FAILURES TO SCRAM-CONTROL ROD DRIVE AND ORIFICE ASSEMBLIES

FORT ST. VRAIN NUCLEAR GENERATING STATION

PUBLIC SERVICE COMPANY OF COLORADO

TABLE OF CONTENTS

Section	Title	Page
	ABSTRACT	vi
1	INTRODUCTION	1-1
1.1	DESCRIPTION OF CONTROL ROD DRIVE AND ORIFICE ASSEMBLY	1-1
1.1.1	Function	1-1
1.1.2	Location and Environment	1-1
1.1.3	Description and Operation	1-1
1.1.3.1	Drive Motor	1-3
1.1.3.2	Friction Brake	1-4
1.1.3.3	Dynamic Braking	1-4
1.1.3.4	Reduction Gear Mechanism	1-5
1.1.3.5	Cable Drum and Cable	1-6
1.1.3.6	Lubricant	1-6
1.2	SUMMARY OF SCRAM FAILURES	1-7
1.2.1	During Design Testing in 1968 and 1969	1-7
1.2.2	During Operation on February 22, 1982	1-8
1.2.3	During Operation on June 23, 1984	1-9
1.2.4	During Back EMF Measurements in January 1985	1-9
1.3	REFERENCES FOR SECTION 1	1-10
2	QUALITATIVE EVALUATION OF POSSIBLE FAILURE MECHANISMS	2-1
2.1	MOTOR BRAKE ASSEMBLY MALFUNCTION	2-1
2.1.1	Possible Failure Mechanisms	2-1
2.1.2	Observations and Inspections	2-1
2.1.3	Analysis and Conclusions	2-2
2.2	REDUCTION GEAR MECHANISM MALFUNCTION	2-2
2.2.1	Possible Failure Mechanisms	2-2
2.2.2	Observations and Inspections	2-2
2.2.3	Analyses and Conclusions	2-2
2.3	MOTOR MALFUNCTION	2-5
2.3.1	Possible Failure Mechanisms	2-5
2.3.2	Observations and Inspections	2-5
2.3.3	Analyses and Conclusions	2-5
3	QUANTITATIVE DETERMINATION OF FAILURE MECHANISM AND CRDOA OPERABILITY	3-1
3.1	MOTOR POWER MEASUREMENTS	3-1
3.1.1	Purpose	3-1
3.1.2	Description of Tests	3-1
3.1.3	Conclusions	3-1
3.2	CONTROL ROD DROP TIME MEASUREMENTS	3-2
3.2.1	Purpose	3-2
3.2.2	Description of Tests	3-2
3.2.3	Conclusions	3-3
3.3	BACK EMF MEASUREMENTS AND ANALYSES	3-3
3.3.1	Purpose	3-3
3.3.2	Test Equipment	3-4
3.3.3	Description of Tests	3-4

TABLE OF CONTENTS (Continued)

Section	Title	Page
3.3.4	Methods of Data Analysis	3-5
3.3.5	Test Results	3-7
3.3.5.1	Waveform Analyses	3-7
3.3.5.2	Comparison of Unrefurbished CRDOAs	3-7
3.3.5.3	Repeatability of Tests	3-11
3.3.5.4	Effect of Variation in Capacitance	3-11
3.3.5.5	Effect of Refurbishment	3-11
3.3.6	Uncertainties	3-17
3.4	ROTOR ANGULAR VELOCITY MEASUREMENTS	3-19
3.4.1	Purpose	3-19
3.4.2	Description of Tes	3-19
3.4.3	Conclusions	3-19
3.5	MOTOR BEARING TESTS AND ANALYSES	3-19
3.5.1	Purpose	3-19
3.5.1.1	Breakaway Torque Tests	3-19
3.5.1.2	Bearing Debris Analyses	3-20
3.5.2	Description of Tests	3-20
3.5.2.1	Breakaway Torque Tests	3-20
3.5.2.2	Bearing Debris Analysis	3-20
3.5.3	Conclusions	3-21
3.6	REFERENCES FOR SECTION 3	3-22
4	REMEDIAL ACTIONS	4-1
4.1	MOTOR AND REDUCTION GEAR MECHANISM REFURBISHMENT	4-1
4.1.1	Purpose	4-1
4.1.2	Procedures and Tests	4-1
4.1.3	Refurbishment Acceptance Criteria	4-1
4.2	RISE TO POWER TESTING	4-2
4.2.1	Purpose	4-2
4.2.2	Procedures and Tests	4-3
4.3	OPERATING TESTS AND SURVEILLANCE PROCEDURES	4-3
4.3.1	Purpose	4-3
4.3.2	Procedures and Tests	4-3
5	SUMMARY	5-1
5.1	FAILURE MECHANISM	5-1
5.2	REMEDIAL ACTIONS	5-1

LIST OF APPENDICES

Appendix A - Data Analysis Program

Appendix B - Frequency versus Time Plot - CRDOA 8

Appendix C - Voltage Fourier Analysis - CRDOA 7

Appendix D - Repeatability of Voltage, Frequency, and Torque versus Time Plots

Appendix E - Effect of Capacitance on Voltage, Frequency, and Torque versus Time Plots

Appendix F - Effect of Refurbishment on Voltage, Frequency, and Torque versus Time Plots and Acceleration Fourier Analysis

Appendix G - Shaft Encoder Measurements versus Electrical Frequency

Appendix H - Average Starting Torque versus Peak Torque at "Steady-State"

Appendix I - Voltage, Frequency, and Torque versus Time - As Found for CRDOAs

LIST OF TABLES

Table No.	Title
1.1-1	HELIUM PURGE SYSTEM
2.2-1	CONTROL ROD DRIVE COMPONENTS COMPARATIVE SENSITIVITY
3.3-1	BACK EMF TEST DATA - PRIOR TO REFURBISHMENT
3.3-2	TEST COMPARISON
3.3-3	EFFECT OF CAPACITANCE VARIATION
3.3-4	EFFECT OF REFURBISHMENT - CRDOA 44
3.3-5	PERFORMANCE DEGRADATION - CRDOA 7

LIST OF FIGURES

Figure No.	Title
1.1-1	Control Rod Drive and Orifice Assembly
1.1-2	Control Rod Drive Mechanism
1.1-3	Motor and Brake Assembly
1.1-4	Characteristic Curves for Control Rod Drive Motor
1.1-5	Control Rod Drive Motor Current versus Rod Weight
1.1-6	Motor Bearing
1.1-7	Control Rod Drive Brake
1.1-8	Reduction Gear Mechanism
3.1-1	CRD Back EMF Test Configuration

ABSTRACT

During a scram, a friction brake on the control rod cables is released allowing the cable drum, reduction gear mechanism, and motor rotor to be driven by the weight of the control rod pairs. The control rod pairs drop into the core under the force of gravity, with their speed controlled by a dynamic brake.

On June 23, 1984, 6 of 37 control rod pairs failed to scram. This report examines mechanisms which could have caused a failure of any of the components of the control rod drive and orifice assembly. The report also sets forth a proposed plan for refurbishment of the control rod drive and orifice assemblies, a refurbishment acceptance criteria, and a plan for development of interim and final operational acceptance criteria. Refurbished control rod drive and orifice assemblies which meet the stringent refurbishment acceptance criteria will provide reliable service while operational performance data is acquired and evaluated and the final operational acceptance criteria is developed.

SECTION 1

INTRODUCTION

1.1 DESCRIPTION OF CONTROL ROD DRIVE AND ORIFICE ASSEMBLY

1.1.1 Function

The control rod drive system makes possible the control of nuclear reactions in the reactor core by means of neutron absorbing rods which are withdrawn from or released to drop into the core. The plant was designed for a total of 74 control rods to be operated in pairs by 37 control rod drive mechanisms (CRDMs). Each CRDM is mounted in a control rod drive and orifice assembly (CRDOA). Seven spare CRDOAs are stored in equipment storage wells. Temporary modifications to two CRDOAs have been made by removing one control rod and adding an instrument package which occupies the space vacated by the removed control rod. The instrument package is not connected to the CRDOA.

A reserve shutdown hopper and an orifice control mechanism, consisting of an orifice valve and an electric stepping motor controlled by an indexer, are also mounted in each CRDOA. The purpose of the orifice control mechanisms is to control the orifice valves, which compensate for core power generation variations in different regions by adjusting coolant flow. The purpose of the reserve shutdown hopper is to provide an alternate method of inserting neutron absorbing material into the core. Operation of these mechanisms is, therefore, not directly related to operation of the CRDMs. Further discussions will focus upon operation of the CRDMs. The orifice control mechanisms and reserve shutdown hoppers will be discussed only when their presence has an impact on inspection, testing, or refurbishment of the CRDOAs.

1.1.2 Location and Environment

The CRDOAs, shown in Figure 1.1-1, are located in the refueling penetrations in each of the 37 core regions in the top head of the prestressed concrete reactor vessel. Each CRDOA has a flange approximately 45 inches below its top face. A counterbore is provided in each refueling penetration, approximately 46 inches deep, into which each CRDOA is bolted (Reference 1).

A radiation shield is contained in the housing just below each CRDM. This shielding limits the radiation level at the CRDM to approximately 1 rad per hour (Reference 2).

During operation, purified helium (about 0.17 ACFM) is introduced through the primary closure, which forms the top housing of each CRDOA, and flows through the radiation shield via cable guide holes and other spaces, and finally into the reactor inlet plenum. The purified helium is distributed to the 37 core regions by means of eight subheaders, as summarized in Table 1.1-1 (Reference 3).

1.1.3 Description and Operation

Figure 1.1-2 is a general arrangement drawing of a CRDM. The principal components of the CRDM, sometimes referred to as a 200 Assembly, are listed below and described in greater detail in subsequent sections:

Table 1.1-1

HELIUM PURGE SYSTEM

Subheader	Regions Served
1	1, 5, 7**, 28**, 34
2	14*, 15, 29, 30, 31
3	32, 33, 35, 36
4	2, 3, 8, 22
5	23, 24, 25*, 26, 27
6	6*, 16, 17, 18, 20
7	9, 10*, 19, 21, 37
8	4, 11, 12, 13

* Failure of CRDOA to automatically scram on June 23, 1984

** Failure of CRDOA to automatically scram on February 22, 1982, and June 23, 1984

- drive motor - lifts control rod pairs from core; control rod pairs drop under the force of gravity during a scram, with the drive motor and capacitors providing dynamic braking to limit control rod drop velocity; can be operated in reverse to drive control rod pairs into core

- reduction gear mechanism - provides interface between drive motor and cable drum

- cable drum - rotates to allow control rod cables to wind and unwind

Other components of the CRDM include a rod position potentiometer; limit switches and limit switch cams to provide rod position indication; a slack cable indication device to provide indication of loss of weight during insertion; and control rod guide tubes.

1.1.3.1 Drive Motor

A control rod drive motor is shown in Figure 1.1-3. Each of the control rod drive motors is a four-pole squirrel-cage induction machine with a rated full-load output of 13.0 inch-pounds at approximately 1650 RPM. The motors require a three-phase 105 V ac power supply to their wye (Y) connected stator windings. Each motor is designed to have a starting torque of approximately 23.0 inch-pounds. The average measured torque on the rotor during withdrawal of a control rod pair has been measured to be 24.2 inch-ounces. The torque on the rotor derived from the weight of two rods, the moment arm of the cable on the drum, and the gear ratio is 19.8 inch-ounces. When compared with other types of electrical drive units, the motors are rugged inexpensive units which are capable of being started and reversed without complicated controls.

Due to the high gear ratio and the flat torque/speed curve of the motor, input current is insensitive to motor load conditions. Variations of less than 6 percent were measured for a 26 percent change in rod weight. There is a 3 percent change between raising and lowering the rods. Figure 1.1-4 shows the typical motor characteristics and Figure 1.1-5 shows the motor current as a function of rod weight.

The maximum duty that each motor is designed to experience is 450 successive start-run-stop cycles at 2 seconds per cycle followed by 93 start-run-stop cycles at 5 minutes per cycle. Under these conditions, the life expectancy of non-wearing parts in the motors is expected to be 30 years.

Each motor is designed to operate in an environment of dry helium. Also, each motor is designed to withstand a maximum radiation dose rate of 1 rad per hour gamma.

Magnet wire with heavy ML insulation is used for the windings. The stator windings are vacuum impregnated using Shell Epon 828 with Shell Z curing agent. The entire stator is encapsulated in Shell Epon 828 with Shell Z curing agent and glass fiber filler.

A permanent magnet made of Index 1 is mounted on each rotor shaft and is suitably covered with aluminum to prevent damage. The permanent magnet ensures that capacitive self-excitation is achieved when scramming the control rod drives (Reference 4).

Each CRDM motor has two motor bearings on the gear end and one bearing on the brake end of the motor. The bearings were provided by New Departure, a division of General Motors Corporation, and were customized for use as CRDM motor bearings by Gulf General Atomic.

A motor bearing, as modified, is shown in Figure 1.1-6. The outer and inner races of each bearing are solid stainless steel, AISI 440C, New Departure 3203 races. Nine tungsten carbide grade 25 balls, 0.28125 inches in diameter, manufactured by Industrial Tectonics, were utilized in each bearing. The radial clearance was specified to be 0.0008 to 0.0012 inches; the inner race was honed, if necessary to provide the specified clearance.

The retainer was manufactured from solid nitralloy 135, AMS 6472. The retainer assembly was heated to 400°F to 450°F and a bearite ring provided by Everlube Corporation of America, was impregnated with molybdenum disulfide, inserted and seated under pressure. The bearing was run in with blowing nitrogen.

1.1.3.2 Friction Brake

The friction brake is a modified Bendix multiple-disc EFL model. The changes from a standard unit consist of a reduction in the number of brake discs, use of sintered metal friction facings, and use of additional release plungers. The brake body assembly is made of carbon steel. For greater reliability in a helium environment, special windings were introduced; these windings were impregnated and encapsulated with Epon 828 compound. Special retaining rings were added to prevent the magnetic coil from interfering with the armature plate and jamming the brake in the event of an encapsulation failure. Under normal conditions the encapsulation retains the coil in position. The retaining rings serve only as a back-up.

The brake is rated at 24 V dc. Holding torque is 15 - 25 inch-pounds at room temperature with 22 V dc applied.

In Figure 1.1-7, the brake is shown energized and engaged (i.e., the electromagnet is energized resulting in a flux path through the iron magnet body and the armature plate). This magnetic field causes the armature plate to be drawn toward the magnet body, clamping the center disc between the two friction discs. The friction discs are constrained from rotating by the spline on the magnet body. The center disc has clearance over the spline but is keyed by three slots that engage with the arms of the spider. The spider is keyed to the rotor shaft. Thus, when energized and applied, the brake retains the control rods in a withdrawn position.

When the magnet is de-energized by removal of dc power, the spring plungers push the armature plate away from the magnet body, allowing the three plates to separate. The center disc, the spider, and the rotor shaft are then free to rotate (i.e., the brake is disengaged and the control rods are free to drop). The springs, constructed of 0.018 inch diameter spring wire, have a 0.407 inch free length and a 0.25 inch length with a 15 ounce compressed load.

1.1.3.3 Dynamic Braking

Dynamic braking limits control rod drop velocity following release of the friction brake to approximately 1.25 inches per second. A three phase, wye

(Y) connected capacitor array is connected to the drive motor stator in the control rod drive motor control centers. When the drive motor is rotated under the influence of the dropping control rods, it functions as an induction generator, supplying a capacitive-resistive load, the characteristic frequency of which determines the limiting speed of the motor and, consequently, the control rod insertion velocity. The initial excitation of the motor for operation as an induction generator is provided by residual magnetism built into the motor.

Each capacitor was nominally specified as 45 μF in the original design. Testing in July 1984 showed that the capacitances ranged from 34 to 50 μF at that time.

1.1.3.4 Reduction Gear Mechanism

A pinion gear on the end of the rotor shaft drives a set of reduction gears, which then turn the cable drum. Figure 1.1-8 shows the reduction gear mechanism. Gear numbers, locations, and gear ratios are shown. Bearing locations are also indicated. During a scram, the dynamic brake limits motor rotor angular velocity to approximately 2400 rpm (40 rps). At this speed the first stage gear axle (3P) is rotating at 4.1176 rps, and the second stage gear axle (5P) is rotating at 0.5003 rps. The gear ratio between the motor and the cable drum is 1:1151.365.

The pinions and gears of the gear train are fabricated of modified nitralloy 135. The gear surfaces are nitrided to provide greater wear resistance. This material was selected for ease of fabrication with excellent resistance to scoring and abrasion because of its high hardness.

Selection of the nitralloy material was based on the good results obtained from tests (References 5, 6 and 7). In those tests, the mechanism with gears manufactured from the modified nitralloy 135 was jogged a total of 212,630 times (travel of 21,753 feet) in the Phase I test. No detectable wear had taken place. In Phase II testing, operating in helium atmosphere, the mechanism was jogged 200,686 times (30,784 feet travel), and the study after disassembly showed that the gears were in very good condition with only negligible wear.

The reduction gear mechanisms utilize bearings of either tungsten carbide (WC) or Type 440C stainless steel in steel races. Type 440C is a martensitic stainless steel which is readily heat treated to a very high hardness and remains hard up to approximately 600°F.

Gears and bearings are provided with slingers and guards to minimize ingress of foreign particles. The mechanism is essentially enclosed within the cable drum, minimizing the possibility of external debris and particles entering the mechanism. In certain areas, additional space was created to permit planned accumulation buildup. Also, magnetic parts, which would tend to attract metallic particulate matter, were eliminated where feasible. This limits the possibility of a particle "jamming" the motor pinion-gear mesh. This "jamming" effect of a particle depends upon its size and composition. Quite large, soft particles could be squeezed through the gear tooth without stalling the drive.

Considerable debris, both metallic and molybdenum disulfide, was generated around the motor pinion at one time during the prototype testing. No effect on drive performance was noted until the pinion failed completely in Phase II of the testing (Reference 6). Since that time, changes have been made to prevent debris from accumulating. The failure of the pinion occurred at a point in time well beyond its design life. The failure was attributed to normal wear of the mating gear bearings coupled with a gear pitch line manufacturing error.

1.1.3.5 Cable Drum and Cable

The cable drum has a pair of deep grooves in which the control suspension cables are wound. The 1/4 inch diameter AISI 347 stranded stainless steel cables are attached to the dual drum by swiveling cable anchors and wound in a "pancake" or spiral manner around the cable drum grooves. The existing cable is composed of a center, middle, and outer strand. Each strand is composed of a center wire around which six wires are layed. The cable weighs 0.1135 pounds/foot. The drum surface essentially follows a spiral curve with a radius of (5.953 + 0.280/360 X θ) inches, as shown in Figure 1.1-8.

Directly below the drum is a group of three guide pulleys which maintain the cables at the correct center distance where they enter the radiation shield below the drive mechanism. The entire drive assembly is supported within the drive housing at three points, two of which are axially aligned to form a fulcrum. The third point, an extension of the spindle carrying the drum bearings, rests in a pillow block having a vertically elongated bore. A spring plunger contacts the underside of the drum spindle on which it exerts an upward force sufficient to raise the drive mechanism (causing it to pivot about the above-mentioned fulcrum) in the event that one control rod cable becomes slack. The plunger normally maintains a microswitch in a free position. The switch is, therefore, actuated in the event that either cable goes slack (i.e., the rod weight is relieved from either cable). In the unlikely event of a failure of the drum spindle, the third point of support is shifted to a support arm device which is mounted at the drum support-guide pulley interface. This arm permits limited rotation of the drive mechanism such that retraction of the control rods is possible.

1.1.3.6 Lubricant

Bearings and gears in the drive assembly are treated with a thoroughly tested dry-film lubrication which is essentially unaffected by the existing radiation and temperature levels. These dry film lubricants have a MoS_2 base. The MoS_2 is combined with an organic (epoxy) binder, commercially know as Molycote X106. There is no evidence that the coefficient of friction of this solid film lubricant is affected by helium or lack of moisture. (The compound has only 3 percent graphite that could increase in frictional characteristics in the absence of H_2O.) There is a reported tendency for a reduced coefficient under radiation. However, radiation seen by all mechanisms is low - about 1 rad/hour. General Atomic environmental testing on EBOR, ESADA, and Fort St. Vrain control rod drives substantiates all but radiation exposure. Peach Bottom operational experience, which includes various levels of radiation exposures, has not indicated any additional problems.

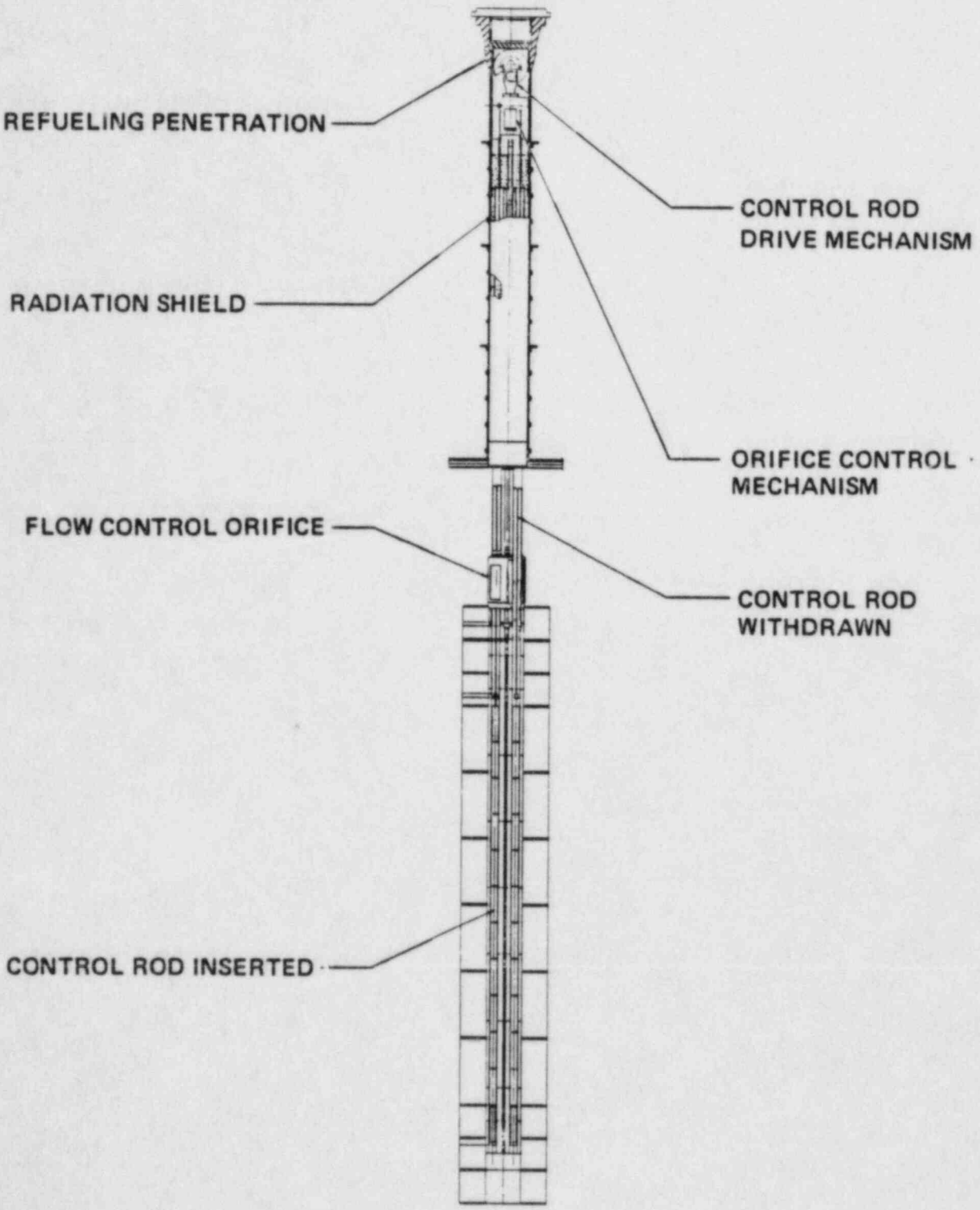

CONTROL ROD DRIVE AND ORIFICE ASSEMBLY
FIGURE 1.1-1

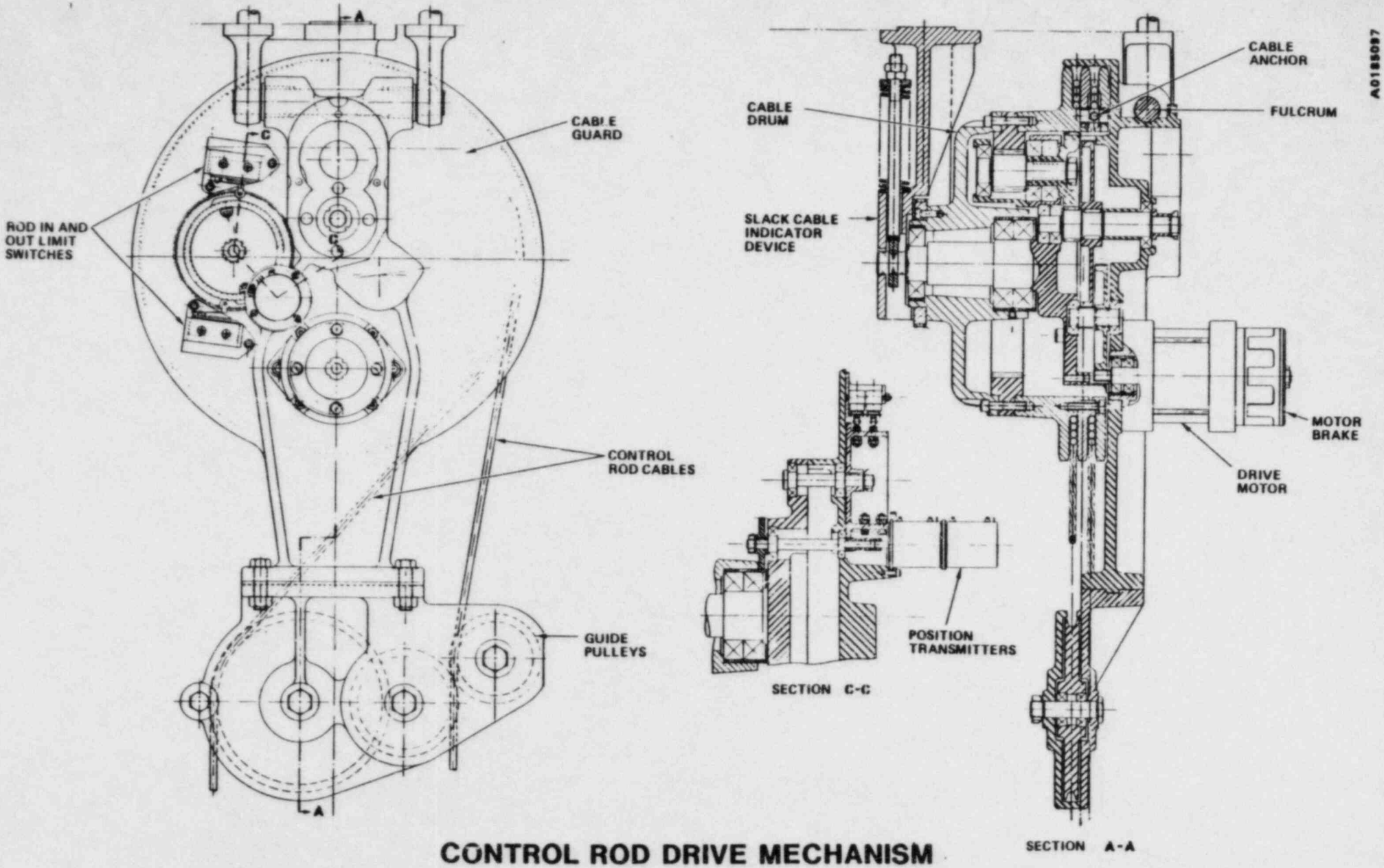

CONTROL ROD DRIVE MECHANISM
FIGURE 1.1-2

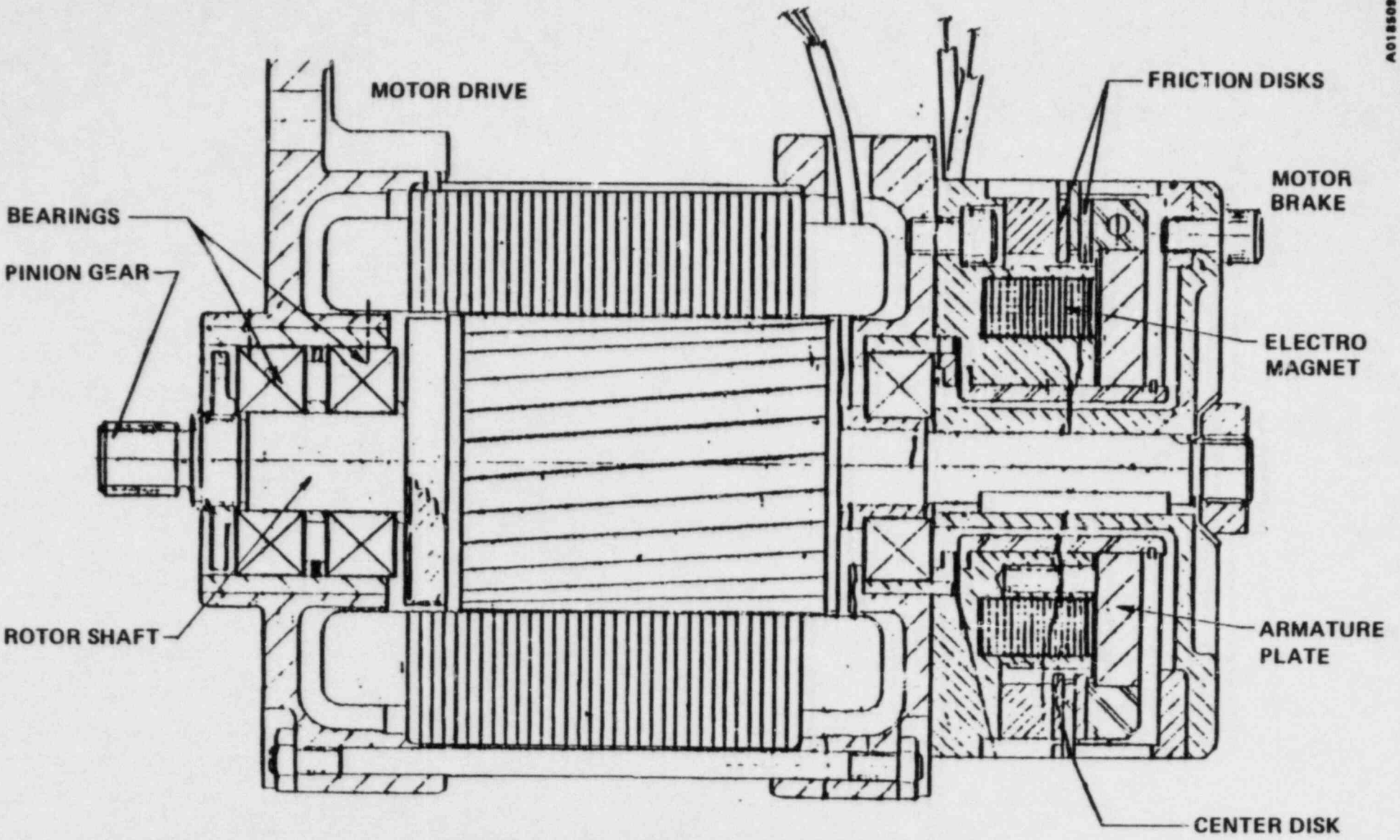

MOTOR AND BRAKE ASSEMBLY
FIGURE 1.1-3

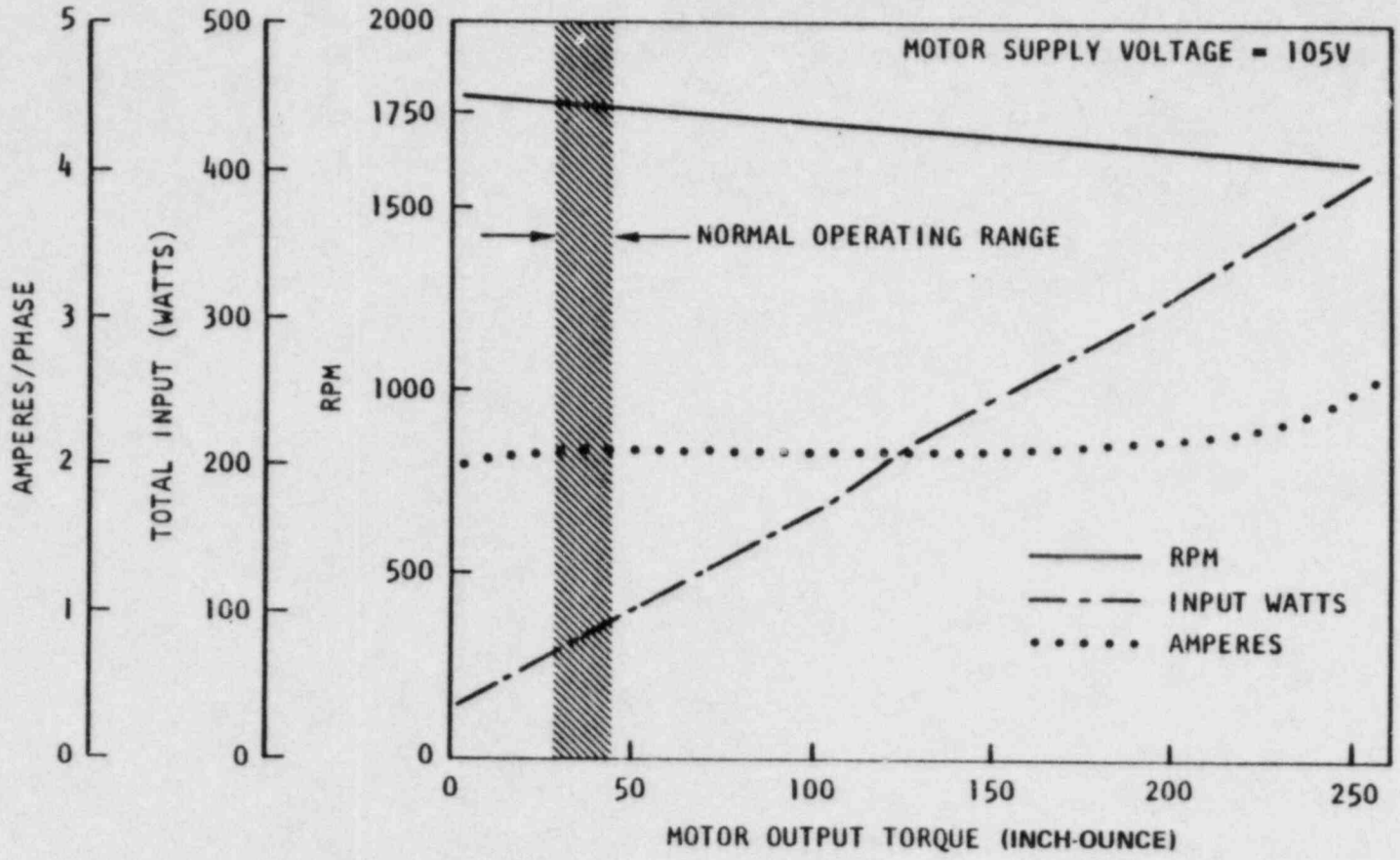

CHARACTERISTIC CURVES
FOR CONTROL ROD DRIVE MOTOR
FIGURE 1.1-4

A0188100

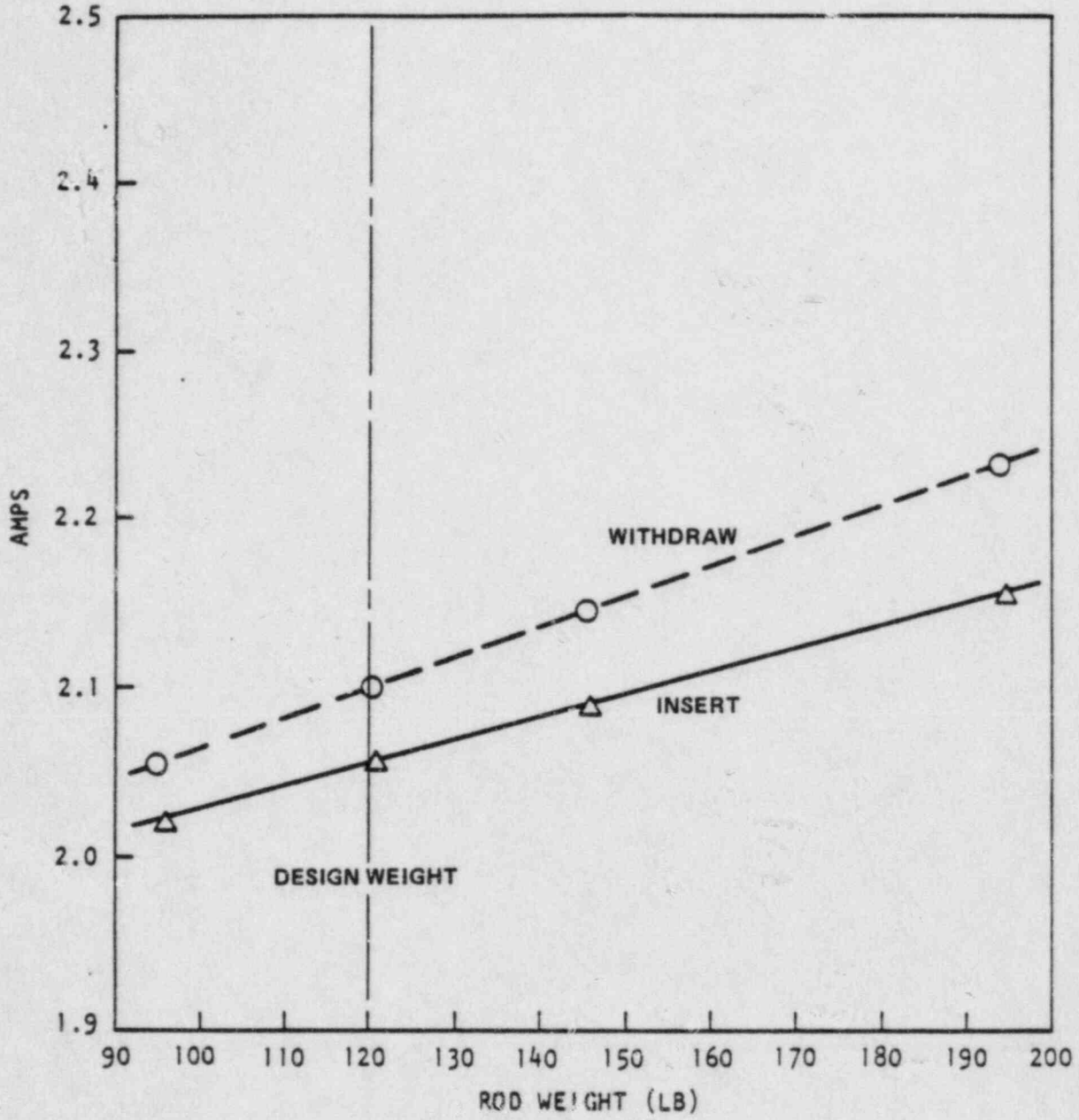

CONTROL ROD DRIVE MOTOR CURRENT VERSUS ROD WEIGHT
FIGURE 1.1-5

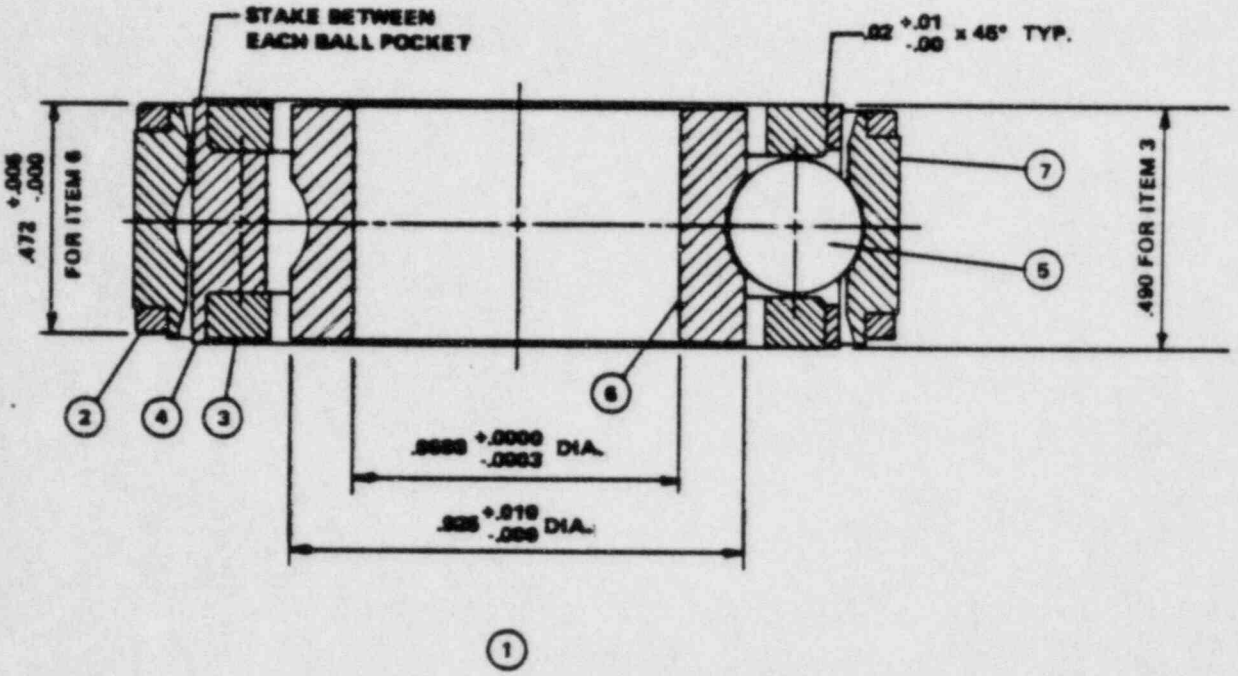

LIST OF MATERIAL			
ITEM	DESCRIPTION	MATL.	MATL. SPEC.
1	ASSEMBLY		
2	RETAINING RING	SST	AISI 430 ANNEALED
3	RING	BEARITE	
4	RETAINER	NITRALLOY 135 MOD	AMS 6472
5	BALL .28125 DIA.	TUNGSTEN CARBIDE GRADE 25	
6	INNER RACE	SST	AISI 440C
7	OUTER RACE	SST	AISI 440C

FIGURE 1.1-6
MOTOR BEARING

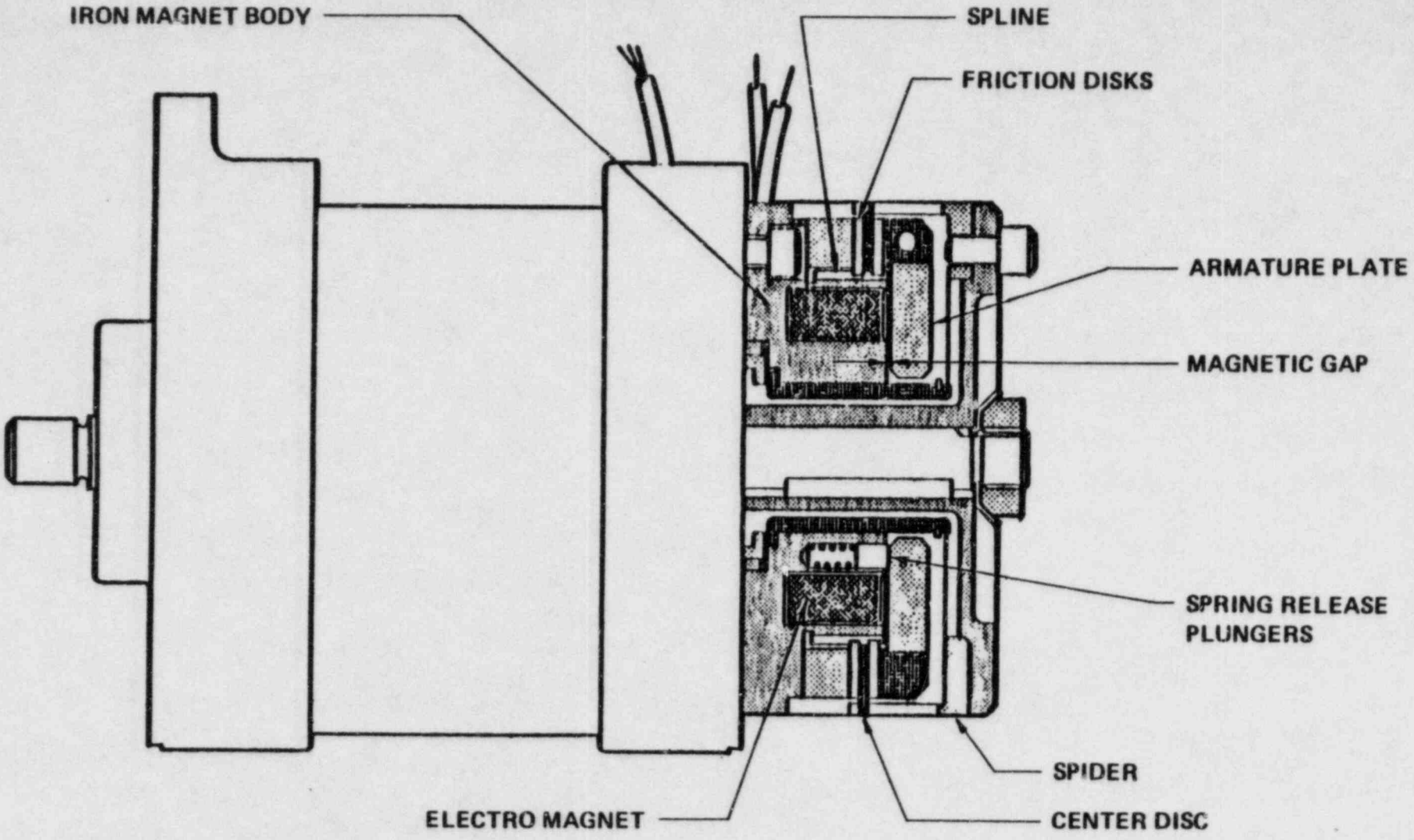

CONTROL ROD DRIVE BRAKE
FIGURE 1.1-7

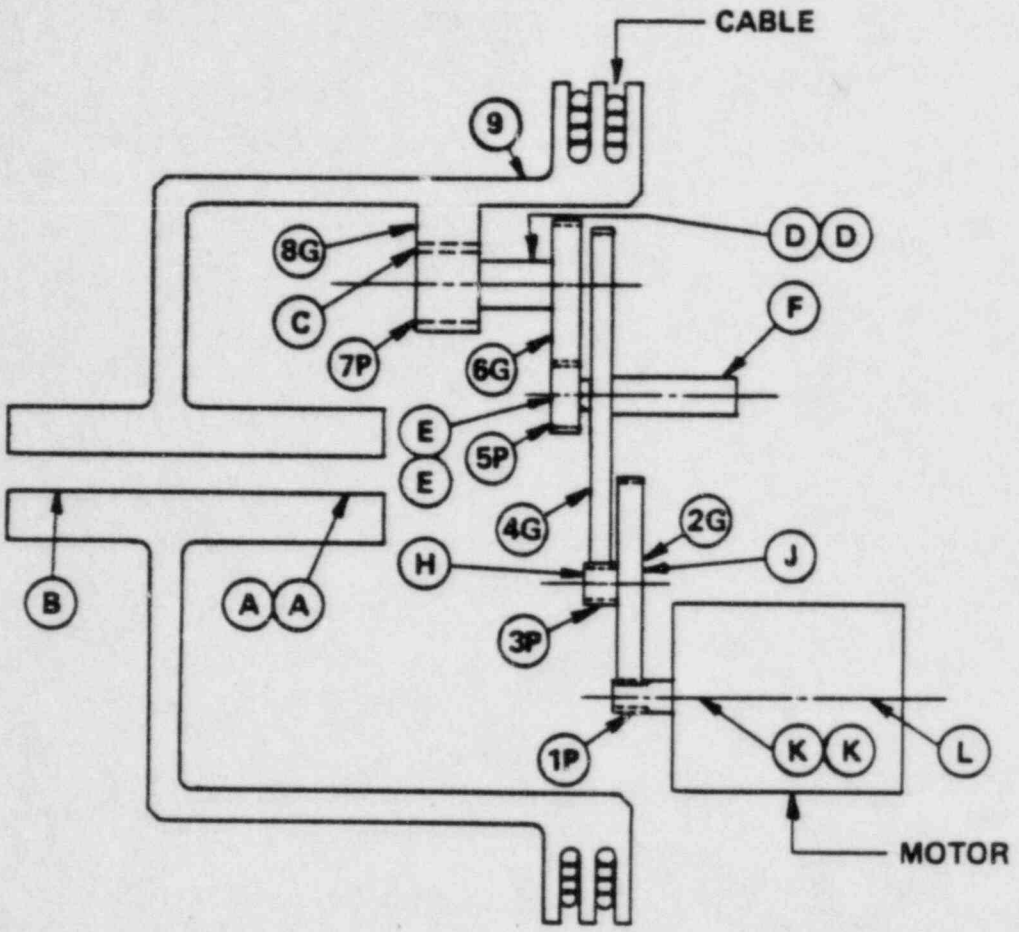

A0185102

GEAR DESIGN CHARACTERISTICS, SHIM MODE		
GEAR NUMBER	MG, GEAR RATIO, (Teeth Out / Teeth In)	R.P.M.
1 P	9.714	1730
2 G		178
3 P	8.231	178
4 G		22
5 P	2.400	22
6 G		9
7 P	6.000	9
8 G		1.5

REDUCTION GEAR MECHANISM
FIGURE 1.1-8

1.2 SUMMARY OF SCRAM FAILURES

1.2.1 During Design Testing in 1968 and 1969

A prototype CRDOA underwent a series of tests to demonstrate its operability. Phase I of the testing program involved testing of the CRDOA in ambient air. No scram failures were observed during this phase of testing. Results of these tests are set forth in Reference 5.

Phase II of the testing began in July 1967 and involved testing of the prototype CRDOA in a helium environment at temperatures representative of planned operating conditions. Results of these tests are set forth in References 6 and 7, summarized below.

Problems with the brake and clutch coils were observed early in the Phase II testing. Failures of the scram clutch on September 28, 1967, and retarder bearings on January 22, 1968, caused test scram failures. Slow clutch disengagement was observed during an ambient checkout of the brake and clutch on August 12, 1968. The scram clutch and retarder bearings were redesigned and subsequently removed as a result of deletion of the fast scram capability requirement. The friction brake was modified to operate at 24 V dc instead of 125 V dc.

Motor bearing failures which resulted in operational failures of the CRDM occurred during the course of Phase II testing. A summary of the motor bearing failures and modifications made to the motor bearings is provided below:

- The original prototype motor bearings were dry film lubricated New Departure 3L03-SS (SST races and balls). These bearings failed on February 1, 1968, after 118,931 jog cycles and were replaced.

- The second set of bearings failed during bench testing on March 16, 1968, following indications of friction in the drive train, and after an additional 246,555 jog cycles. At this time, the bearings were changed to higher capacity New Departure 3203-SS bearings. The number of balls in each bearing was increased from eight to ten and a solid one-piece retainer was introduced.

- The third set of bearings failed on April 9, 1968, after only 65,956 jog cycles and were replaced by bearings consisting of New Departure 3203-SS races, no retainer and a complement of twelve tungsten carbide balls. These bearings lasted for 141,915 job cycles before failing.

- The current design, consisting of New Departure 3203-SS races, solid nitralloy retainer with bearite inserts and nine tungsten carbide balls, was introduced after the fourth failure, on May 16, 1968. These bearings underwent 440,050 jog cycles, 1051 scrams plus an additional 1275 "fast scrams". (The fast scram feature was subsequently deleted as a design requirement.)

On October 24, 1968, failure of the pinion and mating gear occurred and the motor bearings showed signs of wear. This was due to normal wear as the duration of the test was far in excess of the life of the parts.

In an attempt to increase bearing life and improve scram characteristics, the prototype CRDOA was redesigned to incorporate a 600 rpm shim motor in place of the 1800 rpm motor included in the initial design. After the redesigned CRDOA was assembled, it was installed in the Phase I test rig where the functional air tests were repeated for the new configuration. These tests included setting of control rod travel limit switches, adjusting the control rod position indicator circuit, and determining the drive mechanism efficiency and the shim motor operating characteristics.

During the brake torque tests it was discovered that the 600 rpm shim motor was incompatible with the capacitance braking system with the result that actuation of the capacitive scram control failed to provide the necessary retarding effect. When efforts by the manufacturer to correct this condition were unsuccessful, it was decided to revert to the 1800 rpm shim motor design.

Ambient temperature checks revealed a bearing chatter problem which was found to result from a bent motor shaft. After installing a new shaft and bearings the initial checkout tests were successfully performed.

Upon restoration of operating temperature test conditions, a series of capacitive scrams was performed. Following this, brake tests were run. The cycling test, which was initially to consist of a total of 130,000 jogs and 1800 capacitive scrams, was then run. This run was interrupted by a broken cable. The cause of the broken cable was a failure of the cable anchor to pivot due to seizure, thereby causing the cable to bend until it broke. A redesign of the anchor and pivot solved the problem. During the course of the remainder of the cycle test, one scram failure occurred. It was suspected that this failure was due to brake disc hangup.

The final portion of the cycling test was performed with a displaced graphite stack during which a second scram failure occurred. This scram failure was found to have been caused by brake disc hangup. The cycling tests were terminated after completion of 130,000 jogs and 1610 scrams.

The mechanism torque measurement performed after completion of the cycle tests revealed little change from the pretest results. Post test examination revealed some roughness in the two clutch shaft bearings and in the potentiometer drive gear shaft support bearing.

1.2.2 During Operation on February 22, 1982

During routine startup following an extended shutdown, operations personnel initiated a scram in order to comply with LCO 4.2.11, Loop Impurity Levels. The reactor was not critical at the time of the scram. Control rods in regions 7 and 28, operated by CRDOAs 18 and 44, did not drop. The rods were subsequently inserted using normal control rod drive power.

On February 23, 1982, each control rod pair was withdrawn to full out-position and then scrammed. Three other rod pairs exhibited sticking tendencies during this initial exercise, but only the CRDOA in region 7 exhibited repeated sticking. After several tests, the CRDOA began to insert freely.

During the shutdown, levels of moisture had increased in the primary helium coolant. It was postulated that moisture had affected the control rod drive mechanisms, which had been idle during the shutdown, causing the CRDM to

stick and preventing the control rods from dropping under the force of gravity. Binding of the control rods in the drive channel was ruled out as a cause because sensing switches in the CRDOA did not indicate slackness in the cable at any time. Corrective action taken was to require daily exercise of the CRDMs when the plant was in a shutdown condition and weekly exercise of the CRDMs during plant operation. The failure to scram and corrective actions are described in Reference 2.

1.2.3 During Operation on June 23, 1984

With the reactor decreasing in power, a blockage of the helium purification train resulted in a decrease in the inlet temperature of the circulating helium system without a corresponding decrease in reactor pressure. With reactor power at 23 percent, the plant protective system initiated an automatic scram upon sensing higher than normal pressure in the prestressed concrete reactor vessel (PCRV). Control rods in regions 6, 7, 10, 14, and 28, operated respectively by CRDOAs 29, 18, 14, 25, and 44, did not drop. Control rod pairs in region 25, operated by CRDOA 7, dropped 5.2 inches before stopping (Reference 8).

The fuses in the 24 V dc power circuit were removed in order to assure de-energization and release of the friction brake. The control rod pairs were then inserted using normal control rod drive power. The reactor has been in a shutdown condition since this occurrence.

The six CRDOAs were served by five different helium purge subheaders (See Table 1.1-1). Therefore, a malfunction of the helium purge system was eliminated as a likely cause of common mode failure.

1.2.4 During Back EMF Measurements in January 1985

A testing program was undertaken in which Back EMF was measured during control rod drops in-core and in the hot service facility. Section 3.3 describes the testing program. During this extensive testing program, several instances of scram failures have occurred.

On January 14, 1985, during scram testing, CRDOA 36 was being operated in Region 28. One full and ten partial scrams from various rod positions had been run, all of which were successful. Partial scrams are tests in which the control rod pairs are allowed to drop for a specified period of time with the friction brake then reapplied to stop the scram. On runs 12 and 13, from rod position 24.8 inches, no movement was indicated. The rod pairs were raised 10 inches and a successful partial scram was then run. Subsequent successful partial scrams and one full scram were performed.

On January 14, 1985, during scram testing, CRDOA 17 was being operated in Region 31. One full scram from rod position 191.2 inches and five partial scrams from rod positions 191.2, 174.0, 157.5, 140.5, and 123.9 inches had been run, all of which were successful. On the seventh and eighth runs, from rod position 107.3 inches, no movement was indicated. The rod pairs were raised 10 inches and a successful partial scram was then performed on the ninth run. Three more successful partial scrams were then run from rod positions 100.9, 84.2, and 67.2 inches. On runs 13 and 14, from rod position 51.7 inches, no movement was indicated. The rod pairs were then raised two inches and a successful partial scram was performed on run 15. Two more

successful partial scrams were then run from rod positions 36.9 and 20.7 inches. On run 18, from rod position 6.1 inches, no movement was indicated. The rod pairs were raised two inches and lowered back to rod position 6.1 inches. A successful partial scram was then performed on run 19. The rods were then raised to rod position 191.2 inches. No movement was indicated on the next two runs. The rod pairs were raised and lowered back to rod position 191.2 inches and the rod pairs were inserted using normal control rod drive power.

On January 15, 1985, CRDOA 15 was being operated in Region 32. One full scram from rod position 191.2 inches and five partial scrams from rod positions 191.2, 175.5, 158.6, 142.5, and 125.1 inches had been run, all successfully. On run 7, from rod position 107.8 inches, no movement was indicated. Testing of this CRDOA was suspended at that point. Testing of other CRDOAs has continued with no other failures to scram.

1.3 REFERENCES FOR SECTION 1

1. Public Service Company of Colorado. Fort St. Vrain Nuclear Generating Station Updated Final Safety Analysis Report, Section 3.8.

2. Public Service Company of Colorado. Licensee Event Report No. 50-267/82-007, March 8, 1982.

3. Letter, D.J. Kowal (G. A. Technologies, Inc.) to D.W. Warembourg (Public Service Company of Colorado), August 28, 1984.

4. Gulf General Atomic. Design Report for Control Rod Drive Mechanism, GADR-10, Issue L, June 1, 1976.

5. Gulf General Atomic. PSC Prototype Control Rod Drive and Orificing System Test Report - Phase I, GA-P-900-49.

6. Gulf General Atomic. Prototype Control Rod Drive and Orificing System for the PSC 330 MW(e) Reactor (Fort St. Vrain) - Phase II Test - Interim Report, GA-P-158-4, August 20, 1969.

7. Gulf General Atomic. PSC Prototype Control Rod Drive and Orificing System - Phase II Test - Final Report, GA-P-158-5, August 22, 1969.

8. Public Service Company of Colorado. Licensee Event Report No. 50-267/84-008, July 23, 1984.

SECTION 2

QUALITATIVE EVALUATION OF POSSIBLE FAILURE MECHANISMS

2.1 MOTOR BRAKE ASSEMBLY MALFUNCTION

2.1.1 Possible Failure Mechanisms

Operation of the friction brake assembly is described in Section 1.1.3.2. Failure of the friction brake to release, which would prevent rotation of the motor rotor, could be caused by the following phenomena, alone or in combination:

- failure of scram contactor to de-energize dc power to electromagnet
- rust-oxidation on brake discs causing sticking
- remanence or induced magnetism remaining in the electromagnet after removal of the magnetizing force (dc power)
- reduction in spring constant of spring plungers at elevated temperatures

2.1.2 Observations and Inspections

During the June 23, 1984, failure to scram incident described in Section 1.2.3, the fuses were removed in order to be certain that the brake assembly electromagnet had been de-energized. This action did not result in normal operation of the CRDOA.

CRDOA 25 was inspected in its as-found condition in the period between June 28, 1984, and July 1, 1984, as part of Test T-226. The following observations concerning the friction brake assembly were recorded:

- rust deposits existed on and around the brake discs
- there was evidence of moisture on the bottom of the area where the brake assembly connects to the motor
- brake components operated freely, showing no signs of sticking
- disc side of brake pad showed no sign of corrosion
- when energized, the brake functioned properly
- no residual magnetism was noticed following de-energization

CRDOA 18 was inspected in its as-found condition in the period between July 3 and July 7, 1984. The following observations concerning the friction brake assembly were recorded:

- brake pads exhibited some corrosion
- brake electromagnet showed various color shadings

CRDOA 29 was inspected in its as-found condition on August 18, 1984. The friction brakes were found to be in a similar condition to those of previously inspected CRDOAs. A deposit of rust was found on the spring plungers of the brake assembly.

A test (T-228) was performed in which a CRDM motor brake assembly was operated in a helium environment in an oven at high temperature and moisture levels. The brake discs could not be made to stick, although two instances of a slightly delayed brake release occurred during the test. Following the tests,

rust-oxidation on the brake discs was observed which may have caused the delayed release. Prior to the test, the brake disc had no observable rust. However, the brake assembly was exposed to air at various times during the testing, which very likely caused the corrosion process to accelerate.

2.1.3 Analysis and Conclusions

Testing provided no evidence to support attributing the cause of the scram failures to a malfunction of the friction brake. Although no tests were conducted, the spring plunger's spring constant would not be affected in any significant way by higher than normal temperatures and moisture around the CRDOA. Accordingly, it is concluded that the friction brake was not the cause of any of the failures to scram.

2.2 REDUCTION GEAR MECHANISM MALFUNCTION

2.2.1 Possible Failure Mechanisms

Operation of the reduction gear mechanism is described in Section 1.1.3.4. The condition of the reduction gear mechanism could be responsible for or contribute to a failure to scram in any of the following ways:

- damage to a gear tooth or bearing or the existence of large, relatively hard debris in a gear or bearing race could prevent rotation of the reduction gear mechanism
- debris or wear could interfere with a bearing or gear in the reduction gear mechanism, thereby reducing gear train efficiency; with lower efficiency, the torque transmitted to the motor rotor during a scram could be reduced below the level necessary to overcome motor bearing friction.

2.2.2 Observations and Inspections

Various CRDOAs have been inspected in their as-found conditions, as described in Section 2.1.2 As part of these inspections, the reduction gear mechanisms were examined.

No major damage to gear teeth or bearings has been discovered. Dust and rust have been observed inside the gear train housing. Some of the debris appeared to be magnetic. Evidence of moisture in the form of stains and rust were also observed. Bearings in the reduction gear mechanism contained debris and residue.

2.2.3 Analyses and Conclusions

To assess the effect of a resisting force that could be caused by debris at various points within the drive mechanism, a calculation was made (neglecting normal friction) to determine the force of resistance equivalent to applying a one pound force at bearing A of the cable drum (See Figure 1.1-8). The results are given in Table 2.2-1.

In reviewing Table 2.2-1, it can be seen that the most sensitive area to debris is at the motor bearings "K" and "L" with an order of sensitivity of 500 relative to the cable drum bearings. Similarly, the motor bearings are three times as sensitive as the pinion gear mesh "2G" and "1P" to debris.

The gearing, due to the part sliding, part rolling action of the gear teeth, creates a tendency towards self cleaning, which does tend to further reduce their already lesser sensitivity to the presence of debris. This is because the clearances are generally larger in the gear meshes than in the bearings. The open construction of the gearing allows debris to drop out after a single revolution. Also, because gear shifts and supports are more elastic than bearing housings, the gears have more capacity to roll over debris.

The physical size and hardness of the foreign material which might enter the CRDM is of major significance in evaluating the sensitivity of the CRDMs. Examination of the CRDM construction clearly indicates that particles of fairly moderate size (i.e., 0.030 inch diameter or larger) would probably cause mechanical interference and/or damage if the particle is comparable in hardness to the materials in the gears and bearings. Since no known permanent damage has occurred after many years of operation, it is likely that any debris entering the CRDM is smaller in size and/or significantly softer than the CRDM materials.

Inspection of several reduction gear mechanisms has revealed no major damage which would by itself prevent normal operation of a CRDOA. Some debris and wear were observed in the gears and bearings which would affect the efficiency of the reduction gear mechanisms. Cleaning the more sensitive gears and bearings listed in Table 2.2-1 can be expected to improve the performance of CRDOAs.

Table 2.2-1

CONTROL ROD DRIVE COMPONENTS
COMPARATIVE SENSITIVITY

Gear or Bearing	Assumed Applied Force (pounds)	Equivalent Inhibiting Force (pounds)	Order of* Sensitivity
A	1.0	1	1
B		1.3	0.769
8G		0.3	3.333
7P		0.3	3.333
C		0.3	3.333
D		0.25	4
6G		0.15	6.667
5P		0.15	6.667
E		0.166	6.024
F		0.133	7.519
4G		0.028	35.714
3P		0.028	35.714
H		0.020	50
J		0.020	50
2G		0.006	166.667
1P		0.006	166.667
K		0.002	500.00
L		0.002	500.00

*Order of sensitivity is defined as the ratio of force applied at bearing A to the force necessary at the location of interest to oppose the force at A.

2.3 MOTOR MALFUNCTION

2.3.1 Possible Failure Mechanisms

A description of the CRDM motor and motor bearings is given in Section 1.1.3.1. Operation of the motor as an induction generator during scrams is described in Section 1.1.3.3.

Existence of the following conditions could prevent the motor bearings from rolling smoothly through the bearing races, thus interfering with or preventing a scram:

- debris in a bearing race
- wear on a bearing ball or race
- excessive temperature or humidity changing the lubricating properties of the dry bearing lubricant

Debris in the bearings could come from several sources:

- damaged bearing balls, races, and other bearing components
- CRDOA housing debris washed into the bearing races
- atmospheric particulate matter deposited on the bearings
- dry bearing lubricant

2.3.2 Observations and Inspection

Various CRDOAs have been inspected in their as-found conditions, as described in Section 2.1.2. As part of these inspections, the CRDM motors and motor bearings were examined.

Very fine deposits were observed in the bearing races. The outer bearing, away from the reduction gear mechanism, appeared to have the most material in its race of the three examined from CRDOA 18. Debris in a motor bearing from CRDOA 7 appeared not to be magnetic. Chemical analyses of the bearing debris from CRDOAs 44 and 7 were performed, as described in Section 3.5.2.2.

A scanning electron microscope analysis was performed on the inner race of the CRDM motor bearing from CRDOA 37, as described in Section 3.5.2.2. No particulate adhesion and only minor wear was detected.

Roughness in rolling the bearing balls was noted in virtually all of the unrefurbished bearings examined. Measured torques varied depending on the orientation of the inner race to the outer race, and generally decreased after the bearing was exercised, as was observed during CRDOA inspections and in Tests T-226 and T-232.

2.3.3 Conclusions

Debris in the motor ball bearings is quite significant because of the small internal clearances and the small amount of torque required at the motor rotor to prevent a scram (approximately 16-20 inch-ounces). However, there are mitigating features which overcome this sensitivity providing the debris is relatively soft as would be the case for molybdenum disulfide or corrosion product particulates. The combination of ball to race geometry and lack of a wet lubrication on the ball and races creates a situation for small particles

to be wedged between the ball and race rather than being "squeezed" ahead of the ball as it rolls in the raceway. When wedging occurs, there must either be clearance in the bearing to allow the ball to roll over the particle or sufficient force must be created to deform the particle to an acceptable size. The wedging action combined with applied torque from either the weight of the rods in a free fall scram or a larger torque by the drive motor creates relatively high unit loads to crush or otherwise clear the particulate.

For example, a motor torque of 20 inch-pounds (which is slightly less than the rated starting torque of the motor) would create a crushing force of 190 pounds on a particle that was initially 0.004 inch in diameter if that particle was trapped in the motor bearing race. Similarly, a 2 inch-pounds torque at the motor bearings from the rod weight acting on the drum, as is the case for the scram situation, would create a 19 pound crushing force on the same particle trapped at the same location.

Although recent operating and testing experience has shown that rod weight alone may not be sufficient to produce satisfactory crushing forces in the presence of significant debris, at no time has operation by the shim motors been inhibited. The ability of the mechanisms to crush debris and self clean was demonstrated with the measurement of post incident scram times which were all within the limits of acceptability. Test T-232, performed in August 1984, also showed that frictional torque load on motors was reduced by simply exercising them.

It is, therefore, concluded that internally generated normal wear byproducts in the CRDM motor bearings is a likely cause of the scram failures. Additional testing is being conducted to further analyze this failure mechanism as described in Section 3.

SECTION 3

QUANTITATIVE DETERMINATION OF FAILURE MECHANISM AND CRDOA OPERABILITY

3.1 MOTOR POWER MEASUREMENTS

3.1.1 Purpose

The addition of a mechanical load to the rotor of an operating motor will cause an increase in electrical power used by the motor. Mechanical load due to friction can be expected to increase over the operating life of a motor as a result of irregularities cause by debris and wear of moving parts such as motor bearings. The purpose of the motor power measurement tests was to measure motor power consumption during motor operation with an applied friction load on the motor rotor equivalent to that which would prevent operation of a CRDOA during a scram, and develop a surveillance procedure and acceptance criteria to identify CRDOAs which are approaching their limit of operability based upon measured power consumption.

3.1.2 Description of Tests

The tests, the methodologies and results of which are set forth in Reference 1, were conducted in June 1971 on a production model control rod drive assembly. The brake end of the drive motor shaft was adapted to incorporate a miniature drag clutch.

The control rod drive assembly was equipped with 125 pound dummy control rods and suspended by the overhead hoist at the production test facility. The mechanism was operated from the control console which forms part of the production test facility.

Since the diameter of the drum and cable varies as the cable unwinds, the torque also varies. Therefore, tests were conducted at three rod positions corresponding to rod in, mid-stroke, and rod out. At each rod position, the clutch was engaged and adjusted until the clutch drag was just sufficient to inhibit scram operation when the motor brake was de-energized. The torque at the motor shaft required to prevent scram operation was measured and averaged about 16 inch-ounces. The drive motor was then operated to obtain start and run power readings. Motor voltage was also varied and power readings were obtained.

3.1.3 Conclusions

The purpose of this limited test program was to provide information for establishing the motor wattage limits for operable drives based on the power required to operate the motor with a drag friction applied which would prevent a scram. At the time of testing, the method was not a viable one for determining operability for the following reasons:

- The increase in friction torque at the drive motor to inhibit scram operation was only about 16 inch-ounces
- The increase in motor wattage corresponding to 16 inch-ounces additional torque was about 18 watts

- The increase in motor supply voltage (or the error in measuring motor supply voltage) which would correspond to 18 watts was about 8 V at a motor voltage of 105 V, 6 V at a motor voltage of 110 V, and 4 V at a motor voltage of 115 V

- It is apparently a characteristic of the control rod drive that the motor current, and hence the motor wattage, oscillates during normal operation. The wattages shown in the test data were the mean values and the oscillations were observed to be about 8-10 watts peak to peak

- It was observed during the series of tests that the motor supply voltage would vary by about 3 V due to fluctuations in the main power supply. Similar fluctuations may occur in the reactor application

- The accuracy of a fair quality ac voltmeter is probably 2 percent F.S.D. or $\pm$ 6 volts on a 300 V ac range (the Triplett meter used on this series of tests read 1 percent F.S.D. low)

- The accuracy of a fair quality wattmeter is probably 2 percent F.S.D. or $\pm$ 20 watts on the 1000 watt range wattmeter proposed for FSV use. The Voltron wattmeter used for this series of tests had a stated accuracy of 0.5 percent for the transducer and 1.0 percent for the meter (1.5 X 500 watt range = $\pm$ 7.5 watts)

- The motor supply voltages shown in the data for this series of tests were measured at the motor side of the watt transducer. The panel meters in the control console are wired on the supply side of the watt transducer. The difference in indicated voltage varied in the range of 7-12 volts

3.2 CONTROL ROD DROP TIME MEASUREMENTS

3.2.1 Purpose

The length of time for a control rod to drop 24 inches with an applied friction load slightly less than that which would prevent operation of a CRDOA during a scram was measured. The purpose of these tests was to develop a surveillance procedure and acceptance criteria to identify CRDOAs which are approaching their limit of operability based upon changes in measured drop time.

3.2.2 Description of Tests

The tests, the methodologies and results of which are set forth in Reference 2, were conducted in November 1971 on a production model control rod drive assembly. The brake end of the drive motor shaft was adapted to incorporate a miniature drag clutch.

The control rod drive assembly was equipped with 125 pound dummy control rods and suspended by the overhead hoist at the production test facility. The mechanism was operated from the control console which forms part of the production test facility.

A high speed oscillograph (Visicorder) was hooked up to the control console to obtain records of:

- Drive motor voltage
- "Rod-Out" limit switch operation
- Scram signal
- Drive motor current
- Photo-cell pulse to indicate 24 inches from "Rod-Out"
- Rod position

3.2.3 Conclusions

It was found difficult to accurately adjust and measure the friction torque developed by the miniature clutch. This probably accounts for the scatter in the test data at the torque values corresponding to slightly less than that required to prevent scram. The data does indicate that added friction torque at the drive motor in excess of 16 inch-ounces would bring the drive mechanism very close to stall (no scram) condition. Hence, the operability limit probably would correspond to about 16 inch-ounces of added friction torque.

Under this condition at the drive motor:

- the time to scram 24 inches from a fully withdrawn position would increase from about 18 seconds to 20 seconds
- the time to reach the regenerative voltage (first peak) would increase from about 2 seconds to 4 seconds
- the regenerative voltage (first peak) would decrease from about 140 V ac to 100 V ac

The test data indicated that approach of the operability limit for the control rod drive would cause a measurable increase in the control rod drop time over the first two feet of travel. The increase in drop time, however, would be small and its measurement would require instrumentation equivalent to that used during this test program. It was concluded that it would also be necessary to obtain operating data for each drive unit followed by interpretation of this data in order to establish operability limits.

3.3 BACK EMF MEASUREMENTS AND ANALYSES

3.3.1 Purpose

The failure of six CRDOAs to function properly on June 23, 1984, indicated that the performance of each of the 37 CRDOAs should be evaluated separately. When the Back EMF measurement test procedure (T-227) was initially developed, the intention was to establish a surveillance procedure involving partial scrams and an acceptance criteria based upon time to peak Back EMF voltage and magnitude of peak or steady state voltage.

As data was accumulated, questions were raised concerning the effect of capacitance variations on the Back EMF voltage and the existence of fluctuations in the voltage waveforms. In an attempt to resolve these

questions, the capacitors were tested. The Back EMF test data was further analyzed by calculating the rate of change of electrical frequency and correlating the calculated values to accelerations and torques on the motor rotor as it accelerates from zero velocity to "steady-state"; as it experiences small cyclical accelerations and decelerations due to the interaction of torques caused by the electro-mechanical dynamic brake and the weight of the control rod pairs; and as it experiences friction induced decelerations and torques. As a result, the purpose of the Back EMF testing and analyses became to develop multi-parameter acceptance criteria to identify inoperable CRDOAs based upon a wide range of measurements and calculations.

3.3.2 Test Equipment

On June 28, 1984, the Fort St. Vrain Technical Services Department issued a test (T-227) to establish a data base of control rod drive motor characteristics based on visicorder traces of the regenerative voltage (Back EMF) generated during scram testing. This characteristic provides a measure of the performance of the rod drive mechanism.

The test originally used a recording oscillograph which provided a three phase trace of phase to phase voltage. Later an analog voltmeter was connected between phases to provide a separate, supplemental source of data. This equipment only provided a means for obtaining gross characteristics which did not lend themselves to subsequent objective analysis.

On August 6, 1984, testing of Back EMF commenced using more sophisticated instruments. Test equipment was located in the Reactor Building near the control rod drive motor control centers. The test configuration is illustrated in Figure 3.3-1.

A Hewlett-Packard Model 3437A microprocessor controlled digital voltmeter was used to measure Back EMF across a voltage divider connected across the motor stator. The voltmeter is capable of sampling voltages up to 5700 times per second; during the Back EMF testing, the sampling rate was 4000 times per second. An LM 555 timer chip generating a 260 kHz continuous pulse train and a LS 7400 NAND gate comprised the trigger, which was actuated by the scram contactor. Output from the digital voltmeter was stored in the computer, a Hewlett-Packard Model 220.

3.3.3 Description of Tests

Back EMF measurements during scram tests have been conducted on most of the CRDOAs. Most of the tests have been in-core, although some tests have occurred in the hot service facility and equipment storage wells. Scram times and values of angular velocity and acceleration in-core can be expected to be slower than in the hot service facility, due to the interaction of the control rods with the channels in the fuel blocks. A difference in acceleration of between 10 and 15 radians per second^2 has been observed.

When conducting a test, the scram contactor is used to simultaneously release the friction brake and actuate the trigger, which commences operation of the digital voltmeter. The weight of the control rod pairs causes the control rod cable to unwind and the cable drum, reduction gear mechanism, and motor rotor to begin to rotate. As indicated in Section 1.1.3.3, when the rotor is driven, the motor acts as an induction generator. The generated output voltage during the first second of scram is less than 1 V peak to peak.

As the motor is driven by the acceleration of the control rod pairs, its generated Back EMF output voltage rapidly increases, typically to about 200 V peak to peak and dynamic braking begins to restrain the angular velocity of the motor rotor. The electrical frequency and voltage reach a somewhat lower "steady-state" value. Some periodic fluctuation occurs during "steady-state", however, as the electromechanical force responsible for the dynamic braking is opposed by and interacts with the force caused by the dropping control rod pairs.

Measurements of the Back EMF voltage during all scram tests were taken as described above in Section 3.3.2. The data was analyzed and plotted as described below in Section 3.3.4.

3.3.4 Methods of Data Analysis

The Shannon Sampling Theorem requires that a minimum of 10 data points per period on a wave form be known in order to analyze the waveform. The digital voltmeter used in the Back EMF measurements took voltage readings 4000 times per second; ten readings were taken in 2.5 milliseconds. Therefore, a wave form with a frequency as high as 400 cycles per second could be plotted using output from this digital voltmeter. Frequencies observed and plotted in the course of Back EMF measurements were under 100 cycles per second.

A data analysis program was developed, as shown in Appendix A. The frequency (f) of each waveform was calculated by detecting the period of time between minus to plus zero volt crossovers. Angular velocity of the rotor for a four pole motor equals πf. The rate of change of angular velocity, or acceleration, was determined by taking the frequency of two consecutive sine waves, subtracting the first velocity value from the second, and dividing the result by the period of time over which the change took place. Torque values were calculated by multiplying the acceleration values by the moment of inertia of the rotor and gear train assembly. The data analysis program enabled the computer and printer to generate the following plots:

- voltage versus time
- frequency versus time
- voltage versus frequency
- acceleration versus time
- torque versus time

A printout of the following parameters was also generated by the computer:

- peak angular velocity
- time to peak Back EMF and angular velocity
- average torque on motor rotor during acceleration to peak velocity
- maximum torque on motor rotor each 10 second interval
- standard deviation of torque values each 10 second interval
- gear train efficiency

As indicated in Section 3.3.3, the Back EMF voltage generated during the first second of a scram test is less than 1 V. Due to the voltage divider network, shown of Figure 3.3-1, the digital voltmeter makes less accurate measurements

in this comparatively low voltage range than it makes at higher voltages. Voltage data and calculations of frequency, acceleration, and torque based upon the voltage data are somewhat unreliable when based upon voltage measurements of less than 1 V.

When the torque caused by the gravitational acceleration of the control rod pairs is substantially greater than any torques caused by frictional decelerations, the angular velocity of the rotor will increase linearly and acceleration and torque experienced by the rotor will be virtually constant. Therefore, data showing relatively large variations in acceleration and torque due to metering inaccuracies can be linearized and an accurate value of starting torque can be calculated. This was the case for most scram tests, where frequency versus time plots show a linear increase in frequency from time zero.

However, when the torque caused by gravitational acceleration of the control rod pairs is of the same order of magnitude as the torques caused by frictional decelerations, the angular velocity of the rotor will not necessarily increase linearly. The rotor may experience a noticeable delay in breakaway or take an extraordinarily long time to attain peak angular velocity. A frequency versus time plot of partial scram run 6 for CRDOA 8, performed November 1, 1984, is included in Appendix B as an example of this. An extension of the plot to zero frequency on the ordinate axis indicates that the rotor did not begin to rotate until approximately a second after scram was initiated. Therefore, the calculation of starting torque based on a linearization of calculated acceleration values will be somewhat inaccurate. However, the calculations do show the starting torque to be substantially lower than for most CRDOAs and are accurate in showing the very high friction-induced torques at "steady-state" rotor angular velocity.

Measurements were made of rotor angular velocity, as described in Section 3.4. These measurements confirmed that the rotor accelerated steadily and was not subject to large decelerations in this time period. Thus, accurate values of acceleration and startup torque prior to dynamic braking were calculated from voltage measurements based upon linearization of calculated frequency values.

A discrete Fourier analysis program was developed to determine predominant frequencies in the Back EMF voltage versus time waveform plots. A Fourier analysis was performed on the voltage data from several full scram tests, in each case after frequency had reached a "steady-state" value (approximately 80 Hertz). This Fourier analysis of Back EMF was intended to show whether the voltage was characterized by one predominant frequency, with the voltage output therefore taking the form of a smooth sine wave. If so, then the calculations of the rate of change of voltage versus time (acceleration) would be more accurate than if the output voltage were of an irregular shape, as would be the case with two or more predominant frequencies.

Discrete Fourier analyses were also performed on calculated acceleration data after frequency had reached a "steady-state" value. The purpose of these analyses was to determine the predominant frequency of the low frequency oscillatory motion which is seen in the acceleration and torque versus time curves and to investigate whether predominant frequencies can be related to specific components in the reduction gear mechanism.

3.3.5 Test Results and Conclusions

3.3.5.1 Waveform Analyses

Full scram tests were run on various CRDOAs, some of which were unrefurbished and some of which had been partially or completely refurbished. Voltage data during "steady-state" was subjected to a Fourier analysis. The existence of a predominant frequency of approximately 80 Hertz was discovered. Printouts of the Fourier analysis of the voltage waveform for CRDOA 7 are included in Appendix C. The different plots reflect analyses of data for CRDOA 7 before refurbishment, after refurbishment of the motor, and after refurbishment of the motor and reduction gear mechanism.

Fourier analyses confirm that the Back EMF voltage generated during "steady-state" conditions can be characterized as a sine wave. The Fourier plots for CRDOA 7 in Appendix C show that a single predominant frequency exists, regardless of whether the CRDOA is refurbished or not. These curves are characteristic of other CRDOAs for which voltage Fourier analyses have been performed. Therefore, calculations of acceleration and torque can be made on the basis of the rate of change of frequency.

3.3.5.2 Comparison of Unrefurbished CRDOAs

Full scram tests were run on various unrefurbished CRDOAs for the purpose of comparing the characteristics of various CRDOAs. A summary of test results is given in Table 3.3-1. Appendix I contains plots of Back EMF voltage versus time, frequency versus time, and torque versus time for each test listed in Table 3.3-1.

The average acceleration to peak rotor angular velocity, calculated from data measured during a control rod pair drop, is indicative of CRDOA reliability. Values have increased following refurbishment, as indicated by Table 3.3-4. Average acceleration to peak velocity values for various unrefurbished CRDOAs are listed in Table 3.3-1. The values for CRDOAs 7, 14, 15, 17, 18, 25, 29, 36, and 44, each of which has failed to automatically function during an actual or test scram, are all under 95 radians/second^2. Only five other assemblies (CRDOAs 2, 8, 21, 26 and 28) were found to have smaller values during testing of unrefurbished CRDOAs in August 1984. The values for some of the better performing CRDOAs were measured to be over 110 radians/second^2.

The calculated peak "steady-state" torque is also an indicator of CRDOA reliability. Peak torque decreases dramatically following refurbishment, as indicated by Table 3.3-4. Peak torques are listed in Table 3.3-1 for unrefurbished CRDOAs. The peak torques for the CRDOAs that failed to scram are all over 10 inch-ounces with the exception of the peak torque for CRDOA 15, which was calculated to be 6.68 inch-ounces. The peak calculated torques for the better performing CRDOAs were under 5 inch-ounces. Seven assemblies which have functioned to date during scrams (CRDOAs 2, 8, 13, 21, 23, 28, and 35) also have calculated peak torques greater than 10 inch-ounces. With the exception of CRDOA 13, all of these CRDOAs exhibit other very poor performance characteristics, such as long time to peak voltage and low average acceleration to peak velocity.

Table 3.3-1

BACK EMF TEST DATA - PRIOR TO REFURBISHMENT

CRDOA Number	Peak Back EMF (Volts)	Time to Peak (Seconds)	Peak Velocity (Radians/ Second)	Time to Peak (Seconds)	Average Acceleration to Peak Velocity (Radians/ Second^2)	Peak "Steady-State" Torque (Inch-Ounces)	Test Location (Core Region or in Hot Service Facility	Measured Capacitance	Date	Comments
1	191	2.928	280	2.823	102	5.34	26	42	8-17-84	
2	172	3.686	267	3.518	72	16.56	27	41	8-22-84	
3	223	3.059	303	2.962	98	5.35	2	41	8-17-84	
5	210	2.927	286	2.825	97	4.80	22	45	8-17-84	Capacitance ranged from 42 to 49 micro F
6	193	2.942	280	2.849	102	5.84	1	42	8-16-84	
7*	191	3.309	276	3.214	89	10.03	HSF	46	8-23-84	Capacitance ranged from 43 to 50 micro F
8	219	3.412	292	3.322	88	29.87	36	40	8-16-84	
9										Bad shock-in equipment storage
10	207	2.415	283	2.323	124	3.51	5	40	8-16-84	Best Characteristics
11										Frayed Cable-no data yet
12	224	2.709	297	2.632	108	5.27	15	44	8-18-84	
13	192	2.906	273	2.822	105	19.357	HSF	46	9-21-84	Capacitance ranged from 43 to 50 micro F
14*										Refurbished prior to testing

Table 3.3-1 (Continued)

CRDOA Number	Peak Back EMF (Volts)	Time to Peak (Seconds)	Peak Velocity (Radians/ Second)	Time to Peak (Seconds)	Average Acceleration to Peak Velocity (Radians/ Second^2)	Peak "Steady-State" Torque (inch-Ounces)	Test Location (Core Region or in Hot Service Facility	Measured Capacitance	Date	Comments
15***	221	3.303	298	3.215	94	6.68	32	39	8-16-84	
16	201	2.479	279	2.408	118	6.64	13	41	8-17-84	
17***	187	3.349	274	3.219	86	11.40	31	40	8-18-84	
18**										Refurbished prior to testing
19										Bad seal, no motor - no data yet
20										ICRD - no data yet
21	178	3.438	265	3.340	83	24.21	35	39	8-16-84	
22	199	3.100	278	3.006	97	6.44	34	40	8-18-84	
23	180	3.332	273	3.214	94	22.76	24	42	8-13-84	
24	184	3.171	274	3.065	93	7.31	14	39	8-16-84	Capacitance ranged from 34 to 43 micro F
25*										Refurbished prior to testing
26	179	3.469	275	3.340	87	9.71	9	41	8-18-84	
27										No orifice Valve - in equipment storage
28	173	3.283	267	3.161	85	13.10	21	42	8-13-84	
29*	179	3.454	268	3.345	83	21.51	HSF	46	8-17-84	Capacitance ranged from 43 to 50 micro F
30	206	2.547	283	2.467	115	5.38	11	40	8-17-84	
31	197	2.511	279	2.430	117	4.37	4	45	8-17-84	Capacitance ranged from 42 to 50 micro F

Table 3.3-1 (Continued)

CRDOA Number	Peak Back EMF (Volts)	Time to Peak (Seconds)	Peak Velocity (Radians/ Second)	Time to Peak (Seconds)	Average Acceleration to Peak Velocity (Radians/ Second^2)	Peak "Steady-State" Torque (Inch-Ounces)	Test Location (Core Region or in Hot Service Facility	Measured Capacitance	Date	Comments
32	193	2.678	276	2.583	110	5.80	20	39	8-17-84	
33	219	2.936	291	2.847	104	4.75	16	40	8-18-84	
34	188	3.063	273	2.968	95	5.93	33	40	8-16-84	
35	186	3.287	275	3.180	90	10.36	29	45	8-13-84	Capacitance ranged from 41 to 48 micro F
36***	187	3.602	277	3.519	79	15.90	28	40	8-18-84	
37										Bad position pot - no data yet
38	204	2.527	281	2.423	119	6.11	8	41	8-17-84	Capacitance ranged from 38 to 47 micro F
39	190	3.030	273	2.922	95	7.23	23	44	8-18-84	
40	183	3.154	270	3.046	89	7.67	18	42	8-18-84	
41	196	2.923	281	2.830	100	7.21	17	41	8-16-84	
42	184	3.072	273	2.997	94	5.67	12	41	8-17-84	
43										ICRD - no data yet
44**	191	5.277	268	5.073	54	14.2	35	39	8-6-84	

* Failed to operate on June 23, 1984, during operation
** Failed to operate on February 22, 1982, and June 23, 1984, during operation
*** Failed to operate during testing in January 1985

3.3.5.3 Repeatability of Tests

Full scram tests were run at various times on CRDOAs 3, 8, and 10 for the purpose of determining whether an unrefurbished CRDOA consistently exhibited the same performance characteristics. CRDOA 3 is an assembly with average as-found performance characteristics. In contrast, the performance characteristics of CRDOAs 8 and 10 are below and above average, respectively. A summary of test results of each run is given in Table 3.3-2. Appendix D contains plots of Back EMF voltage versus time, frequency versus time, and and torque versus time for each test listed in Table 3.3-2.

The performance characteristics of CRDOA 10 are the most consistent. Average acceleration to peak velocity ranged between 121 and 124 radians/second^2. Time to peak voltage ranged between 2.415 and 2.472 seconds. Peak calculated torque values varied between 3.51 and 3.97 inch ounces.

The performance characteristics of CRDOA 3 are also fairly consistent. Average acceleration to peak velocity ranged from 95 to 101 radians/ second^2. Time to peak voltage ranged between 2.988 and 3.141 seconds. Peak calculated torque values varied between 5.53 and 6.20 inch-ounces.

The performance characteristics of CRDOA 8 varied somewhat between tests but always indicate that the assembly is a below average performer. Average acceleration to peak velocity ranged from 72 to 92 radians/second^2. Time to peak voltage ranged between 3.307 and 3.964 seconds. Peak calculated torque values varied between 16.9 and 34.8 inch-ounces. It is evident that the better performing CRDOAs exhibit the greatest consistency of performance.

3.3.5.4 Effect of Variation in Capacitance

All dynamic brake capacitors were tested (T-235) in July 1984 using a Sprague #TO-6 capacitor tester. Each capacitor was tested for capacitance, power factor, leakage current, opens, and shorts. It was found that 34 out of 114 capacitors did not meet specifications and exhibited widely varying values of capacitance.

Full scram tests were run on the CRDOAs immediately before and after replacement of the old capacitors with new 45 μF capacitors. Table 3.3-3 compares the test results for CRDOAs which had substantially degraded capacitors. Appendix E contains plots of Back EMF voltage versus time, frequency versus time, and torque versus time for each test listed in Table 3.3-3.

Replacement of the degraded capacitors with new ones of higher capacitance appears to reduce the time to peak Back EMF and the magnitude of the peak voltage. However, the degraded capacitors apparently had no effect on average acceleration to peak velocity and the magnitude of the peak "steady-state" torque.

3.3.5.5 Effect of Refurbishment

Full scram tests were run on CRDOA 44 prior to refurbishment, after refurbishment of the motor only, and after refurbishment of the motor and reduction gear mechanism. A summary of test results is given in Table 3.3-4. Appendix F contains plots of Back EMF voltage versus time, frequency versus time, and torque versus time for each test listed in Table 3.3-4.

Table 3.3-2

TEST COMPARISON*

CRDOA Number	Test Date	Peak Back EMF (Volts)	Time to Peak (Seconds)	Peak Velocity (Radians/Second)	Time to Peak (Seconds)	Average Acceleration to Peak Velocity (Radians/Second^2)	Peak "Steady-State" Torque (Inch-Ounces)
3	8-17-84	223	3.059	303	2.962	98	5.35
	10-02-84	221	3.141	301	3.054	95	6.20
	11-19-84	224	2.988	301	2.901	101	5.09
8	8-16-84	219	3.412	292	3.322	88	29.9
	9-19-84	225	3.307	295	3.197	92	34.8
	11-01-84	204	3.964	283	3.838	74	37.2
	11-02-84	214	3.696	289	3.594	72	27.5
	11-05-84	204	3.691	283	3.587	77	16.9
	11-05-84	203	3.678	282	3.552	76	20.7
	11-06-84	210	3.777	287	3.674	79	17.5
	11-06-84	213	3.641	288	3.550	78	17.0
10	8-16-84	207	2.415	283	2.323	124	3.51
	10-03-84	212	2.472	285	2.380	121	3.97

*All tests in-core

Table 3.3-3

EFFECT OF CAPACITANCE VARIATION*

CRDOA Number	Average Capacitance	Peak Back EMF (Volts)	Time to Peak (Seconds)	Peak Velocity (Radians/Second)	Time to Peak (Seconds)	Average Acceleration to Peak Velocity (Radians/Second^2)	Peak "Steady-State" Torque (Inch-Ounces)	Date
1	42 micro F	199	2.932	280	2.839	102	4.93	1-12-85
1	45 micro F	194	2.946	276	2.840	101	3.91	1-15-85
10	40 micro F	210	2.494	280	2.412	121	3.31	1-4-85
10	45 micro F	202	2.387	269	2.303	121	3.06	1-4-85
12	44 micro F	228	2.694	297	2.627	110	4.39	1-7-85
12	45 micro F	225	2.666	292	2.587	110	4.84	1-7-85
30	40 micro F	207	2.598	279	2.515	112	4.41	1-10-85
30	45 micro F	203	2.537	271	2.453	111	3.50	1-12-85
31	45 micro F**	211	2.530	285	2.450	116	3.89	1-4-85
31	45 micro F	201	2.442	275	2.359	117	3.88	1-5-85

* All tests in-core
** Ranged from 42 to 50 micro F

Table 3.3-4

EFFECT OF REFURBISHMENT - CRDOA 44*

Test Date	Peak Back EMF (Volts)	Time to Peak (Seconds)	Peak Velocity (Radians/Second)	Time to Peak (Seconds)	Average Acceleration to Peak Velocity (Radians/Second^2)	Peak "Steady State" Torque (Inch-Ounces)	Comments
8-06-84	191	5.277	268	5.073	54	14.2	Prior to Refurbishment
8-08-84	210	2.82	283	2.726	109	10.0	After Motor Refurbishment
8-10-84	203	3.483	282	3.379	83	6.80	After Motor and Gear Refurbishment - Shim misplaced
8-10-84	180	4.278	272	4.135	65	6.99	After Motor and Gear Refurbishment - Shim misplaced
8-15-84	214	2.666	286	2.575	116	4.84	After Motor and Gear Refurbishment

*All tests listed were performed in Hot Service Facility

Performance of CRDOA 44 improved following refurbishment of the motor and improved further following reduction gear refurbishment. Average acceleration to peak velocity increased from 54 radians/second^2 prior to refurbishment to 109 radians/second^2 following motor refurbishment. Average acceleration further increased to 116 radians/second^2 following refurbishment and proper reassembly of the gear train. Peak "steady-state" torque also showed a marked decrease, going from 14.2 inch-ounces prior to refurbishment to 10.0 inch-ounces following refurbishment of the motor and 4.84 inch-ounces following completion of all refurbishment.

Plots of Fourier analyses of acceleration versus time data, taken during "steady-state" operation are also included. The plots are in various colors corresponding to the following CRDOA conditions:

- brown - as found
- turquoise - after motor refurbishment
- purple - after refurbishment of both motor and reduction gear mechanism

The magnitude of the predominant and background frequencies of the acceleration versus time waveform decreased following motor refurbishment. The magnitude of the predominant frequency decreased further following refurbishment of the reduction gear mechanism. This is not unexpected, since refurbishment should lower the friction induced torques on the rotor.

CRDOA 44 was returned to the core. Subsequent testing has indicated that it is retaining good performance characteristics.

CRDOA 7 was refurbished in August 1984. Table 3.3-5 shows the effect which refurbishment had on its performance. Following motor refurbishment, the acceleration to peak velocity increased and the peak "steady-state" torque decreased. Following refurbishment of the reduction gear mechanism, the performance of the CRDOA improved further, as indicated by these parameters.

Steady-state acceleration versus time data for CRDOA 7 obtained before refurbishment, after refurbishment of the motor only, and after refurbishment of the motor and gear train, was subjected to Fourier analysis. The purpose of the Fourier analysis was to identify the extent to which refurbishment of each reduction gear train component affected magnitude of the frequencies of the acceleration waveform which correspond to the operating frequencies of the first and second stage gears. The Fourier analysis plots of the "steady-state" acceleration versus time waveforms of the tests listed in Table 3.3-5 are included in Appendix F. The frequency of the first stage gear (4.1176 rps) and the second stage gear (0.5003 rps) are also indicated.

Prior to refurbishment, there was a predominant component at approximately 3.0 Hertz. This component corresponds to the frequency of oscillation observed in the acceleration versus time curves of all of the CRDOAs and is thought to be caused by the interaction of the driving torque on the rotor (the weight of the control rod pairs) with the dynamic braking torque. There was also another significant component at approximately 0.5 Hertz, which corresponds to the second stage gear frequency.

The Fourier analysis of the acceleration versus time waveform for CRDOA 7 following motor refurbishment shows no change in the magnitude of the 3.0 Hertz or the 0.5 Hertz component; a reduction in other background frequencies

Table 3.3-5

PERFORMANCE DEGRADATION - CRCOA 7

Test Date	Test Location (Core Region or in Hot Service Facility)	Peak Back EMF (Volts)	Time to Peak (Seconds)	Peak Velocity (Radians/Second)	Time to Peak (Seconds)	Average Acceleration to Peak Velocity Radians/Second^2)	Peak "Steady - State Torque (Inch-Ounces)	Comments
8-23-84	HSF	191	3.309	276	3.214	89	10.03	Prior to Refurbishment
8-24-84	HSF	196	2.954	274	2.835	97	8.08	After Motor Refurbishment
8-25-84	HSF	196	2.737	273	2.641	103	6.06	After Motor and Gear Train Refurbishment
10-02-84	37	188	3.364	269	3.255	83	9.96	
11-20-84	37	191	3.135	269	3.026	88	9.95	
11-23-84	37	201	3.172	275	3.076	87	10.47	
1-19-85	37	191	3.240	267	3.130	87	9.52	

is indicated by the plot, however. Following refurbishment of the reduction gear mechanism, the Fourier analyses of the acceleration versus time waveform shows a significant reduction in the magnitude of the 3.0 Hertz component, a small reduction in the magnitude of the 0.5 Hertz component, and a rise to prominence of a 4.1 Hertz component, which corresponds with the frequency of the first stage gear. This was not see in an analysis of the acceleration versus time waveform performed on CRDOA 44 following refurbishment.

CRDOA 7 was returned to the core. When tested in subsequent months, it has shown noticeable performance degradation. Average acceleration to peak velocity has decreased, and peak "steady-state" torques have increased. The Fourier plots of acceleration versus time data from the subsequent tests show that the 0.5, 3.0 and 4.1 Hertz components have all increased in magnitude.

The Fourier analyses described above for CRDOAs 7 and 44 suggest that it may be possible to detect degraded components in the reduction gear mechanism by examining the frequency components of the acceleration versus time waveforms. This hypothesis will be further investigated as CRDOA 7 and additional CRDOAs are disassembled, the condition of their reduction gear mechanisms is determined, and post refurbishment data collected and analyzed.

3.3.6 Uncertainties

Calculated values of acceleration and torque on the motor rotor are based upon the rate of change of electrical frequency. Although it is apparent that electrical frequency in an induction generator is established by the angular velocity of the rotor, there may be a "slip" between the electrical and mechanical frequencies; mechanical frequency or angular velocity may exceed electrical frequency. If this were the case, then actual accelerations and torques on the rotor would be greater than the calculated values.

A test was performed in which the electrical frequency and rotor angular velocity were simultaneously measured, as described in Section 3.4. The results indicate that there is a very close correlation between electrical frequency and the angular velocity for the rotor. Therefore, if there is a very small slip between the angular velocity of the rotor and the electrical frequency, it cannot be measured and will have no impact on the development of a refurbished CRDOA acceptance criteria.

Another uncertainty involves the relationship between rolling friction-induced torques and breakaway friction-induced torques experienced during startup and operation. If breakaway friction torques were higher than rolling torque, then calculated friction-induced accelerations and torques made during "steady-state" conditions following dynamic braking would not necessarily be indicative of the friction-induced torques which a motor bearing might have to overcome when starting from standstill.

The frequency versus time curves provide some indication that rolling friction-induced torques are not substantially smaller than breakaway friction torques. If the breakaway torque caused a substantial delay in rotor rotation, the frequency versus time curve, if extended, would intersect the time axis at some point after time zero. If breakaway of the rotor was substantially delayed following a scram and calculated peak torques were of small or moderate magnitude, then it might be concluded that breakaway torques were substantially larger than rolling friction-induced torques. Such a delay

is observed in very few of the frequency versus time plots. The frequency versus time plot for CRDOA 8 fcr a test conducted on November 1, 1984, shows a delay in breakaway (See curve in Appendix B). The calculated peak torque for this run is 17.4 inch-ounces, which would indicate that high magnitude torques were also present during the "steady-state" portion of the scram. Additional tests are planned as part of the motor bearing test series, described in Section 3.5.2.1, the purpose of which will be to determine a relationship between breakaway and rolling friction-induced torques. The feasibility of conducting tests to identify holding torques during the refurbishment program is being investigated.

It is uncertain whether the low frequency oscillation that is observable in some acceleration and torque versus time curves has any effect on a motor when scram is initiated. If the oscillation is caused by the interaction between torques applied by the dynamic brake and those due to the weight of the control rod pairs, then the oscillatory torques probably do not affect the rotor prior to when synchronous speed is attained and the dynamic brake is actuated. However, if the oscillations were related to the performance of the reduction gear mechanism, then the oscillations would affect the magnitude of the breakaway torque. Further investigation of the oscillatory acceleration phenomenon will be conducted during CRDOA refurbishment. This information is needed to refine the proposed refurbishment acceptance criteria set forth in Section 4.1.3.

The torques typically measured during steady-state operation of even the worst performing CRDOA will not stop the scram. It is only these same torques when applied to the rotor at startup that are of concern in assessing the operability of a CRDOA. Therefore, the component of torque due to the low frequency oscillation possibly should be taken out of the calculated torques when assessing CRDOA operability.

The Fourier analyses which have been performed on the steady-state acceleration versus time data can identify the predominant frequency of the underlying oscillatory sine wave in the acceleration and torque versus time curves. Efforts are continuing to further analyze the oscillatory phenomenon. Its effects have not been taken out of the calculations of peak torque.

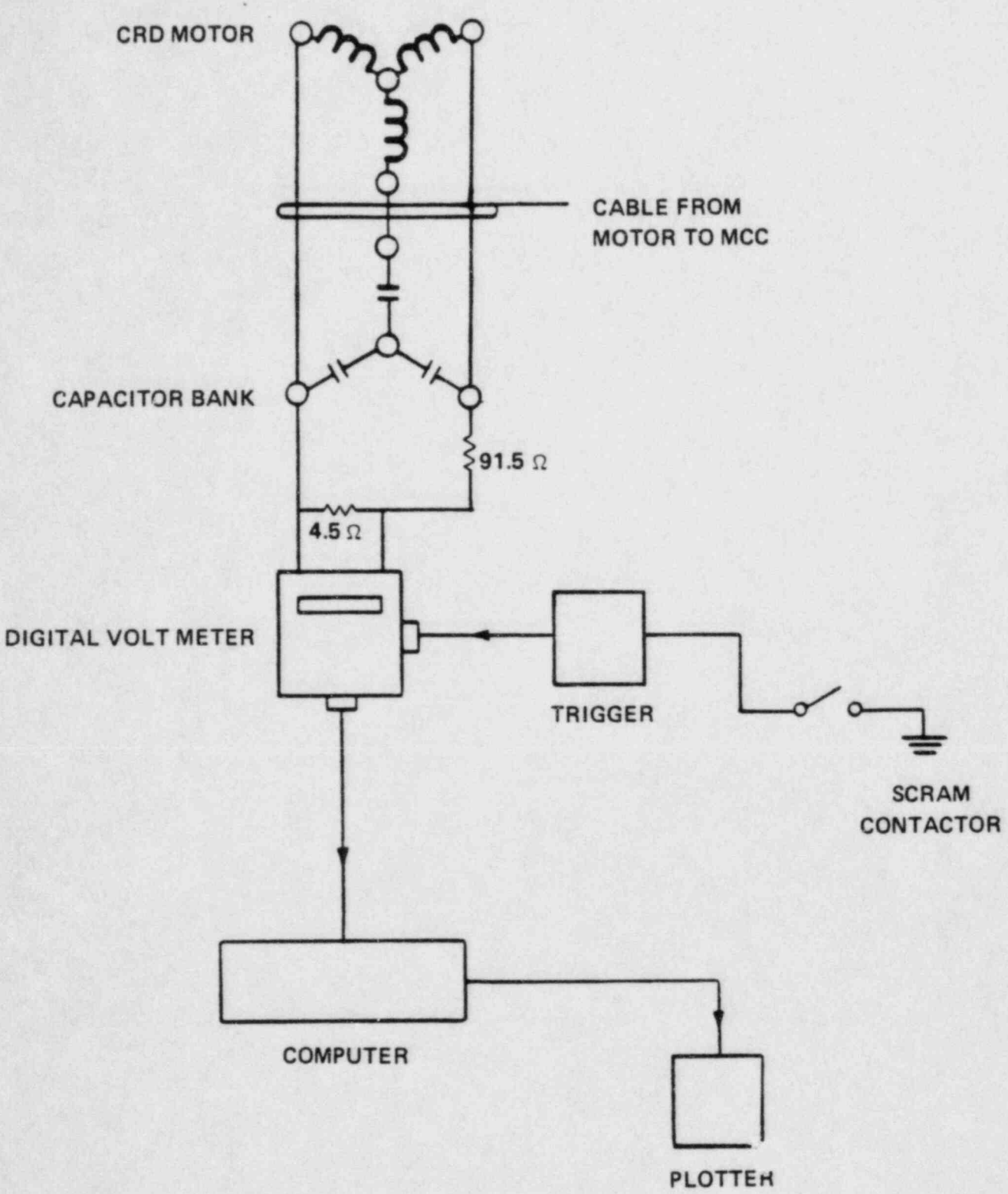

CRD BACK EMF
TEST CONFIGURATION
FIGURE 3.3-1

3.4 ROTOR ANGULAR VELOCITY MEASUREMENTS

3.4.1 Purpose

The purpose of measuring the angular velocity of the rotor, while at the same time measuring Back EMF voltage, was to determine the relationship between rotor angular velocity and Back EMF frequency. With this relationship known, an accurate correlation could be made between the rate of change of Back EMF electrical frequency and the actual acceleration (or friction-induced deceleration) and torque on the motor rotor.

3.4.2 Description of Test

On January 26, 1985, partial scram tests of CRDOA 27 were run in an equipment storage well. Measurements of Back EMF voltage were made with the digital voltmeter, as described in Section 3.3.2.

During these tests, a shaft encoder was used to measure rotor angular velocity. The shaft encoder was an Encoder Products Company Model 713-100-12 unit. It was connected to the motor rotor with a flexible shaft coupling and mounted on a bracket attached to the motor. The shaft encoder generated a 12 V dc pulse signal at the rate of 100 pulses per revolution.

The pulse signal was input to a pulse rate to analog converter. The converter was a Red Lion Controls Model PRA1-103-1/A unit with a full scale range adjustment of 3000 Hertz minimum to 10,000 Hertz maximum with a 0 to 10 V dc output. Response time, defined as the time required for the output to reach 90 percent of final value when the frequency is instantly changed from 0 to full scale, was 8 milliseconds. Ripple voltage for this unit should range from 0.25 V peak to peak at full scale to 0.50 V peak to peak at 10 percent of full scale output. A capacitor was used to reduce the magnitude of the ripple voltage. The accuracy or linearity of the converter was 0.25 percent of full range setting.

Output voltage from the pulse rate to analog converter was provided to a digital voltmeter, identical to the one used to measure Back EMF. Both digital voltmeters used in this test were simultaneously triggered by the scram contactor. Output from the voltmeters was stored on the Hewlett-Packard Model 220 computer and output plots of rpm versus time were made, as described in Section 3.3.2.

3.4.3 Conclusions

Appendix G contains a plot showing both the frequency of the Back EMF and the angular velocity of the rotor as measured by the shaft encoder. The values are almost indistinguishable, indicating that measurements of Back EMF voltage and frequency provide a very accurate indication of actual rotor angular velocity.

3.5 MOTOR BEARING TESTS AND ANALYSES

3.5.1 Purpose

3.5.1.1 Breakaway Torque Tests

Quantitative data concerning breakaway torque of new and used motor bearings

in a helium atmosphere at various humidity levels was obtained to determine which of the following were primary or contributing factors in the past failures of the CRDOAs to scram:

- humidity
- debris in bearing races
- wear

3.5.1.2 Bearing Debris Analyses

Debris in the motor bearings was analyzed to determine its source. This analyses was done to provide evidence to substantiate or disprove the theory that humidity levels had become high enough in the area of the CRDOAs to cause debris from the housing to be washed into the bearings by moisture condensing in the vicinity of the bearings.

3.5.2 Description of Tests

3.5.2.1 Breakaway Torque Tests

The breakaway torque tests were run beginning in November 1984 in the Mechanical Engineering Department of Colorado State University. Results are summarized in References 3 and 4.

Reference 3 describes breakaway torque tests performed on a new bearing (Serial Number 15) and a refurbished used bearing (Serial Number 126). Breakaway torque measurements were obtained in a helium environment at relative humidity ranging from under 10 percent to over 90 percent. Average breakaway torque increased at high humidity for both bearings, although never exceeding 1.0 inch-ounce. It was also observed that the average breakaway torque depends to a small degree upon the position of the inner race in relation to the outer race.

Reference 4 describes additional breakaway torque tests performed on three unrefurbished bearings (Serial Numbers 003, 076, and 086). The measured breakaway torques were significantly higher than for the new and refurbished bearings, with the highest value measured being 3.2 inch-ounces. No evidence of any systematic influence of relative humidity on breakaway torque was observed. It was again observed that the average breakaway torque is dependent upon the position of the inner race in relation to the outer race.

3.5.2.2 Bearing Debris Analysis

Several samples of the bearing cleaning solution were analyzed. It was subsequently discovered that the samples were contaminated by the cleaning solution itself. The cleaning solution may have masked the results somewhat, but the analysis still indicates that all but two of the major constituents can be attributed to the bearing materials. The two exceptions are lead and tin which were the major contaminants in the cleaning solution. Two samples from CRDOAs 44 and 7 were cleaned using a solution which did not contaminate the samples. This also verified that the major debris constituents could all be attributed to the materials of the bearing construction. Some of the minor constituents, such as flourine, titanium, and tungsten, were identified by the motor manufacturer as being constituents or contaminants which could be attributed to the motor.

Due to the method of acquisition and the quantity of material available, it was determined that a meaningful bearing debris particulate size analysis could not be performed. However, some relative idea of particulate size was obtained by filtering the debris solution. A one-half micron filter successfully removed the particulate from solution. While this filter does not provide the exact measurement of the particulate involved, it does provide a general indication of size. Approximately one (1) gram of particulate is required for Fisher Subsize Sieve testing. Since only extremely small quantities are obtained from the cleaning solution, a meaningful particle size analysis test could not be performed. In an attempt to determine if there was any adhered particulate on the surface of the bearing race and the general condition of the race, a scanning electron microscope (SEM) analysis was performed. The SEM was performed on the inner race of CRDOA 37 motor bearing. The SEM did not identify any particulate adhesion and only minor surface wear was detected.

The chemical composition and particle size of the general CRDOA housing debris was also analyzed. In most cases, any appreciable amount of debris that was obtained had to be scraped off of the housing. The chemical analysis indicates that the scrapings and dust were essentially rust with a high content of sodium and boron. Rust flakes, scraped off the ring gear pinion housing of CRDOA 18, were approximately 0.0625 to 0.125 inches in size. However, the average particle size in this sample appears to be approximately 0.02 inches and the debris is relatively uniform in size. Although this sample has not been chemically analyzed, it appears to consist of rust, molybdenum disulfide, and a few silicon particles.

Subsequent to chemical analysis, the remaining sample of CRDOA 44 was examined utilizing a stereomicroscope at 165x. The largest particle found by this method was approximately 0.003 inches. A SEM analysis was then performed on the same CRDOA 44 housing debris. The average particle size was 0.003 inches. The largest particle found was approximately 0.009 inches.

3.5.3 Conclusions

There is evidence that an increase in humidity can be correlated to slight increase in breakaway torque. Effects are less than would be attributable to change in orientation of inner race to outer race of motor bearings, however. Therefore, humidity is presumed not to be the cause of failure.

Bearing debris analyses were performed in an attempt to prove or disprove the theory that the failure of the six CRDOAs to scram resulted from moisture washing foreign particulate matter into the races of the CRDOA shim motor bearings. Since there is a high concentration of sodium and/or boron found on the housing adjacent to the shim motor, if a transport mechanism existed, these constituents should be found in the bearing debris analysis. Sodium is present on the housing due to the leaching of the black oxide coating on the CRDOA gear train. The boron is leached from the biological shield. Since large quantities of sodium and/or boron were not found in the bearing debris samples, the wash-in theory was not supported. Therefore, the CRDOA rust has been discounted as a potential cause of the June 23, 1984, failure to scram. However, the internally generated CRDOA bearing debris can not be discounted as the potential cause of the scram failures.

3.6 REFERENCES FOR SECTION 3

1. Gulf General Atomic. PSC Control Rod Drive - Motor Wattage Limits for Operable Drives, Gulf P-900-141, Experimental Engineering Report Number 1971 - 5, June 25, 1971.

2. Gulf General Atomic. PSC Control Rod Drive - Affect of Frictional Drag at Drive Motor on Control Rod Drop Time, Gulf P-900-148, Experimental Engineering Report Number 1971-8, November 10, 1971.

3. Shakerin, Said and Loehrke, Richard. Control Rod Drive Shim Motor Bearing Tests, Technical Report HT-PSB841, November 1984.

4. Memo, Said Shakerin and Richard Loehrke (Colorado State University) to R.L. Craun (Public Service Company of Colorado), January 9, 1985.

SECTION 4

REMEDIAL ACTIONS

4.1 MOTOR AND REDUCTION GEAR MECHANISM REFURBISHMENT

4.1.1 Purpose

The purpose of refurbishing all of the CRDM motors and reduction gear mechanisms is to provide a margin of safety which will ensure that the CRDOAs will function properly during an interim period in which the final operating surveillance procedures and acceptance criteria are developed. Refurbishment in conjunction with a testing program will ensure the ability to scram until development of final acceptance criteria.

4.1.2 Procedures and Tests

All of the CRDOAs will undergo refurbishment and testing as described below. Back EMF measurements will be made with the digital voltmeter and printouts of voltage versus time, frequency versus time, and torque versus time will be generated for each full scram test conducted before, during, and after refurbishment.

Prior to refurbishment, an in-core full scram test will be run for each CRDOA. The CRDOA will then be taken to the hot service facility where another full scram test will be run. The control rod pairs will then be removed. The remainder of the CRDOA (200 Assembly) will be taken to an equipment storage well.

The 200 Assembly will be refurbished while in the equipment storage well. Details of the refurbishment will be provided in a separate report.

The reduction gear mechanism will be refurbished and a scram test performed using 120 pound dummy weights. The motor will then be removed, a standardized test motor installed, and another full scram test performed with the dummy weights. The motor will be refurbished, the test motor removed, and the refurbished motor reinstalled. The refurbished 200 assembly will then be subjected to a scram test using the dummy weights.

The 200 Assembly will be taken back to the hot service facility where the CRDOA will be reassembled. New Inconel cable will be used to attach the control rod pairs to the cable drum. A full scram test will be performed in the hot service facility. If feasible, measurements of the holding torque will be made. The CRDOA will then be returned to the core, where a full scram test will be performed.

4.1.3 Refurbishment Acceptance Criteria

Refurbishment acceptance criteria have been proposed taking into account the results of the Back EMF voltage measurements and calculations performed to date. These criteria classify all CRDOAs which have failed to scram either during operation or testing as unacceptable.

The performance characteristics of CRDOA 15 were substantially better than those of all other CRDOAs which have failed to scram. Accordingly, the acceptance criteria classifies CRDOA 15 as unacceptable. During the course of the refurbishment program, the cause of CRDOA 15's failure to scram may be determined to be different than that of the other CRDOA's. Use of a less restrictive refurbishment acceptance criteria then may be justifiable if recurrence of the failure mechanism is extremely improbable or if the failure mechanism may be identified through other means, such as Fourier analyses.

Final acceptance of a refurbished CRDOA will be based upon the results of its in-core full scram test. The following acceptance criteria for refurbished CRDOAs is proposed:

- minimum calculated average torque during acceleration to peak velocity of 17.0 inch-ounces; this value corresponds to an average acceleration to peak velocity of 98.83 radians/second^2
- maximum torque calculated during "steady-state" of 7.0 inch-ounces

Appendix H contains a graph showing the calculated average torques and peak "steady-state" torques for each full scram test performed as of January 26, 1985. The proposed acceptance criteria is indicated on the graph.

Following the graph is a list of CRDOAs which have been found not to meet the refurbishment acceptance criteria. A CRDOA is on this list if one or more times during the course of full scram testing its average torque during acceleration to peak velocity was less than 17.0 inch-ounces or its maximum torque calculated during "steady-state" was greater than 7.0 inch-ounces.

During the course of refurbishment, the data obtained from the full scram tests in-core, in the hot service facility, and the equipment storage well will be examined and analyzed in detail. Fourier analyses of the "steady-state" acceleration versus time waveforms will be conducted to determine the effect of gear refurbishment on the predominant waveforms. These analyses will be used to determine the quality and acceptability of the refurbishment process prior to completion of refurbishment of a CRDOA in the equipment storage well and hot service facility. Other measured and calculated values such as magnitude and time to peak of the Back EMF voltage and Fourier analyses of the voltage and acceleration versus time waveforms prior to steady state will be closely examined. This will be done in order to assist in evaluating the refurbishment and developing operating surveillance procedures.

4.2 RISE TO POWER TESTING

4.2.1 Purpose

The purpose of performing additional tests during rise to power is to determine the effect of operation at power on the performance of the CRDOAs. Based upon the tests performed to date, additional testing to be performed during refurbishment, and the tests performed while in-core at power, operating surveillance procedures and acceptance criteria will be developed and revised as necessary.

4.2.2 Procedures and Tests

A detailed program defining the rise to power testing program will be developed. This program will be submitted to the Nuclear Regulatory Commission prior to the resumption of operation.

4.3 OPERATING TESTS AND SURVEILLANCE PROCEDURES

4.3.1 Purpose

Tests and surveillance procedures will be developed for the purpose of determining the operability of the CRDOAs.

4.3.2 Procedures and Tests

An interim suveillance program has been developed and submitted in a separate report. An interim surveillance test procedure and acceptance criteria will be submitted to the Nuclear Regulatory Commission for review and approval prior to the resumption of operation.

Information concerning CRDOA performance obtained during refurbishment and operational testing is needed to deve˙p a final surveillance procedure and operational acceptance criteria. The stringent refurbishment criteria will ensure the operability of the CRDOAs in the interim period between startup with the preliminary acceptance criteria and development of the final acceptance criteria.

SECTION 5

SUMMARY

5.1 FAILURE MECHANISM

A variety of mechanisms which might explain the failure of the CRDOAs to function during scram have been investigated. Some have been eliminated from further consideration based upon qualitative analyses and quantitative testing.

Testing and analyses indicate that the failures to scram were caused by the physical degradation of moving parts in the motor bearings and reduced gear mechanism efficiencies. The net result was a lowering in torque applied to the motor rotor by the weight of the control rod pairs and an increase in friction-induced torques which opposed rotation of the rotor during scram.

5.2 REMEDIAL ACTIONS

All of the CRDOAs will be refurbished and tested. A refurbishment acceptance criteria has been proposed. This criteria will ensure that any degradation which might occur as a result of wear or deposition of debris on the moving parts of the CRDOA will not prevent operation of the reduction gear mechanism or rotation of the motor rotor during scram.

A plan for development of interim and final operational acceptance criteria has been proposed. Refurbishment of the CRDOAs will ensure operability of the CRDOAs while the final operational acceptance criteria is being developed.

APPENDIX A

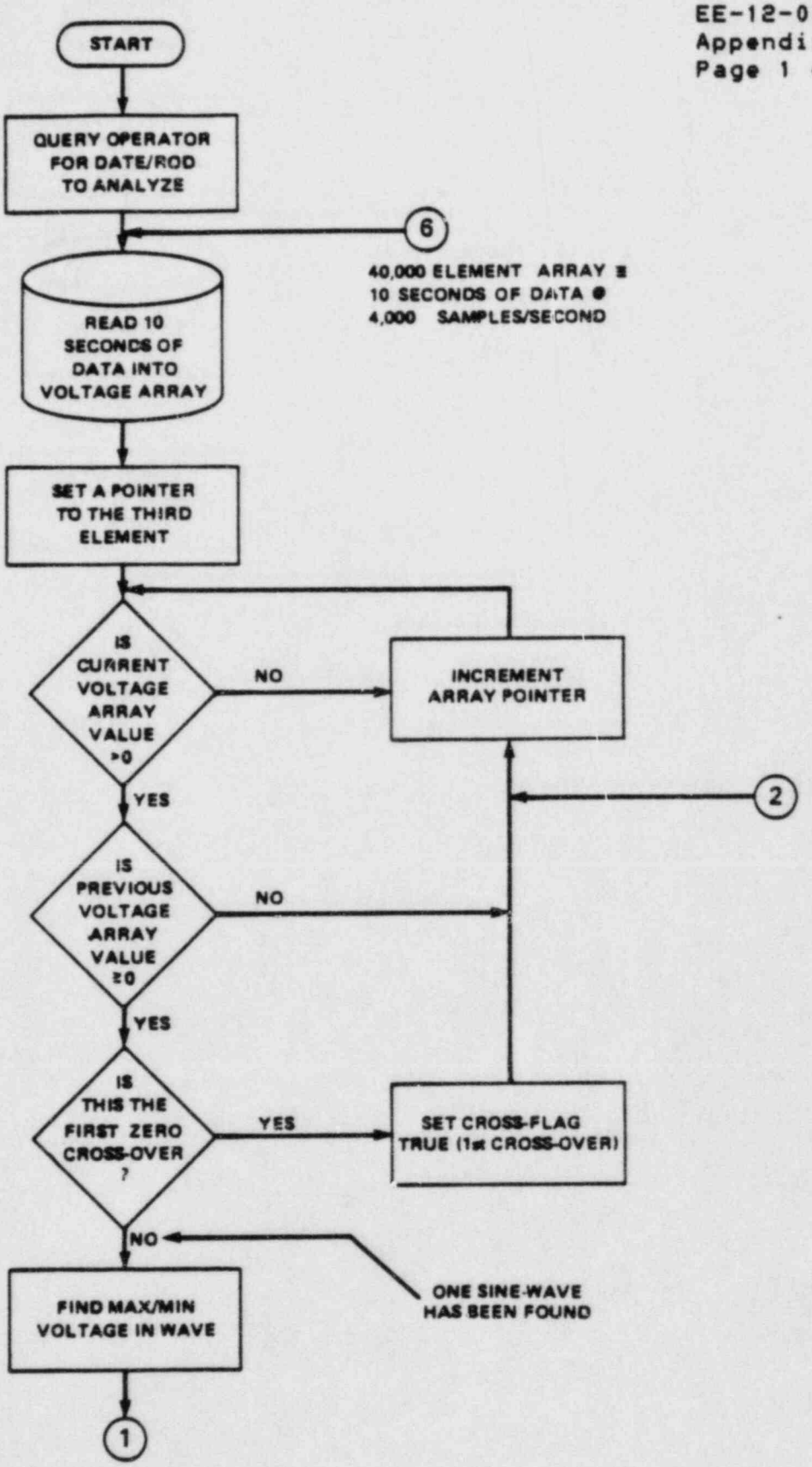

DATA ANALYSIS PROGRAM

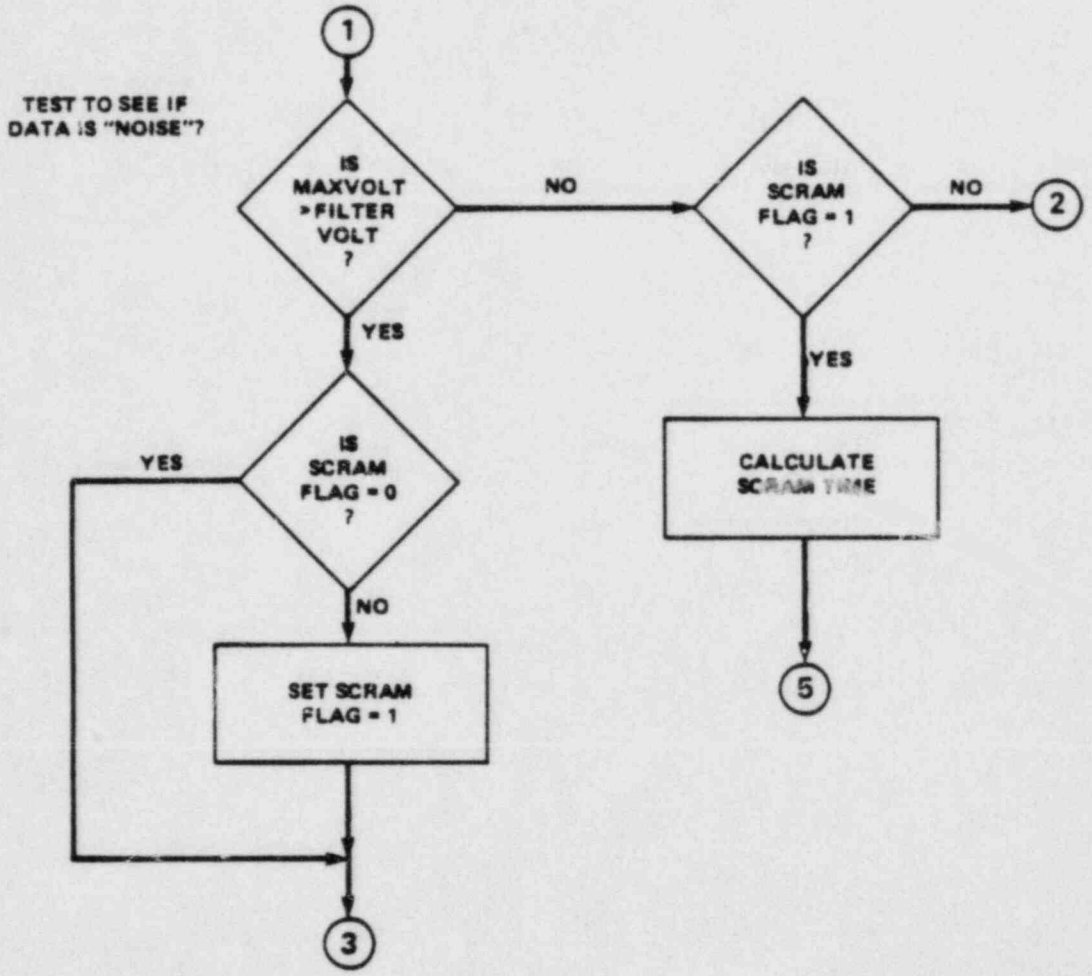
1
TEST TO SEE IF DATA IS "NOISE"?
IS MAXVOLT > FILTER VOLT ?
NO
IS SCRAM FLAG = 1 ?
NO
2
YES
YES
IS SCRAM FLAG = 0 ?
YES
CALCULATE SCRAM TIME
NO
SET SCRAM FLAG = 1
5
3

TEST TO SEE IF DATA IS NOT "NOISE"

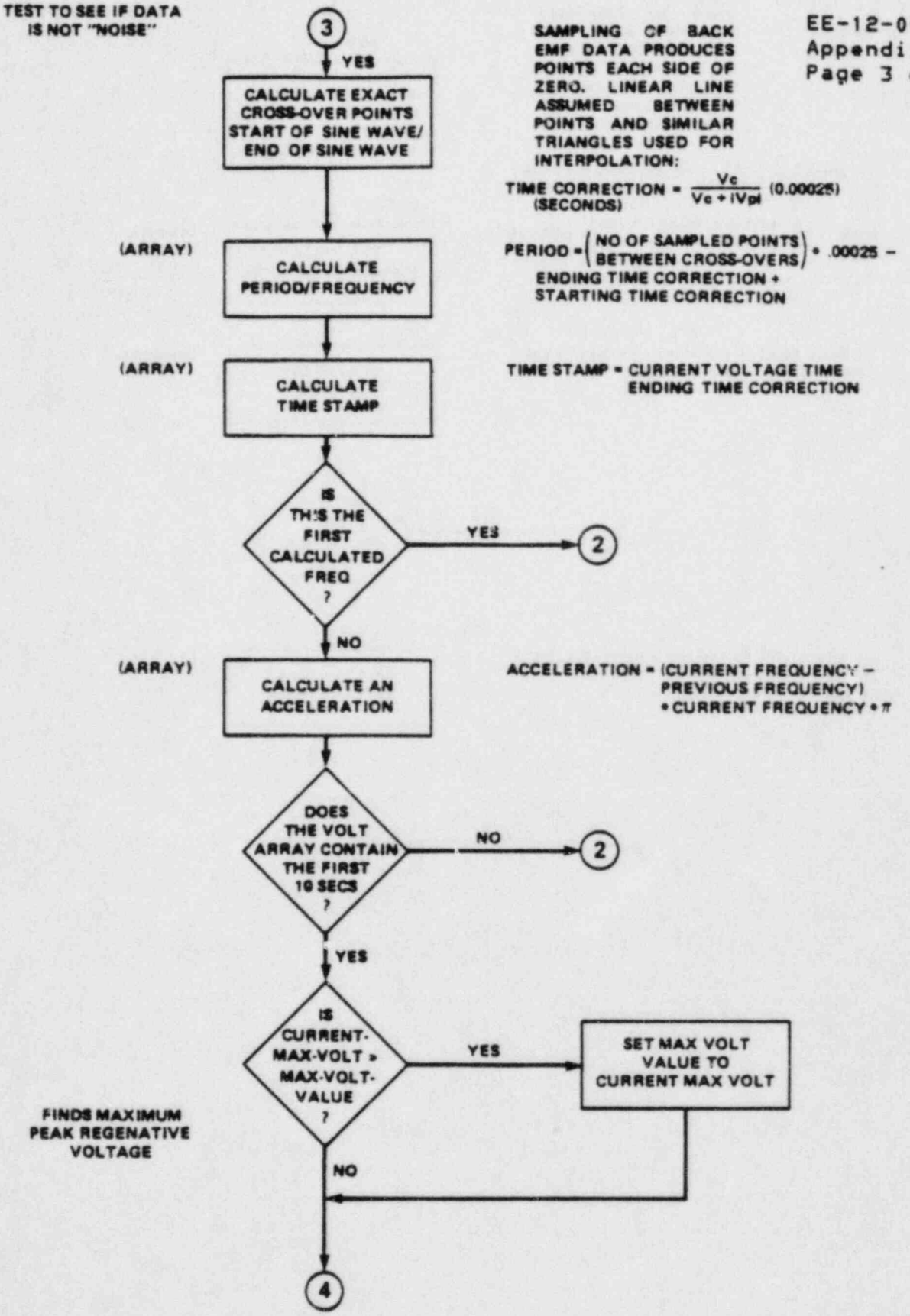

SAMPLING OF BACK EMF DATA PRODUCES POINTS EACH SIDE OF ZERO. LINEAR LINE ASSUMED BETWEEN POINTS AND SIMILAR TRIANGLES USED FOR INTERPOLATION:

$$\text{TIME CORRECTION (SECONDS)} = \frac{Vc}{Vc + |Vpl|}\ (0.00025)$$

$$\text{PERIOD} = \left(\frac{\text{NO OF SAMPLED POINTS}}{\text{BETWEEN CROSS-OVERS}}\right) * .00025 - \text{ENDING TIME CORRECTION} + \text{STARTING TIME CORRECTION}$$

TIME STAMP = CURRENT VOLTAGE TIME ENDING TIME CORRECTION

ACCELERATION = (CURRENT FREQUENCY − PREVIOUS FREQUENCY) * CURRENT FREQUENCY * π

FINDS MAXIMUM PEAK REGENATIVE VOLTAGE

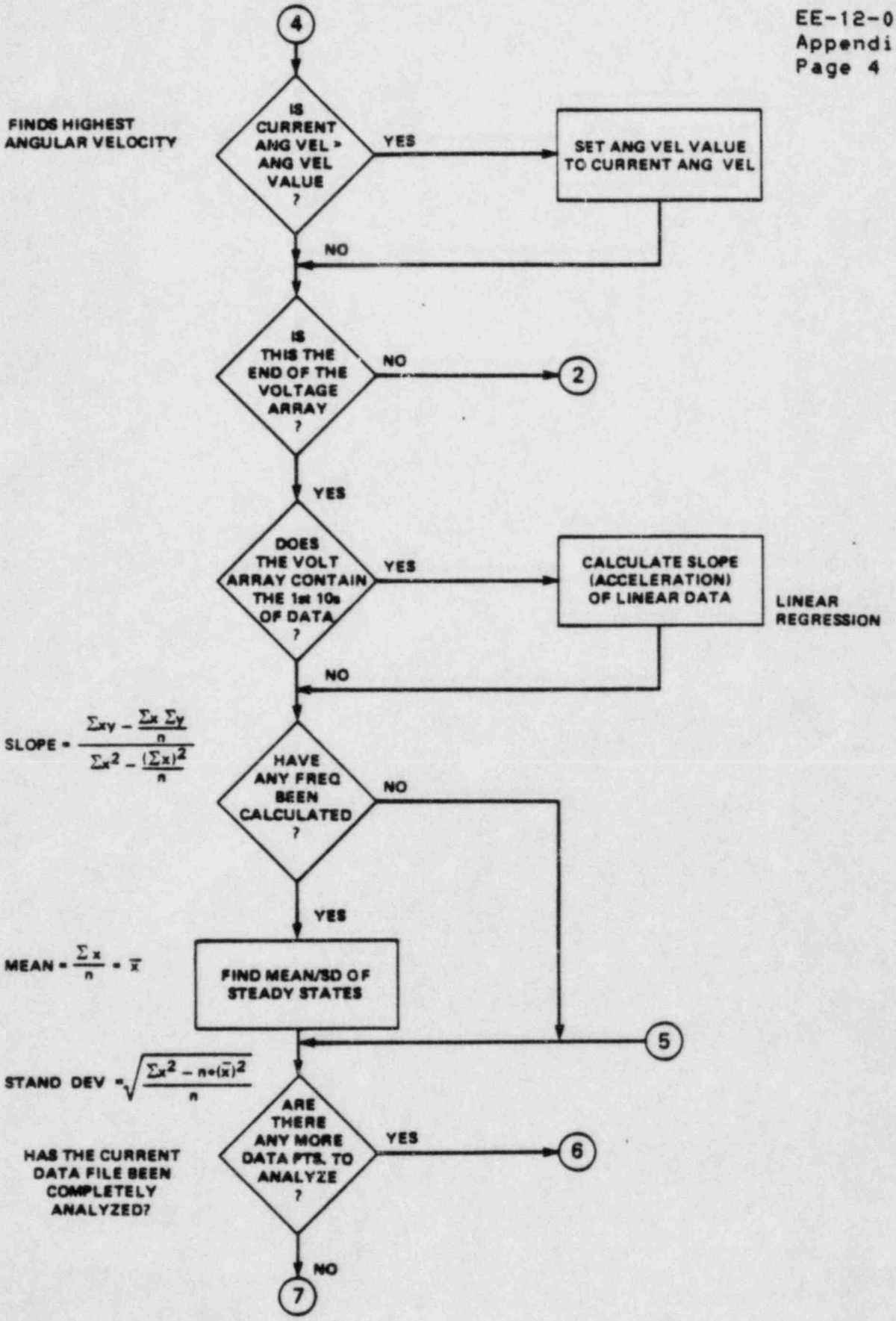
4
FINDS HIGHEST ANGULAR VELOCITY
IS CURRENT ANG VEL > ANG VEL VALUE ?
YES
SET ANG VEL VALUE TO CURRENT ANG VEL
NO
IS THIS THE END OF THE VOLTAGE ARRAY ?
NO
2
YES
DOES THE VOLT ARRAY CONTAIN THE 1st 10% OF DATA ?
YES
CALCULATE SLOPE (ACCELERATION) OF LINEAR DATA
LINEAR REGRESSION
NO
SLOPE = $\frac{\Sigma xy - \frac{\Sigma x \Sigma y}{n}}{\Sigma x^2 - \frac{(\Sigma x)^2}{n}}$
HAVE ANY FREQ BEEN CALCULATED ?
NO
YES
MEAN = $\frac{\Sigma x}{n} = \bar{x}$
FIND MEAN/SD OF STEADY STATES
5
STAND DEV = $\sqrt{\frac{\Sigma x^2 - n*(\bar{x})^2}{n}}$
HAS THE CURRENT DATA FILE BEEN COMPLETELY ANALYZED?
ARE THERE ANY MORE DATA PTS. TO ANALYZE ?
YES
6
NO
7

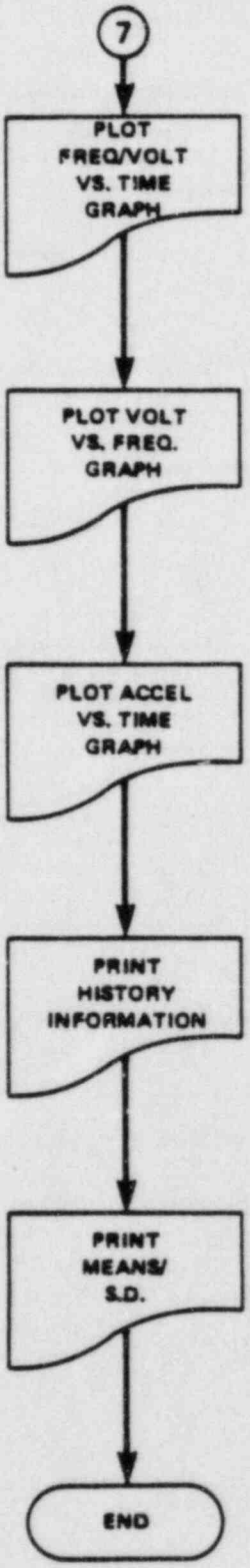
7
PLOT FREQ/VOLT VS. TIME GRAPH
PLOT VOLT VS. FREQ. GRAPH
PLOT ACCEL VS. TIME GRAPH
PRINT HISTORY INFORMATION
PRINT MEANS/ S.D.
END

APPENDIX B

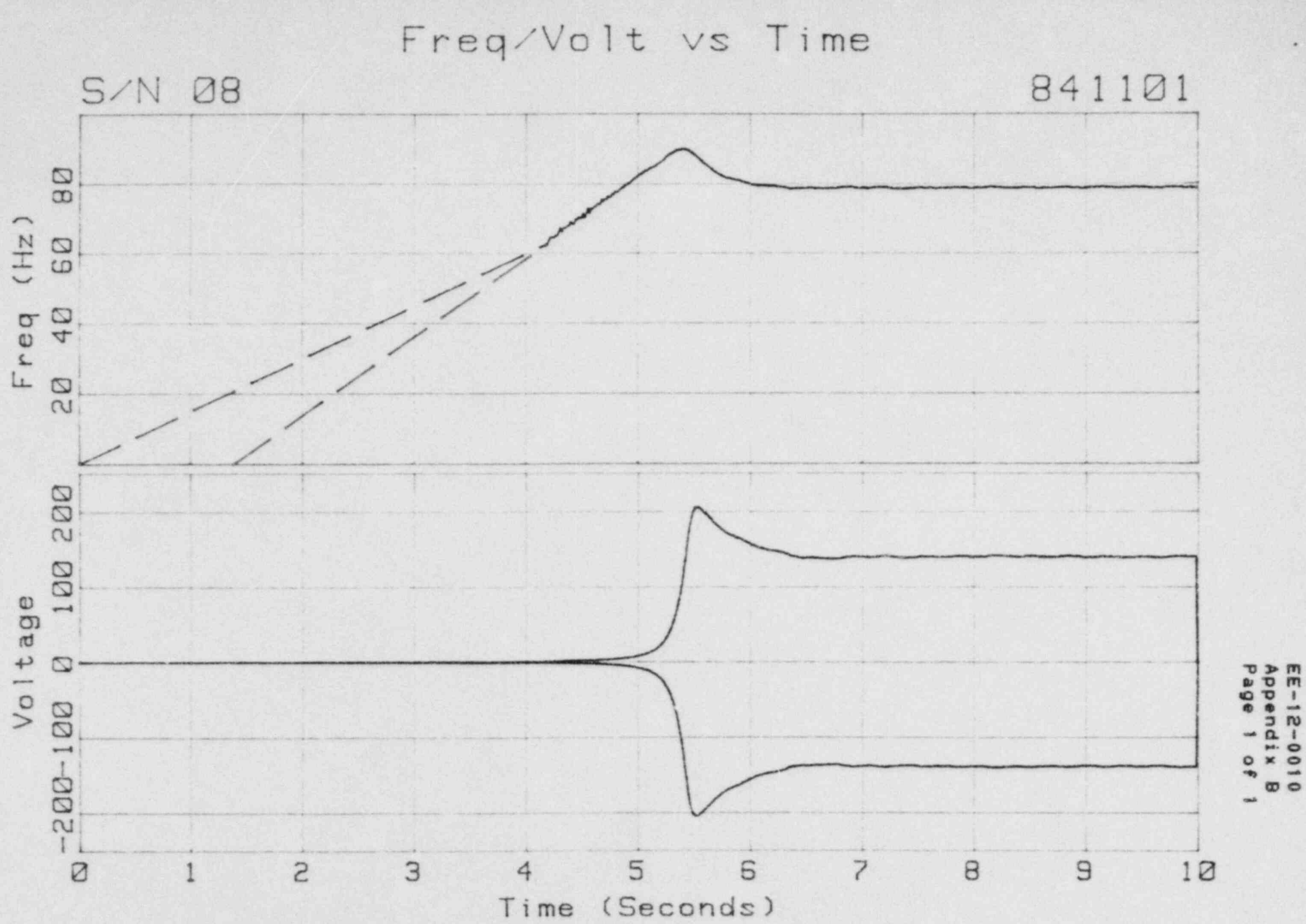
Freq/Volt vs Time
S/N 08
841101
Freq (Hz)
20 40 60 80
Voltage
-200 -100 0 100 200
0 1 2 3 4 5 6 7 8 9 10
Time (Seconds)

APPENDIX C


07840823
MAX @ 78
21.0
42.0
63.0
84.0
74.0
78.0
82.0
86.0

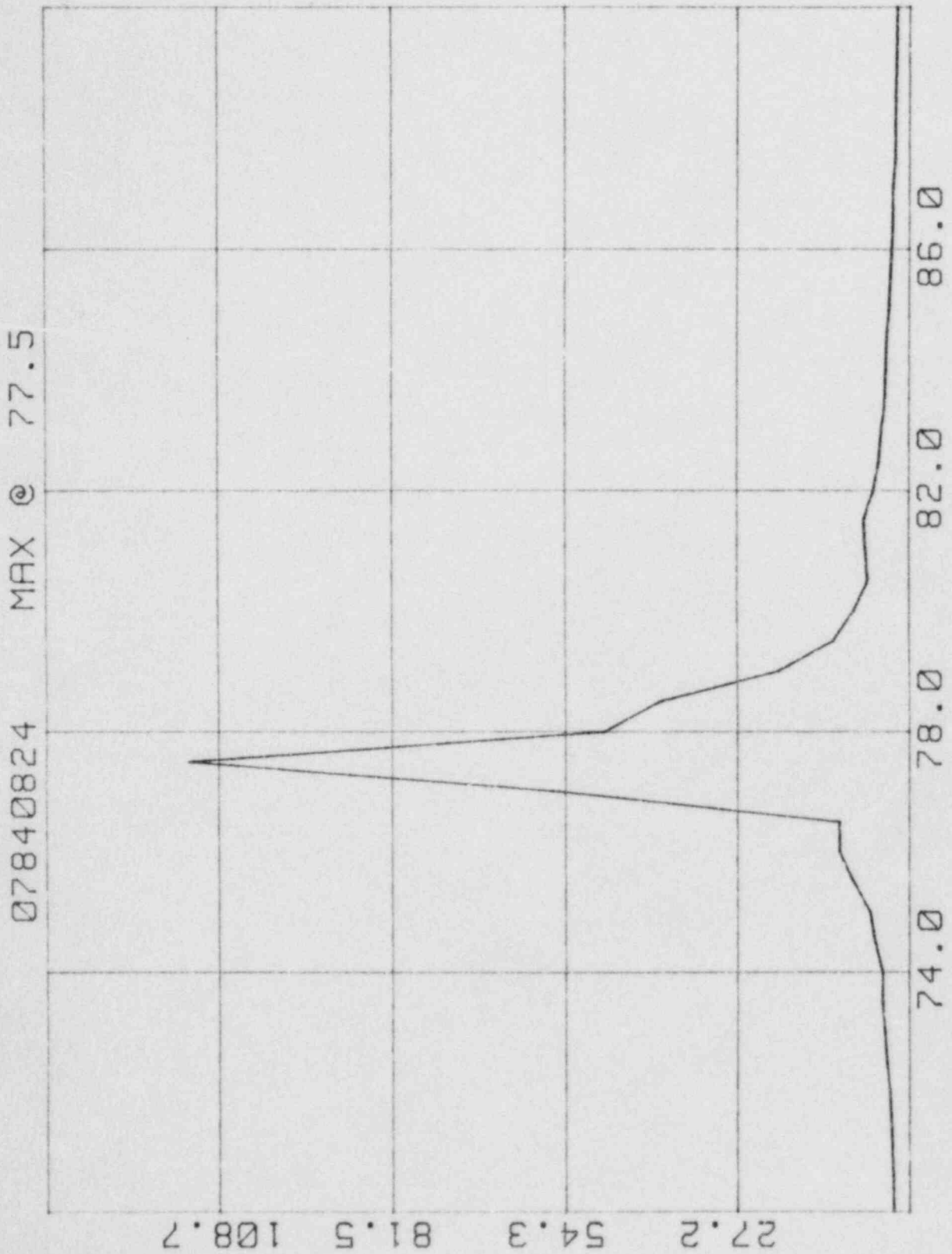
07840824
MAX @ 77.5
74.0
78.0
82.0
86.0
27.2
54.3
81.5
108.7

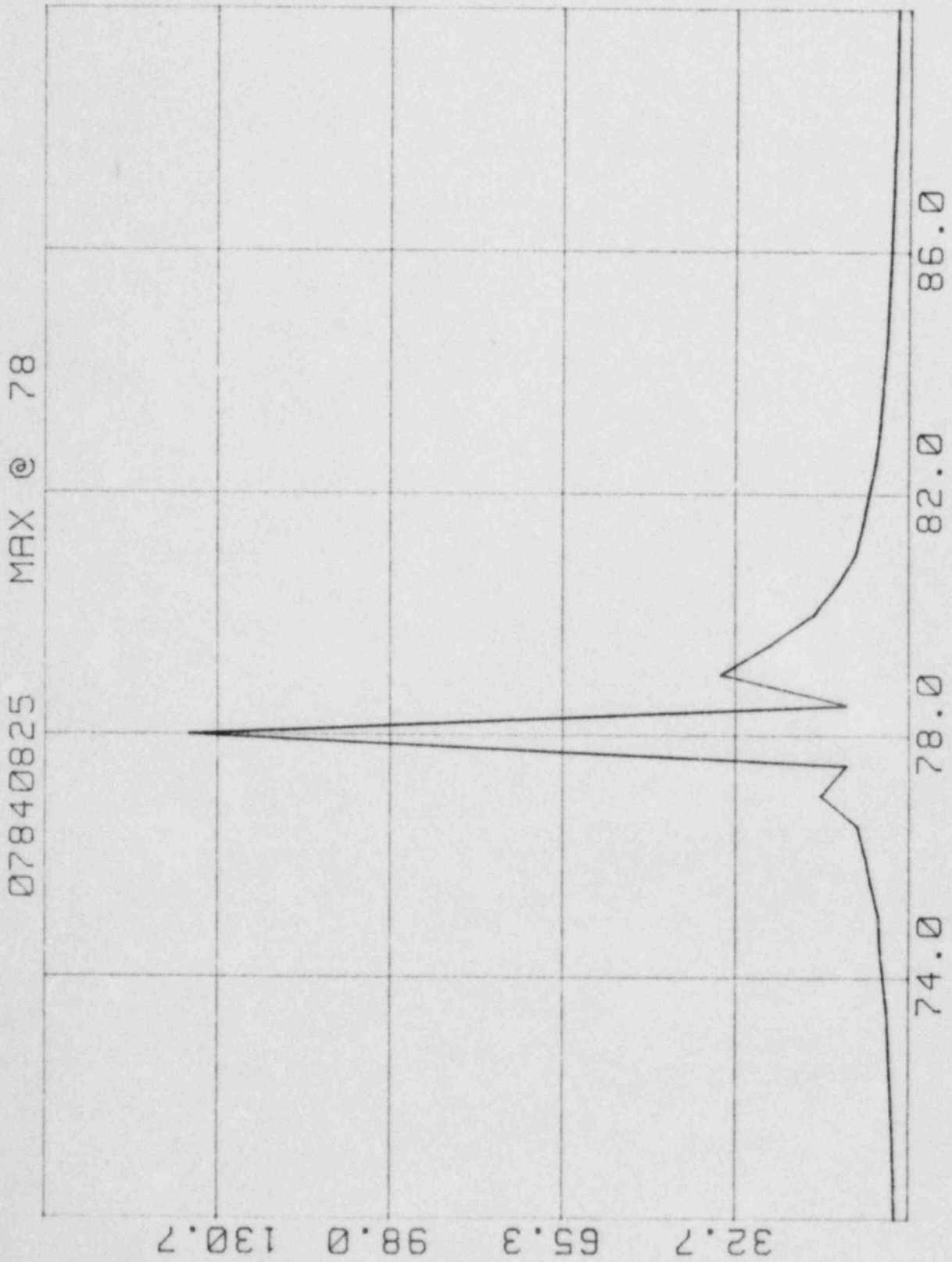
07840825
MAX @ 78
32.7
65.3
98.0
130.7
74.0
78.0
82.0
86.0

APPENDIX D

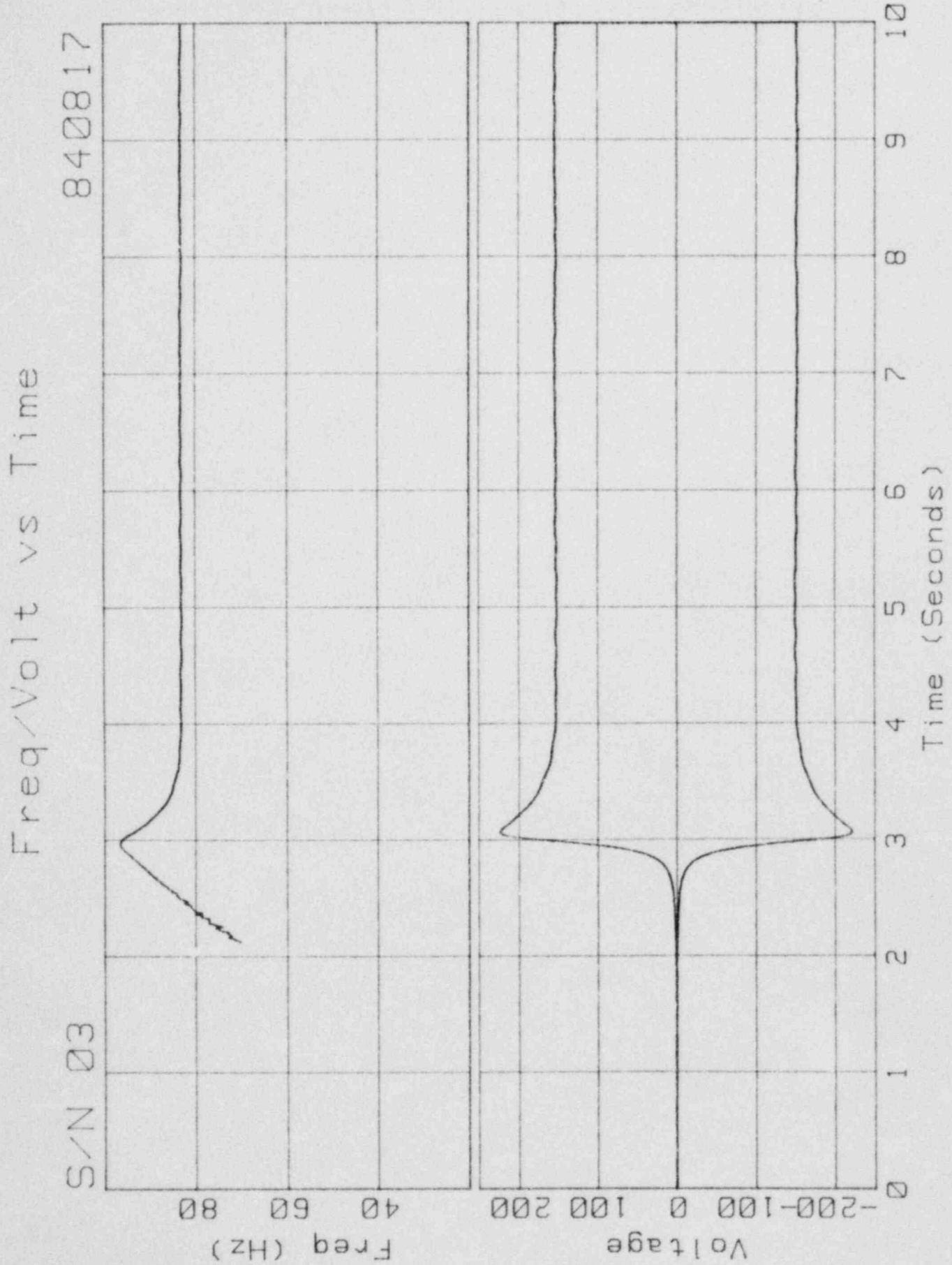
Freq/Volt vs Time
8408817
S/N 03
Freq (Hz)
40
60
80
Voltage
-200
-100
0
100
200
0
1
2
3
4
5
6
7
8
9
10
Time (Seconds)

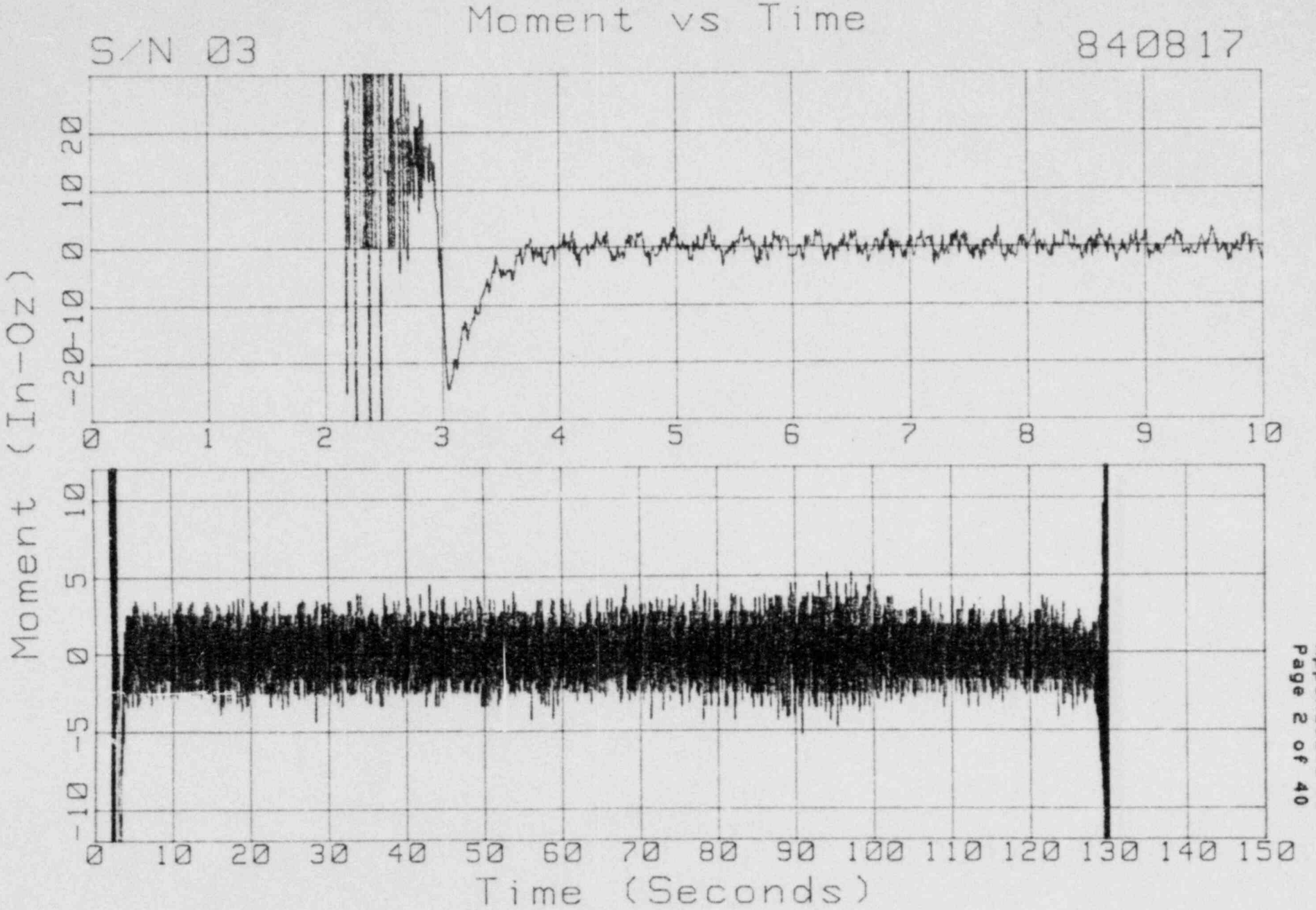
Moment vs Time
S/N 03
840817
Moment (In-Oz)
-20 -10 0 10 20
0 1 2 3 4 5 6 7 8 9 10
-10 -5 0 5 10
0 10 20 30 40 50 60 70 80 90 100 110 120 130 140 150
Time (Seconds)

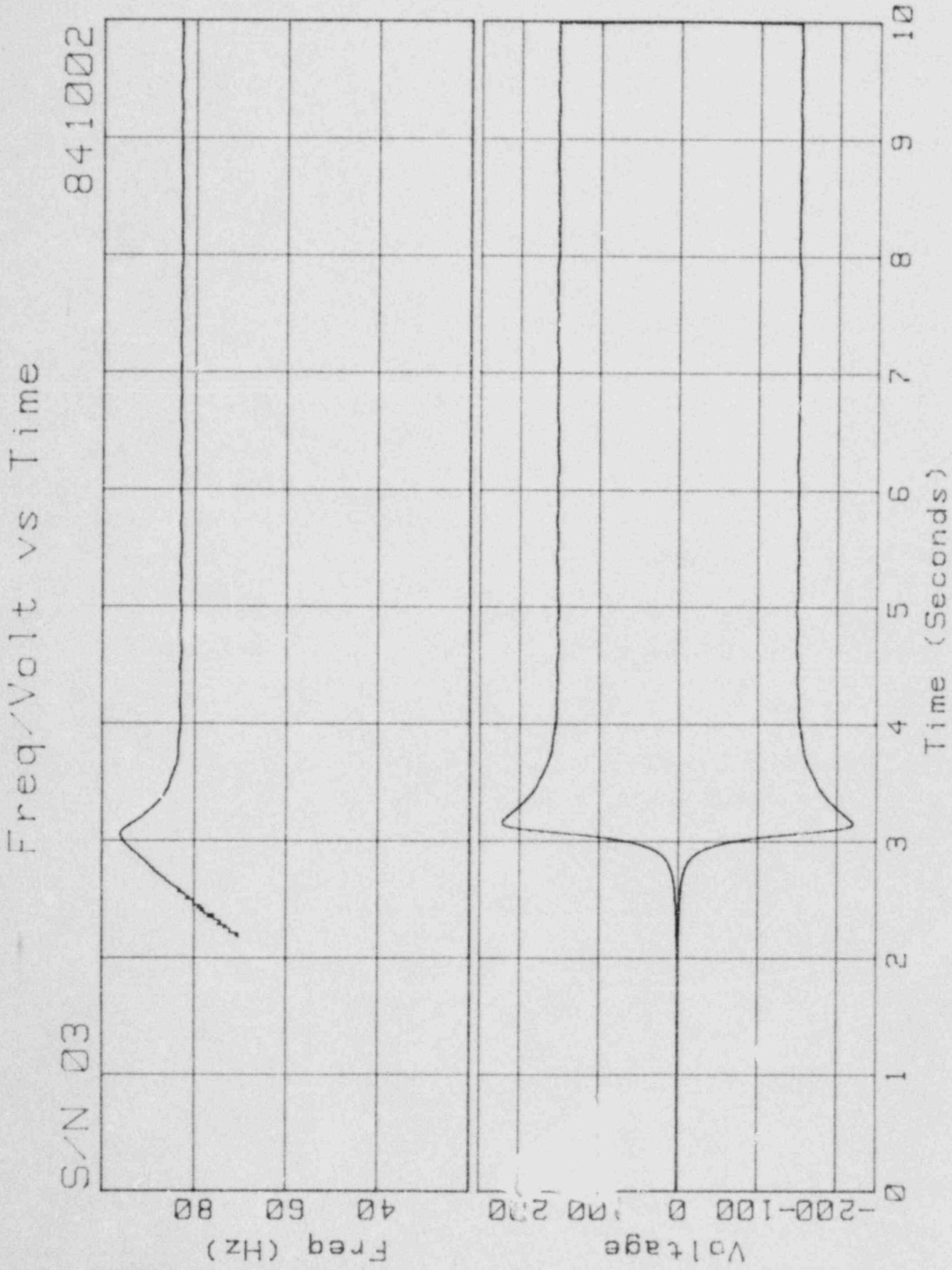
Freq/Volt vs Time
841002
S/N 03
Freq (Hz)
40
60
80
Voltage
-200
-100
0
100
200
0
1
2
3
4
5
6
7
8
9
10
Time (Seconds)

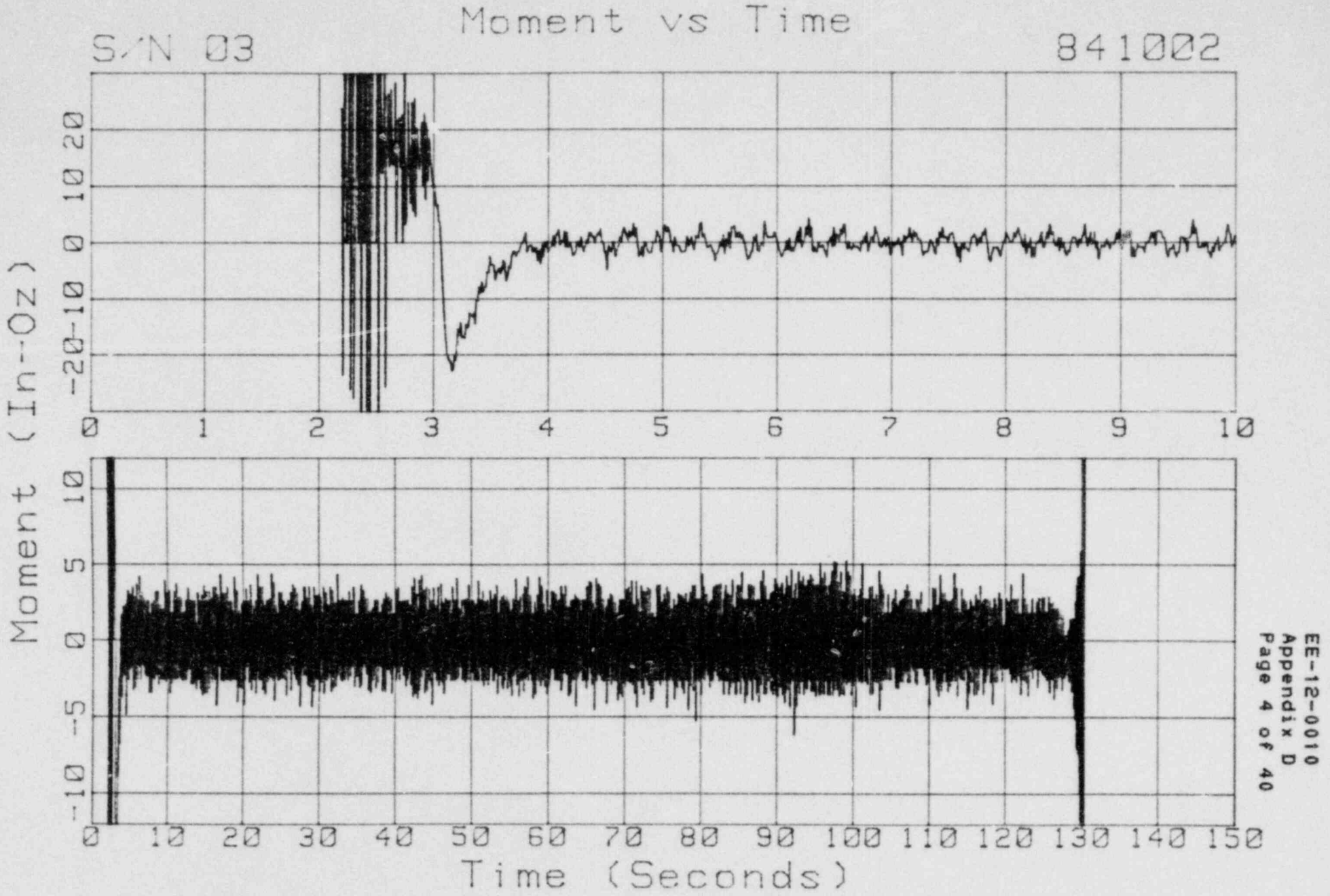
Moment vs Time
S/N 03
841002
Moment (In--Oz)
-20 -10 0 10 20
0 1 2 3 4 5 6 7 8 9 10
-10 -5 0 5 10
0 10 20 30 40 50 60 70 80 90 100 110 120 130 140 150
Time (Seconds)

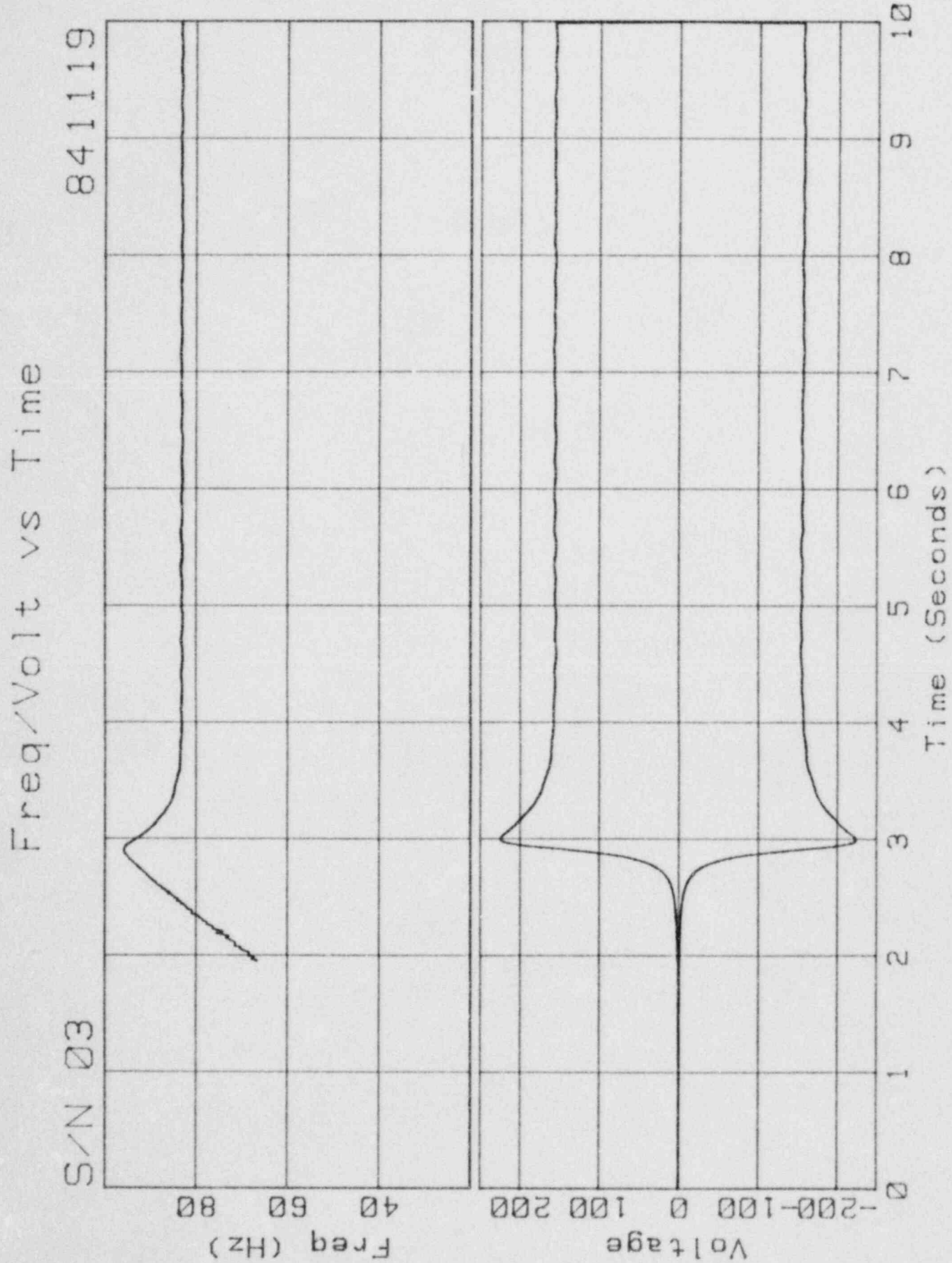
Freq/Volt vs Time
8411119
S/N 03
Freq (Hz)
40
60
80
Voltage
-200
-100
0
100
200
0
1
2
3
4
5
6
7
8
9
10
Time (Seconds)

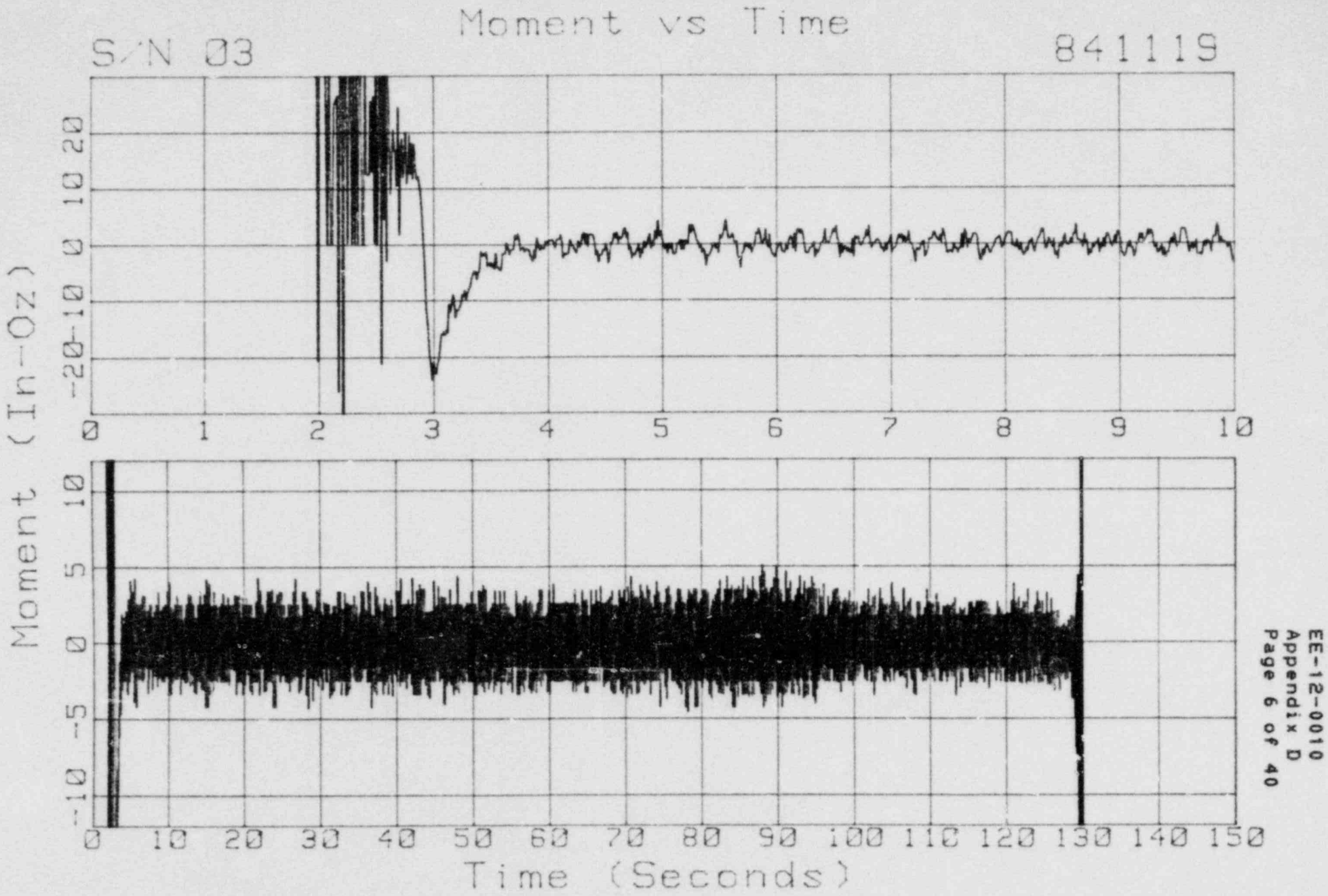
Moment vs Time
S/N 03
841119
Moment (In-Oz)
-20 -10 0 10 20
0 1 2 3 4 5 6 7 8 9 10
-10 -5 0 5 10
0 10 20 30 40 50 60 70 80 90 100 110 120 130 140 150
Time (Seconds)

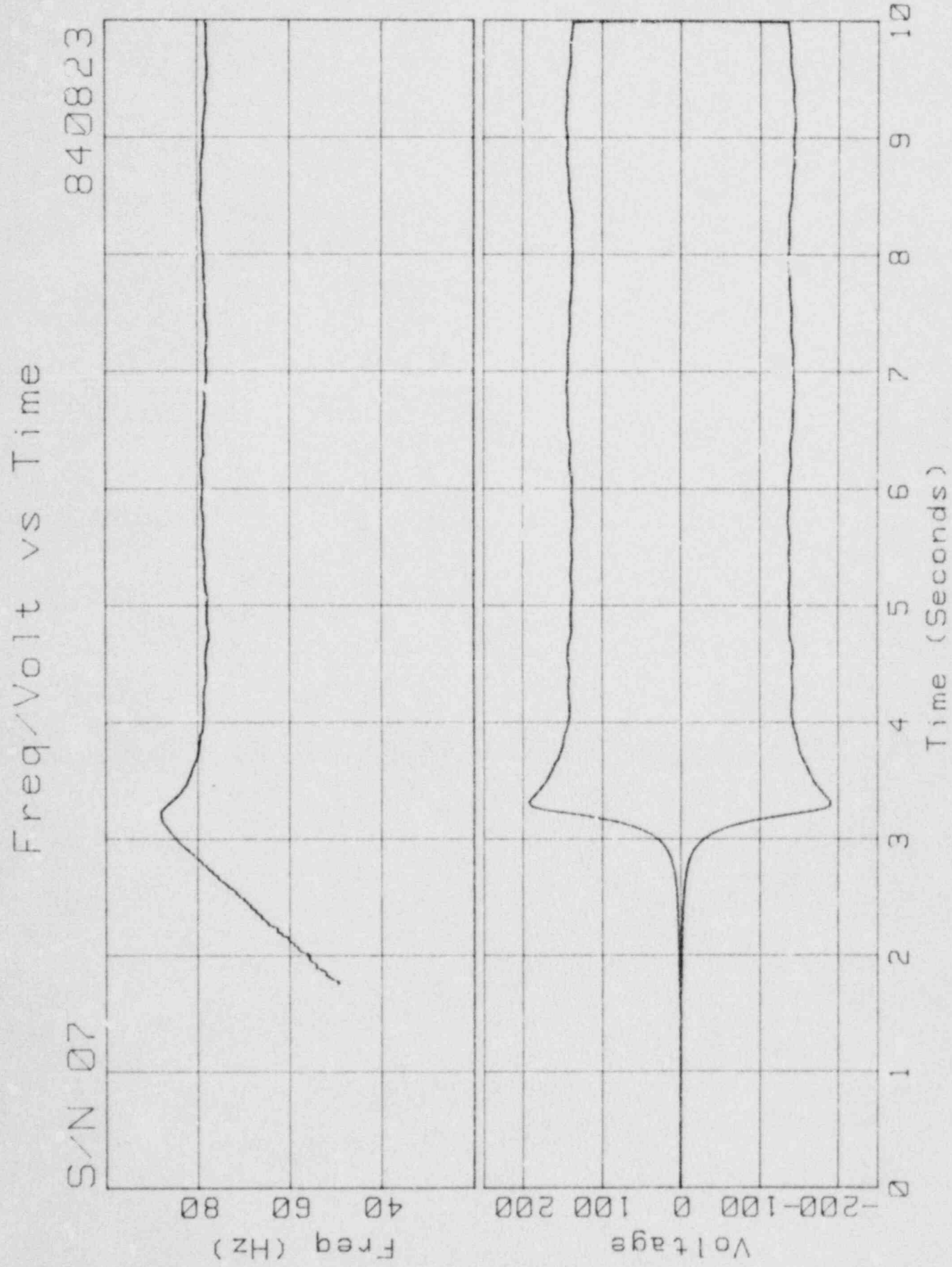
Freq/Volt vs Time
840823
S/N 07
Freq (Hz)
40
60
80
Voltage
-200
-100
0
100
200
0
1
2
3
4
5
6
7
8
9
10
Time (Seconds)

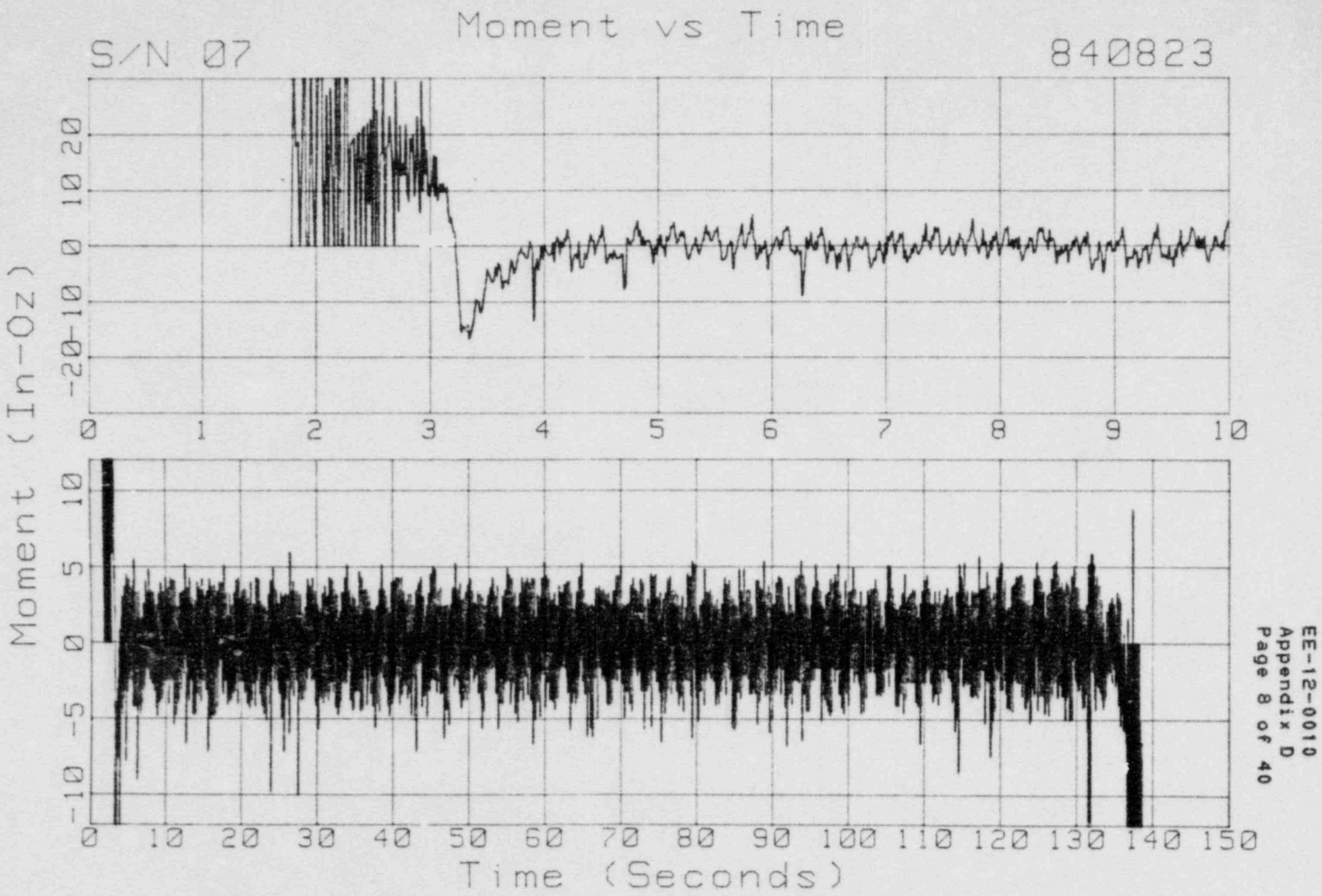
Moment vs Time
S/N 07
840823
Moment (In-Oz)
-20 -10 0 10 20
0 1 2 3 4 5 6 7 8 9 10
-10 -5 0 5 10
0 10 20 30 40 50 60 70 80 90 100 110 120 130 140 150
Time (Seconds)

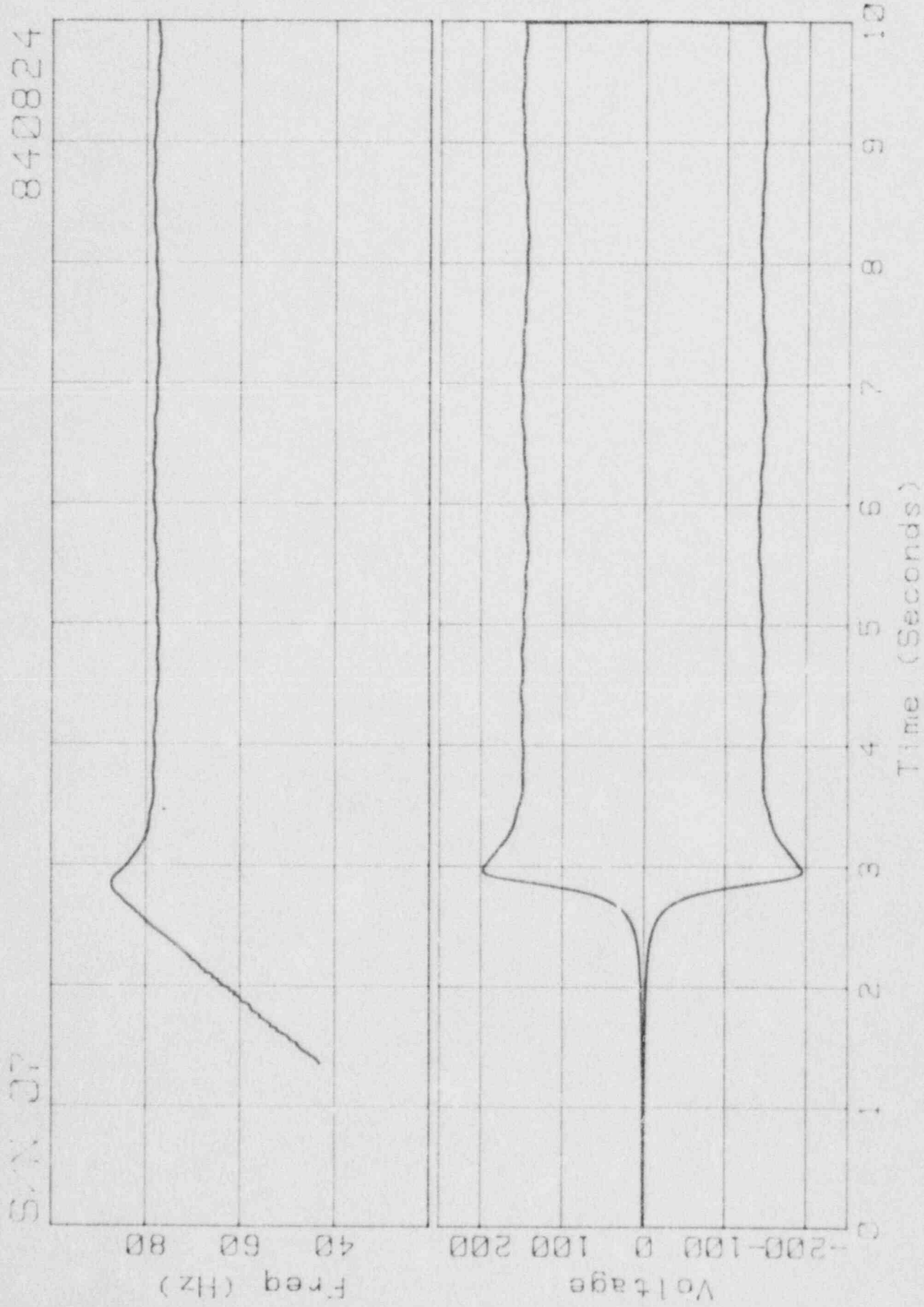
Freq, Volt vs Time
840824
S/N 02
Freq (Hz)
40
60
80
Voltage
-200
-100
0
100
200
Time (Seconds)
0
1
2
3
4
5
6
7
8
9
10

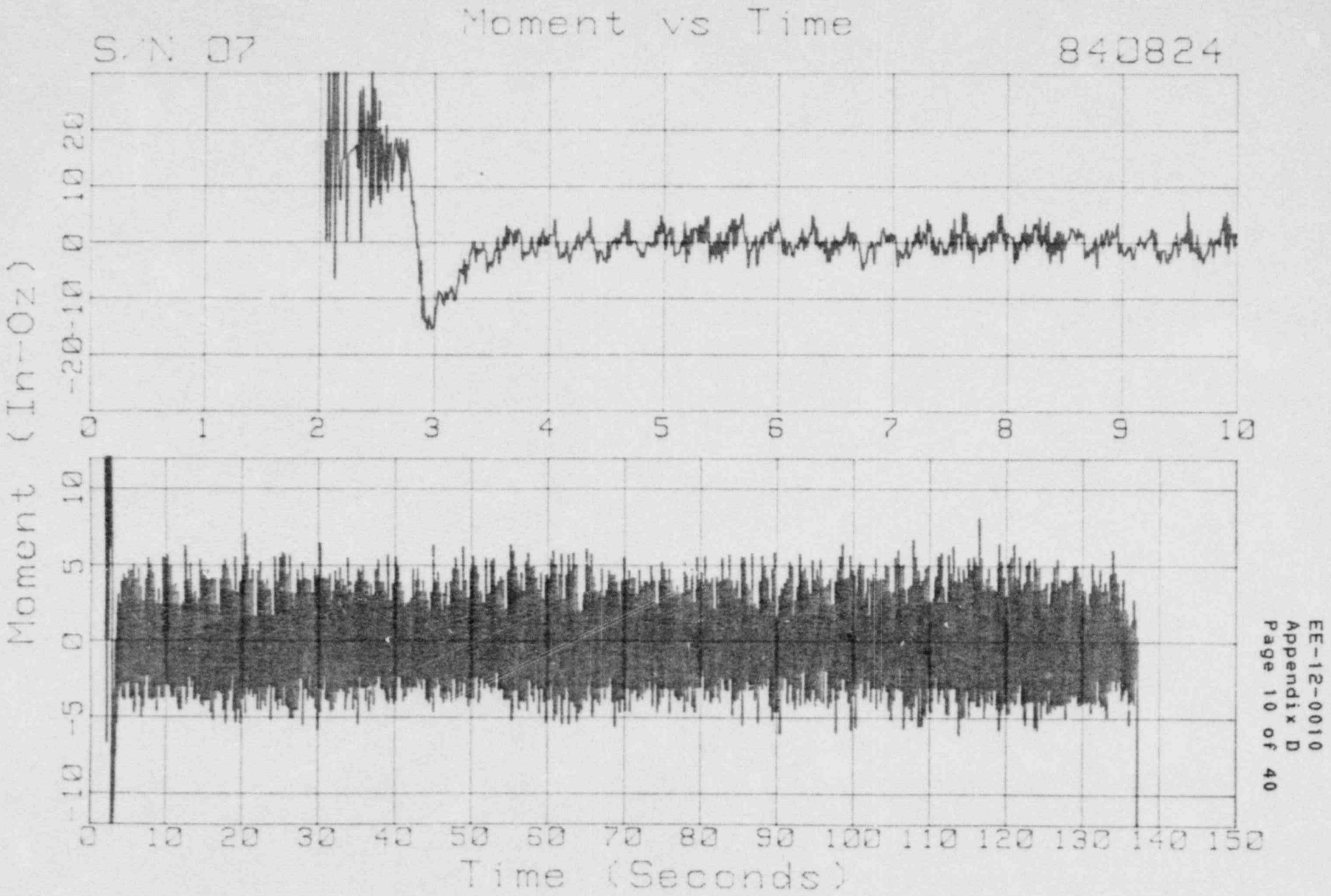
Moment vs Time
S/N 07
840824
Moment (In-Oz)
-20-10 0 10 20
0 1 2 3 4 5 6 7 8 9 10
-10 -5 0 5 10
0 10 20 30 40 50 60 70 80 90 100 110 120 130 140 150
Time (Seconds)

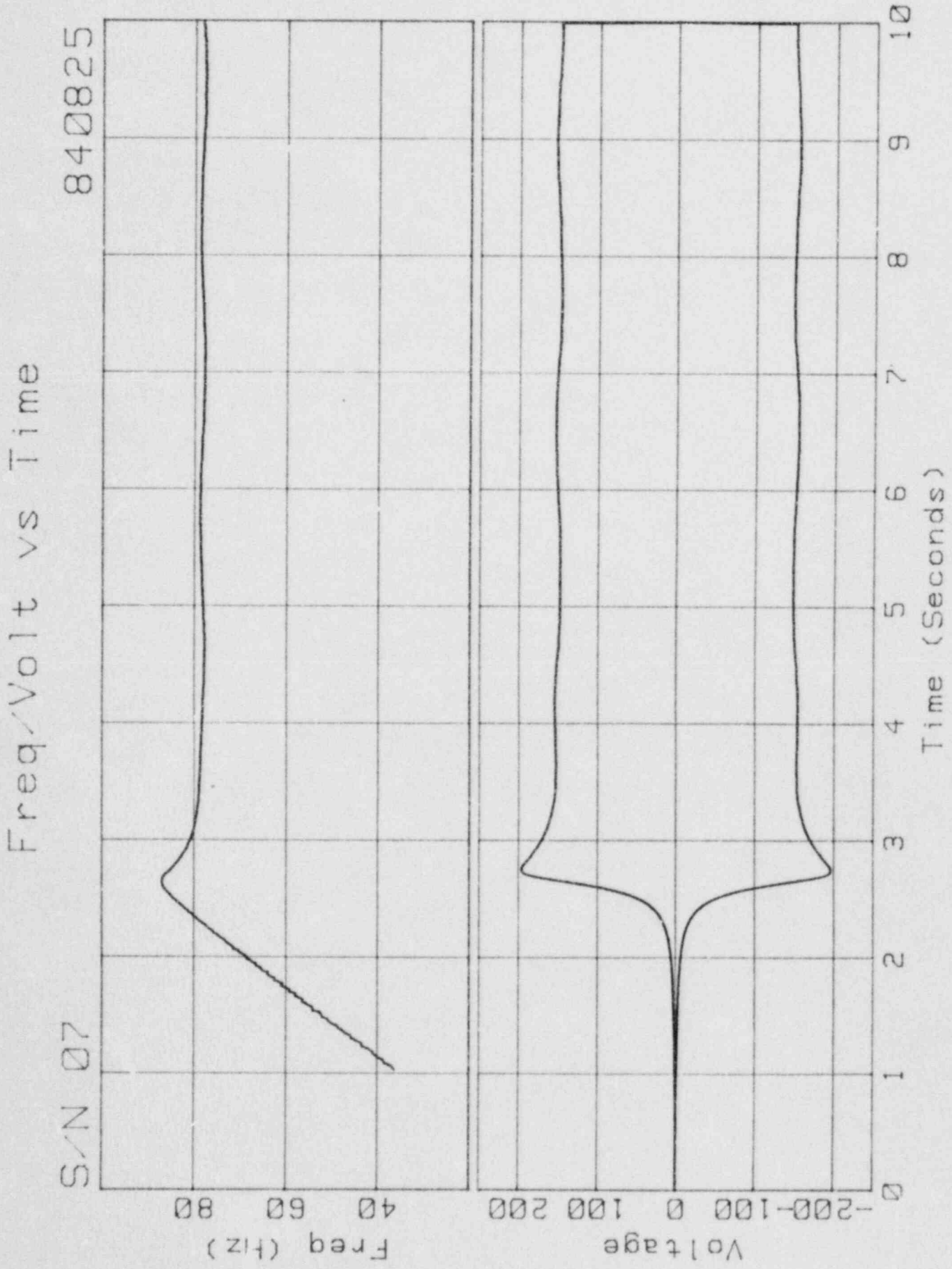
Freq/Volt vs Time
840825
S/N 07
Freq (Hz)
40
60
80
Voltage
-200
-100
0
100
200
0
1
2
3
4
5
6
7
8
9
10
Time (Seconds)

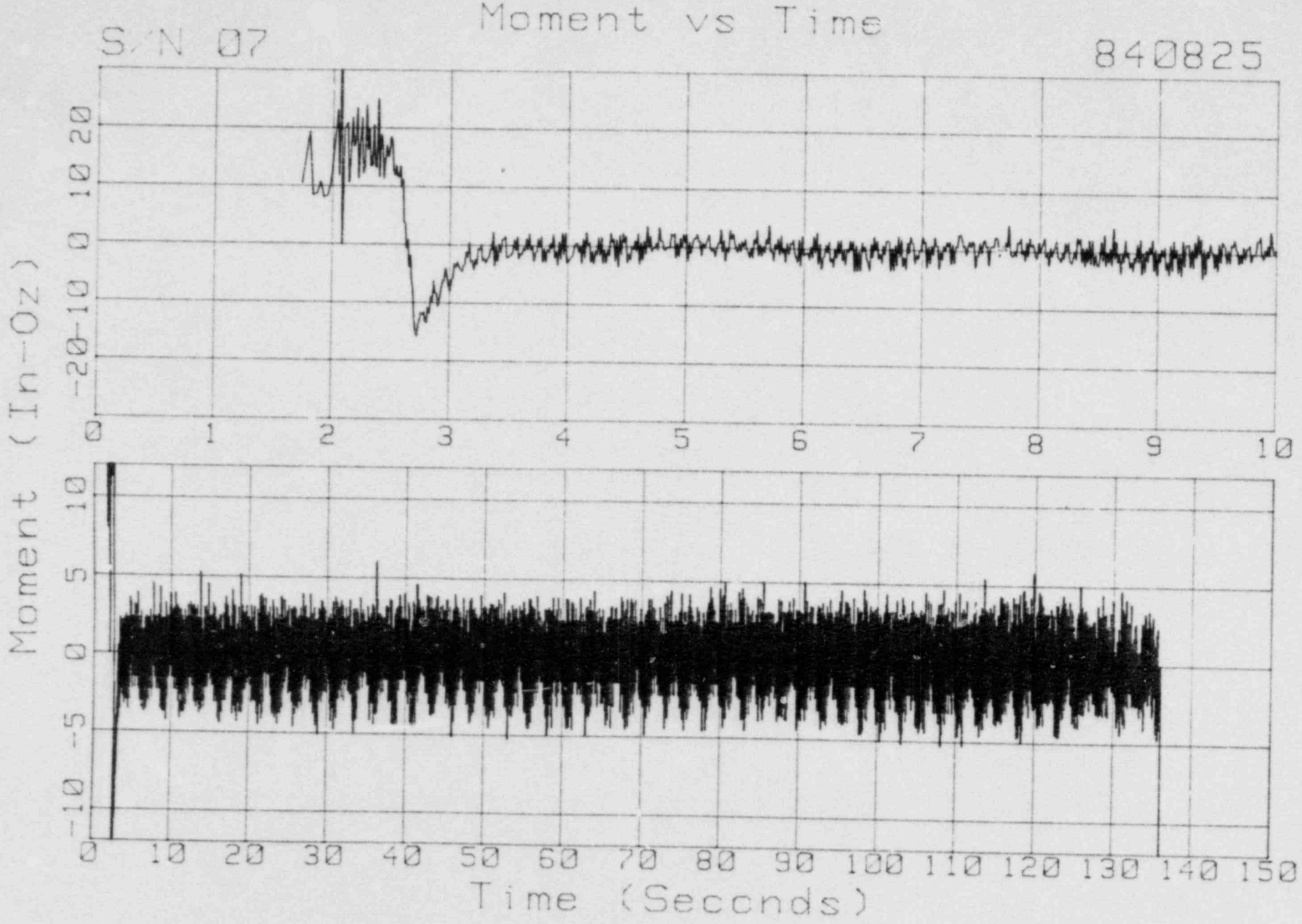
Moment vs Time
S/N 07
840825
Moment (In-Oz)
-20 -10 0 10 20
0 1 2 3 4 5 6 7 8 9 10
-10 -5 0 5 10
0 10 20 30 40 50 60 70 80 90 100 110 120 130 140 150
Time (Seconds)

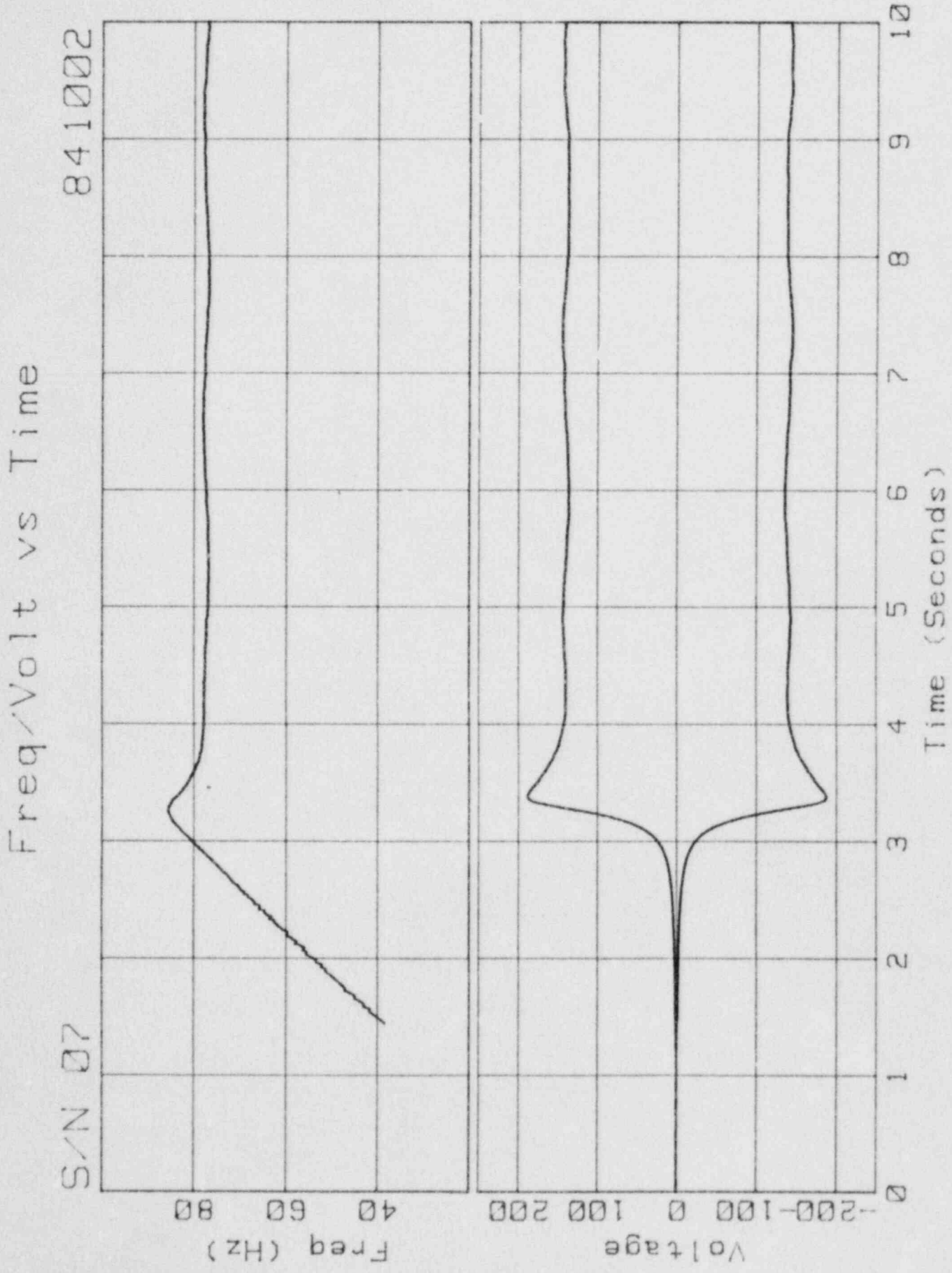
Freq/Volt vs Time
841002
S/N 07
Freq (Hz)
40
60
80
Voltage
-200
-100
0
100
200
0
1
2
3
4
5
6
7
8
9
10
Time (Seconds)

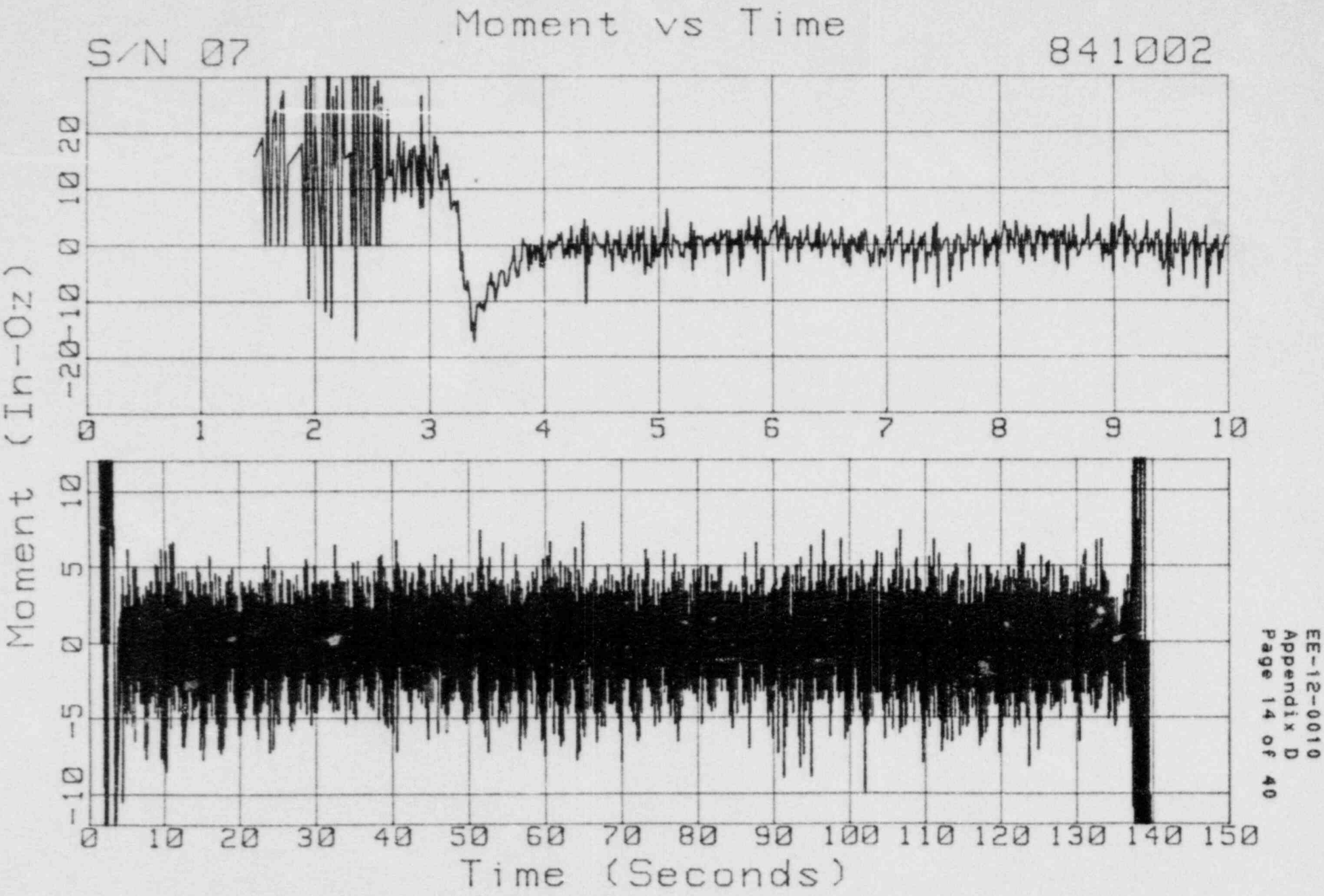
Moment vs Time
S/N 07
841002
Moment (In-Oz)
20
10
0
-10
-20
0
1
2
3
4
5
6
7
8
9
10
10
5
0
-5
-10
0
10
20
30
40
50
60
70
80
90
100
110
120
130
140
150
Time (Seconds)

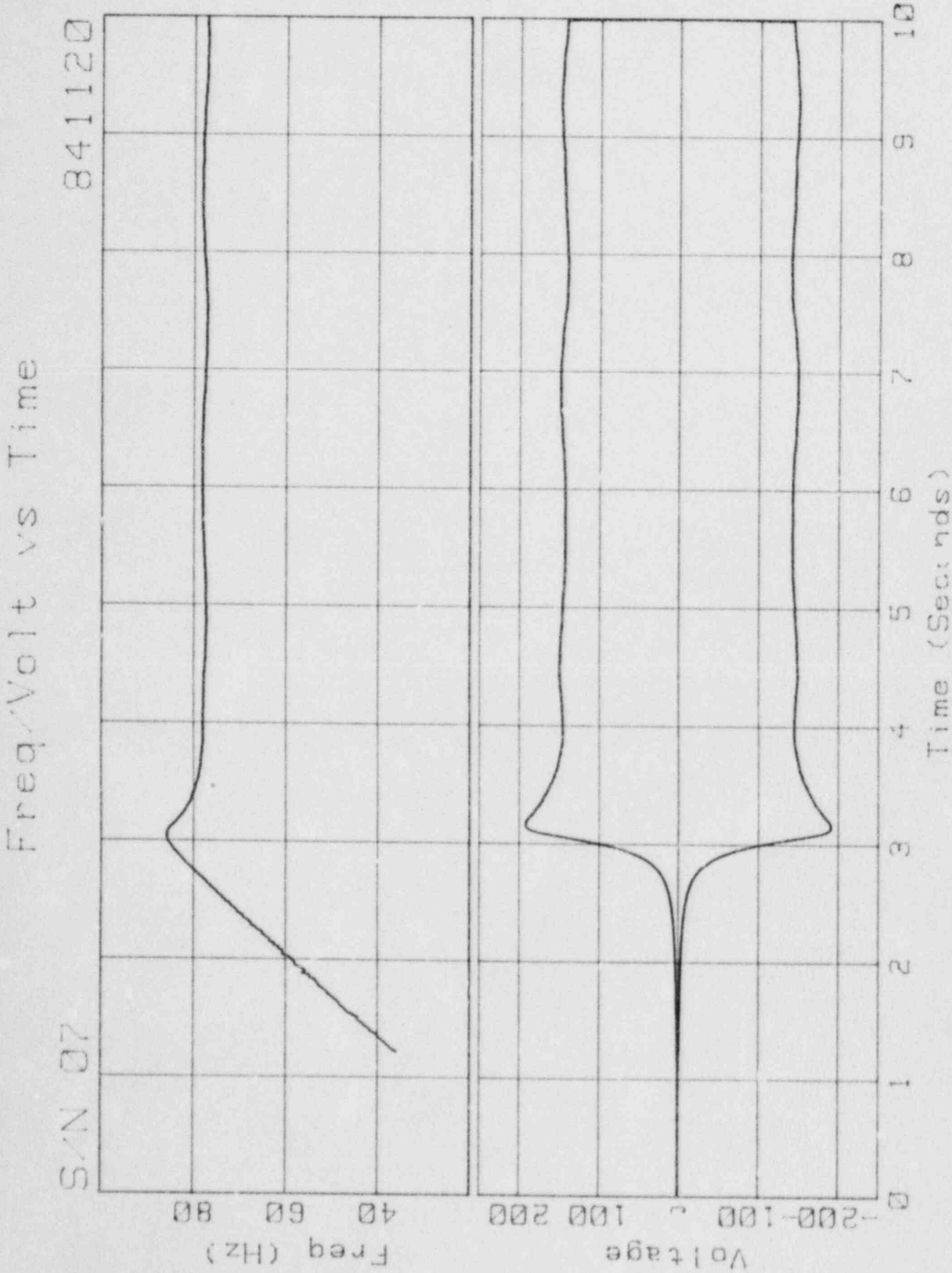
Freq/Volt vs Time
8411120
S/N 07
Freq (Hz)
40
60
80
Voltage
-200
-100
0
100
200
0
1
2
3
4
5
6
7
8
9
10
Time (Seconds)

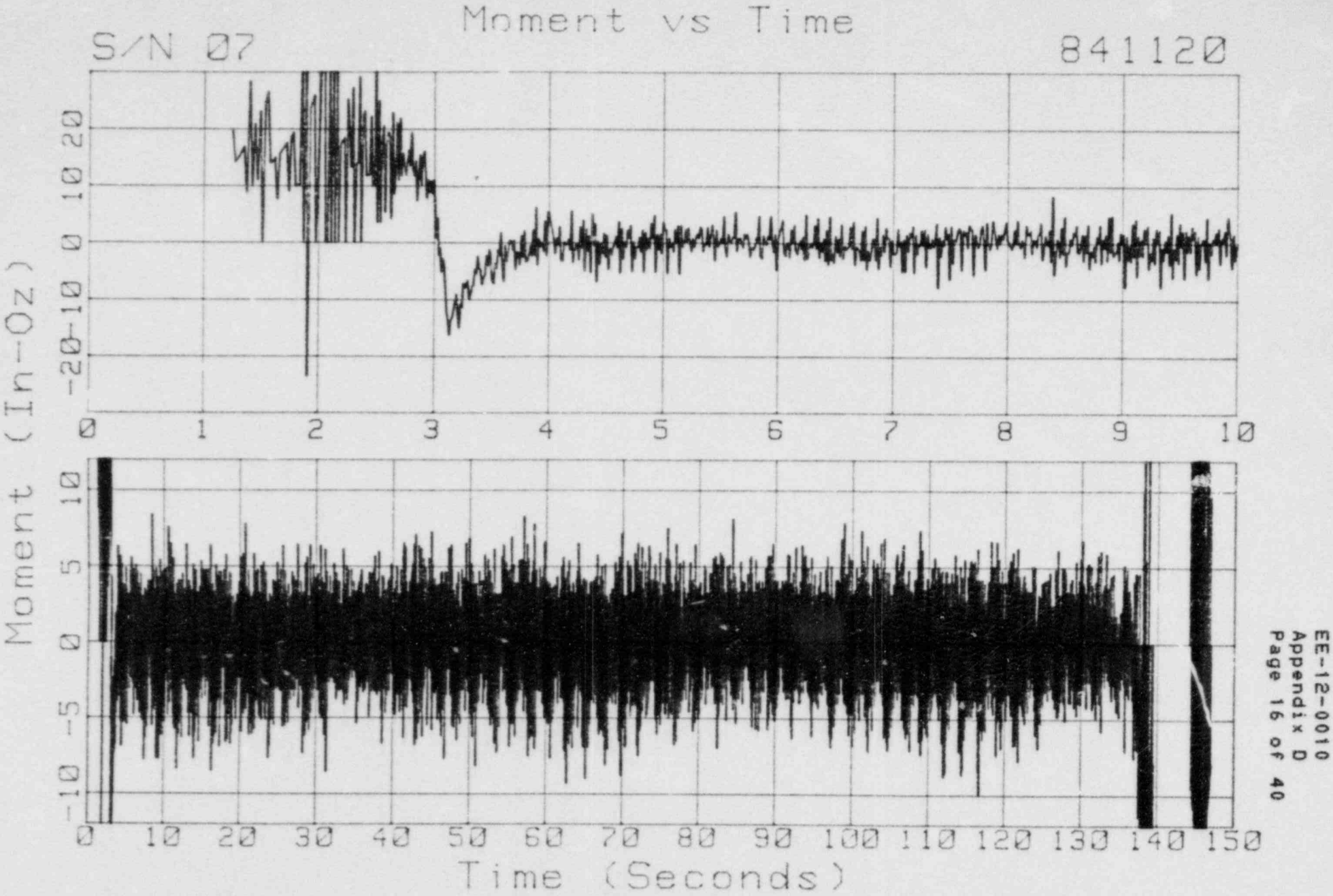
Moment vs Time
S/N 07
841120
Moment (In-Oz)
-20 -10 0 10 20
0 1 2 3 4 5 6 7 8 9 10
-10 -5 0 5 10
0 10 20 30 40 50 60 70 80 90 100 110 120 130 140 150
Time (Seconds)

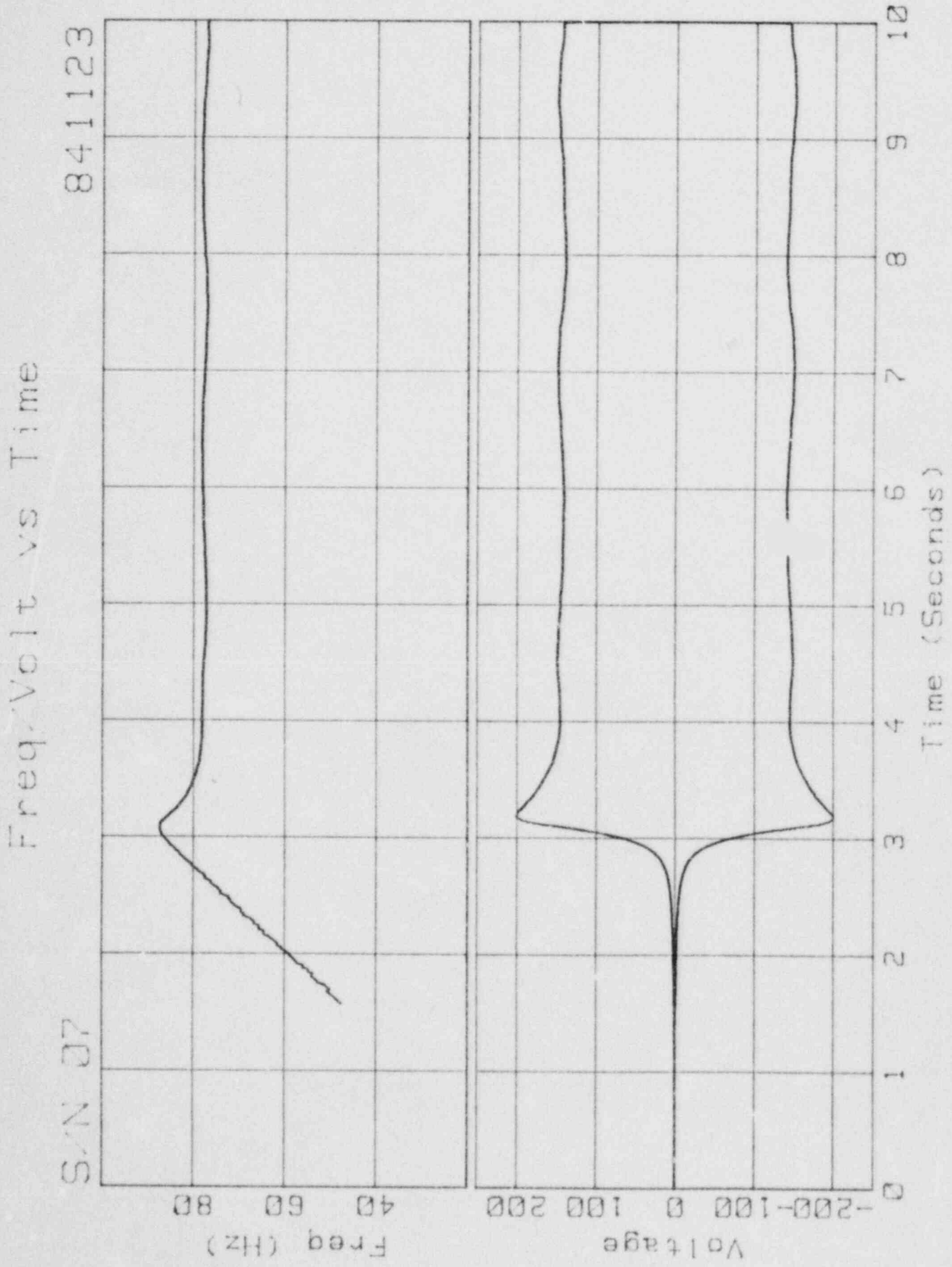
S/N 07
841123
Freq/Volt vs Time
Freq (Hz)
40
60
80
Voltage
-200
-100
0
100
200
0
1
2
3
4
5
6
7
8
9
10
Time (Seconds)

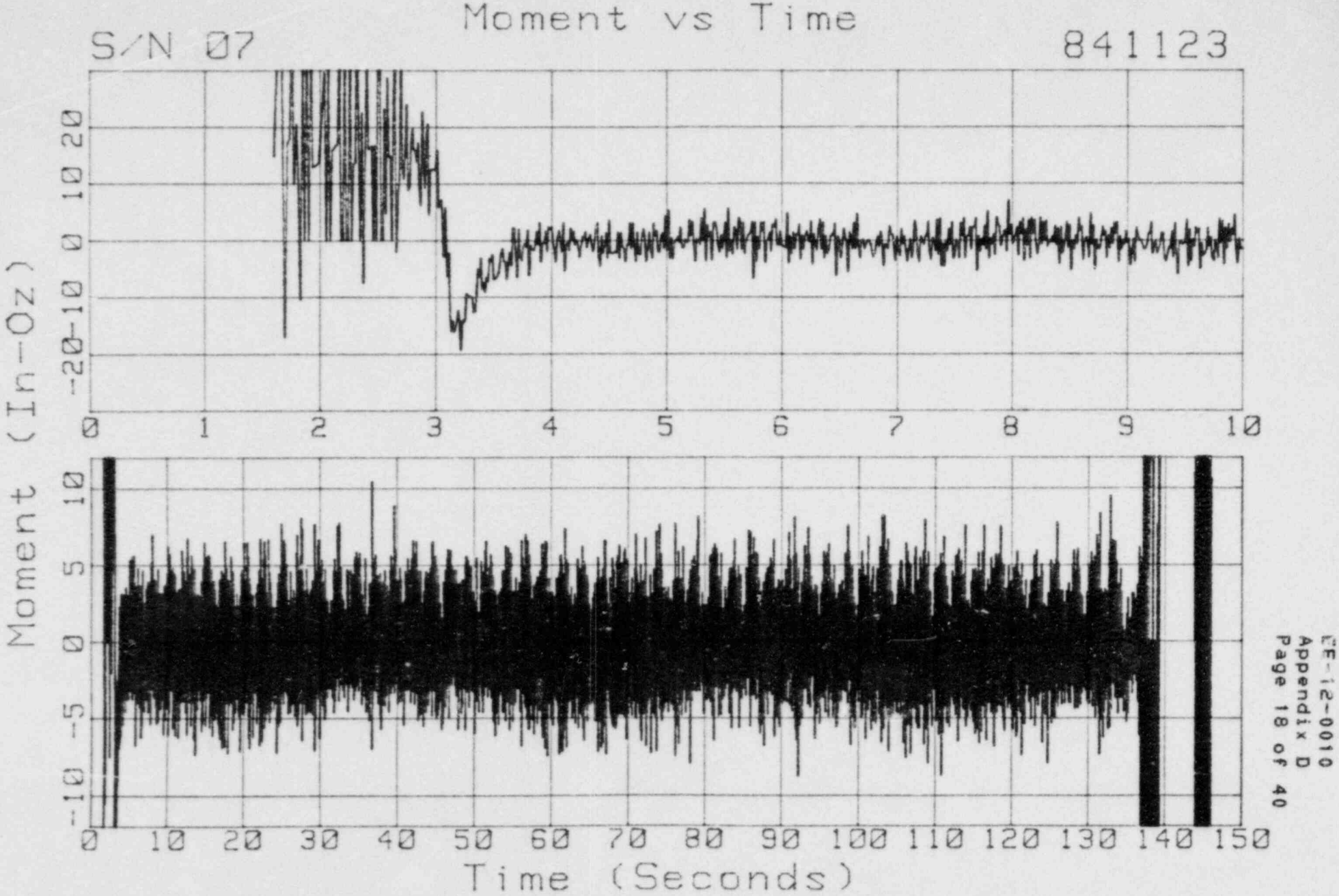
Moment vs Time
S/N 07
841123
Moment (In-Oz)
-20 -10 0 10 20
0 1 2 3 4 5 6 7 8 9 10
-10 -5 0 5 10
0 10 20 30 40 50 60 70 80 90 100 110 120 130 140 150
Time (Seconds)

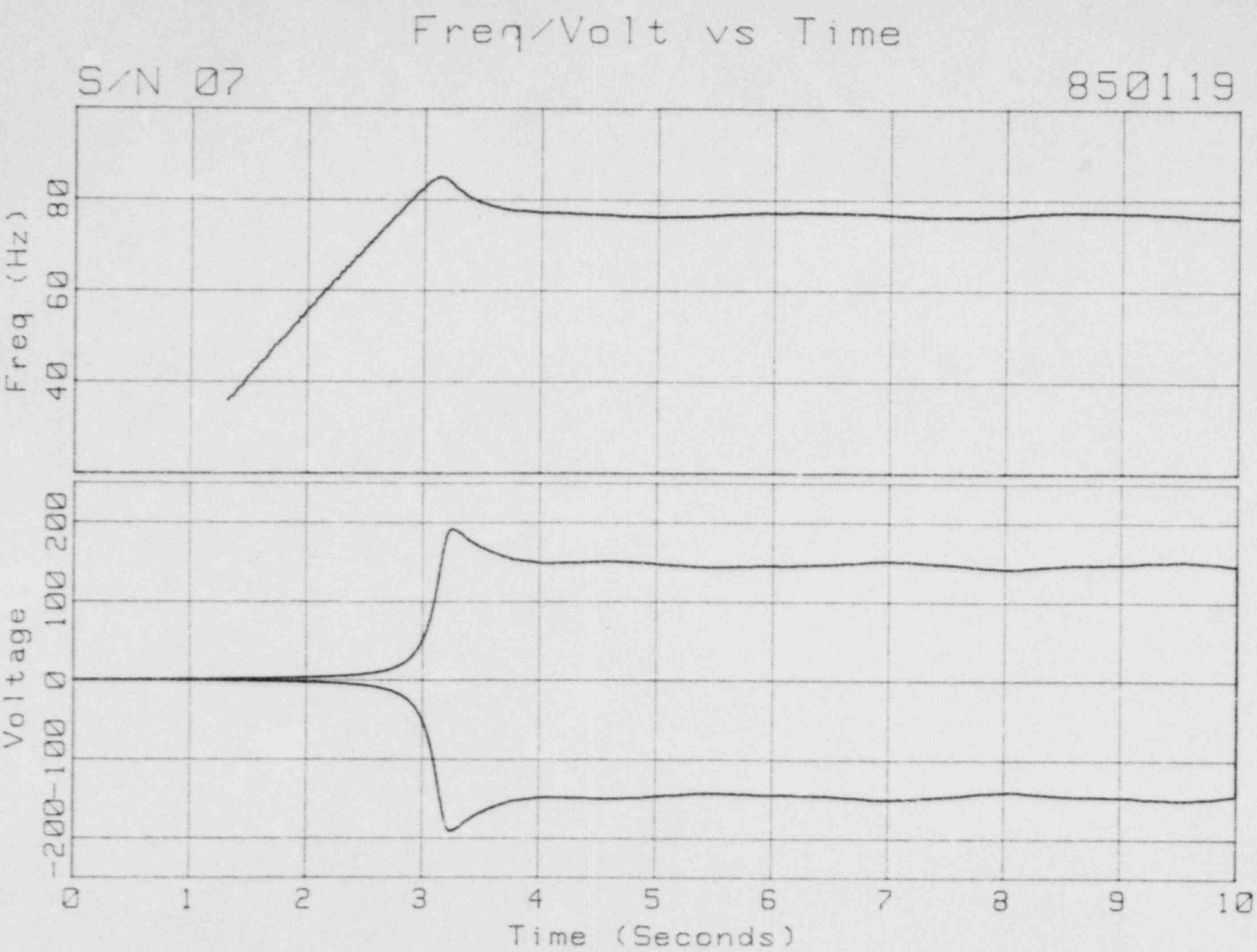
Freq/Volt vs Time
S/N 07
850119
Freq (Hz)
40
60
80
Voltage
-200
-100
0
100
200
0
1
2
3
4
5
6
7
8
9
10
Time (Seconds)

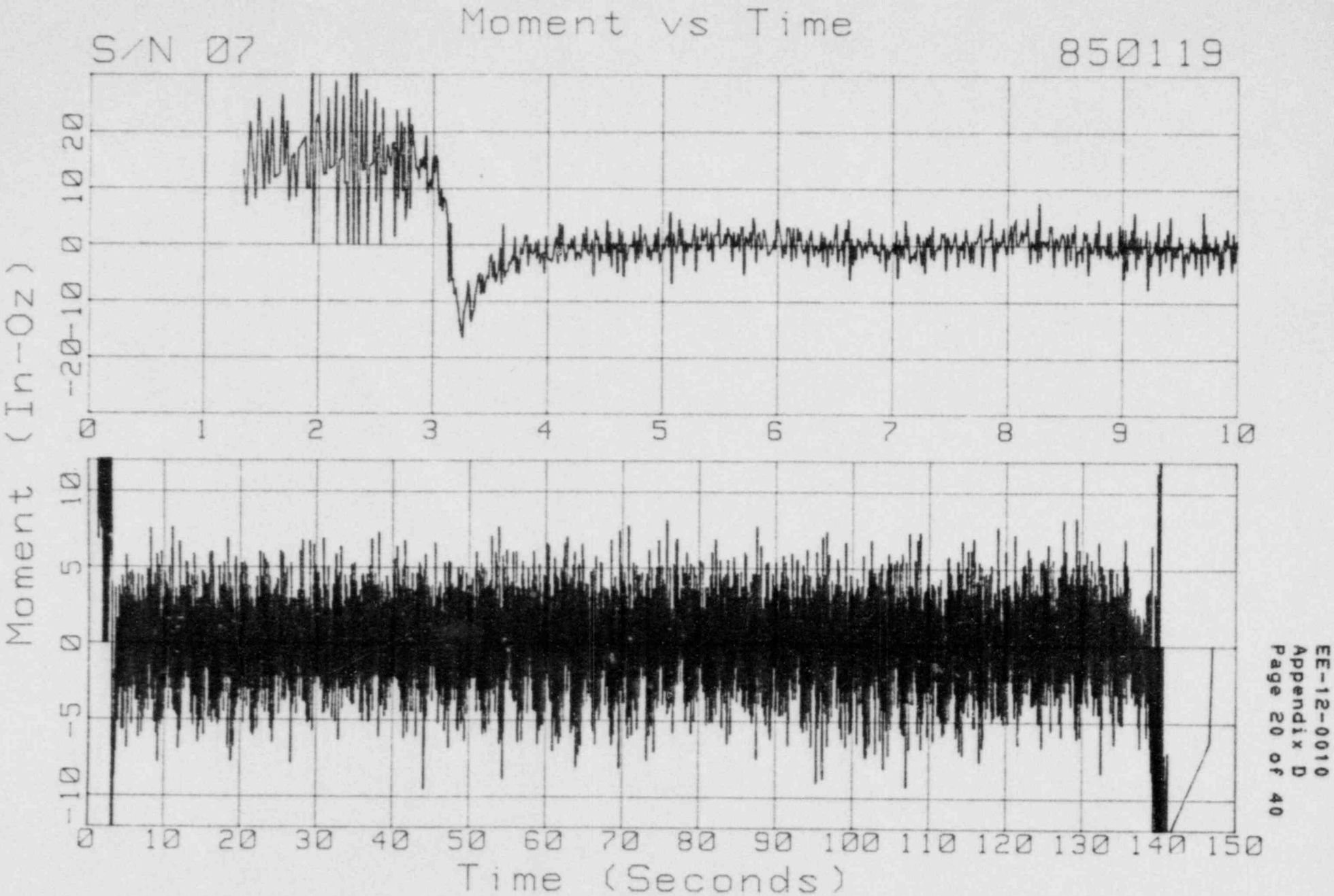
Moment vs Time
S/N 07
850119
Moment (In-Oz)
-20 -10 0 10 20
0 1 2 3 4 5 6 7 8 9 10
-10 -5 0 5 10
0 10 20 30 40 50 60 70 80 90 100 110 120 130 140 150
Time (Seconds)

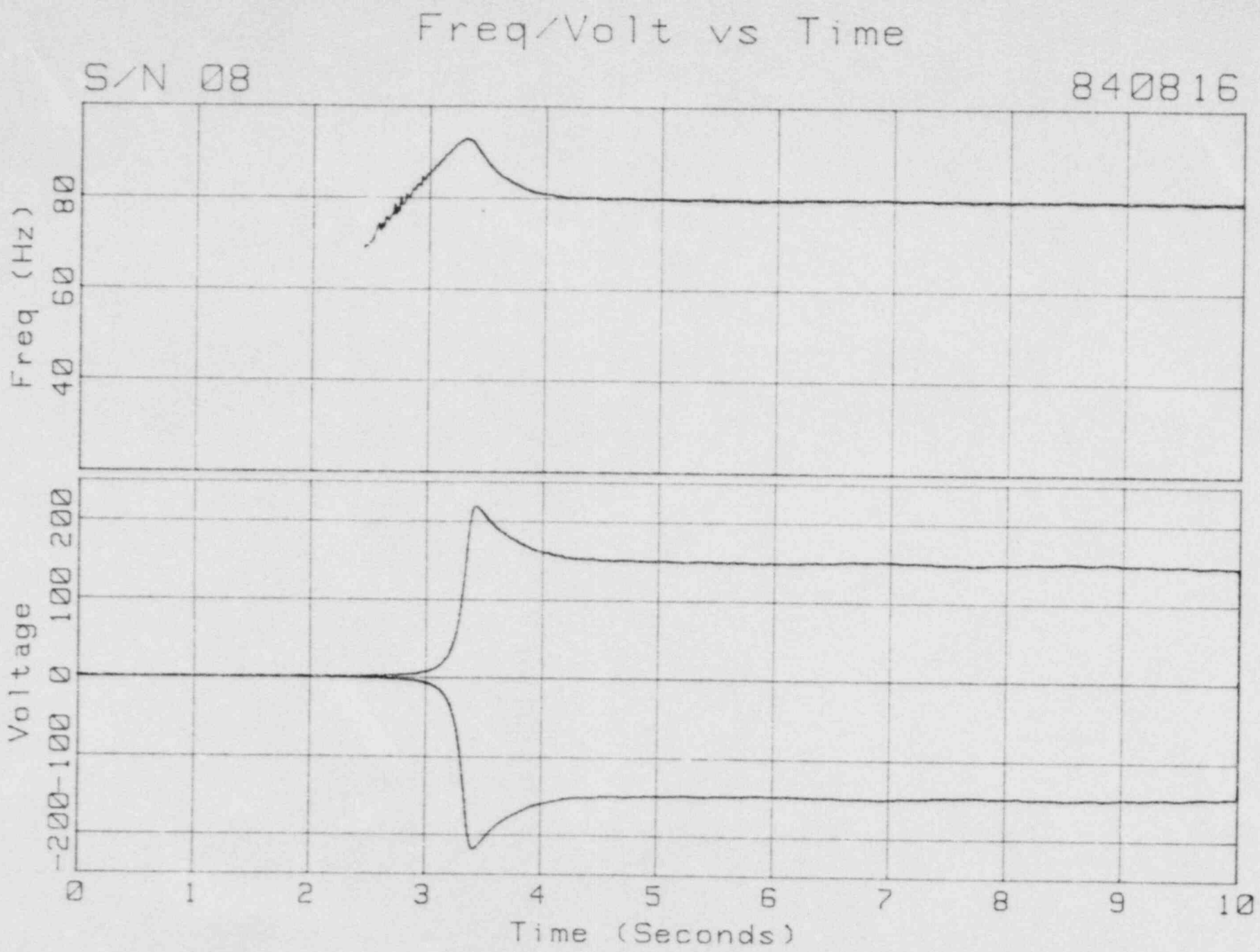
Freq/Volt vs Time
S/N 08
840816
Freq (Hz)
40
60
80
Voltage
-200
-100
0
100
200
0
1
2
3
4
5
6
7
8
9
10
Time (Seconds)

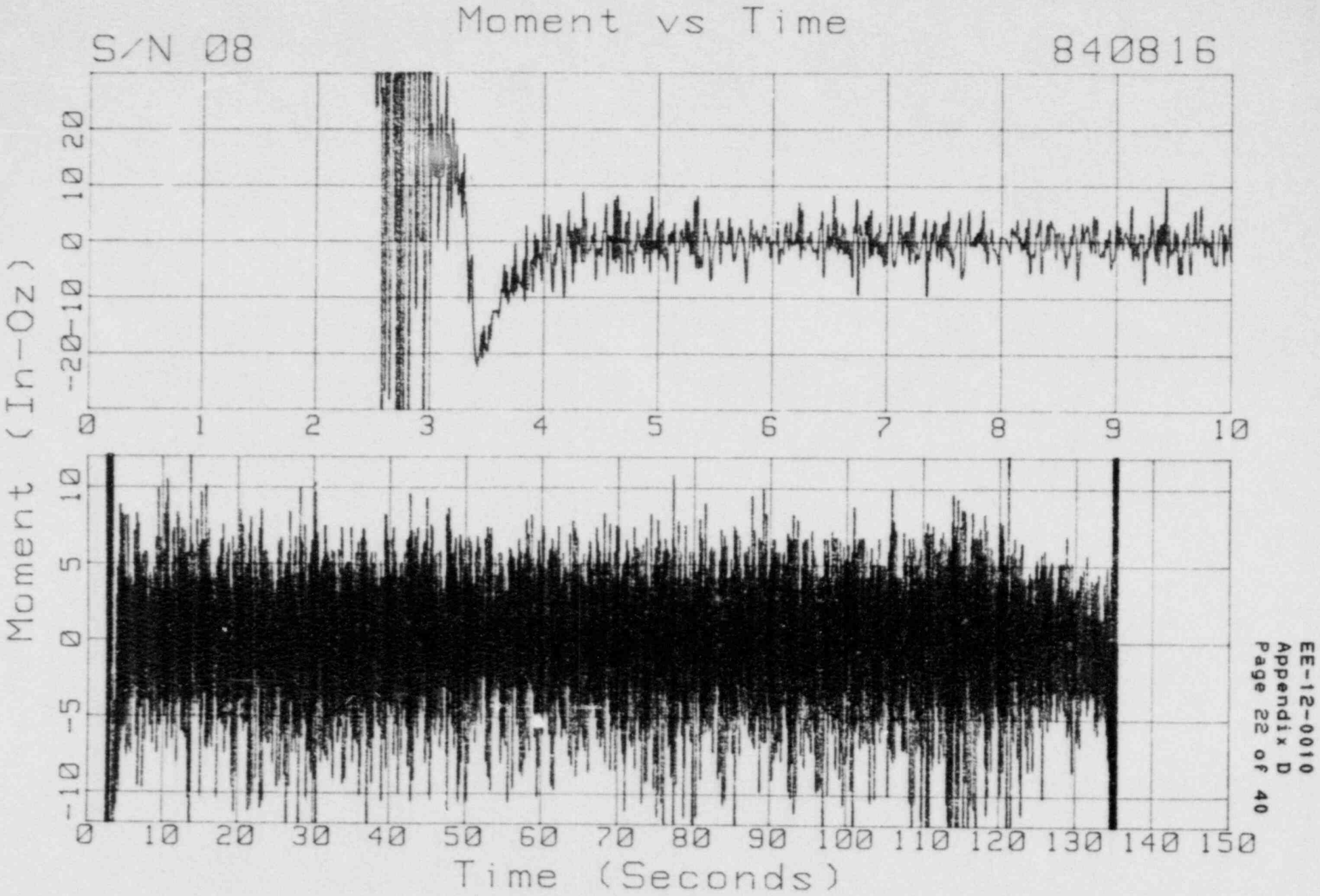
Moment vs Time
S/N 08
840816
Moment (In-Oz)
-20 -10 0 10 20
0 1 2 3 4 5 6 7 8 9 10
-10 -5 0 5 10
0 10 20 30 40 50 60 70 80 90 100 110 120 130 140 150
Time (Seconds)

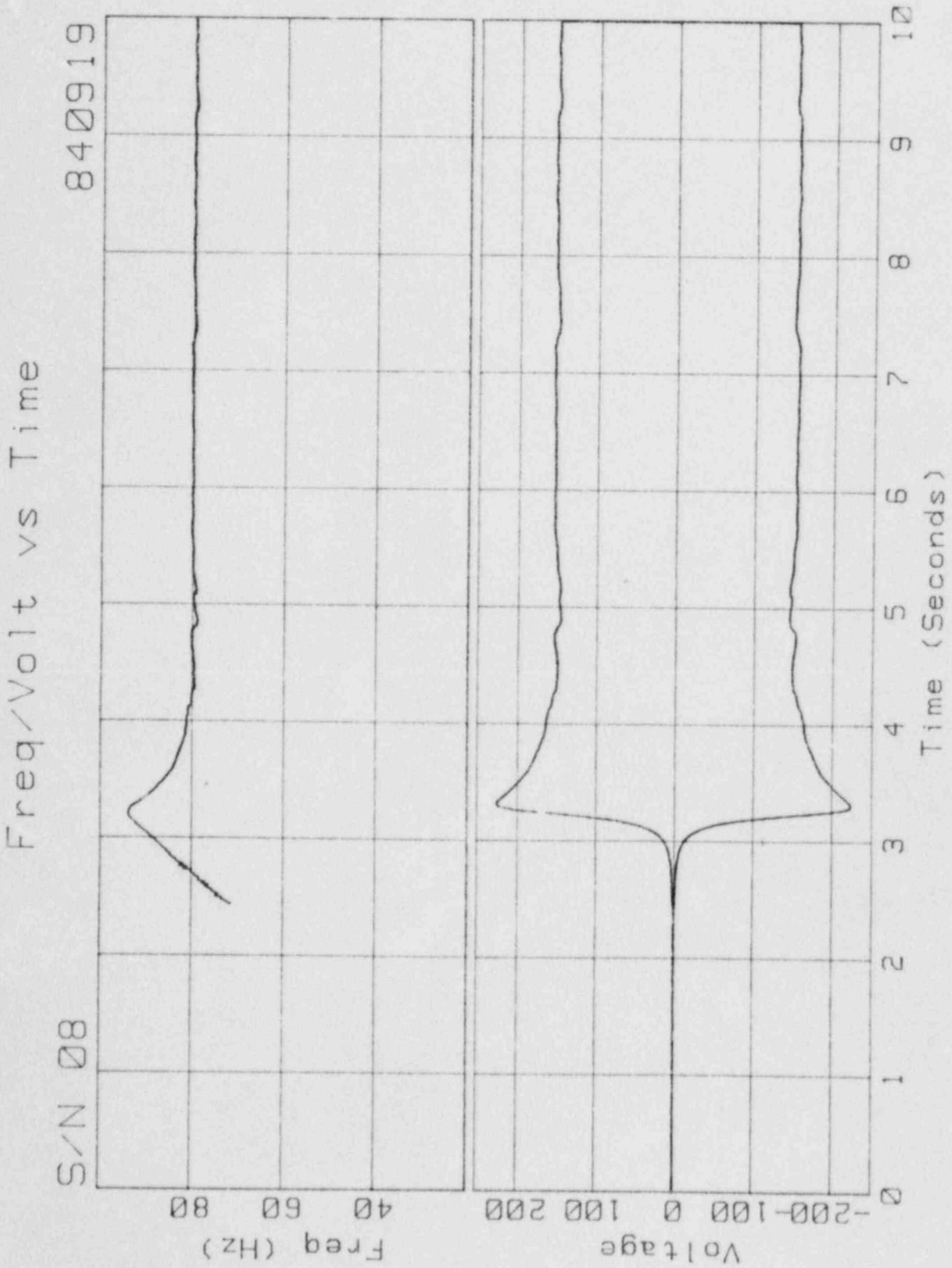
Freq/Volt vs Time
840919
S/N 08
Freq (Hz)
40
60
80
Voltage
-200
-100
0
100
200
0
1
2
3
4
5
6
7
8
9
10
Time (Seconds)

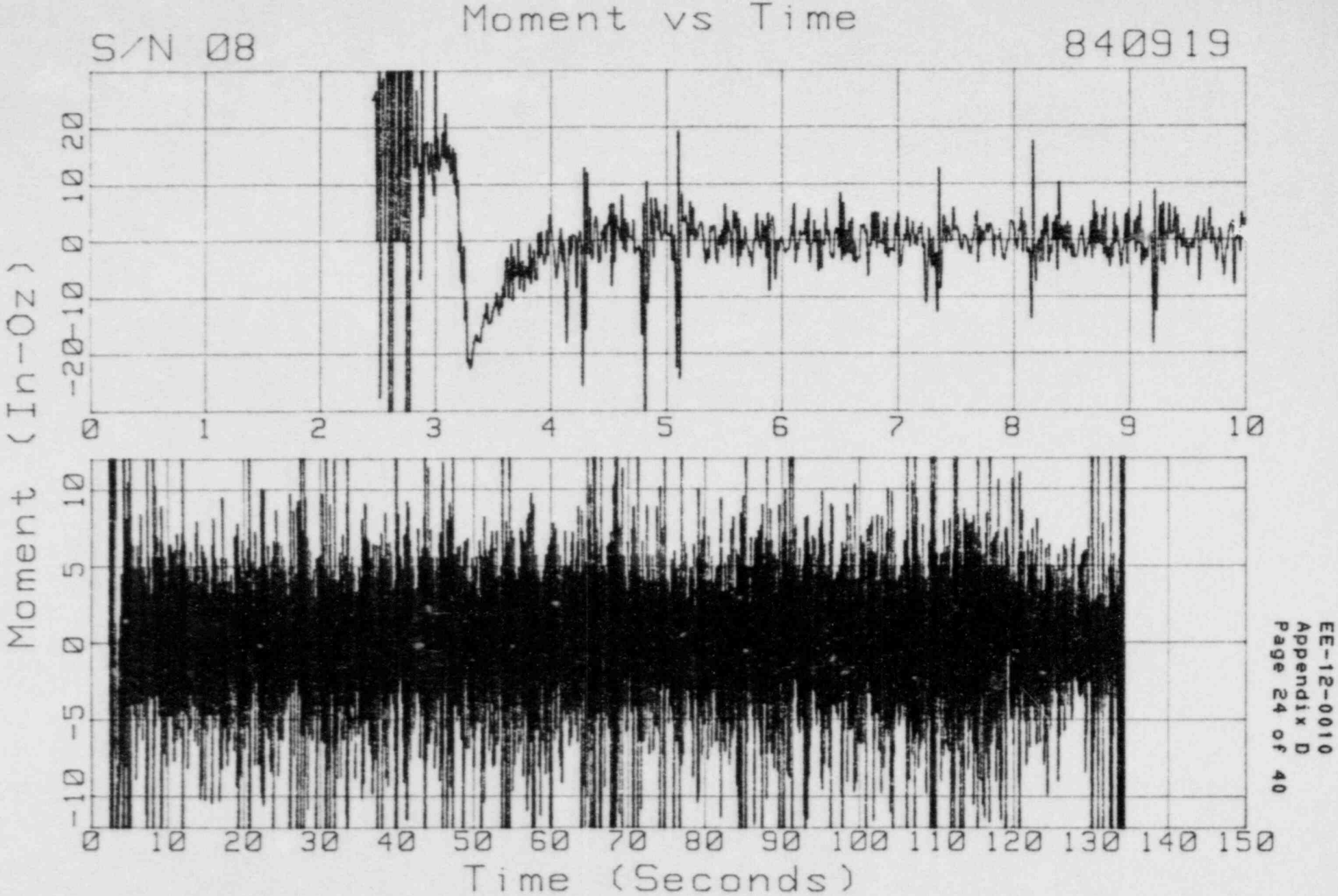
Moment vs Time
S/N 08
840919
Moment (In-Oz)
-20 -10 0 10 20
0 1 2 3 4 5 6 7 8 9 10
-10 -5 0 5 10
0 10 20 30 40 50 60 70 80 90 100 110 120 130 140 150
Time (Seconds)

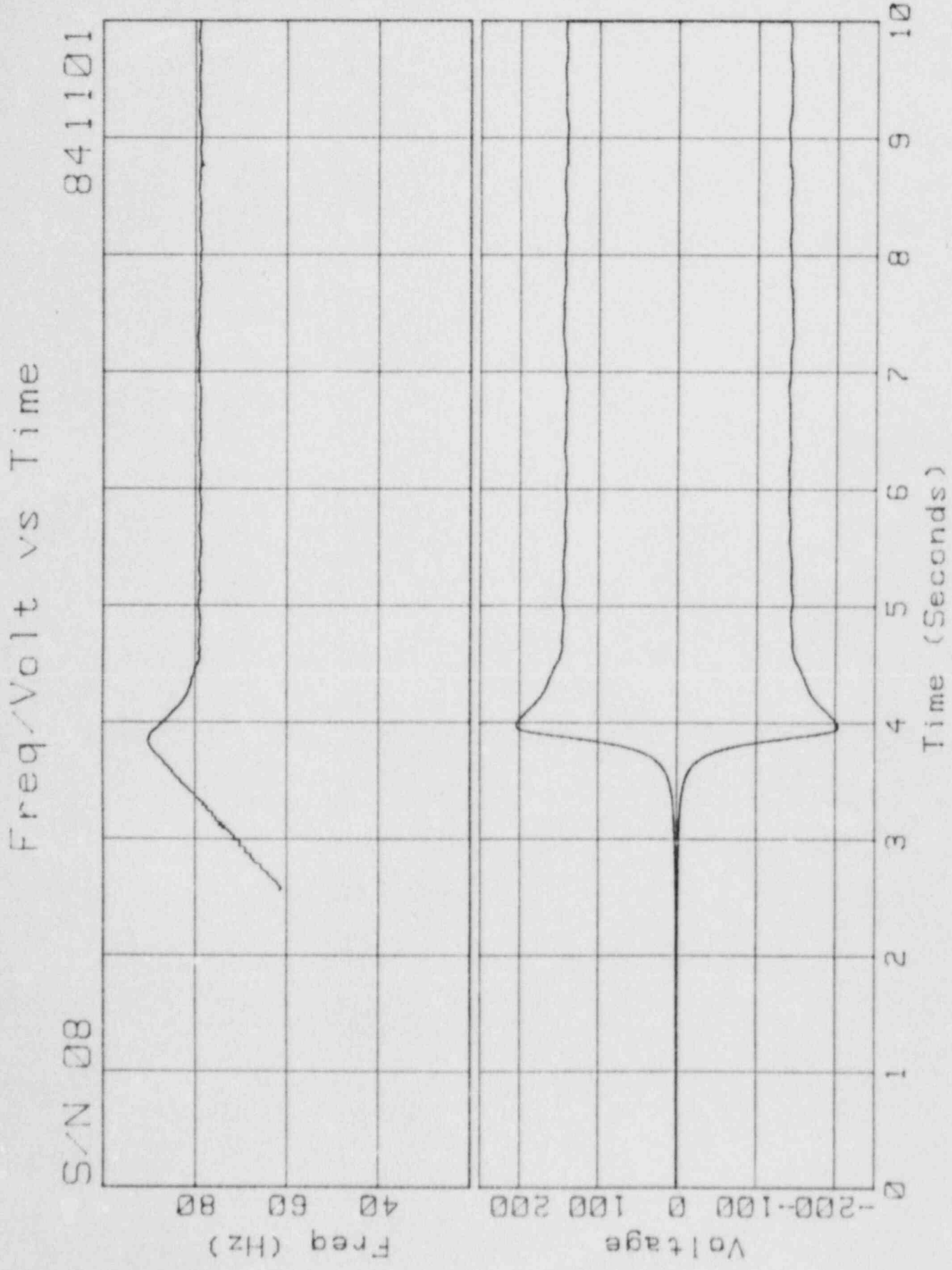
Freq/Volt vs Time
841101
S/N 08
Freq (Hz)
40
60
80
Voltage
-200
-100
0
100
200
Time (Seconds)
0
1
2
3
4
5
6
7
8
9
10

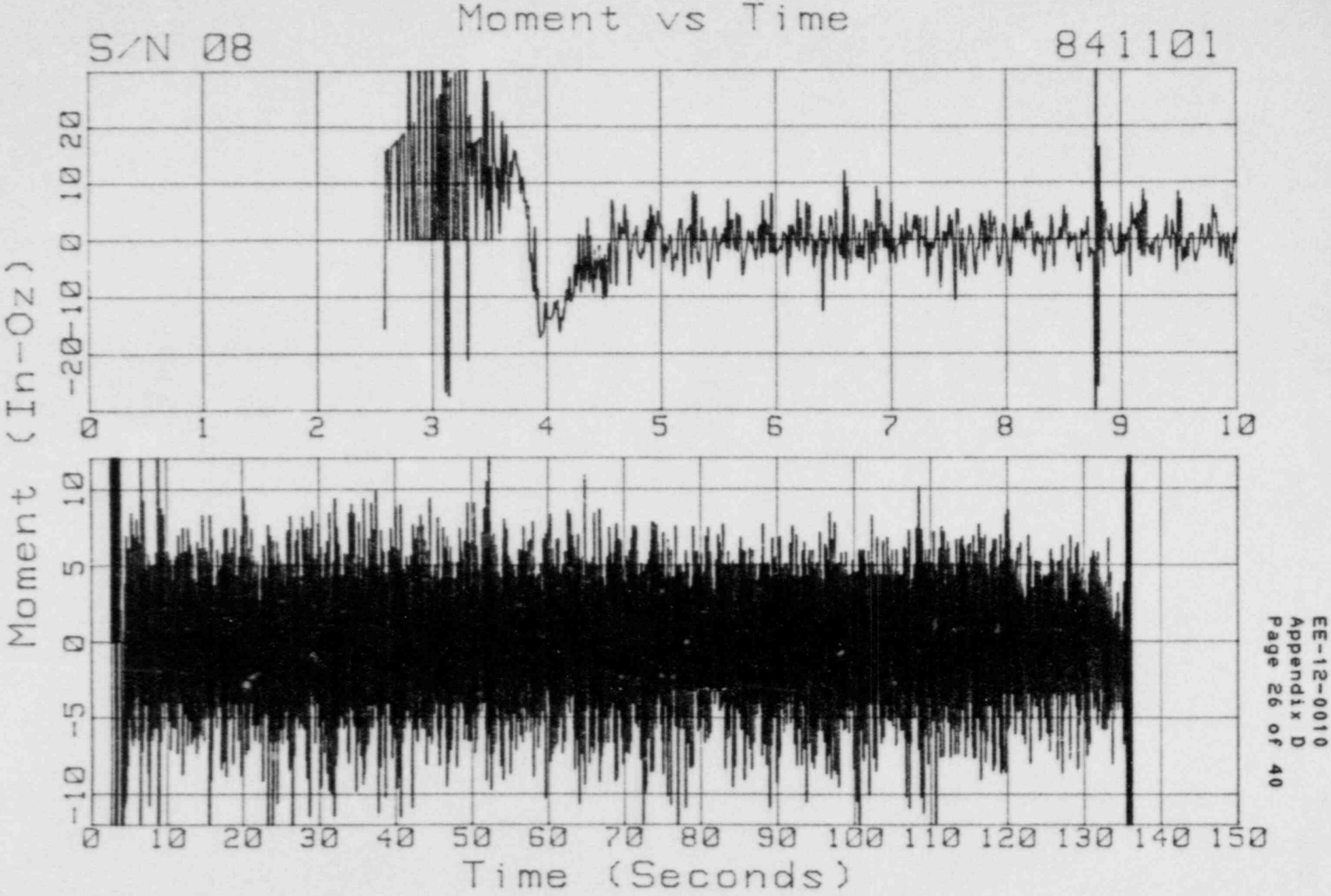
Moment vs Time
S/N 08
841101
Moment (In-Oz)
-20 -10 0 10 20
0 1 2 3 4 5 6 7 8 9 10
-10 -5 0 5 10
0 10 20 30 40 50 60 70 80 90 100 110 120 130 140 150
Time (Seconds)

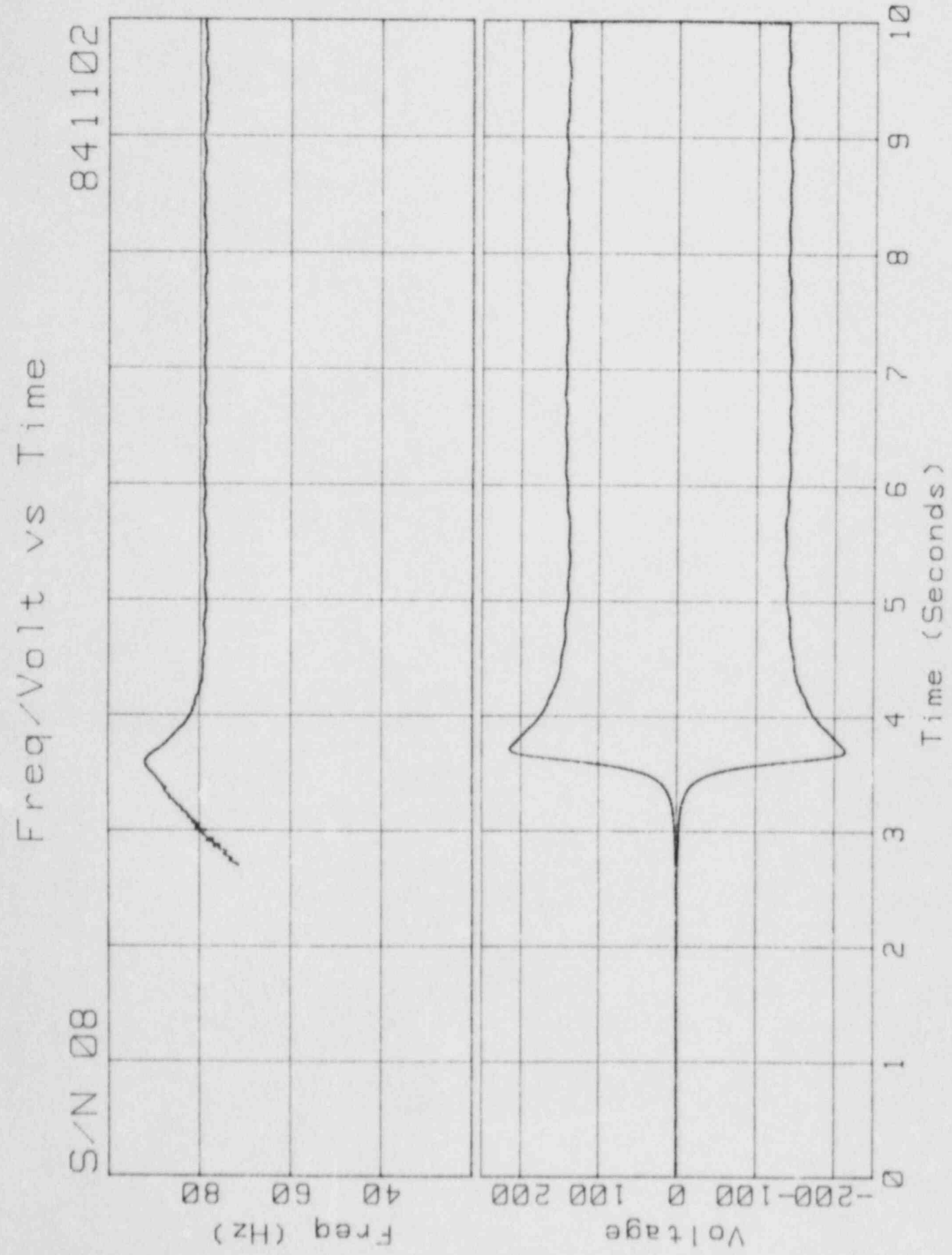
Freq/Volt vs Time
8411102
S/N 08
Freq (Hz)
40
60
80
Voltage
-200
-100
0
100
200
0
1
2
3
4
5
6
7
8
9
10
Time (Seconds)

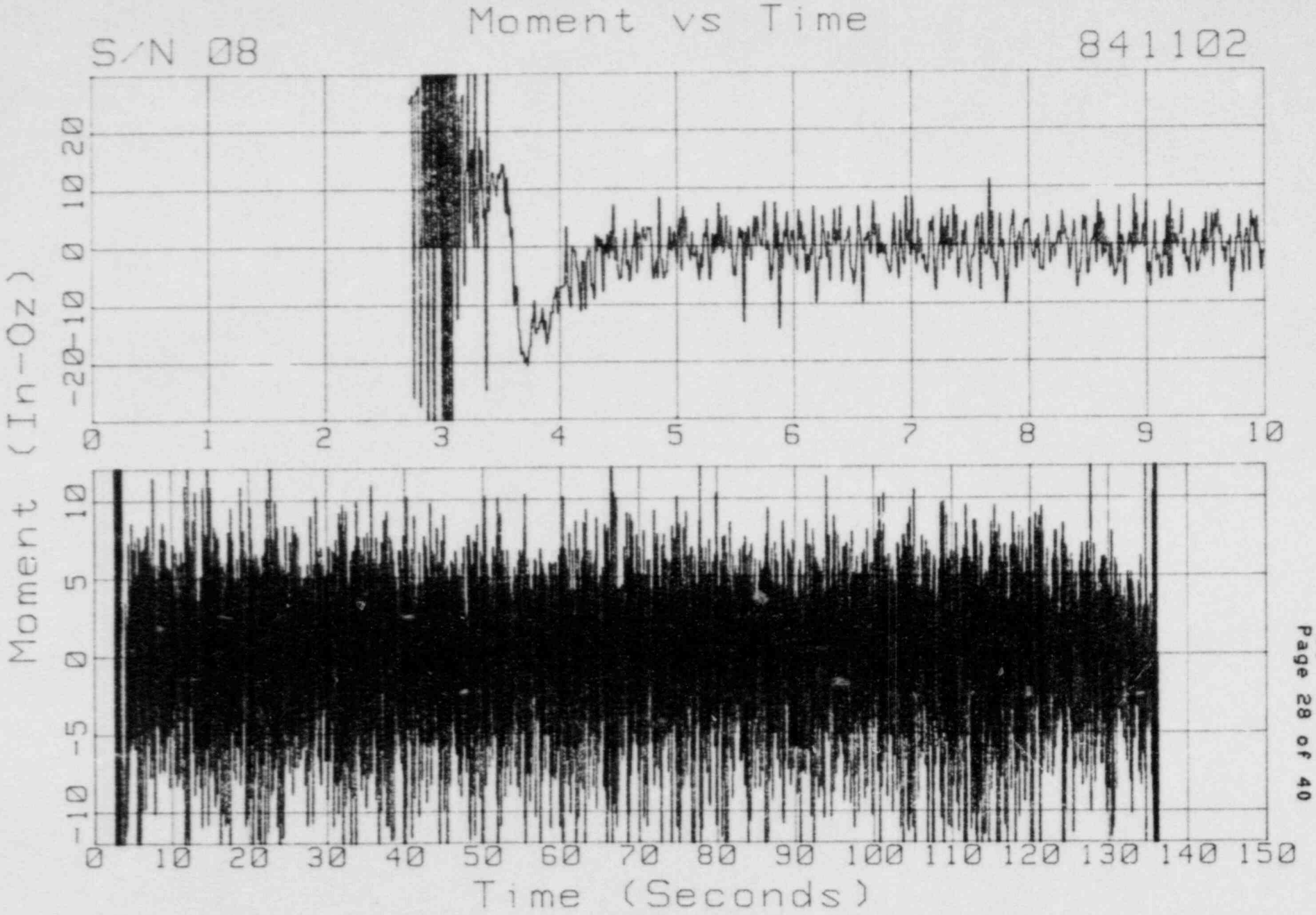
Moment vs Time
S/N 08
841102
Moment (In-Oz)
-20 -10 0 10 20
0 1 2 3 4 5 6 7 8 9 10
-10 -5 0 5 10
0 10 20 30 40 50 60 70 80 90 100 110 120 130 140 150
Time (Seconds)

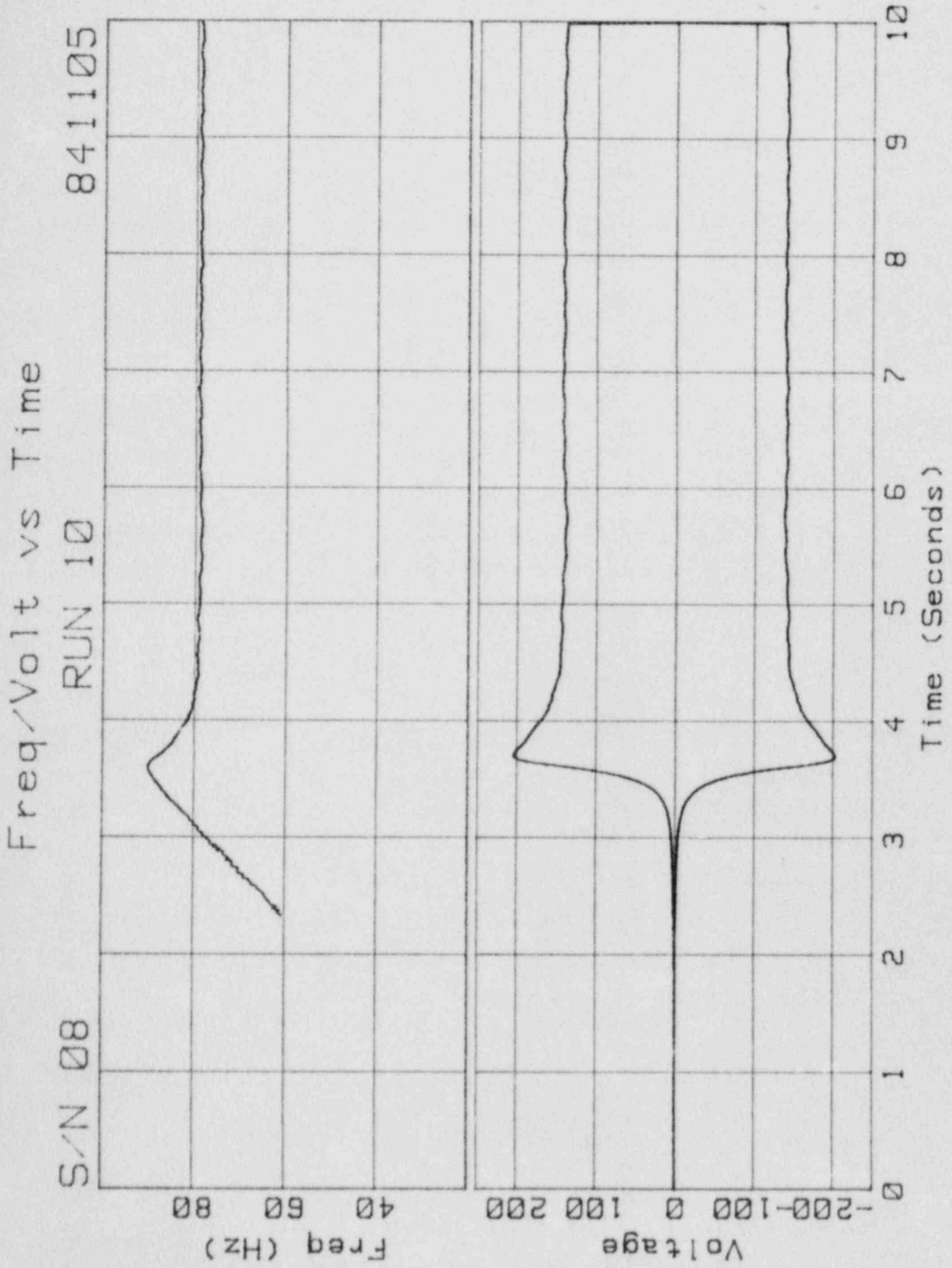
Freq/Volt vs Time
RUN 10
841105
S/N 08
Freq (Hz)
40
60
80
Voltage
-200
-100
0
100
200
0
1
2
3
4
5
6
7
8
9
10
Time (Seconds)

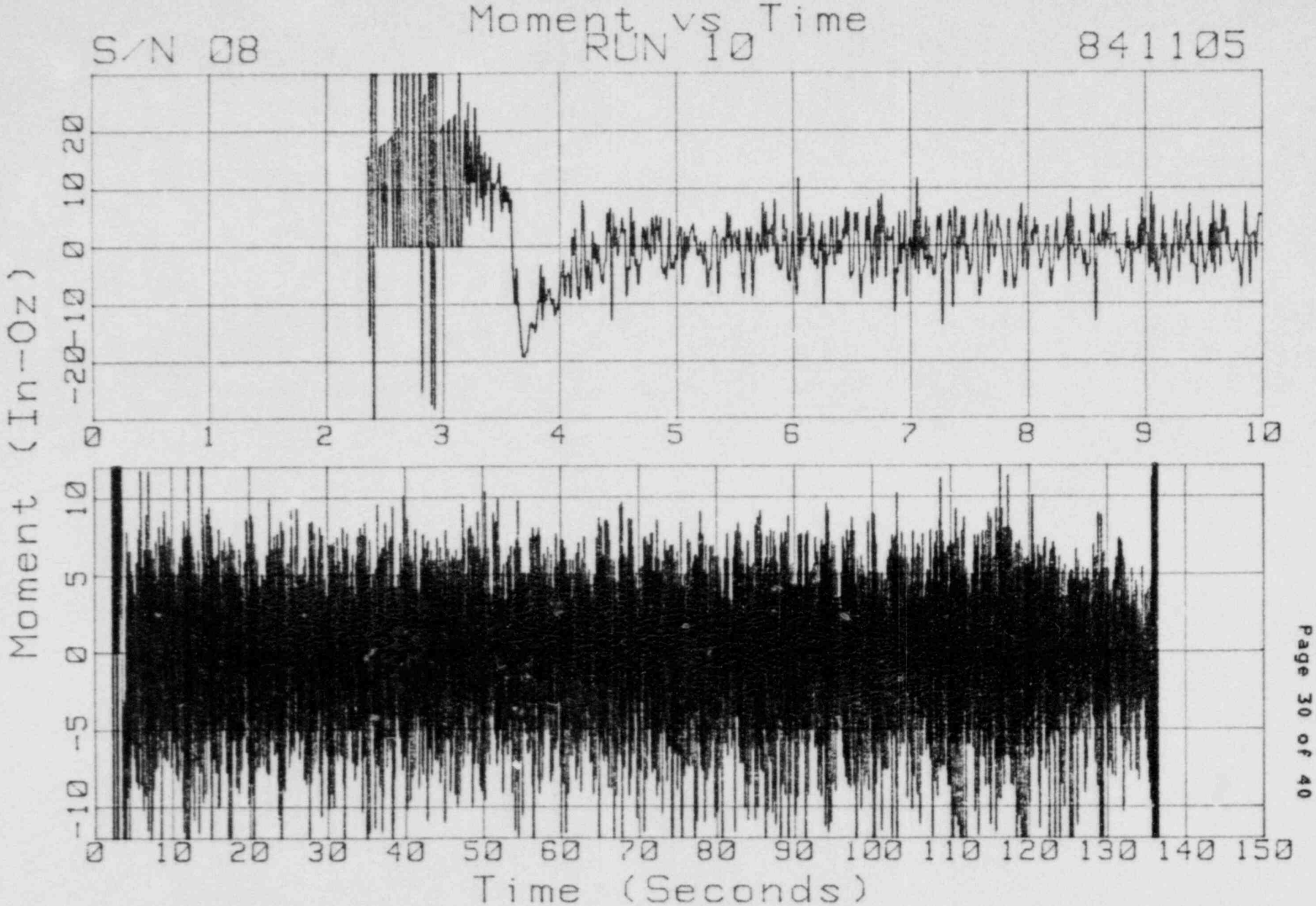
Moment vs Time
S/N 08
RUN 10
841105
Moment (In-Oz)
-20 -10 0 10 20
0 1 2 3 4 5 6 7 8 9 10
-10 -5 0 5 10
0 10 20 30 40 50 60 70 80 90 100 110 120 130 140 150
Time (Seconds)

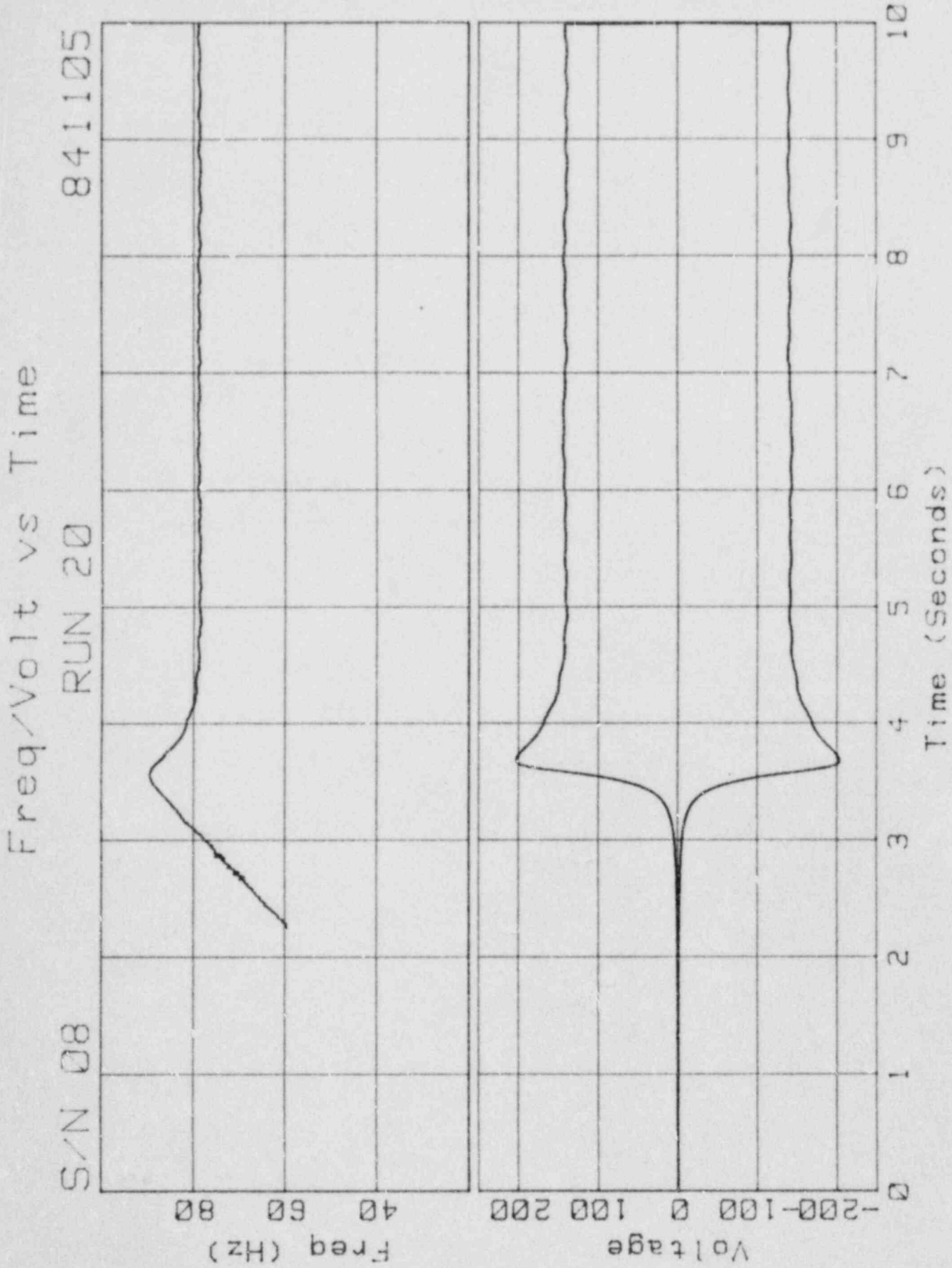
Freq/Volt vs Time
RUN 20
841105
S/N 08
Freq (Hz)
40
60
80
Voltage
-200
-100
0
100
200
Time (Seconds)
0
1
2
3
4
5
6
7
8
9
10

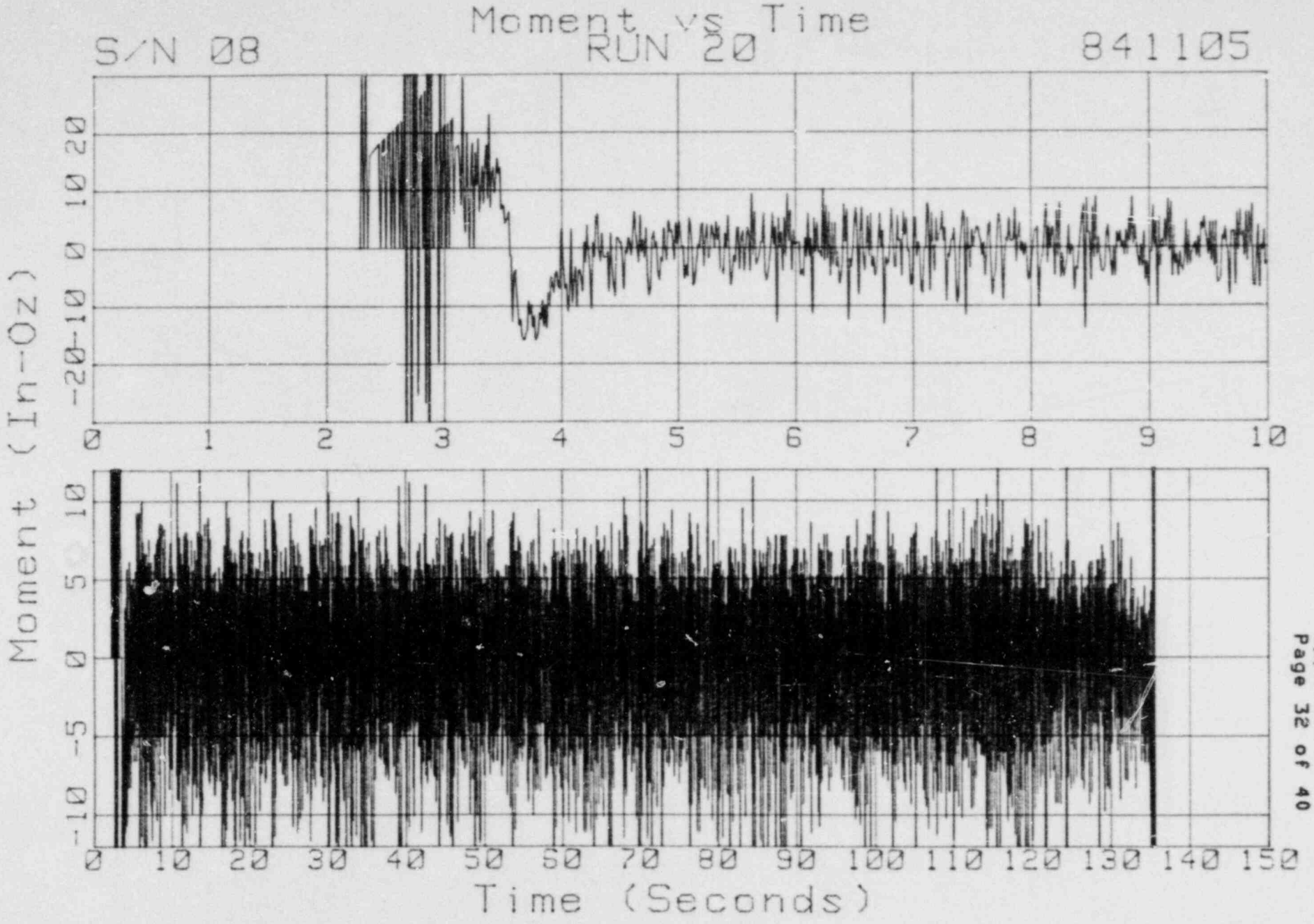
Moment vs Time
S/N 08
RUN 20
841105
Moment (In-Oz)
-20 -10 0 10 20
0 1 2 3 4 5 6 7 8 9 10
-10 -5 0 5 10
0 10 20 30 40 50 60 70 80 90 100 110 120 130 140 150
Time (Seconds)

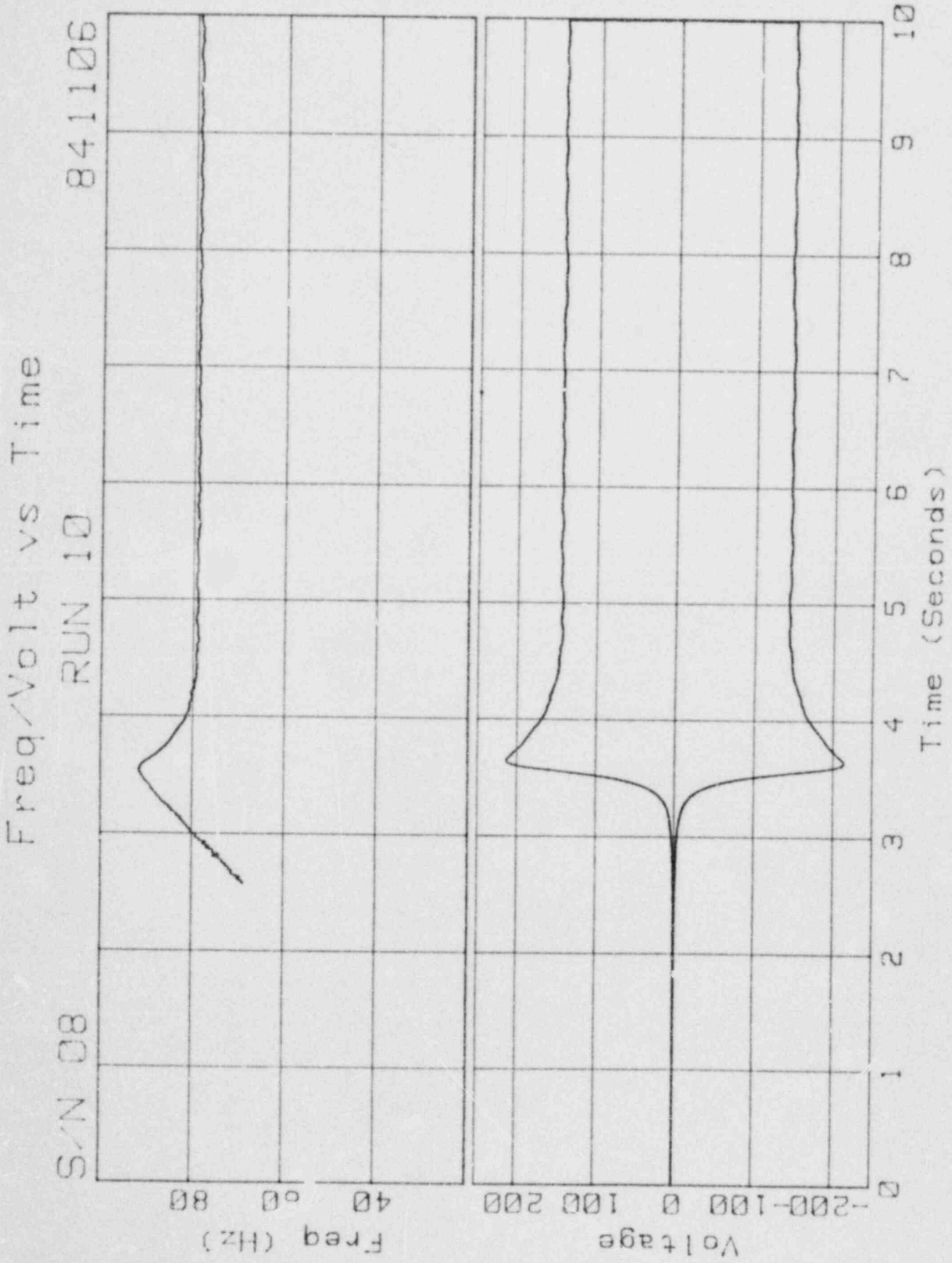
Freq/Volt vs Time
RUN 10
8411106
S/N 08
Freq (Hz)
80
0°
40
Voltage
-200 -100 0 100 200
0 1 2 3 4 5 6 7 8 9 10
Time (Seconds)

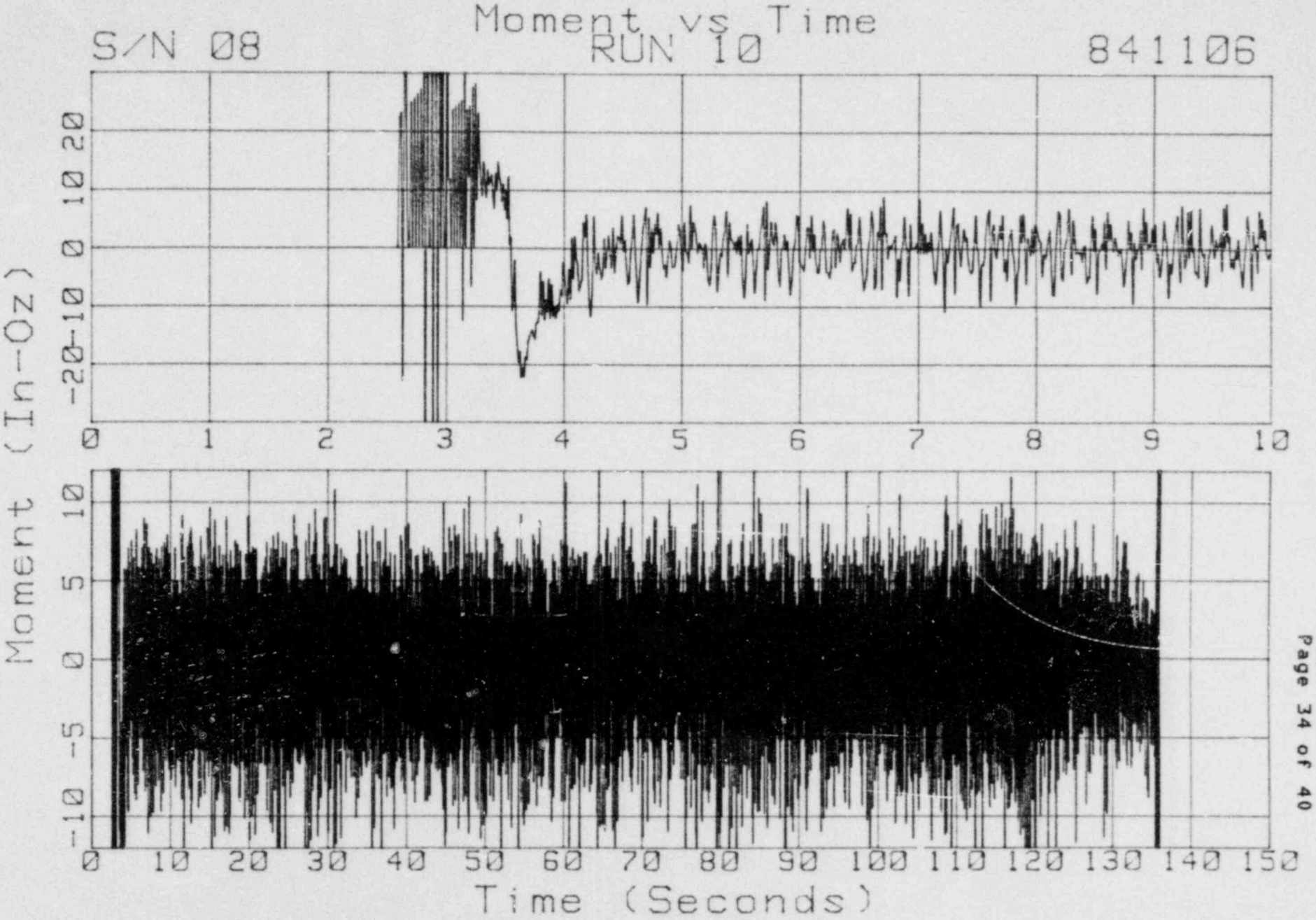
Moment vs Time
S/N 08
RUN 10
841106
Moment (In-Oz)
-20 -10 0 10 20
0 1 2 3 4 5 6 7 8 9 10
-10 -5 0 5 10
0 10 20 30 40 50 60 70 80 90 100 110 120 130 140 150
Time (Seconds)

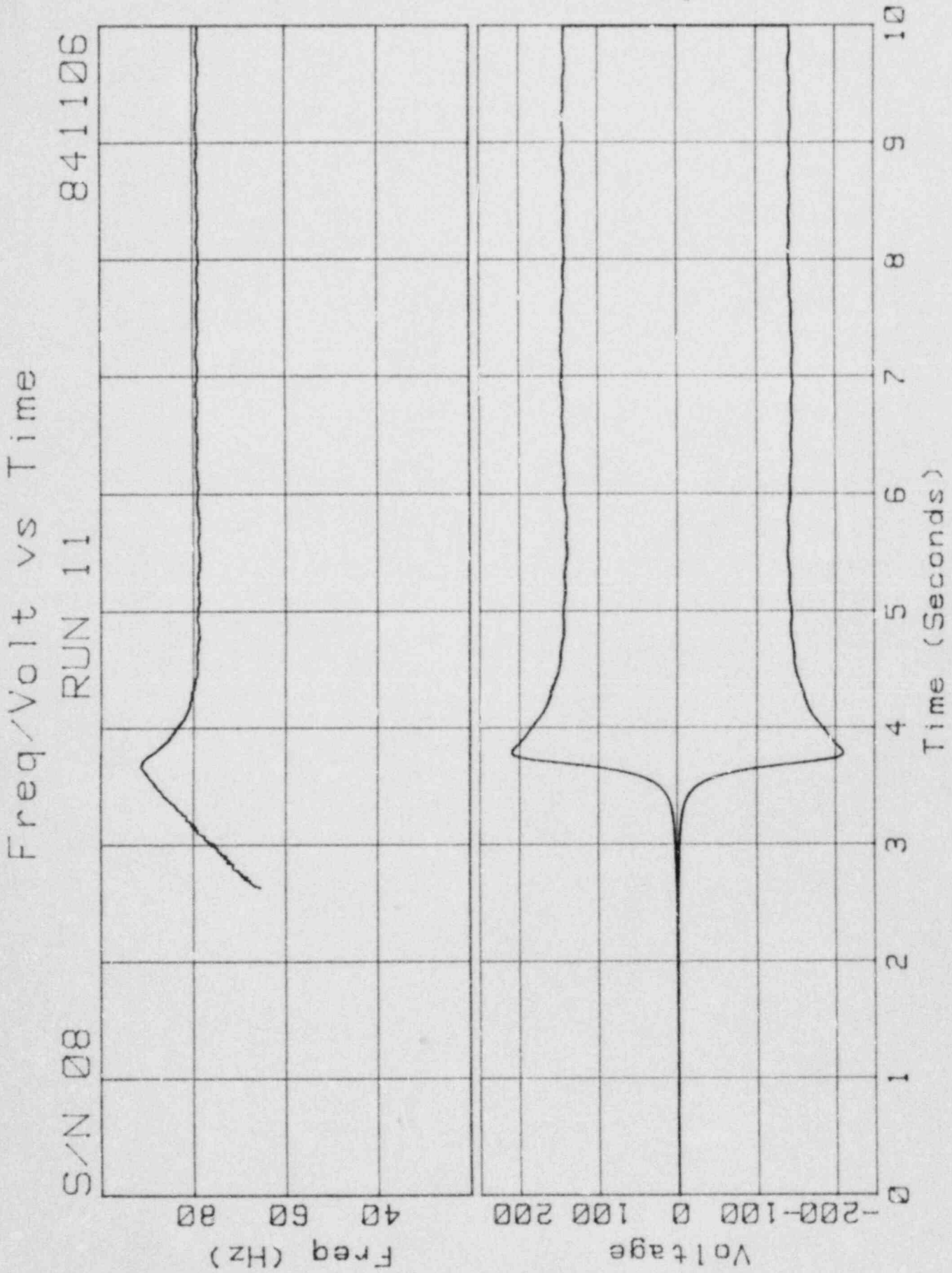
Freq/Volt vs Time
RUN 11
841106
S/N 08
Freq (Hz)
40
60
80
Voltage
-200
-100
0
100
200
0
1
2
3
4
5
6
7
8
9
10
Time (Seconds)

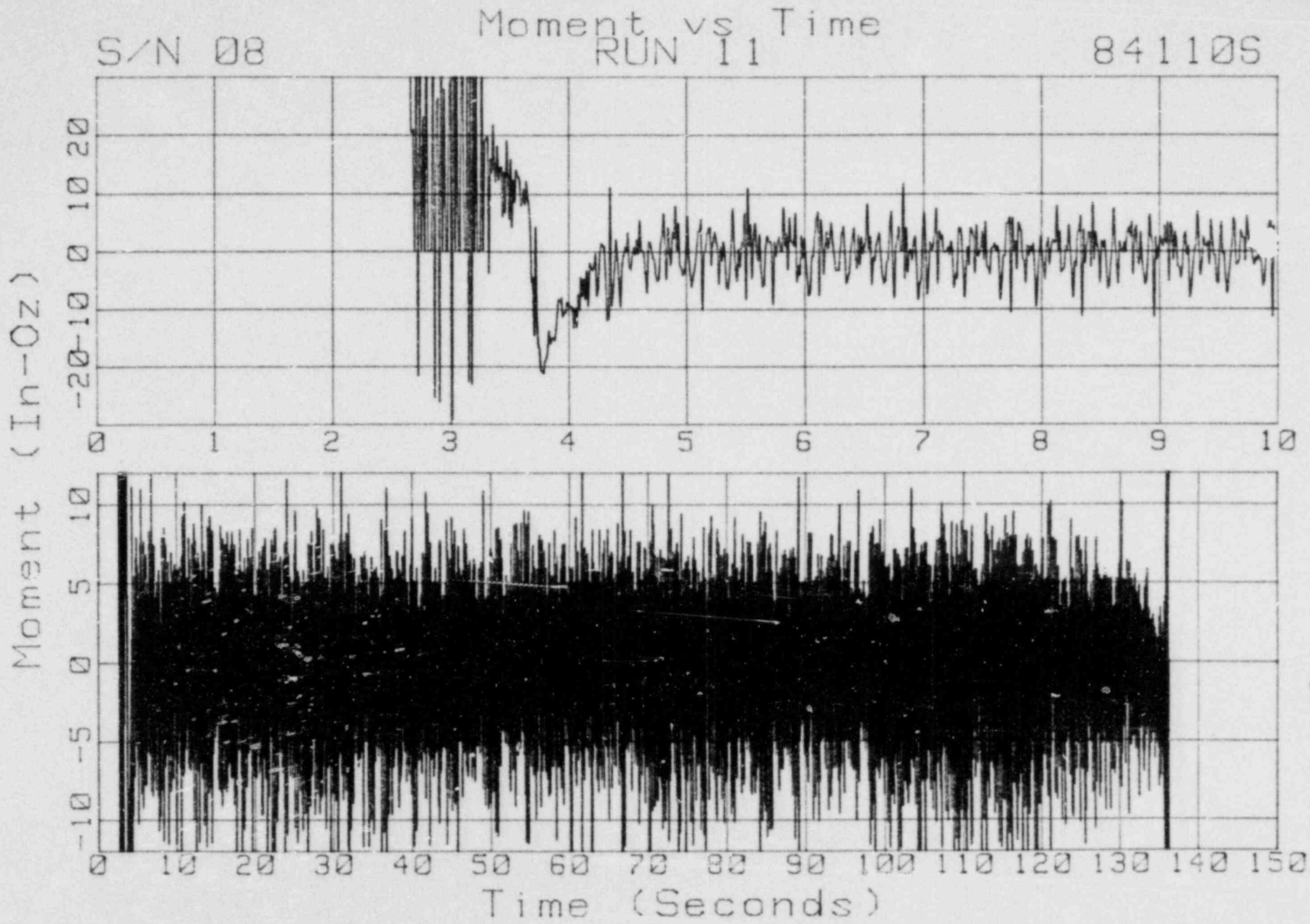
Moment vs Time
S/N 08
RUN 11
841105
Moment (In-Oz)
-20 -10 0 10 20
0 1 2 3 4 5 6 7 8 9 10
-10 -5 0 5 10
0 10 20 30 40 50 60 70 80 90 100 110 120 130 140 150
Time (Seconds)

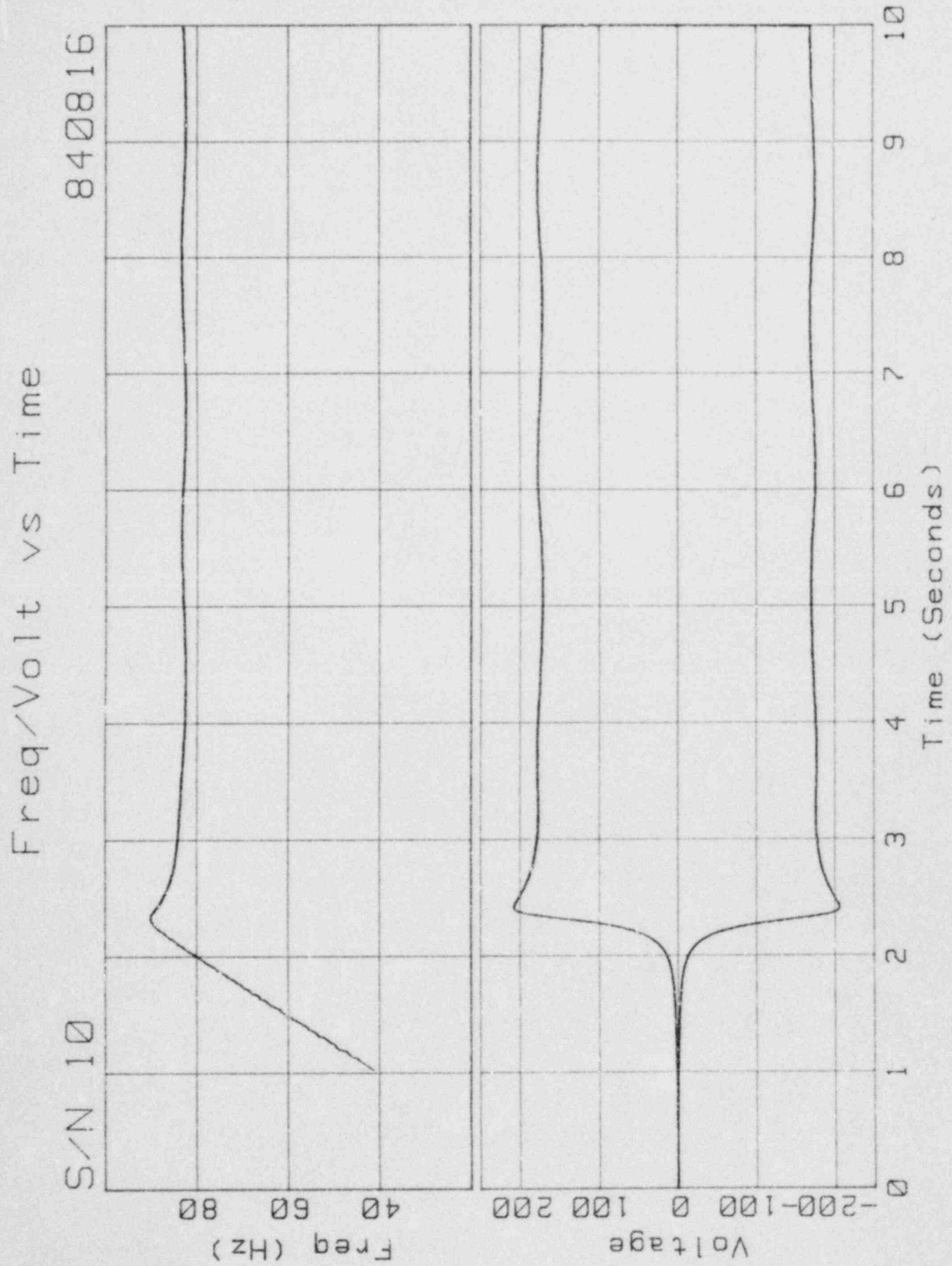
Freq/Volt vs Time
8408816
S/N 10
Freq (Hz)
40
60
80
Voltage
-200
-100
0
100
200
0
1
2
3
4
5
6
7
8
9
10
Time (Seconds)

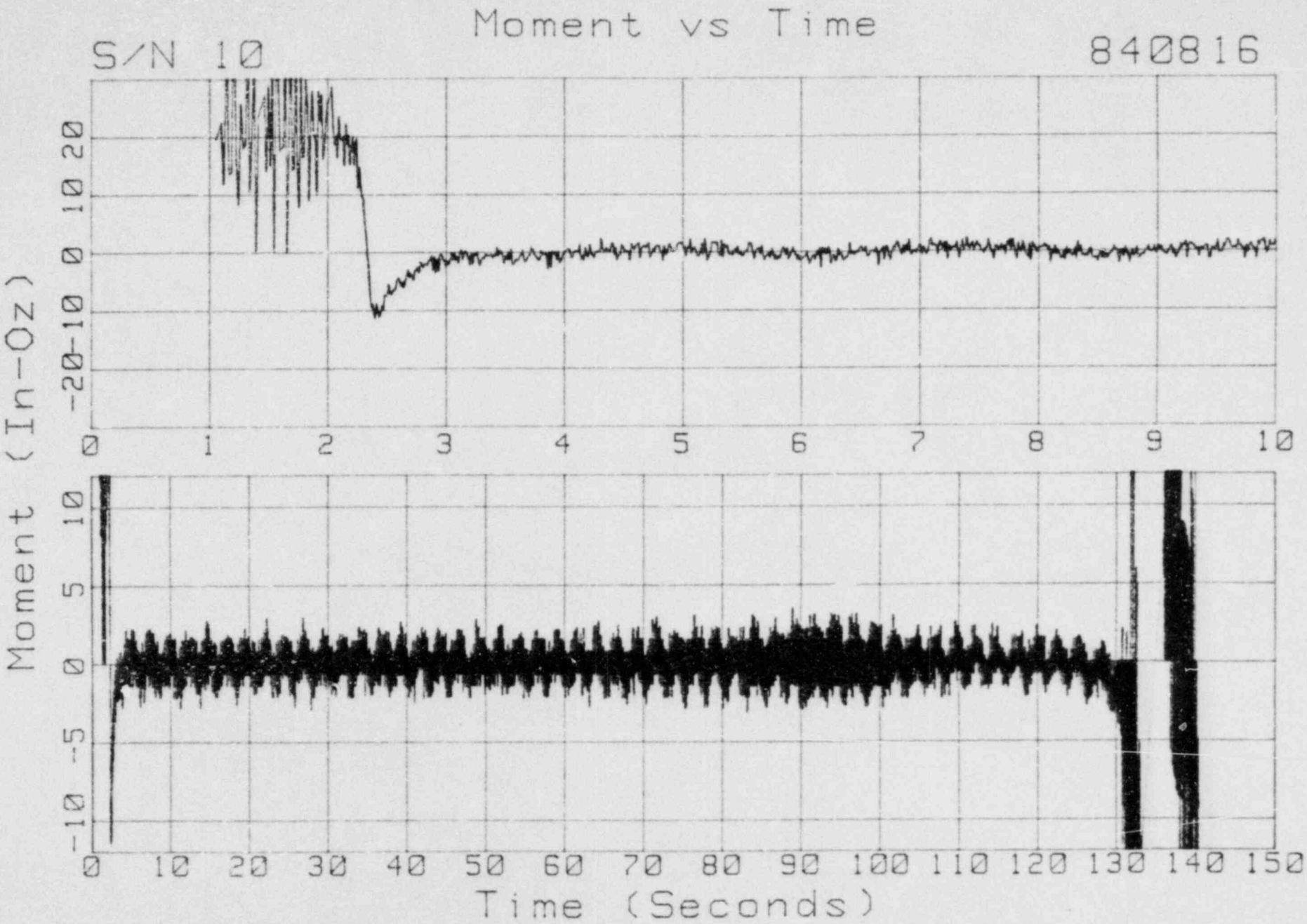
Moment vs Time
S/N 10
840816
Moment (In-Oz)
-20 -10 0 10 20
0 1 2 3 4 5 6 7 8 9 10
-10 -5 0 5 10
0 10 20 30 40 50 60 70 80 90 100 110 120 130 140 150
Time (Seconds)

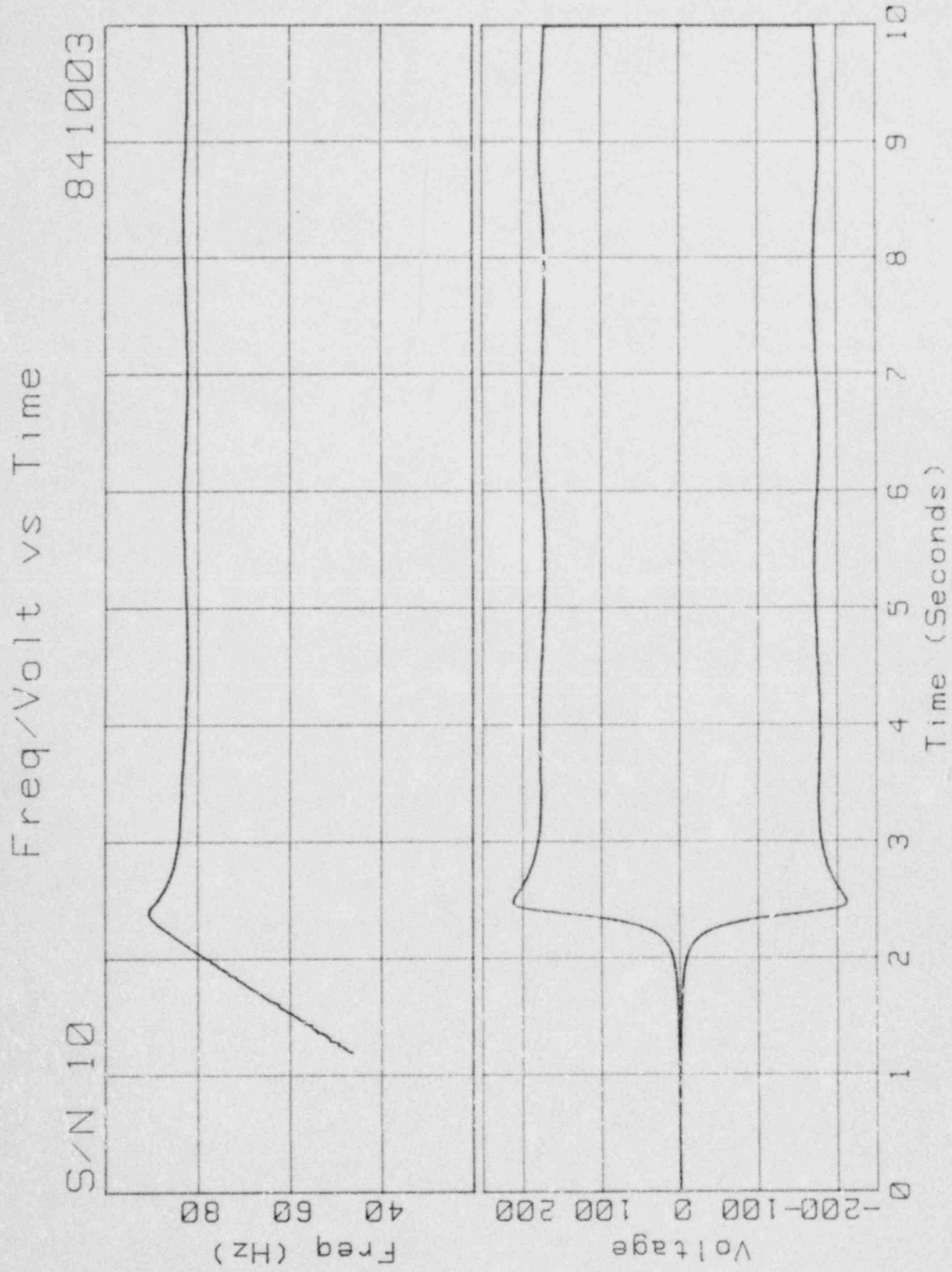
Freq/Volt vs Time
841003
S/N 10
Freq (Hz)
40
60
80
Voltage
-200
-100
0
100
200
0
1
2
3
4
5
6
7
8
9
10
Time (Seconds)

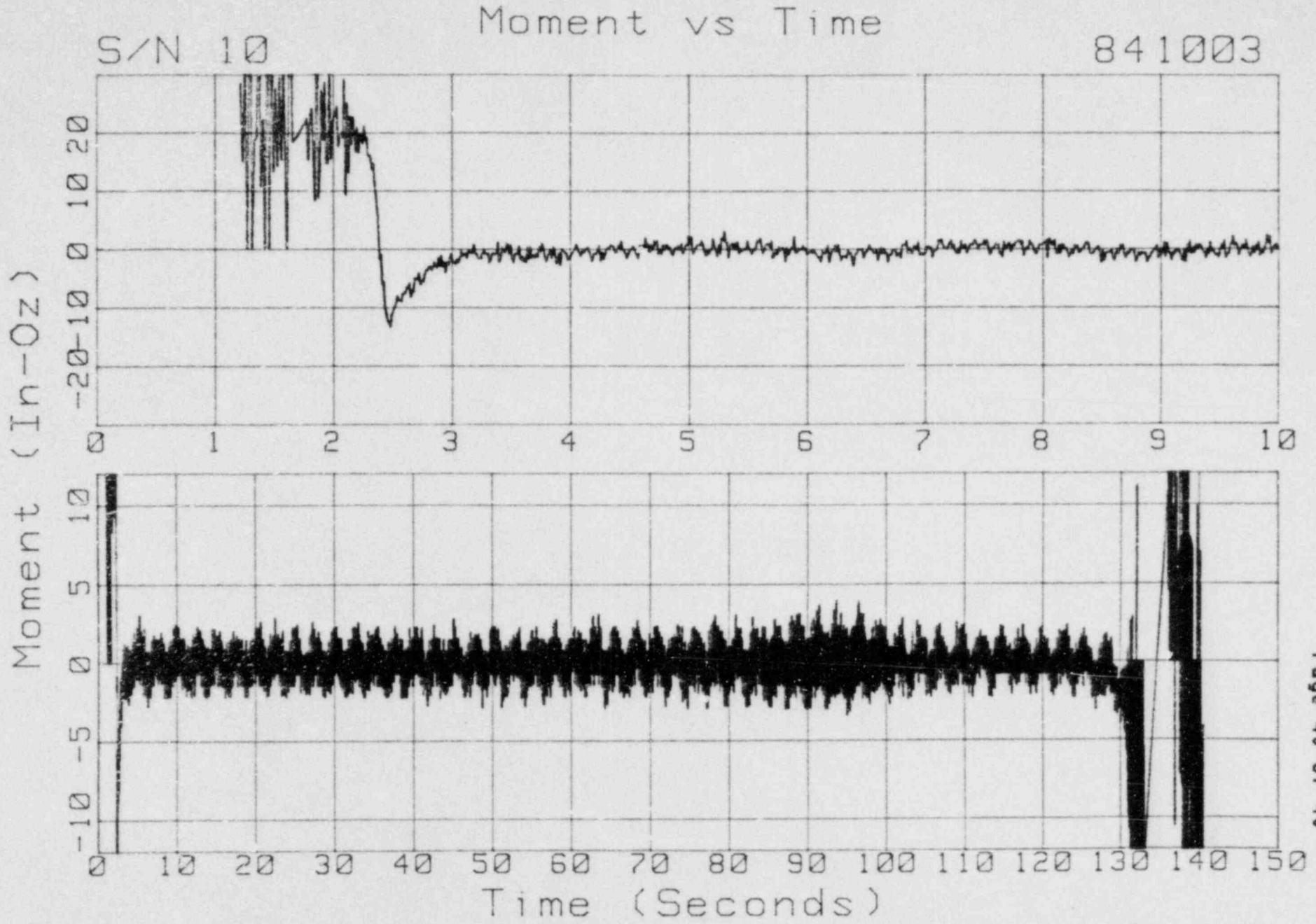
Moment vs Time
S/N 10
841003
Moment (In-Oz)
20
10
0
-10
-20
0
1
2
3
4
5
6
7
8
9
10
10
5
0
-5
-10
0
10
20
30
40
50
60
70
80
90
100
110
120
130
140
150
Time (Seconds)

APPENDIX E

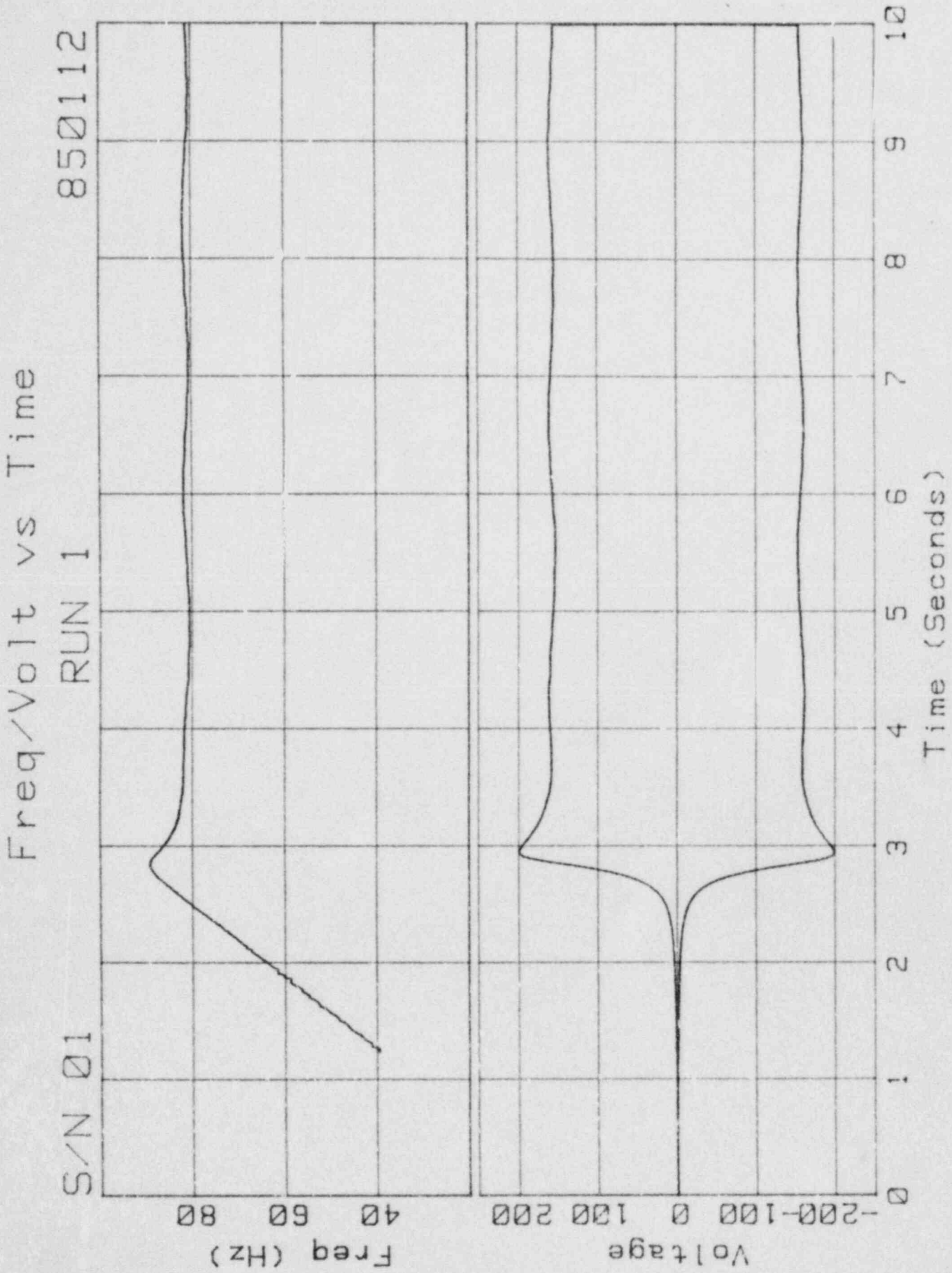
Freq/Volt vs Time
RUN 1
8501112
S/N 01
Freq (Hz)
40
60
80
Voltage
-200
-100
0
100
200
Time (Seconds)
0
1
2
3
4
5
6
7
8
9
10

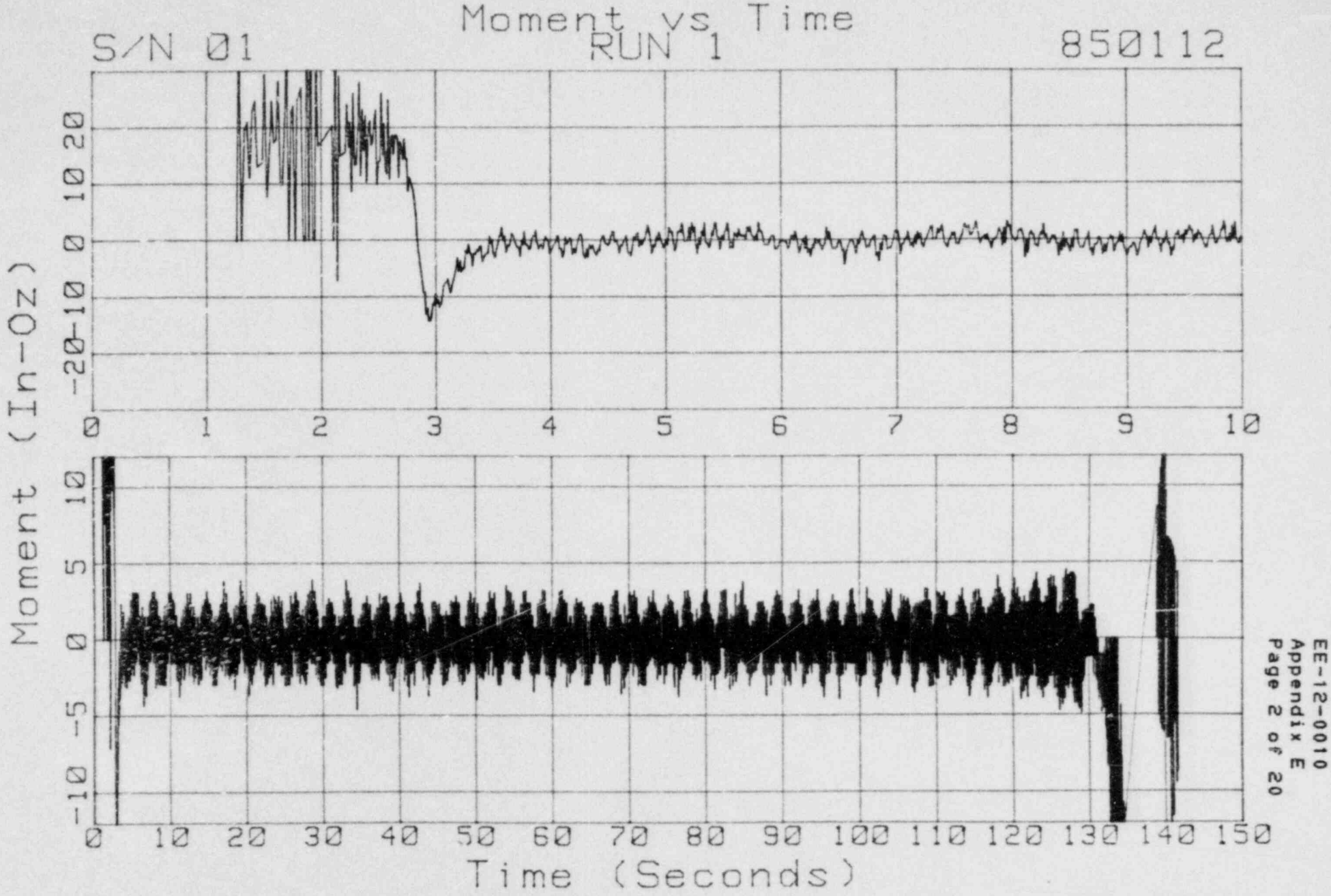
Moment vs Time
S/N 01
RUN 1
850112
Moment (In-Oz)
-20 -10 0 10 20
0 1 2 3 4 5 6 7 8 9 10
-10 -5 0 5 10
0 10 20 30 40 50 60 70 80 90 100 110 120 130 140 150
Time (Seconds)

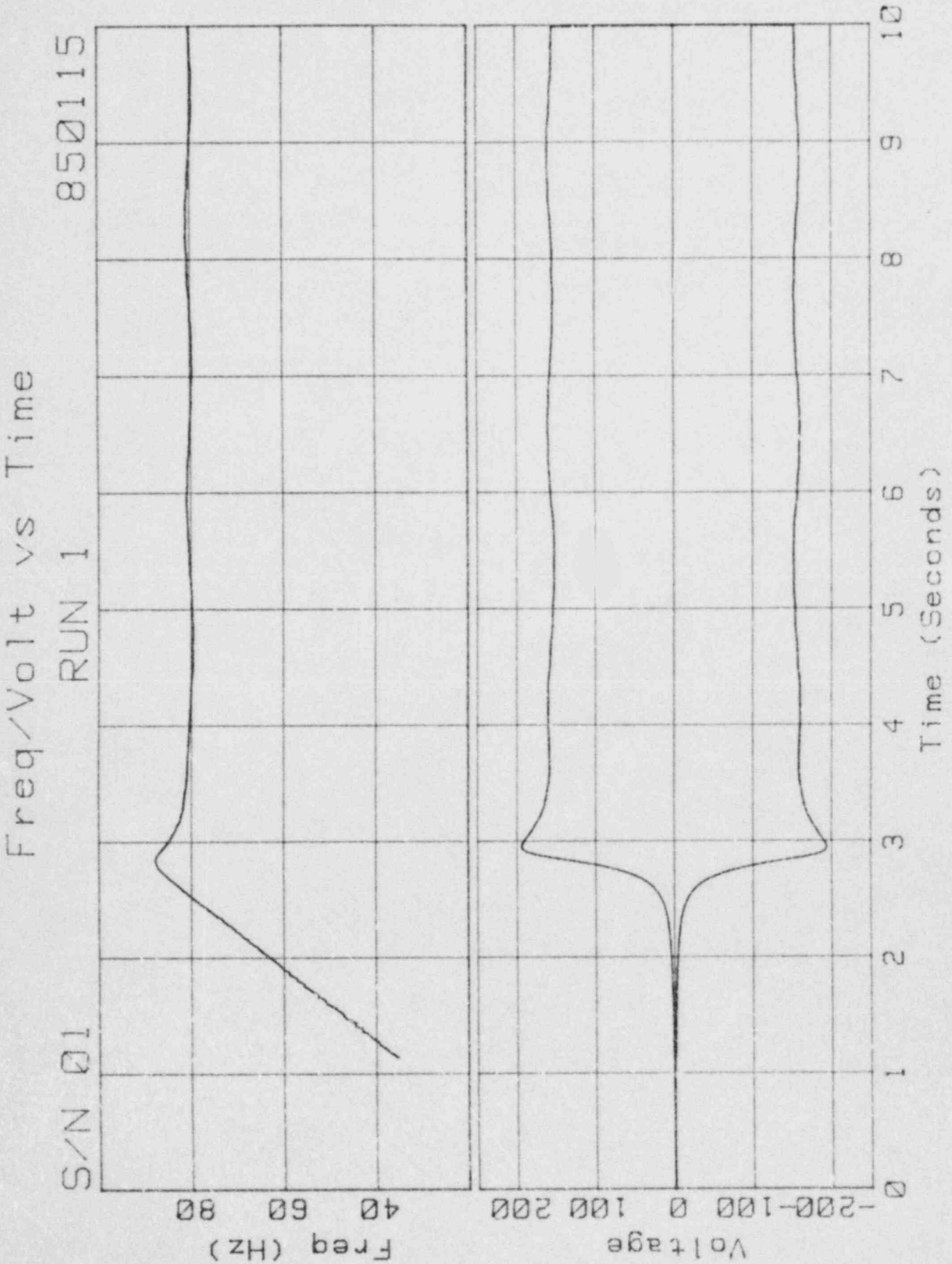
Freq/Volt vs Time
RUN 1
S/N 01
8501115
Freq (Hz)
40
60
80
Voltage
-200
-100
0
100
200
Time (Seconds)
0
1
2
3
4
5
6
7
8
9
10

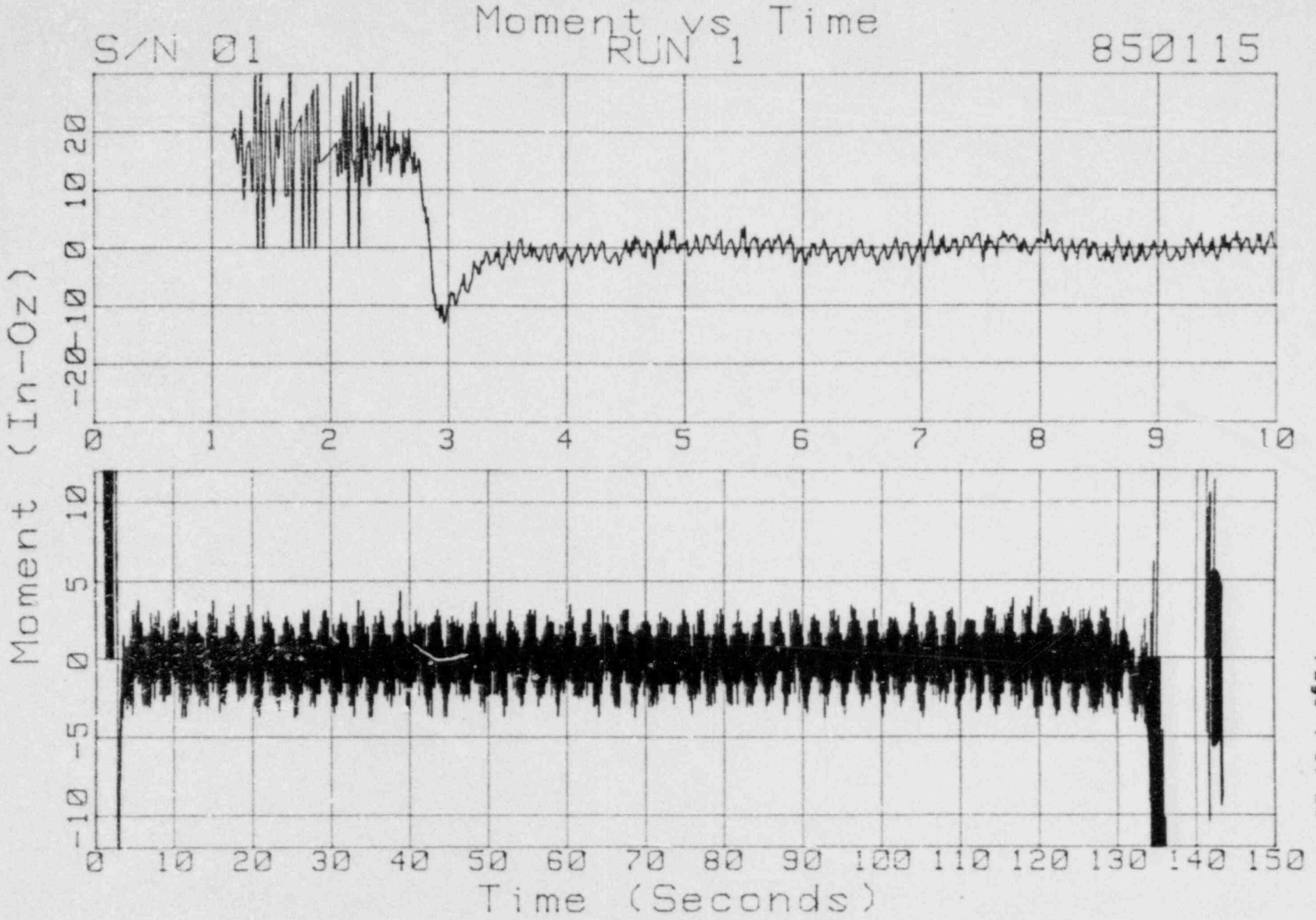
Moment vs Time
S/N 01
RUN 1
850115
Moment (In-Oz)
-20 -10 0 10 20
0 1 2 3 4 5 6 7 8 9 10
-10 -5 0 5 10
0 10 20 30 40 50 60 70 80 90 100 110 120 130 140 150
Time (Seconds)

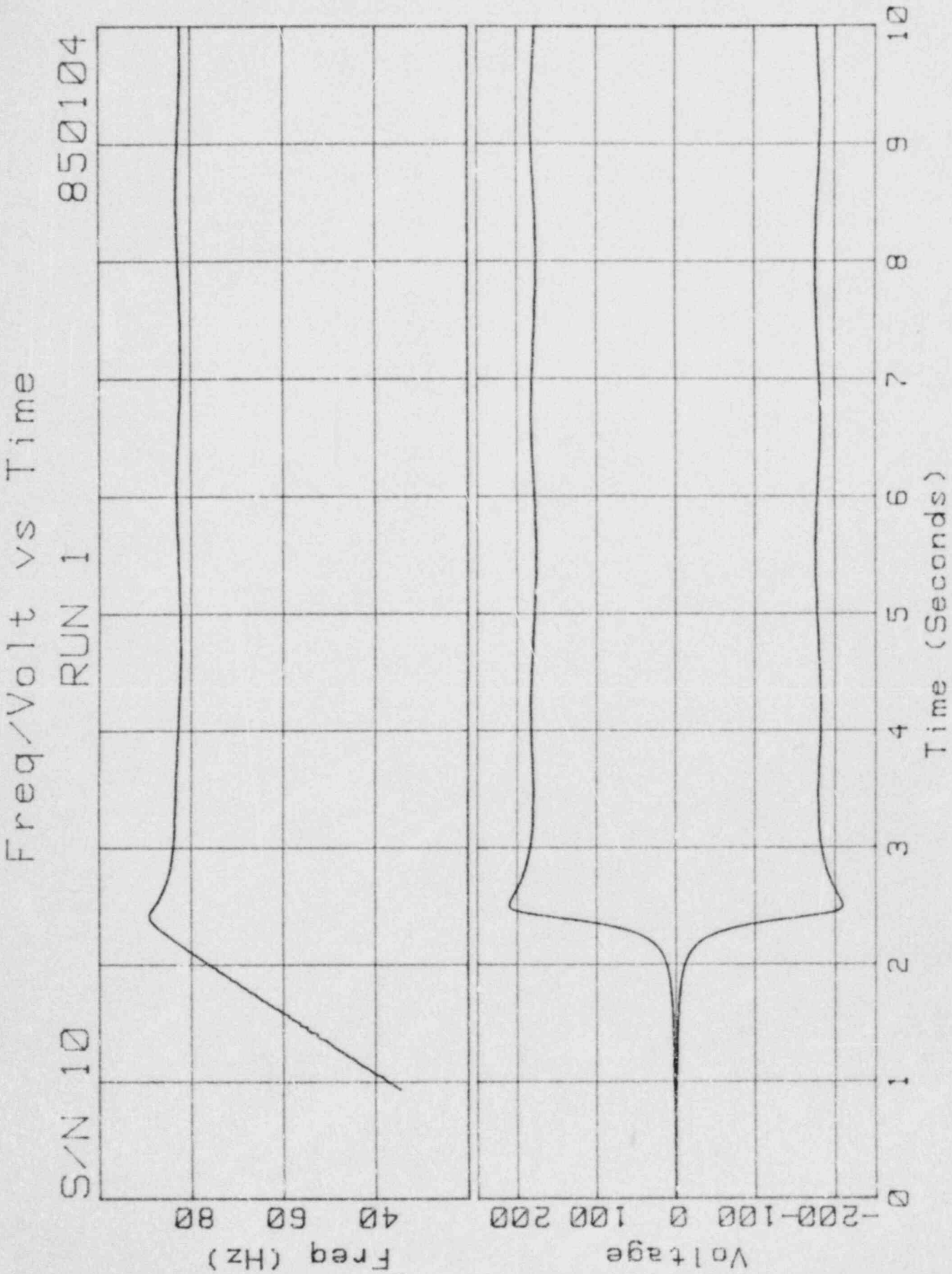
Freq/Volt vs Time
RUN 1
850104
S/N 10
Freq (Hz)
40
60
80
Voltage
-200
-100
0
100
200
Time (Seconds)
0
1
2
3
4
5
6
7
8
9
10

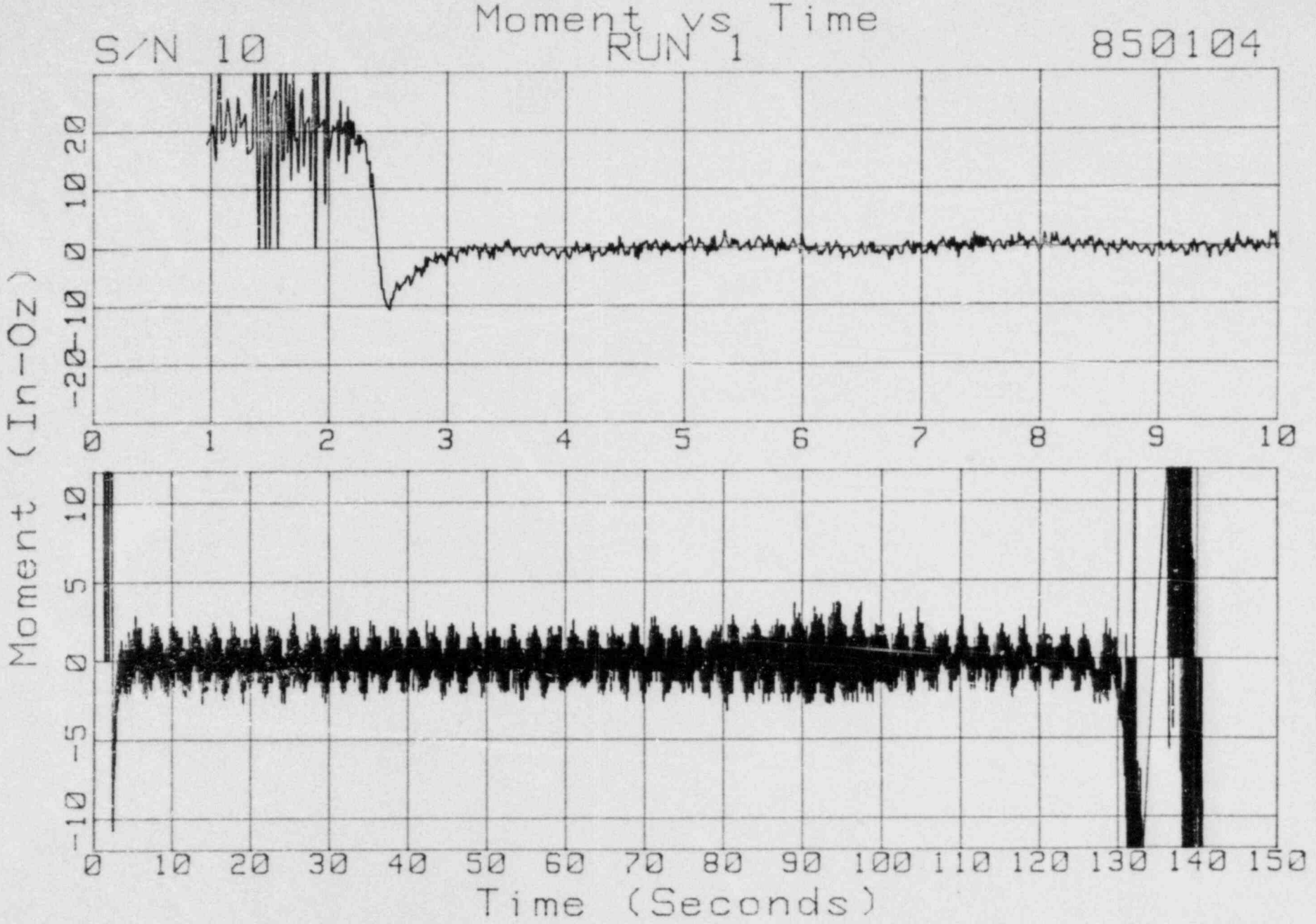
Moment vs Time
S/N 10
RUN 1
850104
Moment (In-Oz)
-20 -10 0 10 20
0 1 2 3 4 5 6 7 8 9 10
-10 -5 0 5 10
0 10 20 30 40 50 60 70 80 90 100 110 120 130 140 150
Time (Seconds)

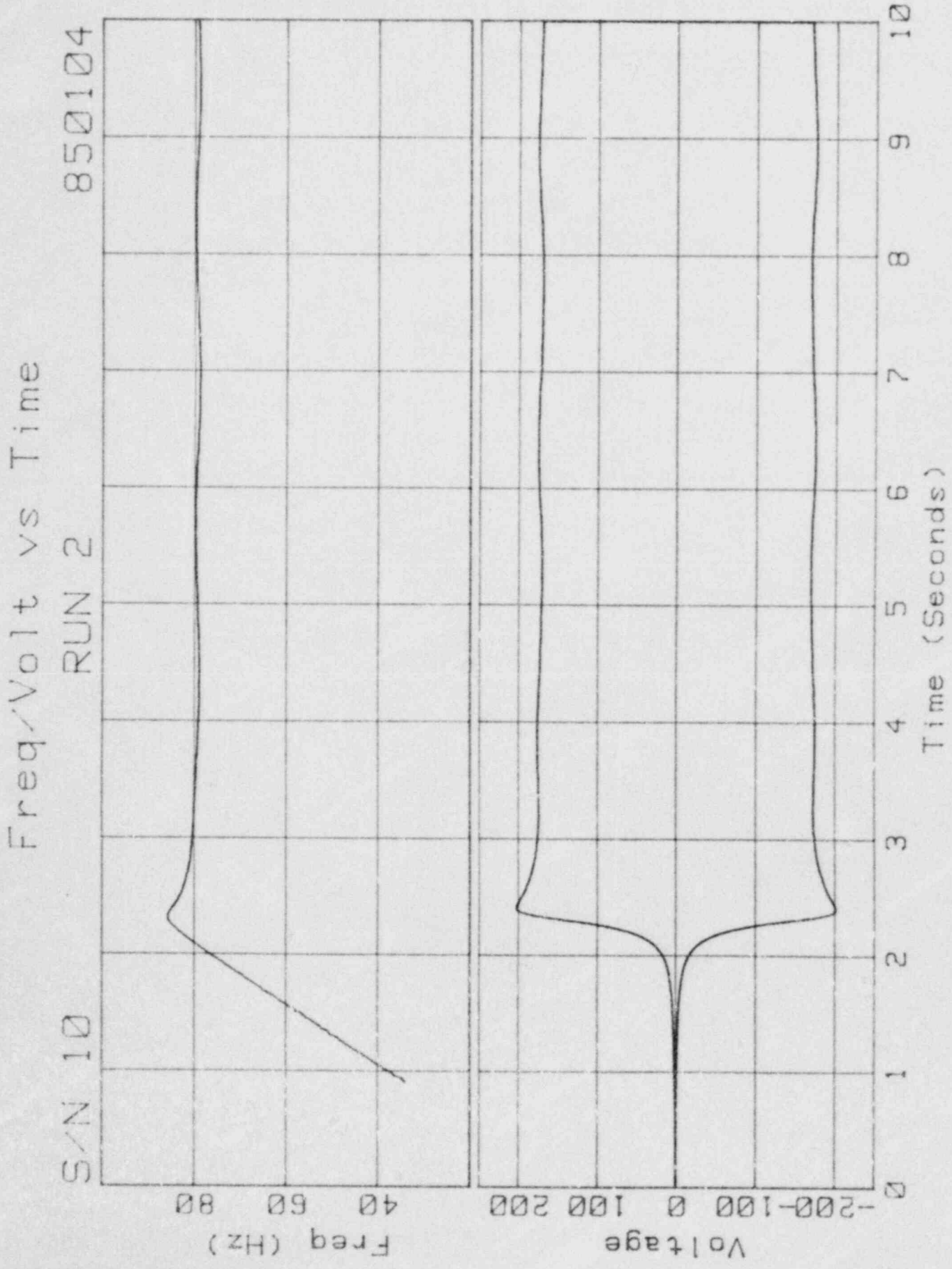
Freq/Volt vs Time
RUN 2
S/N 10
850104
Freq (Hz)
40
60
80
Voltage
-200
-100
0
100
200
Time (Seconds)
0
1
2
3
4
5
6
7
8
9
10

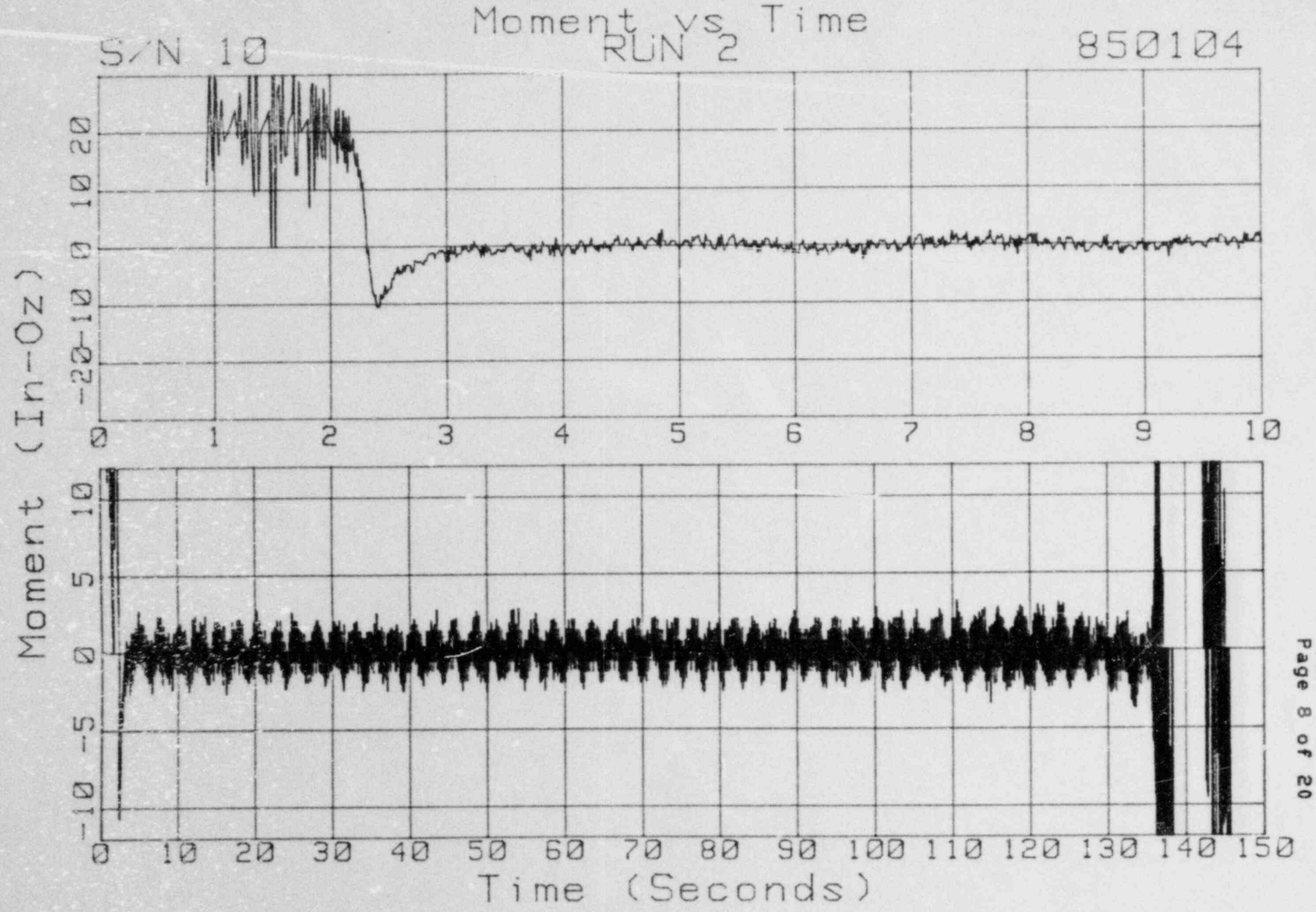
Moment vs Time
S/N 10
RUN 2
850104
Moment (In-Oz)
-20 -10 0 10 20
0 1 2 3 4 5 6 7 8 9 10
-10 -5 0 5 10
0 10 20 30 40 50 60 70 80 90 100 110 120 130 140 150
Time (Seconds)

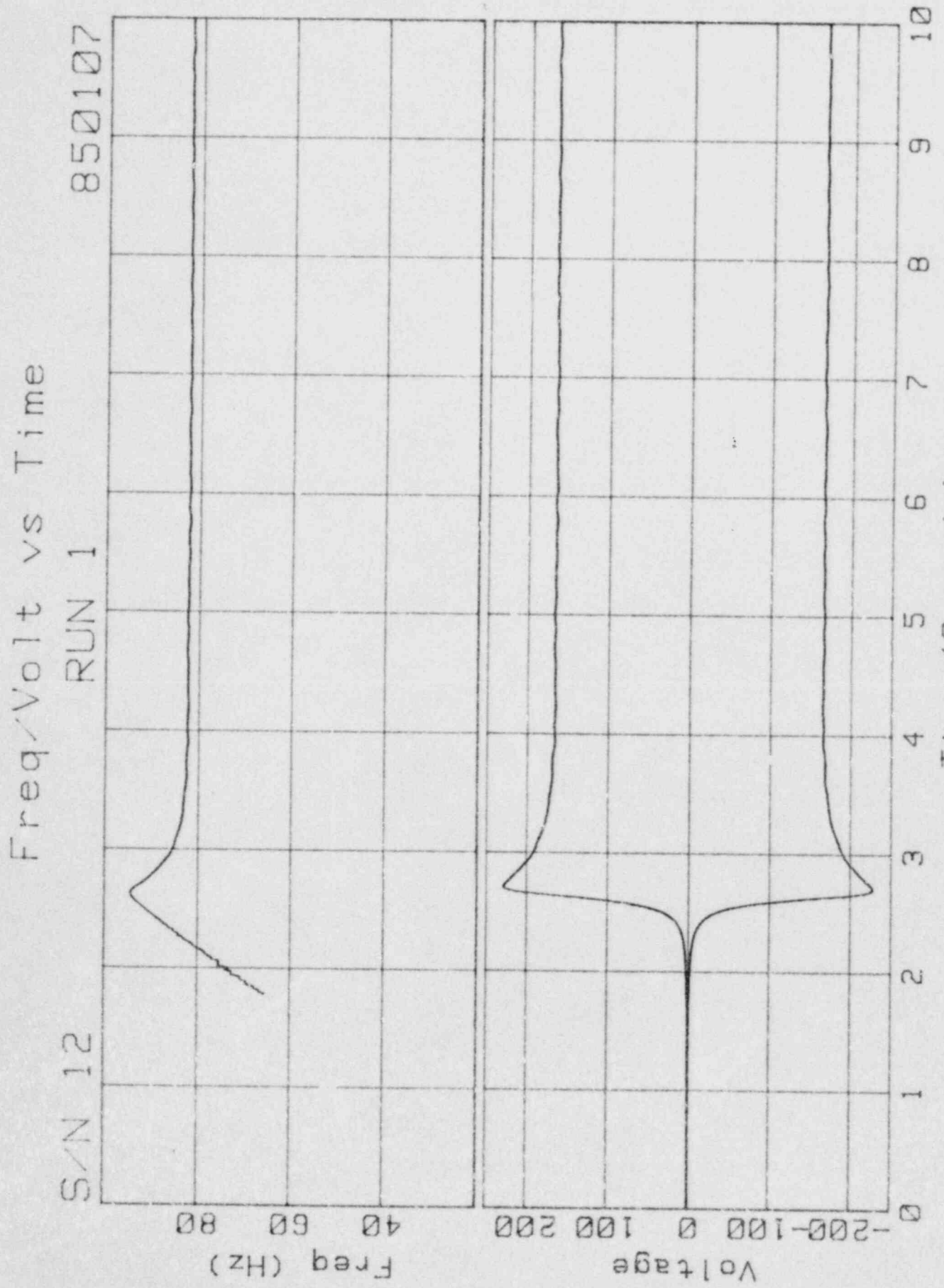
Freq/Volt vs Time
RUN 1
850107
S/N 12
Freq (Hz)
40
60
80
Voltage
-200
-100
0
100
200
0
1
2
3
4
5
6
7
8
9
10
Time (Seconds)

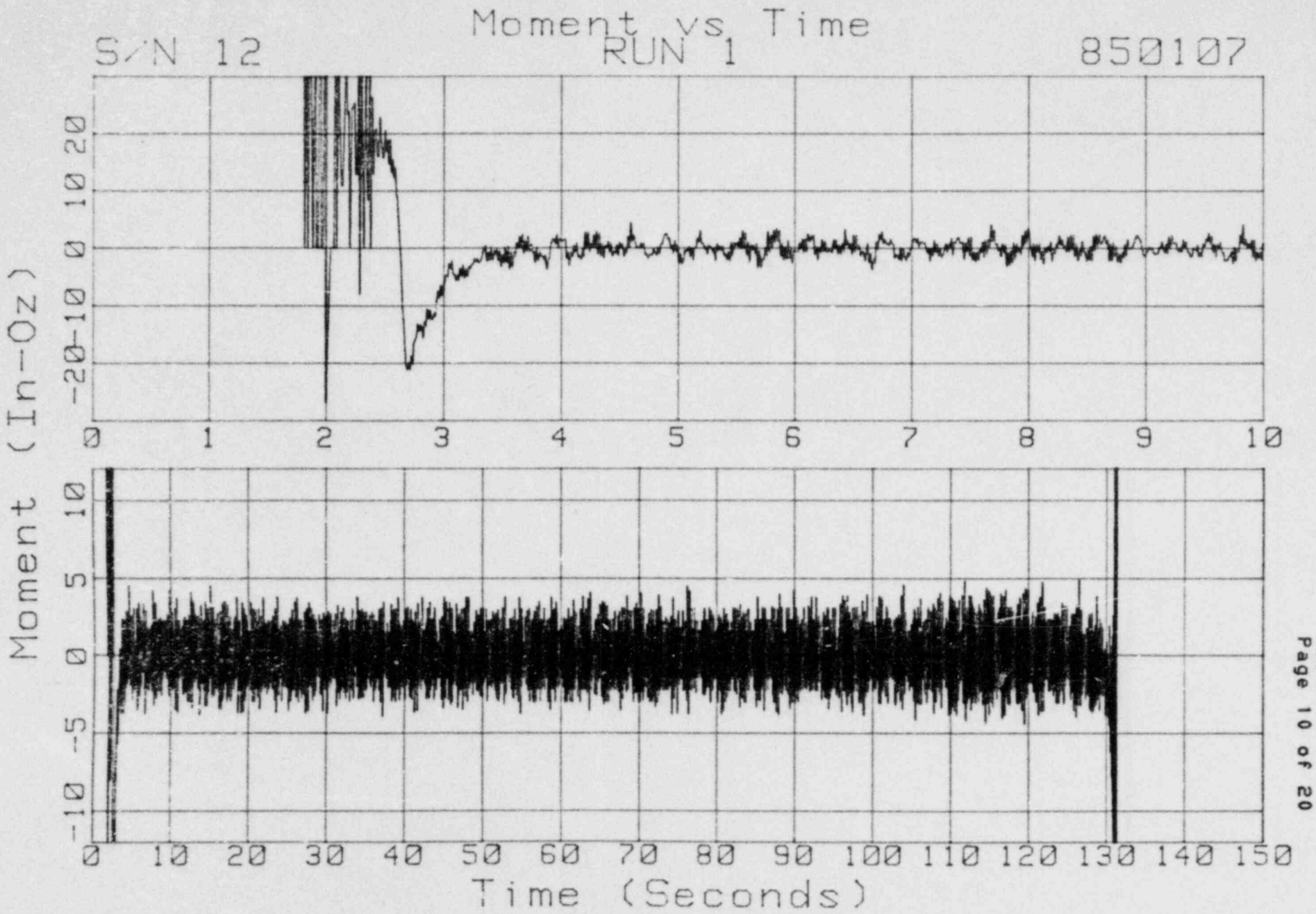
Moment vs Time
S/N 12
RUN 1
850107
Moment (In-Oz)
-20 -10 0 10 20
0 1 2 3 4 5 6 7 8 9 10
-10 -5 0 5 10
0 10 20 30 40 50 60 70 80 90 100 110 120 130 140 150
Time (Seconds)

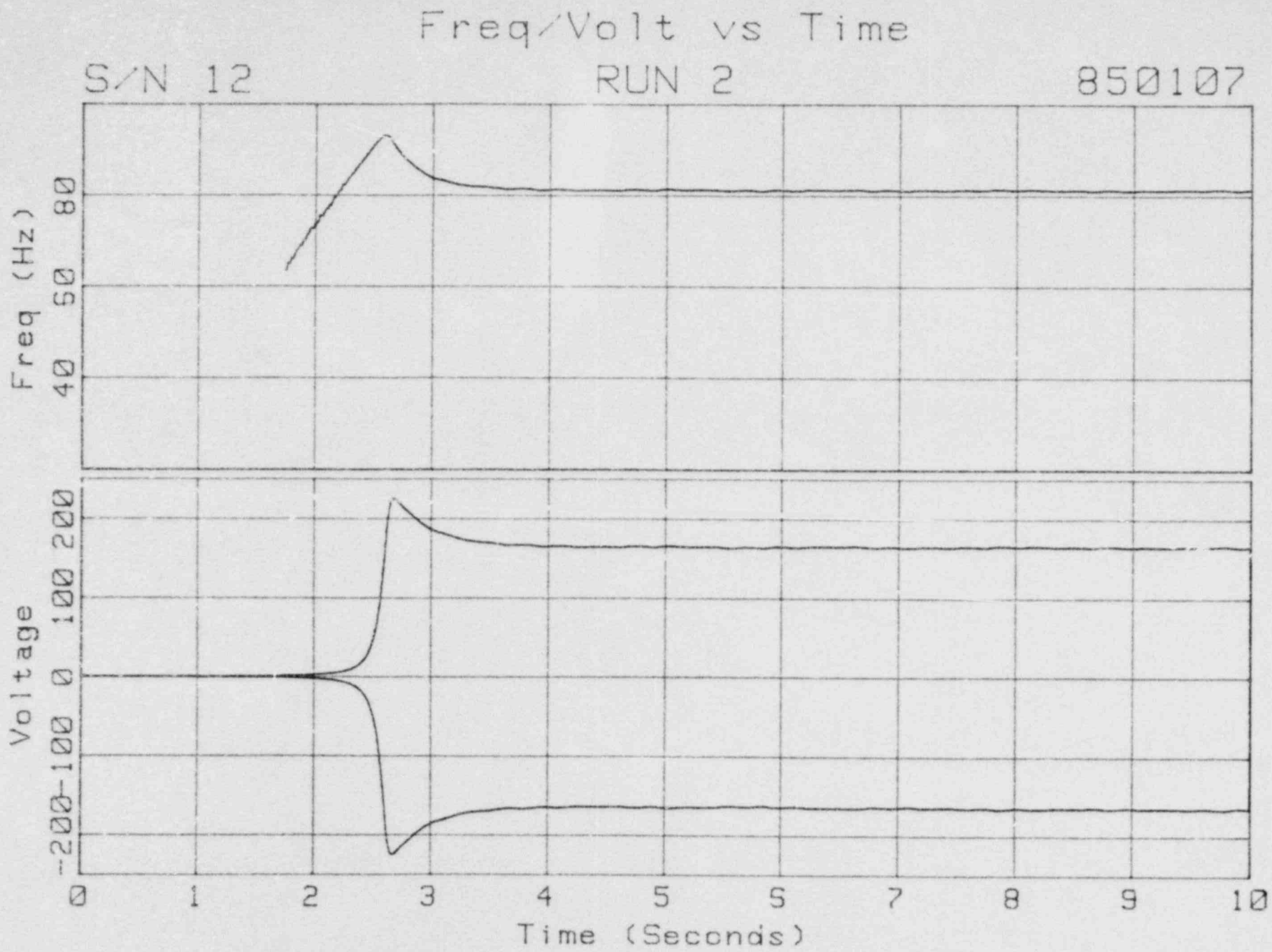
Freq/Volt vs Time
S/N 12
RUN 2
850107
Freq (Hz)
40
60
80
Voltage
-200
-100
0
100
200
0
1
2
3
4
5
6
7
8
9
10
Time (Seconds)

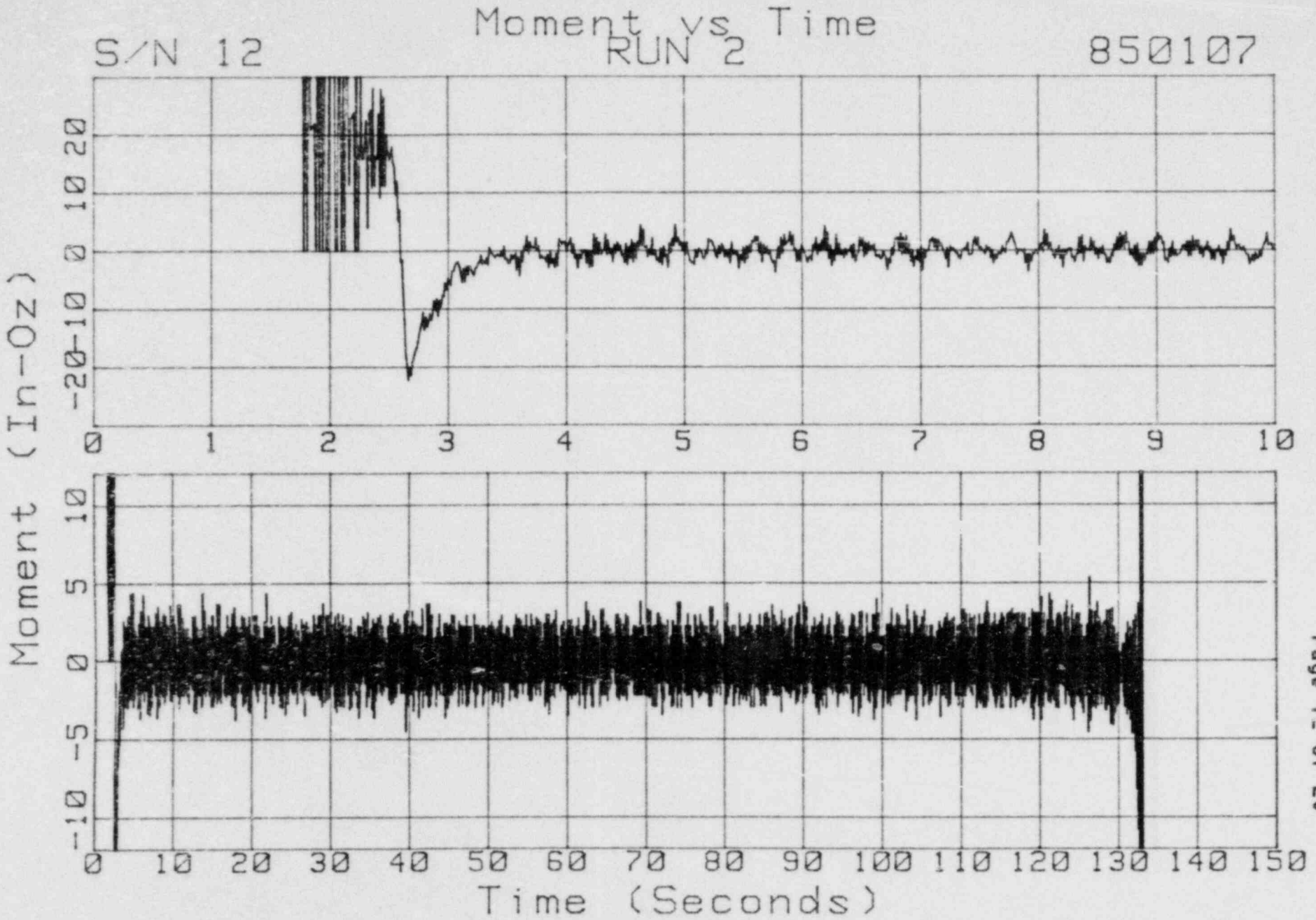
Moment vs Time
S/N 12
RUN 2
850107
Moment (In-Oz)
-20 -10 0 10 20
0 1 2 3 4 5 6 7 8 9 10
-10 -5 0 5 10
0 10 20 30 40 50 60 70 80 90 100 110 120 130 140 150
Time (Seconds)

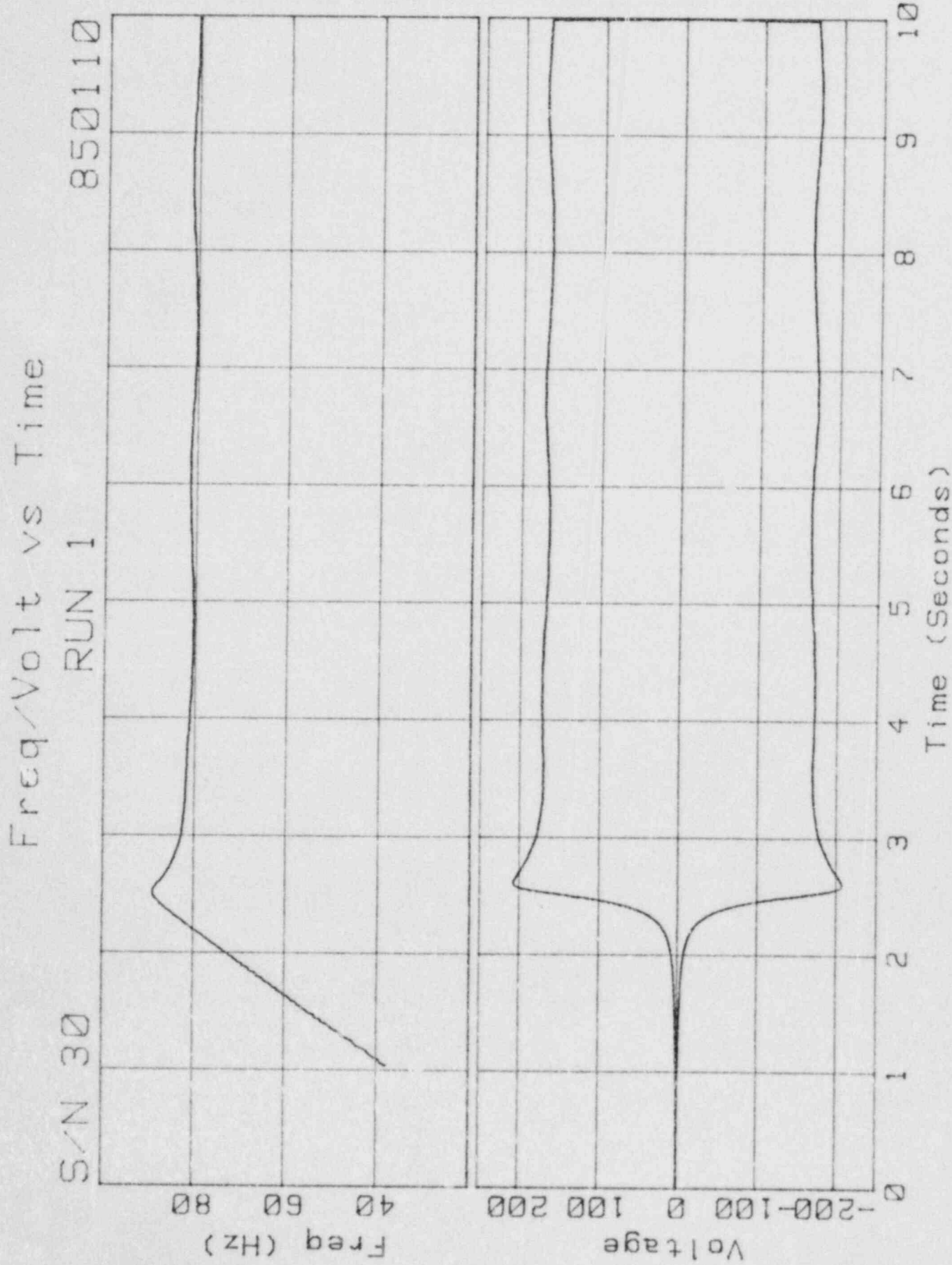
Freq/Volt vs Time
RUN 1
850110
S/N 30
Freq (Hz)
40
60
80
Voltage
-200
-100
0
100
200
Time (Seconds)
0
1
2
3
4
5
6
7
8
9
10

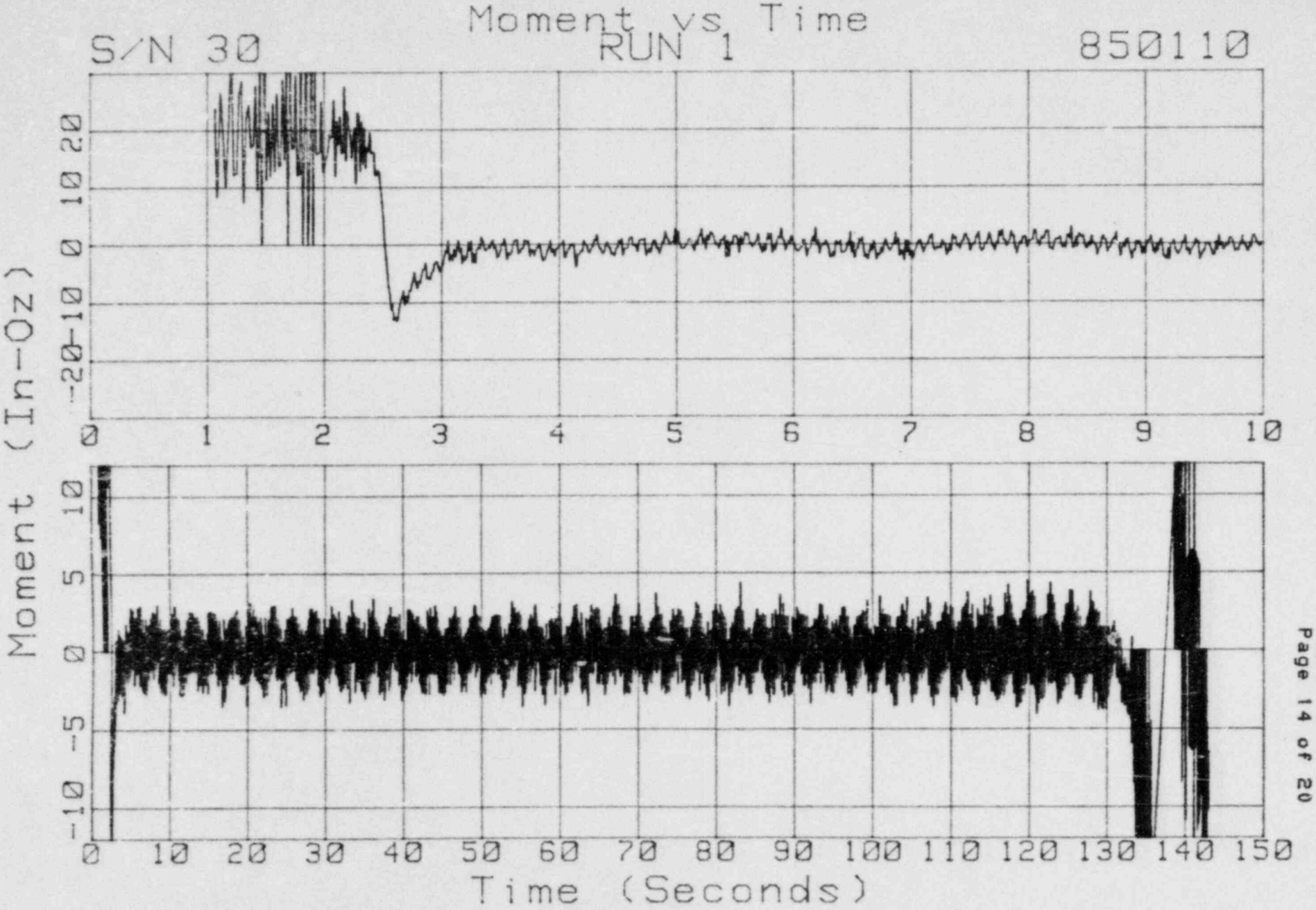
Moment vs Time
S/N 30
RUN 1
850110
Moment (In-Oz)
-20 -10 0 10 20
0 1 2 3 4 5 6 7 8 9 10
-10 -5 0 5 10
0 10 20 30 40 50 60 70 80 90 100 110 120 130 140 150
Time (Seconds)

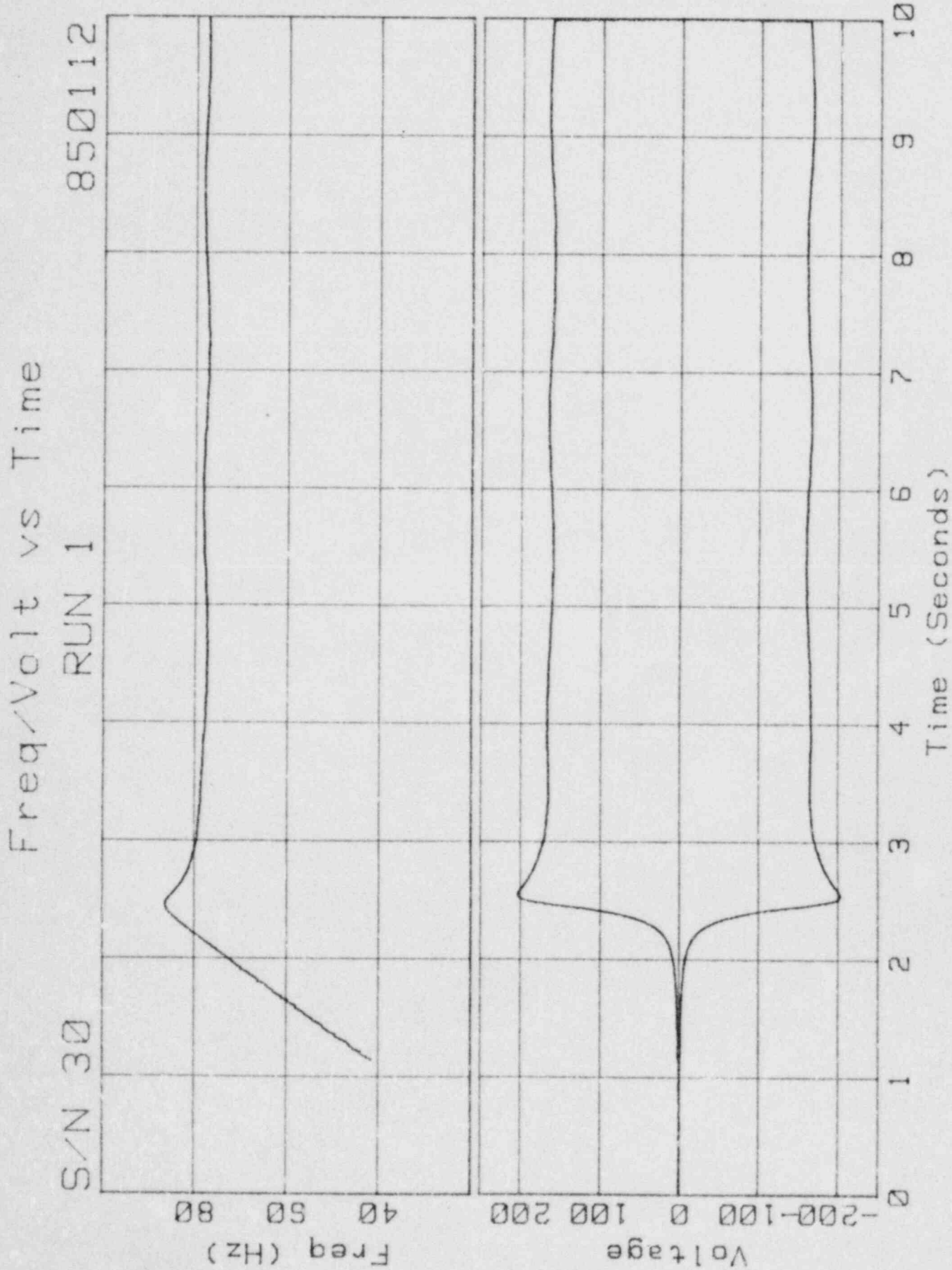
Freq/Volt vs Time
RUN 1
8501112
S/N 30
Freq (Hz)
40
50
60
Voltage
-200
-100
0
100
200
0
1
2
3
4
5
6
7
8
9
10
Time (Seconds)

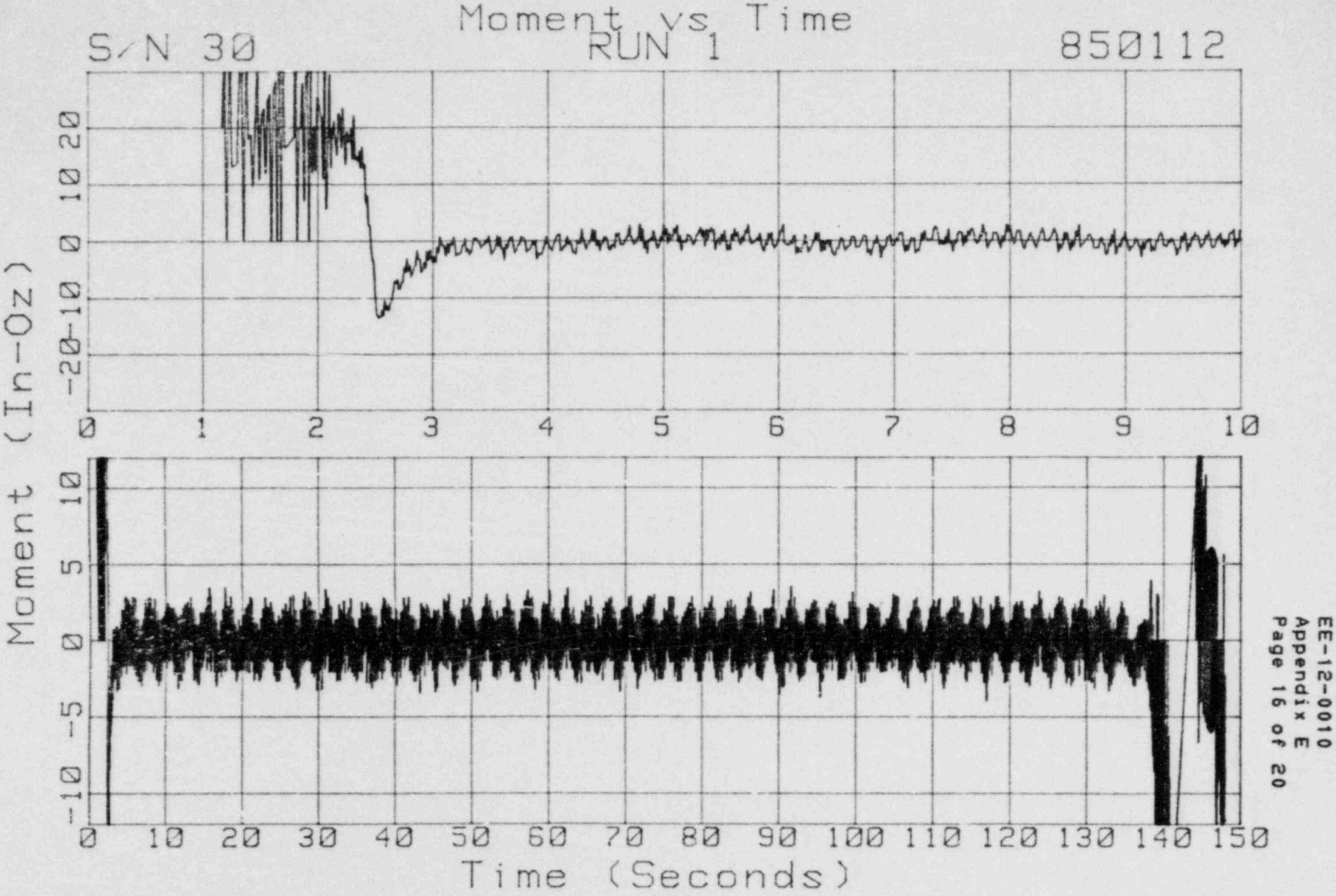
Moment vs Time
S/N 30
RUN 1
850112
Moment (In-Oz)
-20 -10 0 10 20
0 1 2 3 4 5 6 7 8 9 10
-10 -5 0 5 10
0 10 20 30 40 50 60 70 80 90 100 110 120 130 140 150
Time (Seconds)

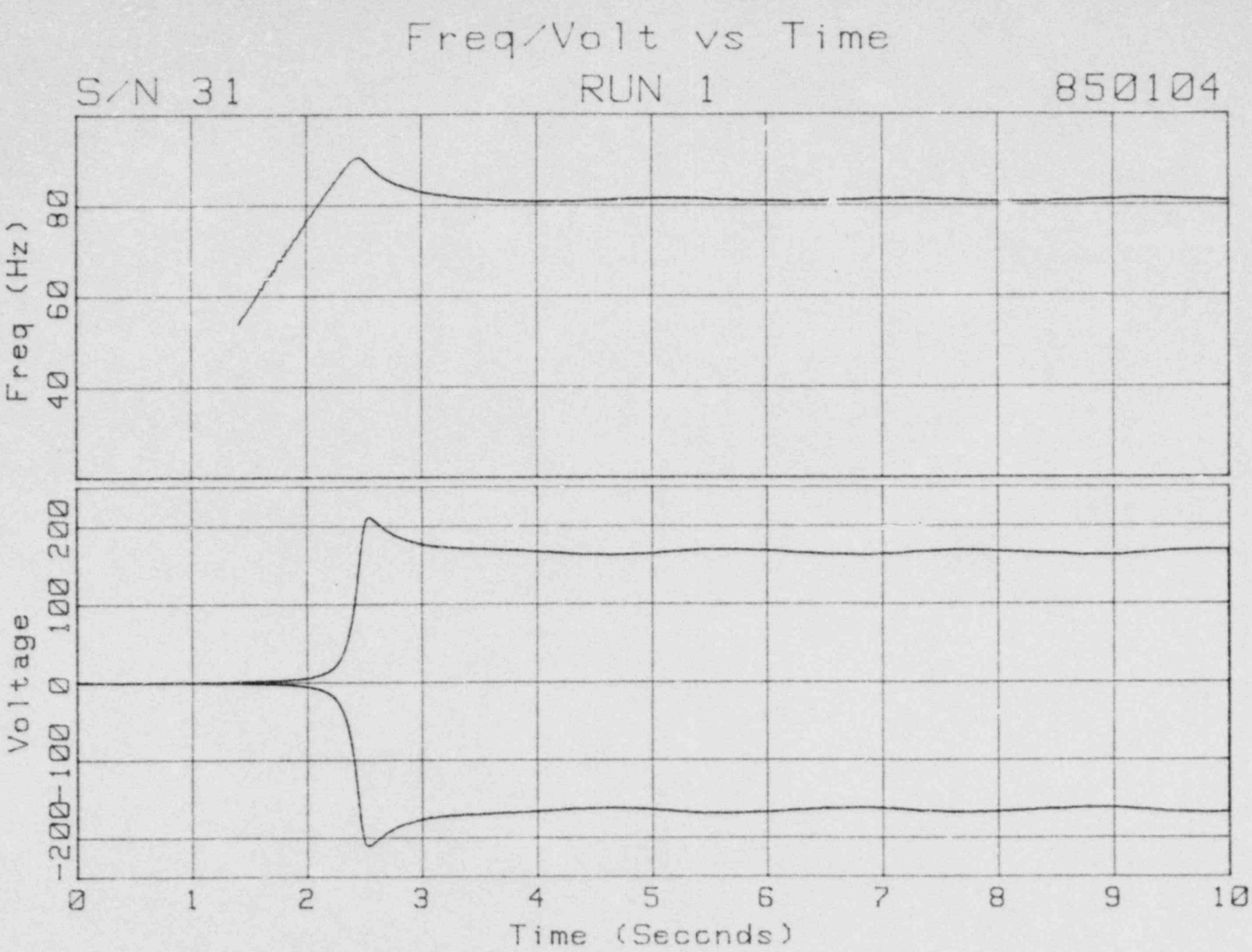
Freq/Volt vs Time
S/N 31
RUN 1
850104
Freq (Hz)
40
60
80
Voltage
-200
-100
0
100
200
0
1
2
3
4
5
6
7
8
9
10
Time (Seconds)

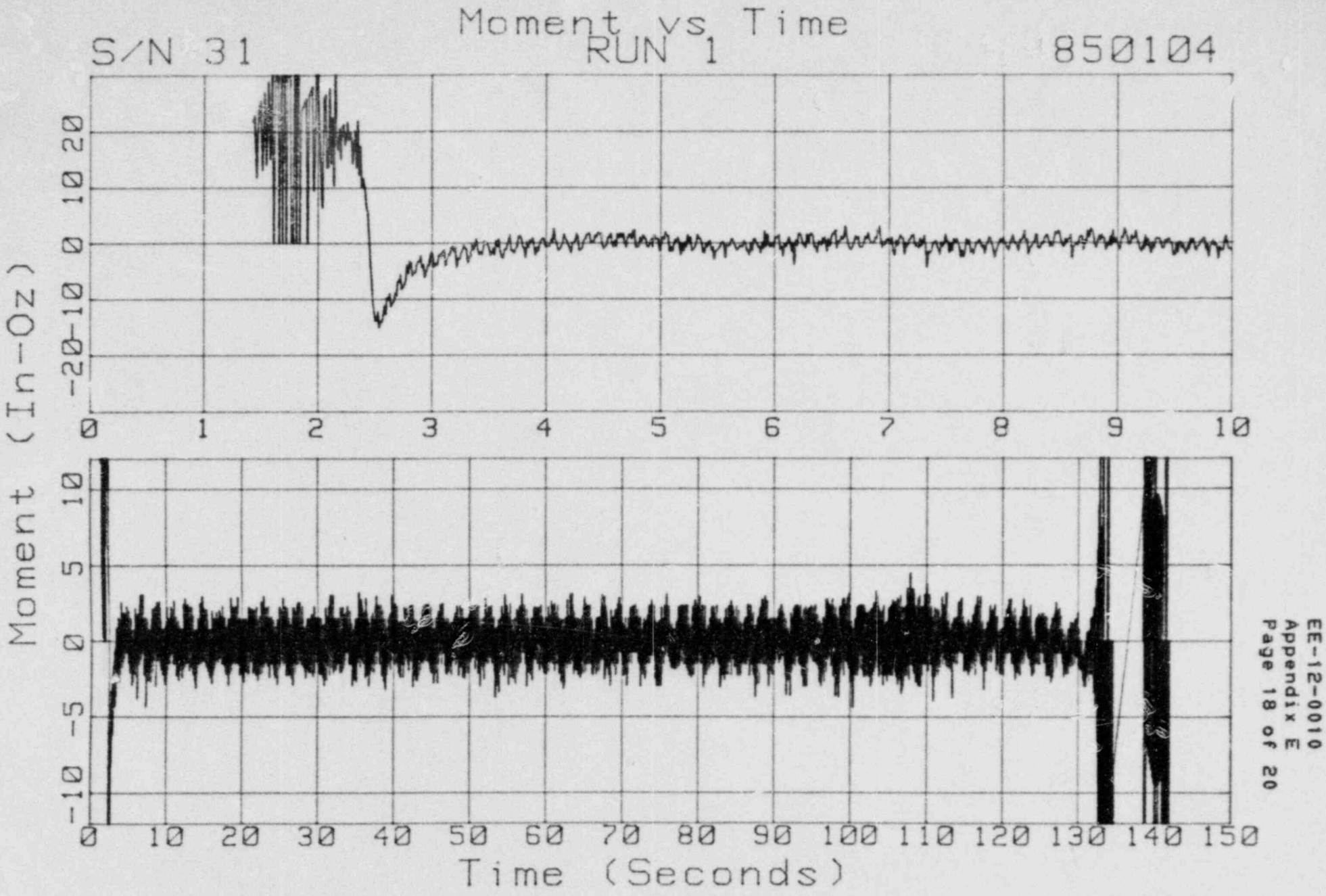
Moment vs Time
S/N 31
RUN 1
850104
Moment (In-Oz)
-20 -10 0 10 20
0 1 2 3 4 5 6 7 8 9 10
-10 -5 0 5 10
0 10 20 30 40 50 60 70 80 90 100 110 120 130 140 150
Time (Seconds)

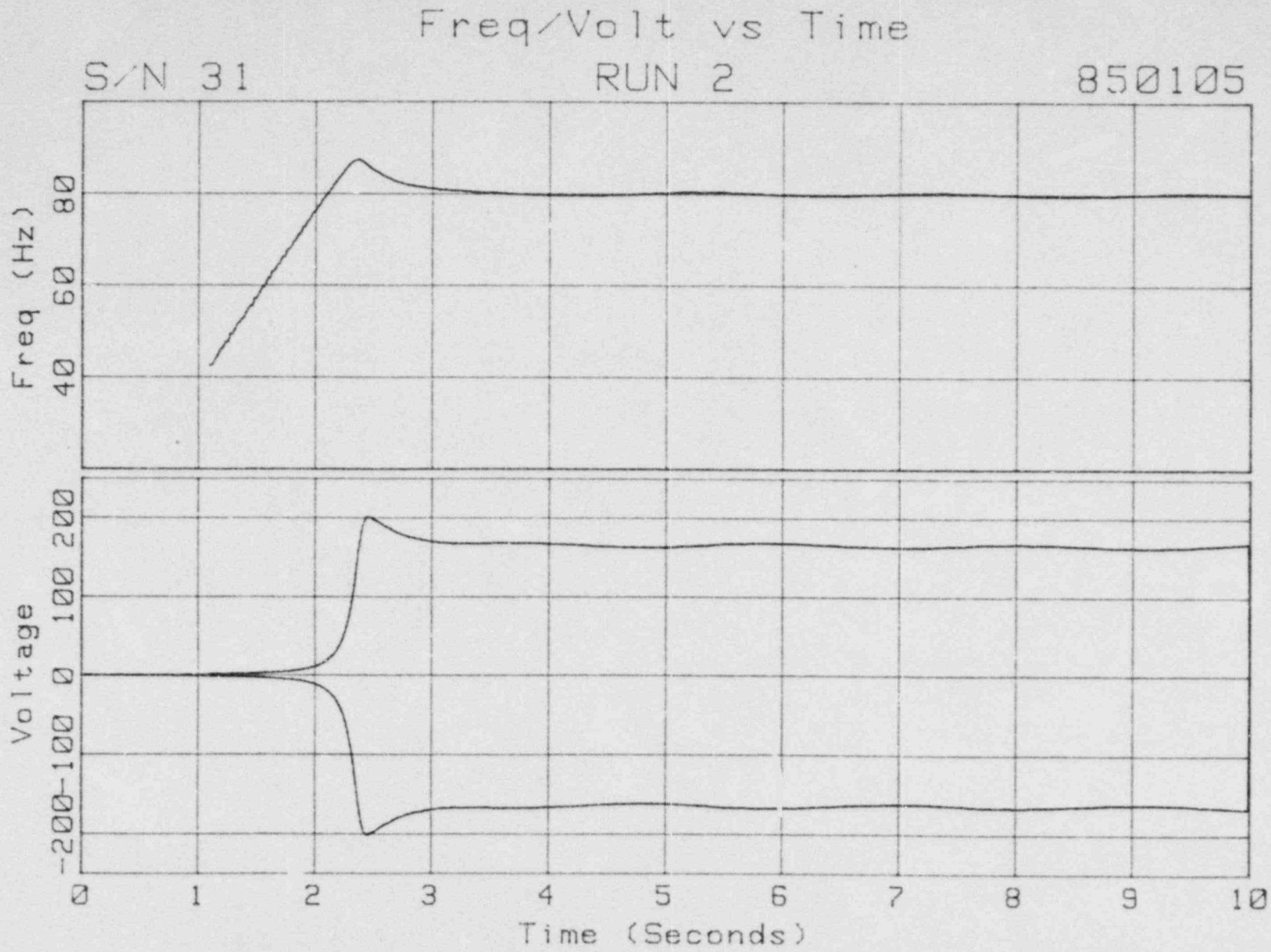
Freq/Volt vs Time
S/N 31
RUN 2
850105
Freq (Hz)
40
60
80
Voltage
-200
-100
0
100
200
0
1
2
3
4
5
6
7
8
9
10
Time (Seconds)

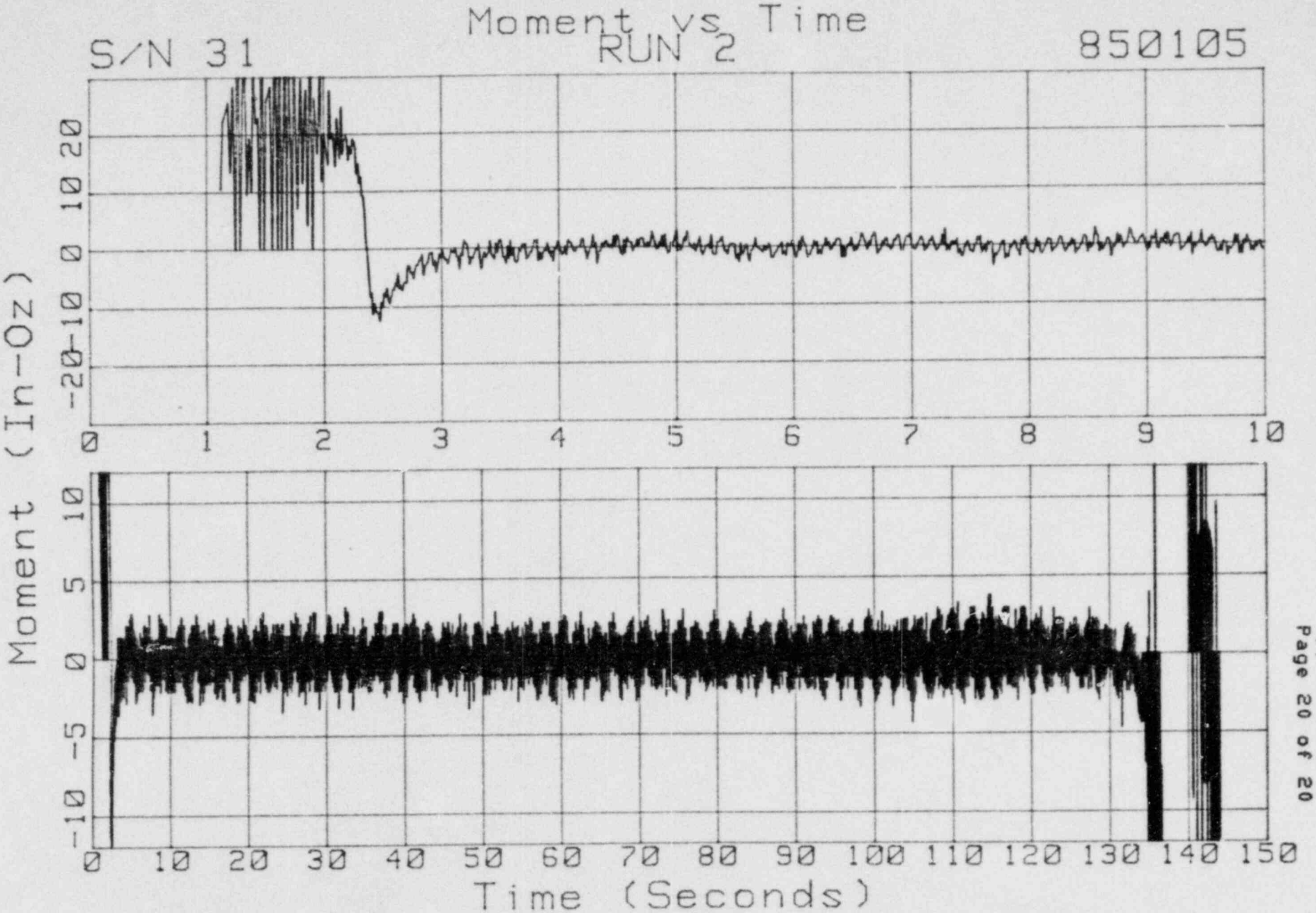
Moment vs Time
S/N 31
RUN 2
850105
Moment (In-Oz)
-20 -10 0 10 20
0 1 2 3 4 5 6 7 8 9 10
-10 -5 0 5 10
0 10 20 30 40 50 60 70 80 90 100 110 120 130 140 150
Time (Seconds)

APPENDIX F

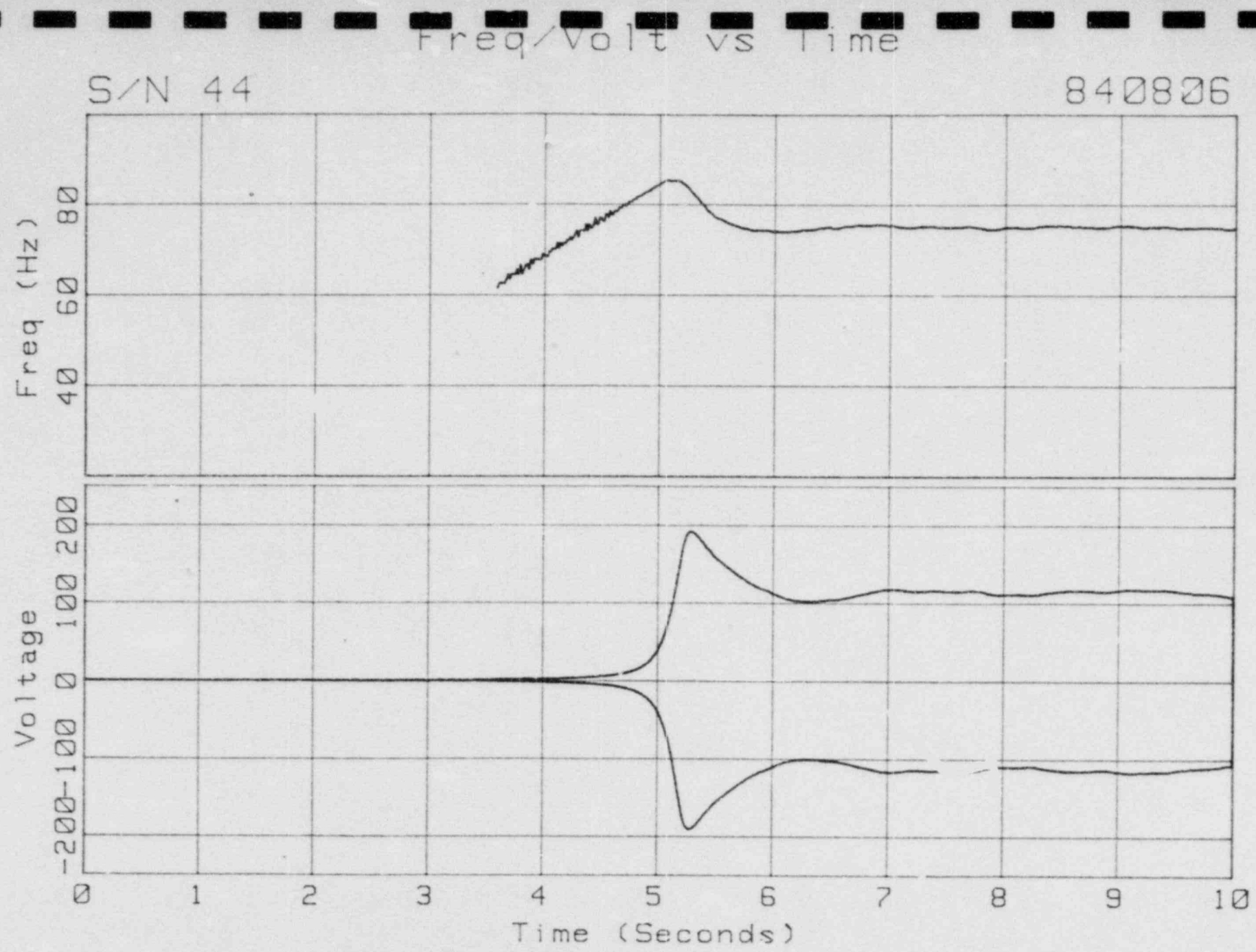
Freq/Volt vs Time
S/N 44
840806
Freq (Hz)
40
60
80
Voltage
-200
-100
0
100
200
0
1
2
3
4
5
6
7
8
9
10
Time (Seconds)

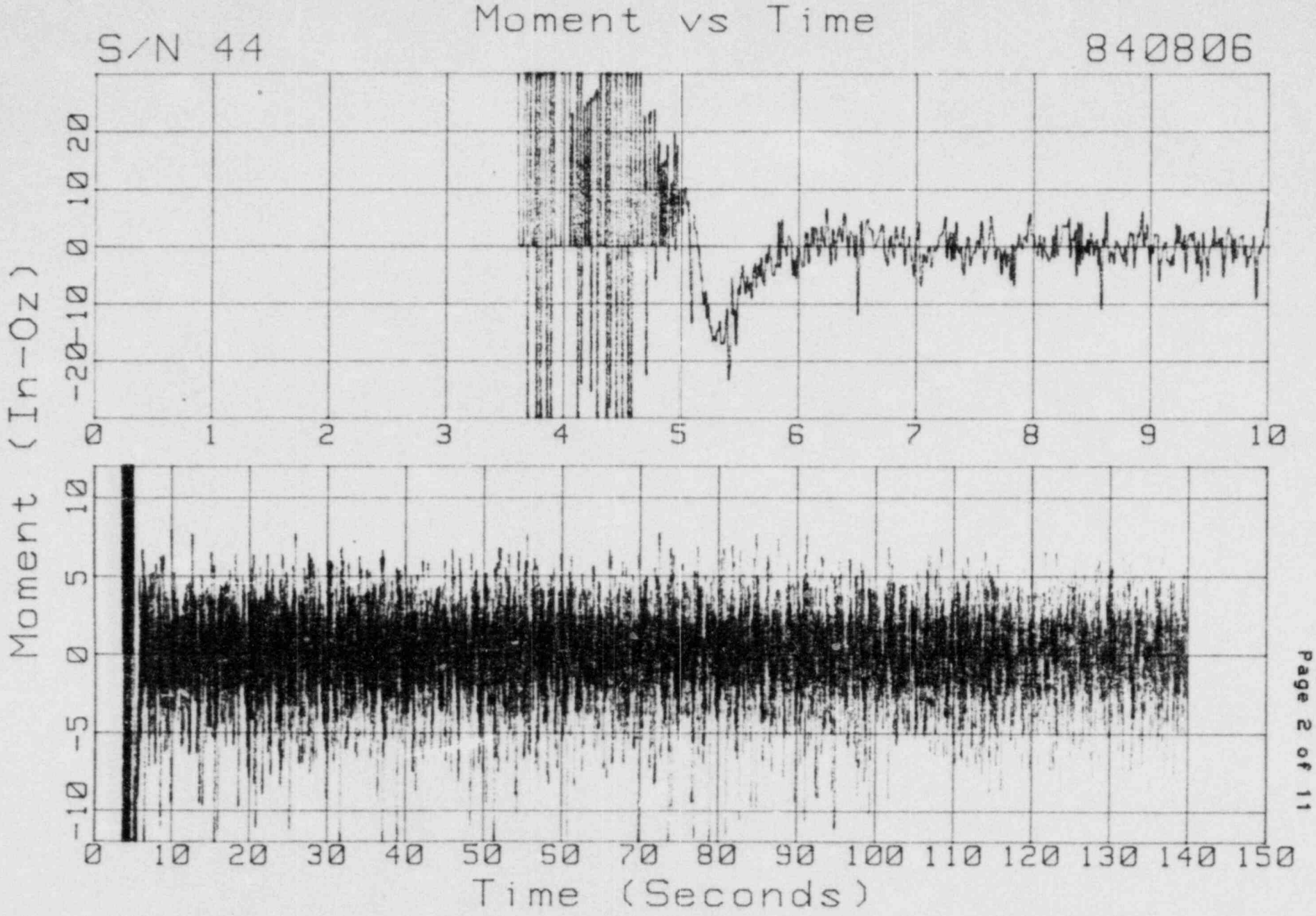
Moment vs Time
S/N 44
840806
Moment (In-Oz)
-20 -10 0 10 20
0 1 2 3 4 5 6 7 8 9 10
-10 -5 0 5 10
0 10 20 30 40 50 50 70 80 90 100 110 120 130 140 150
Time (Seconds)

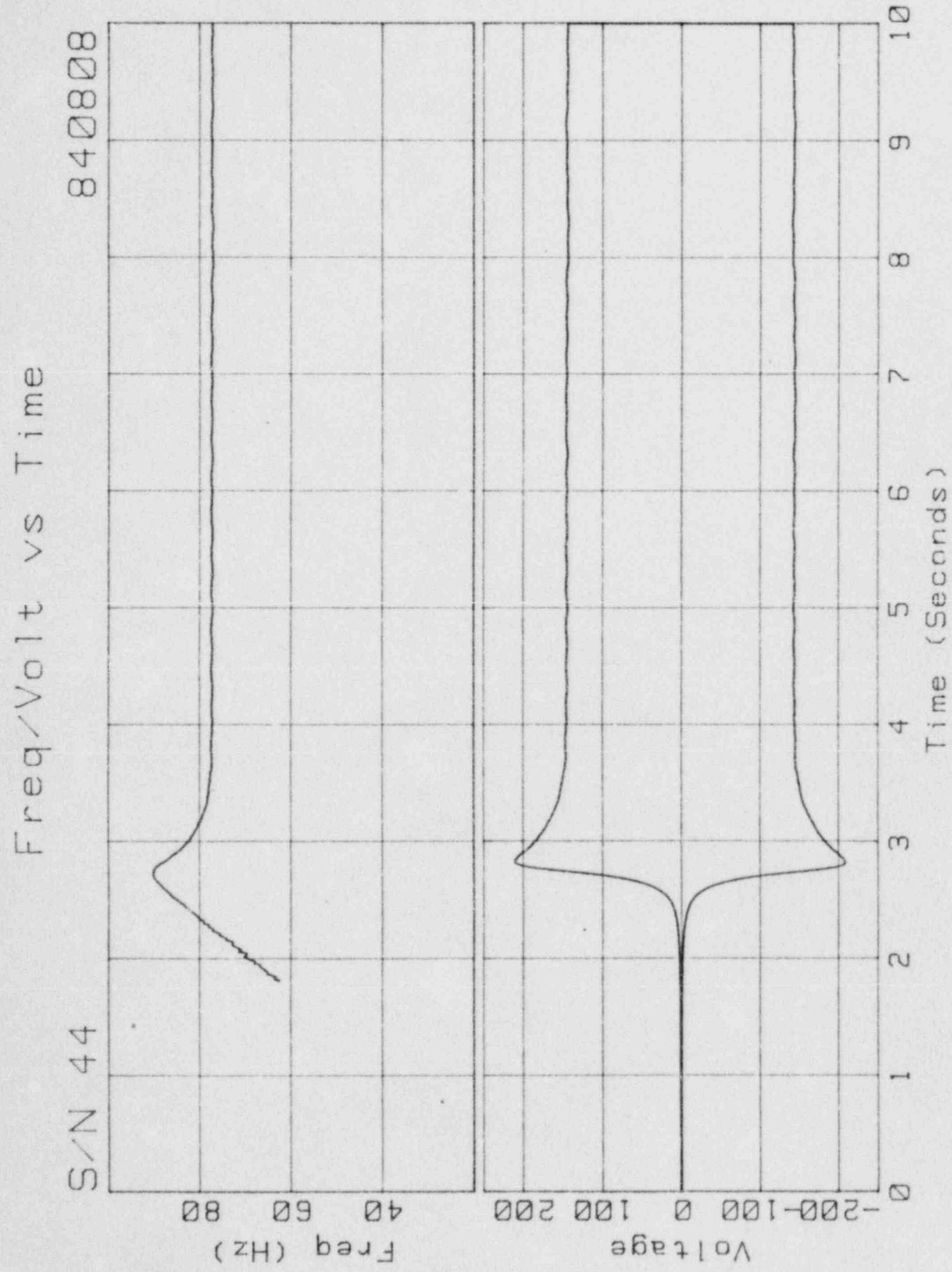
Freq/Volt vs Time
840808
S/N 44
Freq (Hz)
40
60
80
Voltage
-200
-100
0
100
200
Time (Seconds)
0
1
2
3
4
5
6
7
8
9
10

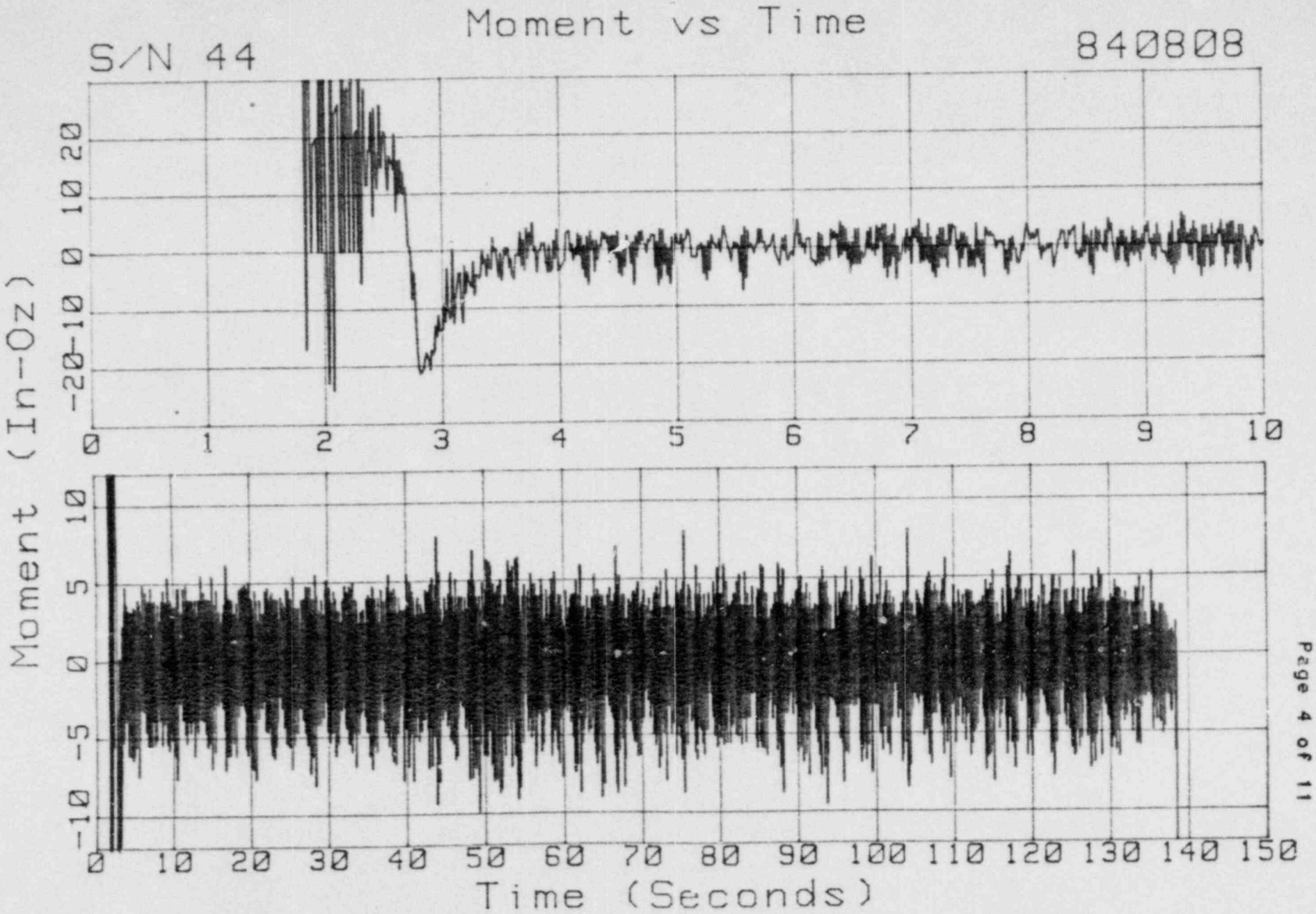
Moment vs Time
S/N 44
840808
Moment (In-Oz)
-20 -10 0 10 20
0 1 2 3 4 5 6 7 8 9 10
-10 -5 0 5 10
0 10 20 30 40 50 60 70 80 90 100 110 120 130 140 150
Time (Seconds)

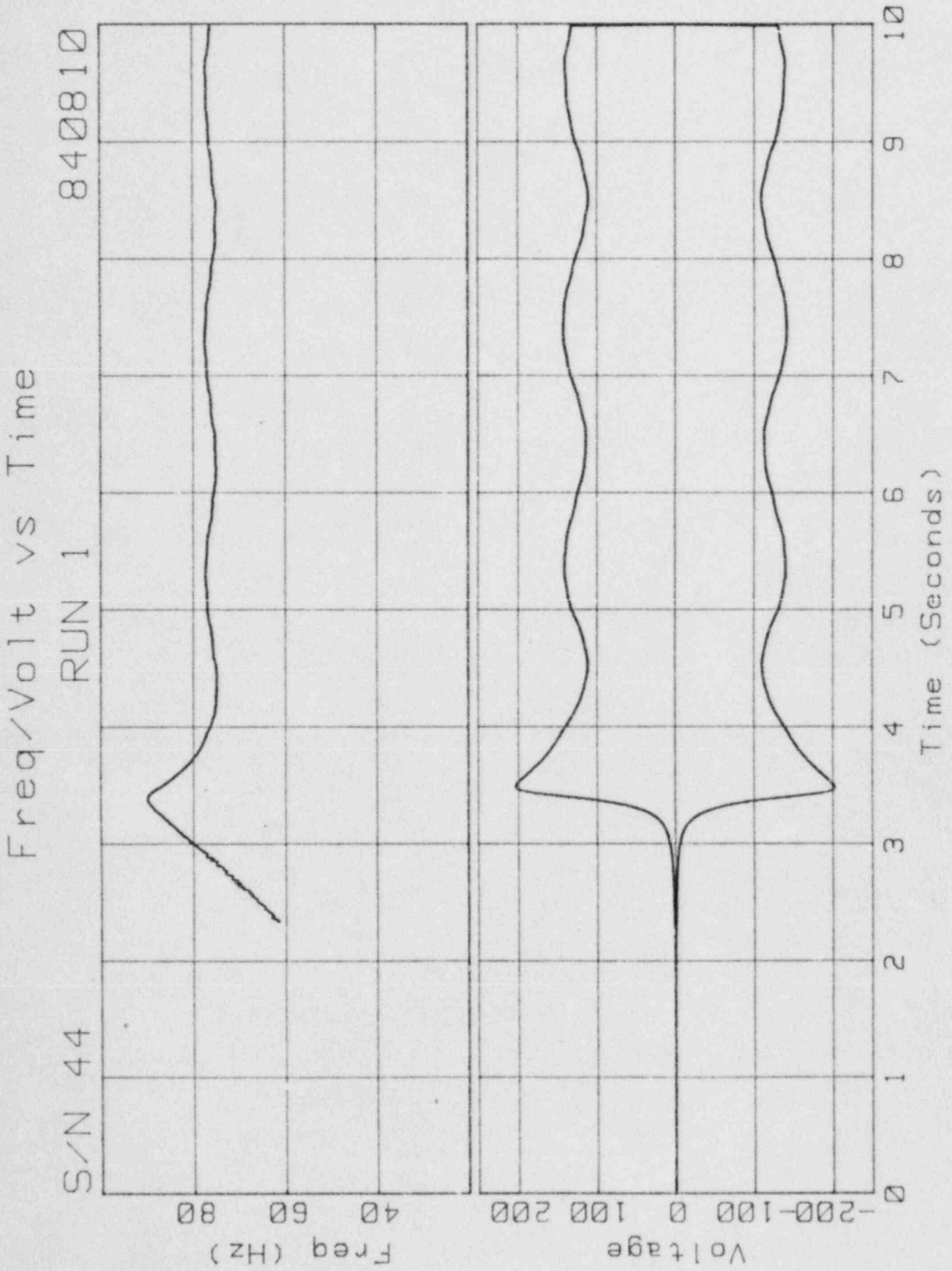
Freq/Volt vs Time
RUN 1
840810
S/N 44
Freq (Hz)
40
60
80
Voltage
-200
-100
0
100
200
0
1
2
3
4
5
6
7
8
9
10
Time (Seconds)

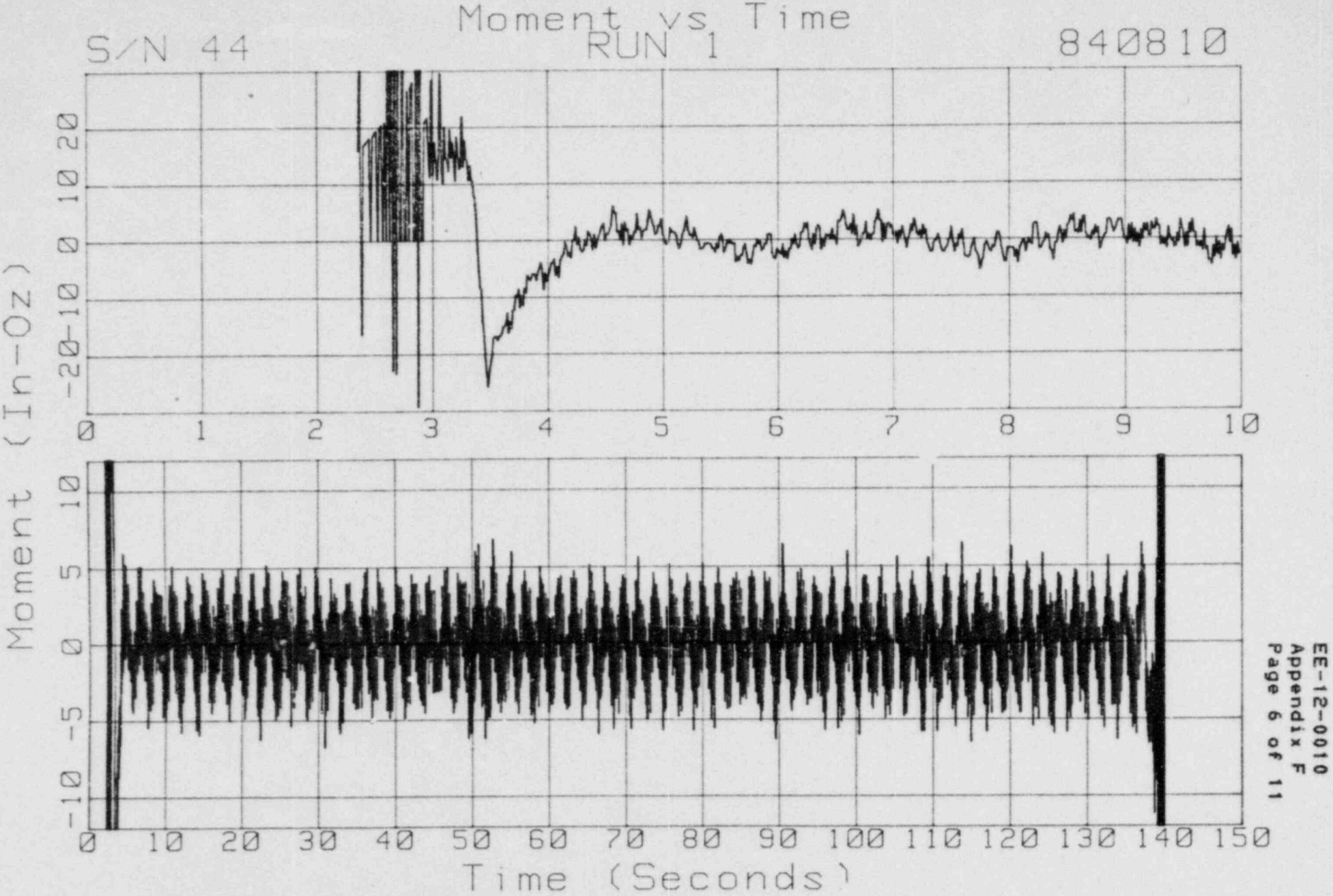
Moment vs Time
S/N 44
RUN 1
840810
Moment (In-Oz)
-20 -10 0 10 20
0 1 2 3 4 5 6 7 8 9 10
-10 -5 0 5 10
0 10 20 30 40 50 60 70 80 90 100 110 120 130 140 150
Time (Seconds)

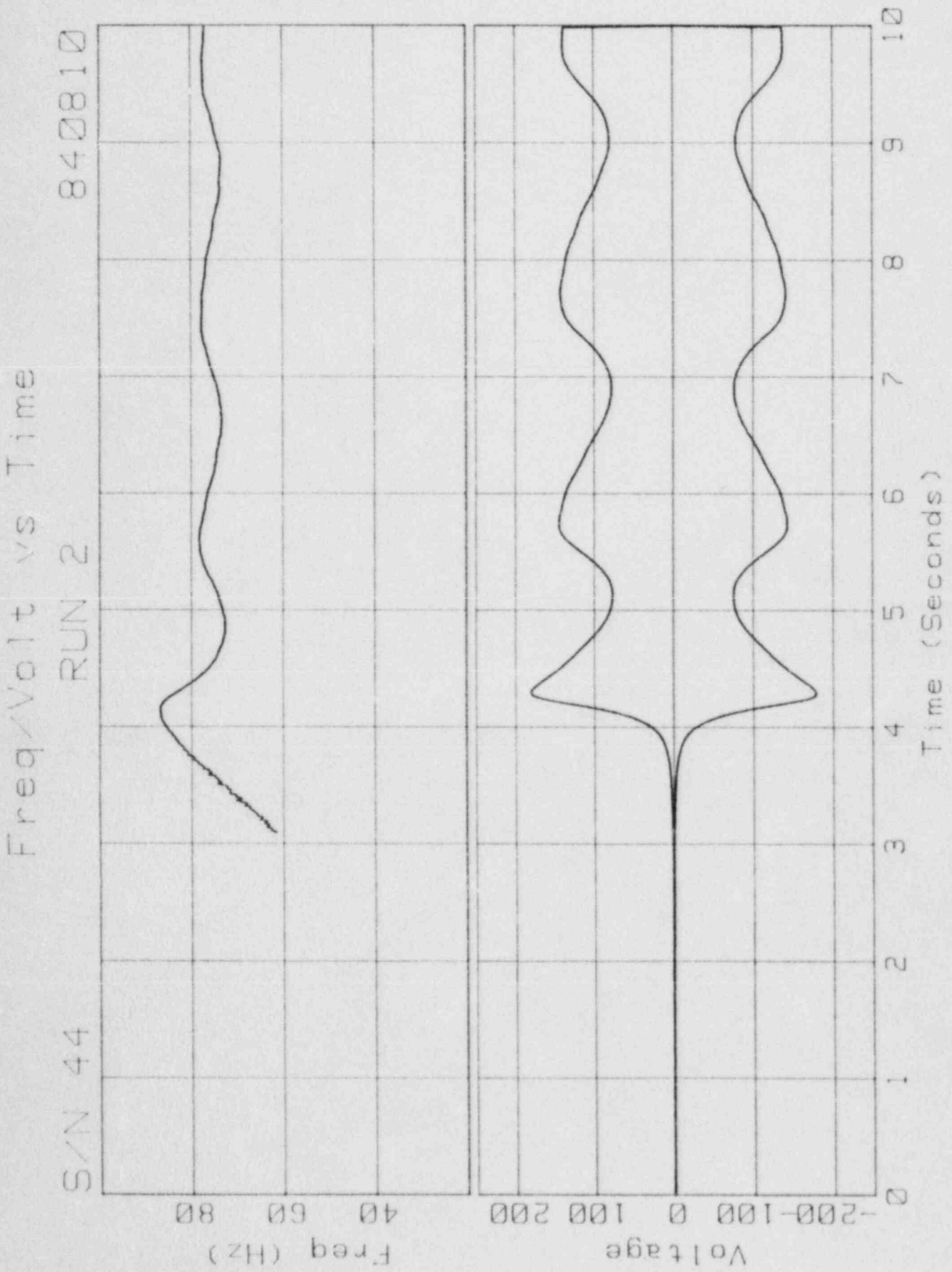
Freq/Volt vs Time
RUN 2
8408810
S/N 44
Freq (Hz)
40
60
80
Voltage
-200
-100
0
100
200
Time (Seconds)
0
1
2
3
4
5
6
7
8
9
10

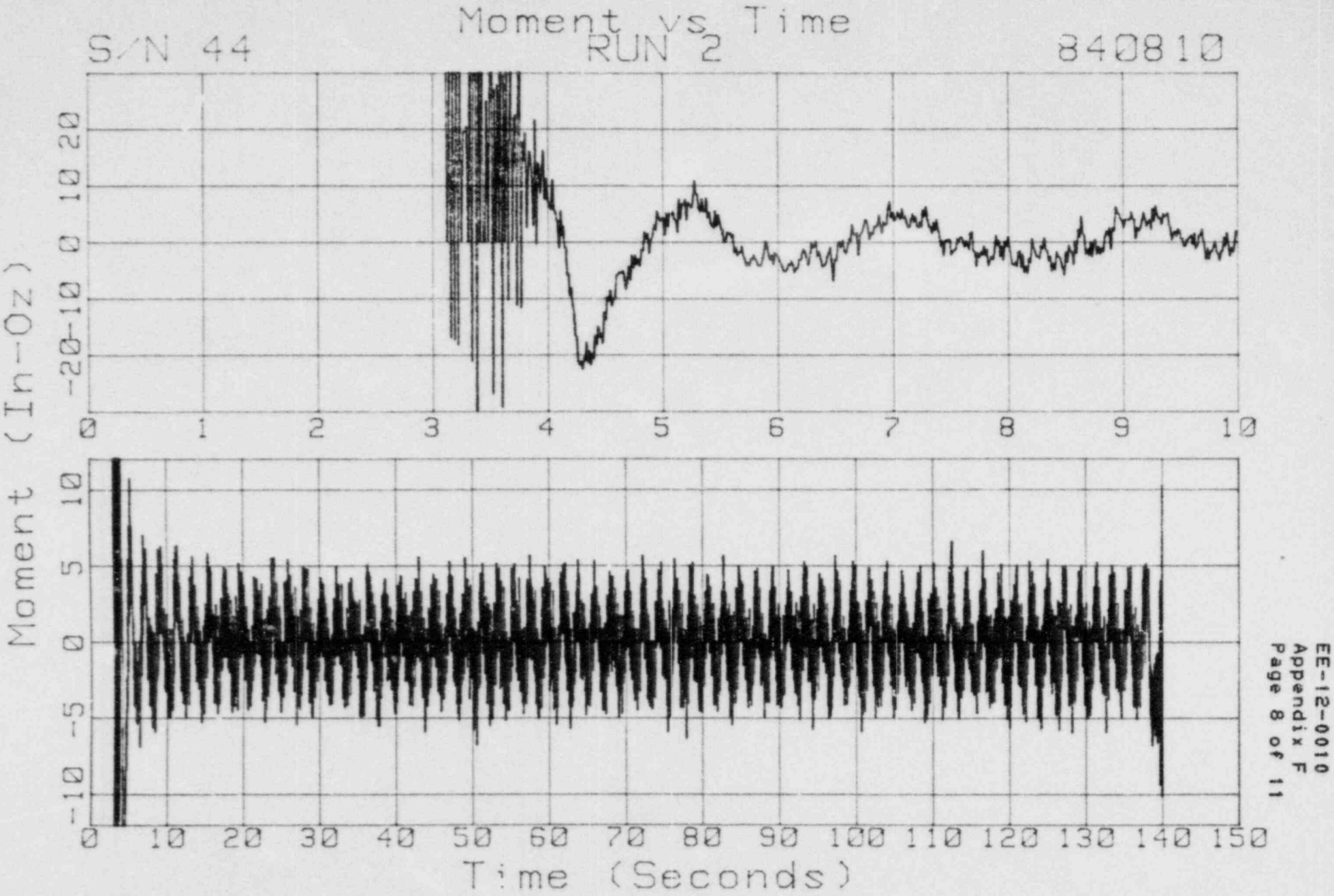
Moment vs Time
S/N 44
RUN 2
840810
Moment (In-Oz)
-20 -10 0 10 20
0 1 2 3 4 5 6 7 8 9 10
-10 -5 0 5 10
0 10 20 30 40 50 60 70 80 90 100 110 120 130 140 150
Time (Seconds)

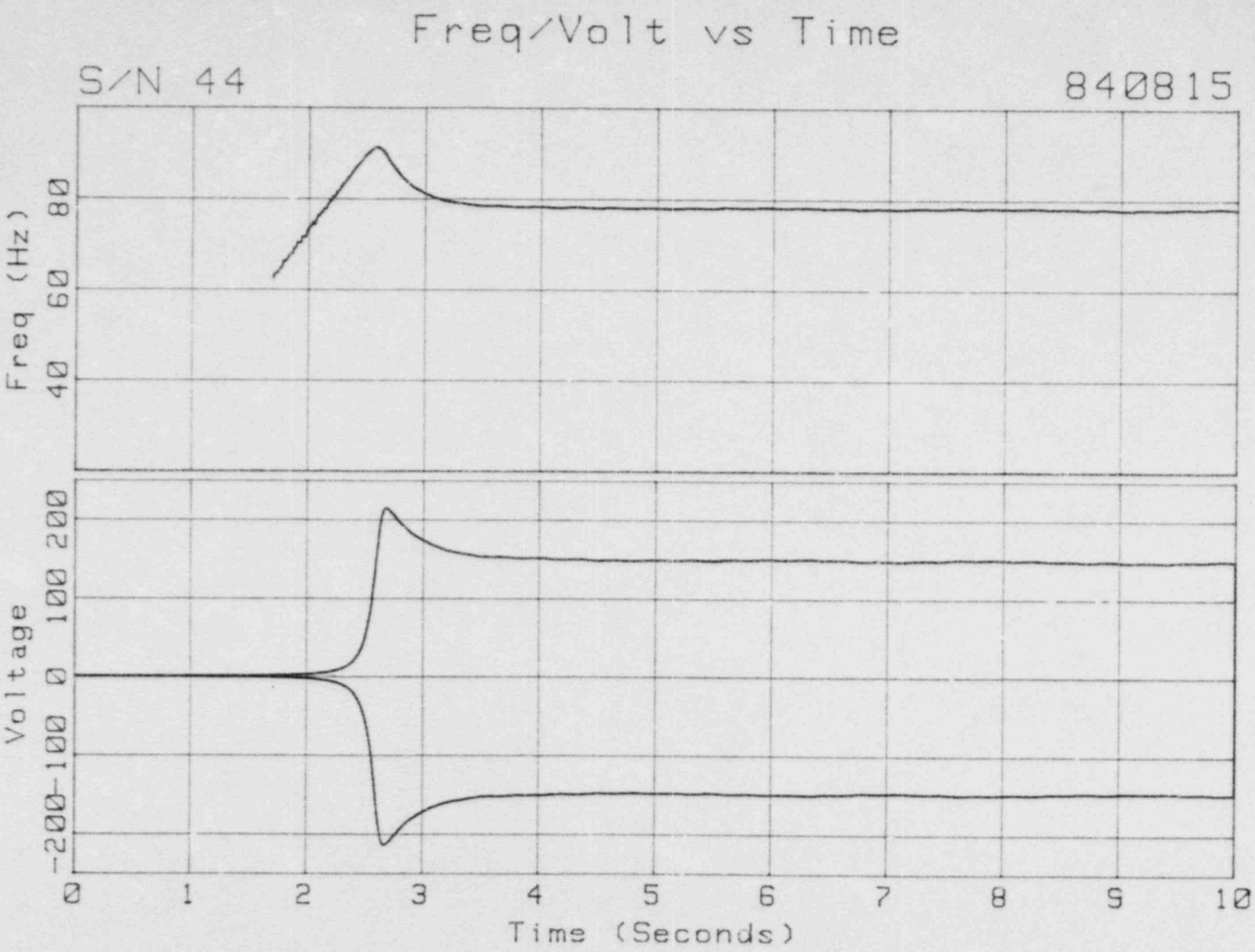
Freq/Volt vs Time
S/N 44
840815
Freq (Hz)
40
60
80
Voltage
-200
-100
0
100
200
0
1
2
3
4
5
6
7
8
9
10
Time (Seconds)

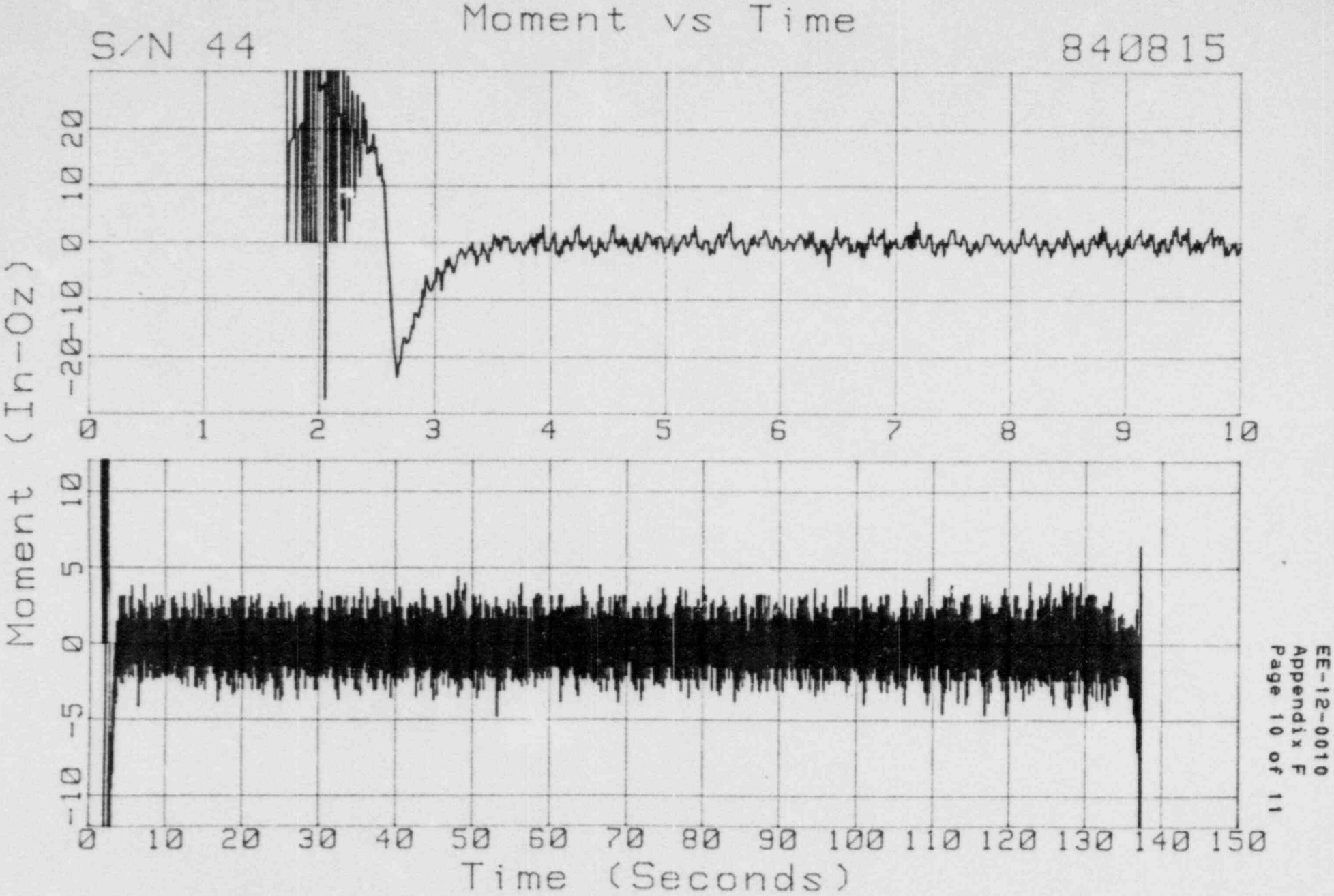
Moment vs Time
S/N 44
840815
Moment (In-Oz)
-20 -10 0 10 20
0 1 2 3 4 5 6 7 8 9 10
-10 -5 0 5 10
0 10 20 30 40 50 60 70 80 90 100 110 120 130 140 150
Time (Seconds)

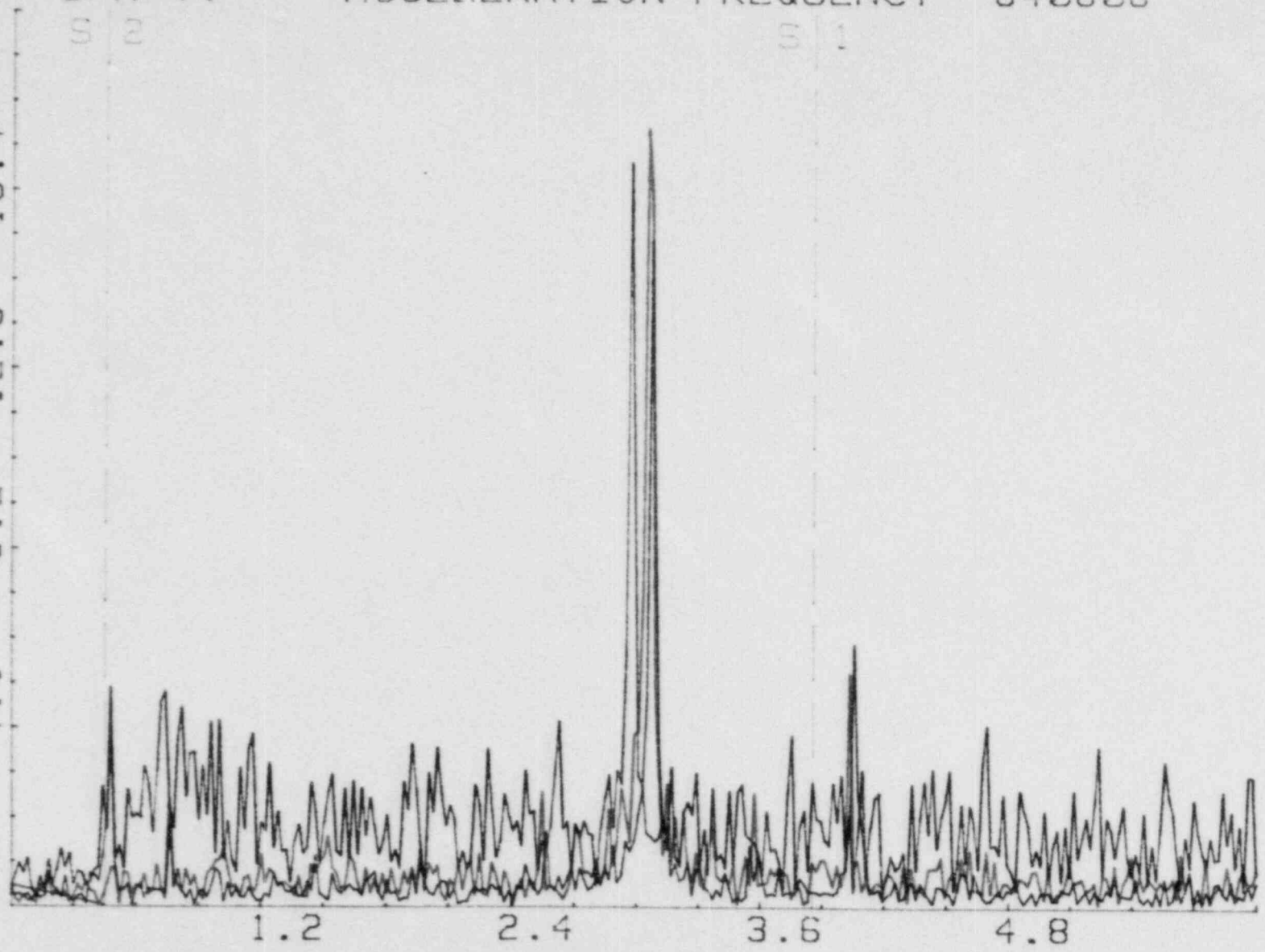
S/N 44 ACCELERATION FREQUENCY 840806
S 2
S 1
4.1
8.2
12.3
16.4
1.2
2.4
3.6
4.8

APPENDIX G

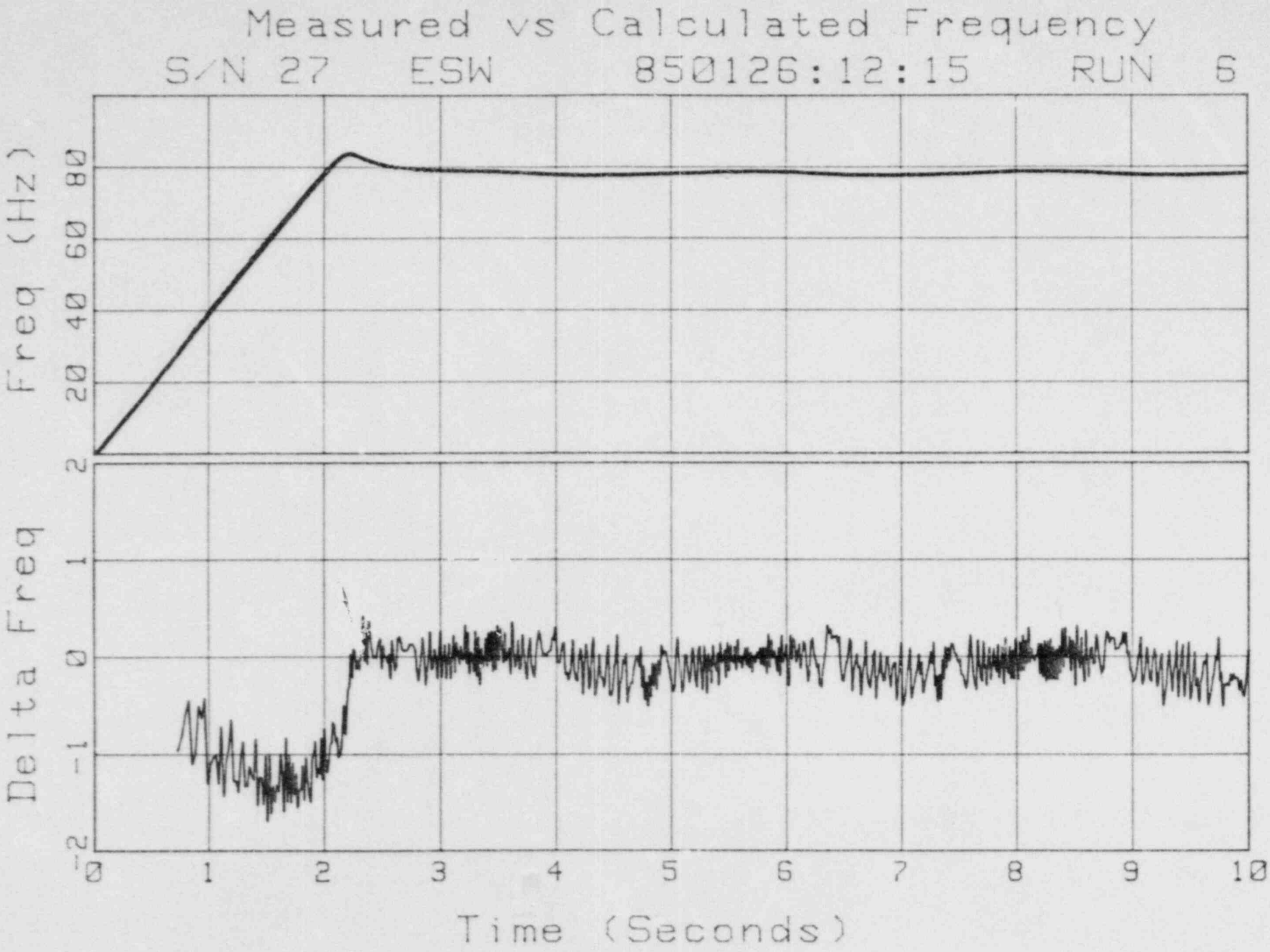
Measured vs Calculated Frequency
S/N 27 ESW 850126:12:15 RUN 6
Freq (Hz)
2
20
40
60
80
Delta Freq
2
1
0
-1
-2
0
1
2
3
4
5
6
7
8
9
10
Time (Seconds)

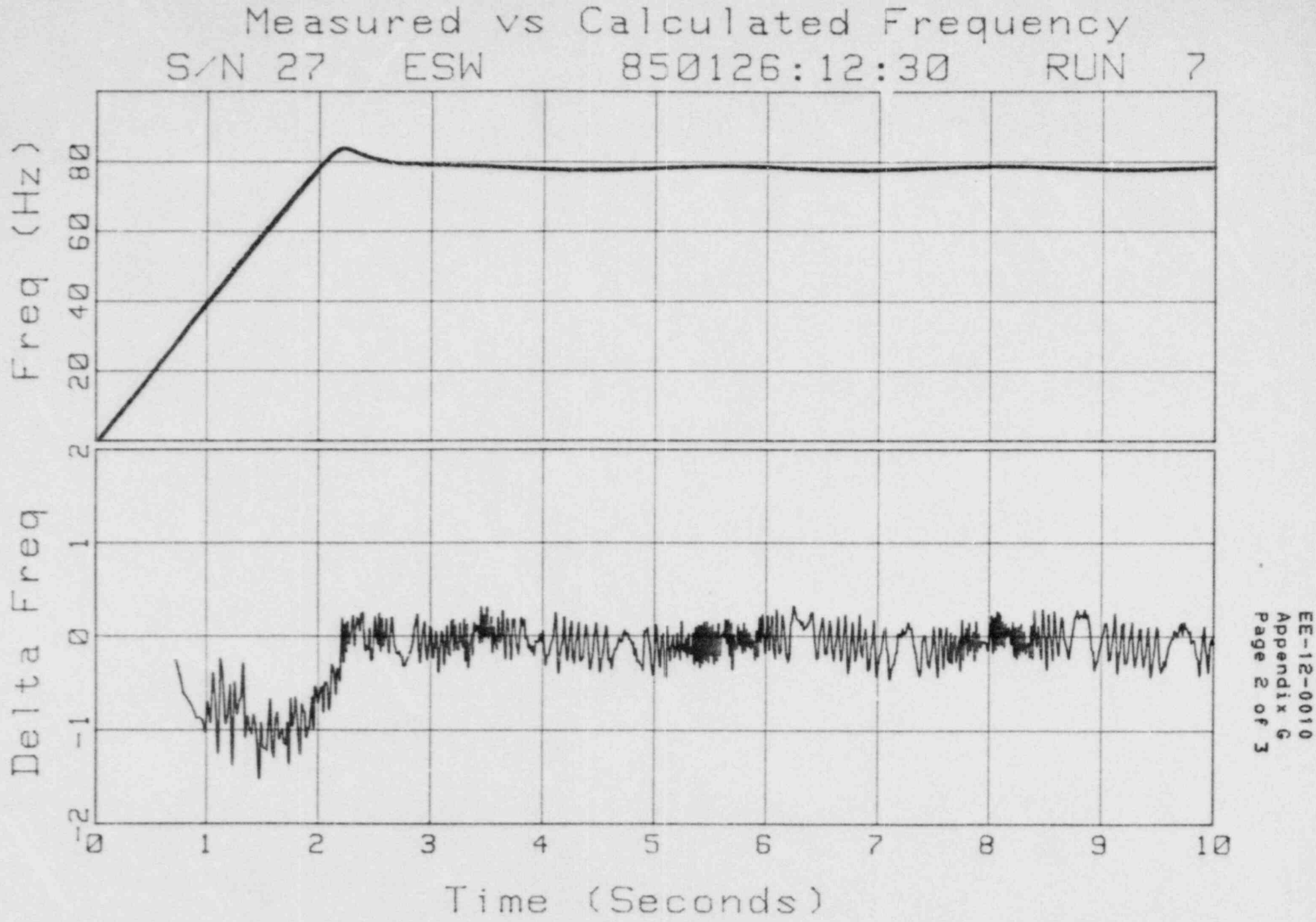
Measured vs Calculated Frequency
S/N 27 ESW 850126:12:30 RUN 7
Freq (Hz)
20 40 60 80
Delta Freq
2 1 0 -1 -2
0 1 2 3 4 5 6 7 8 9 10
Time (Seconds)

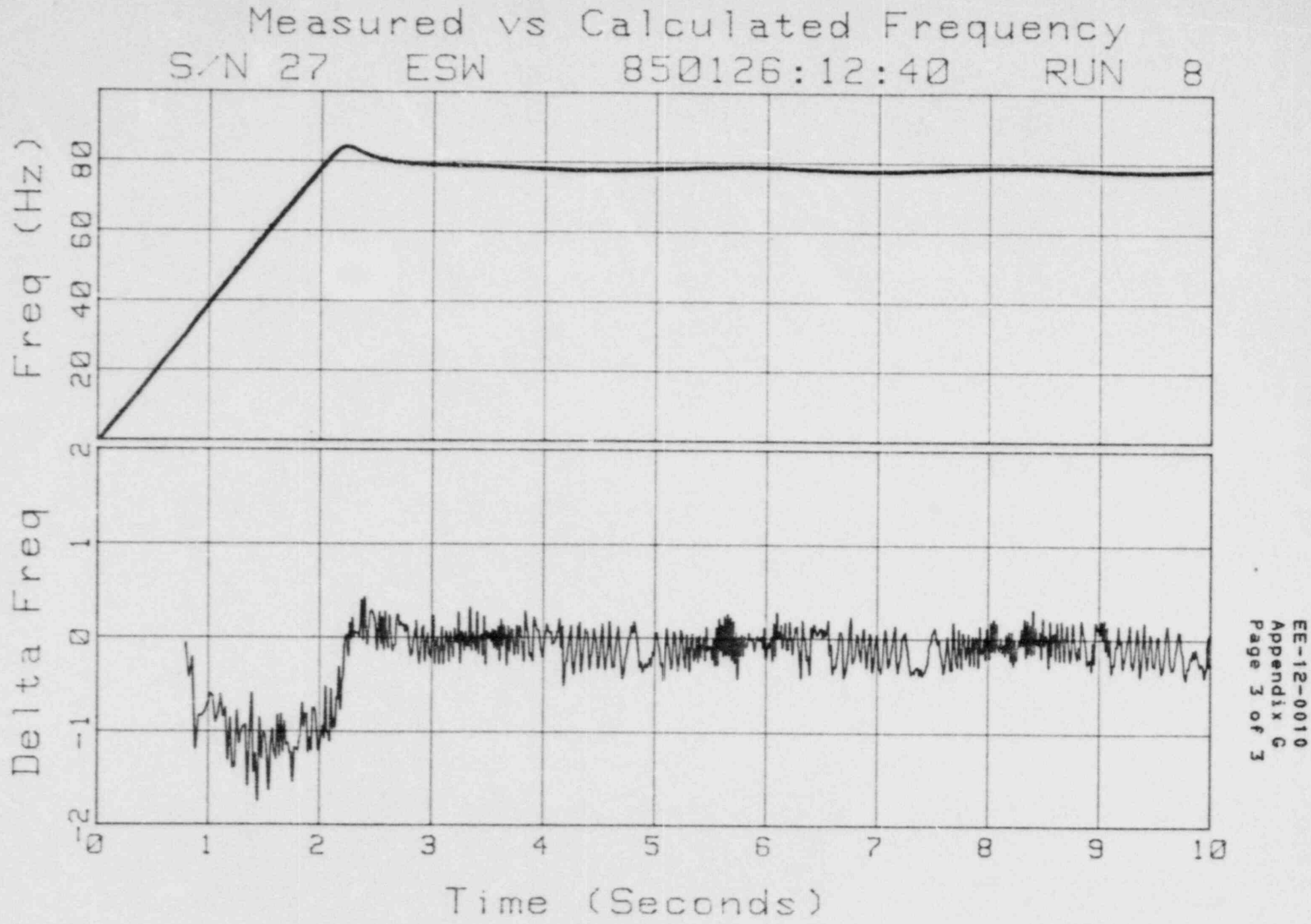
Measured vs Calculated Frequency
S/N 27 ESW 850126:12:40 RUN 8
Freq (Hz)
20 40 60 80
Delta Freq
2
1
0
-1
-2
0 1 2 3 4 5 6 7 8 9 10
Time (Seconds)

APPENDIX H

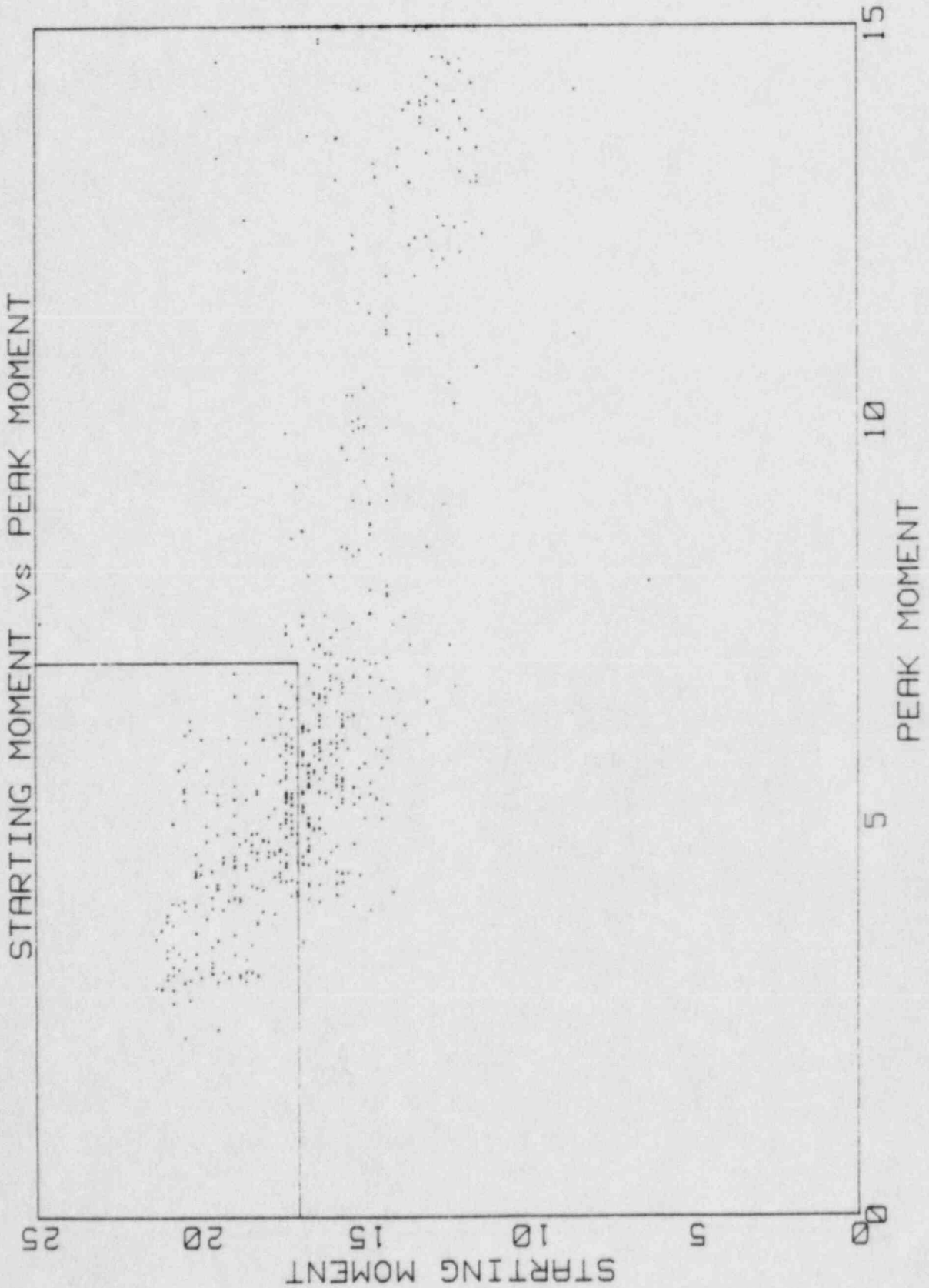
STARTING MOMENT vs PEAK MOMENT
STARTING MOMENT
PEAK MOMENT
0
5
10
15
20
25

EVALUATION OF CRDOAS (AS-FOUND)

Meets Acceptance Criteria	Does Not Meet Acceptance Criteria	No Test Data Yet
1	2	19
10	3	20
12	4	27
30	5	37
31	6	43
32	7	
38	8	
	9	
	11	
	13	
	14	
	15	
	16	
	17	
	18	
	21	
	22	
	23	
	24	
	25	
	26	
	28	
	29	
	33	
	34	
	35	
	36	
	39	
	40	
	41	
	42	
	44	

APPENDIX I

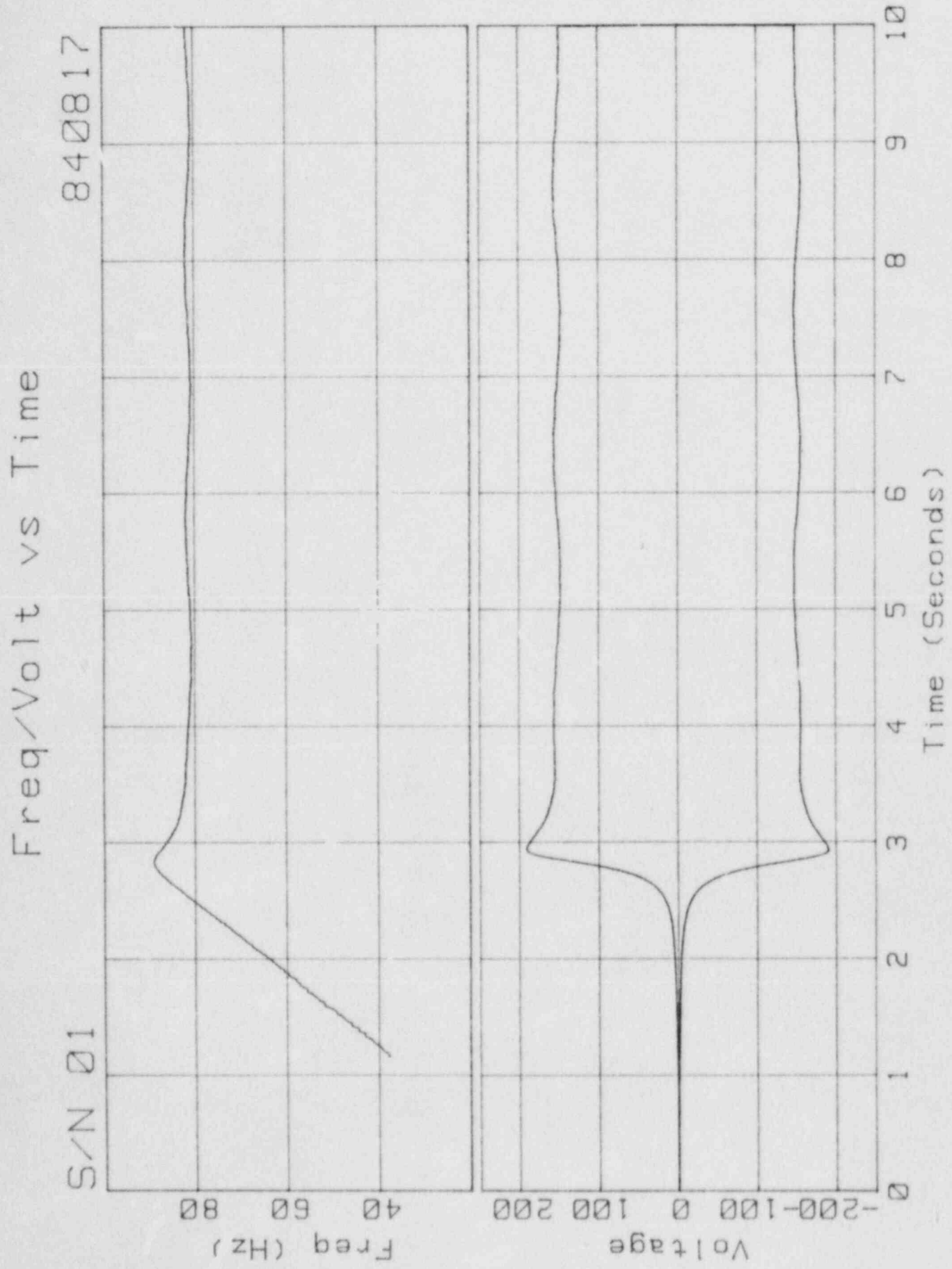
Freq/Volt vs Time
840817
S/N 01
Freq (Hz)
40
60
80
Voltage
-200
-100
0
100
200
0
1
2
3
4
5
6
7
8
9
10
Time (Seconds)

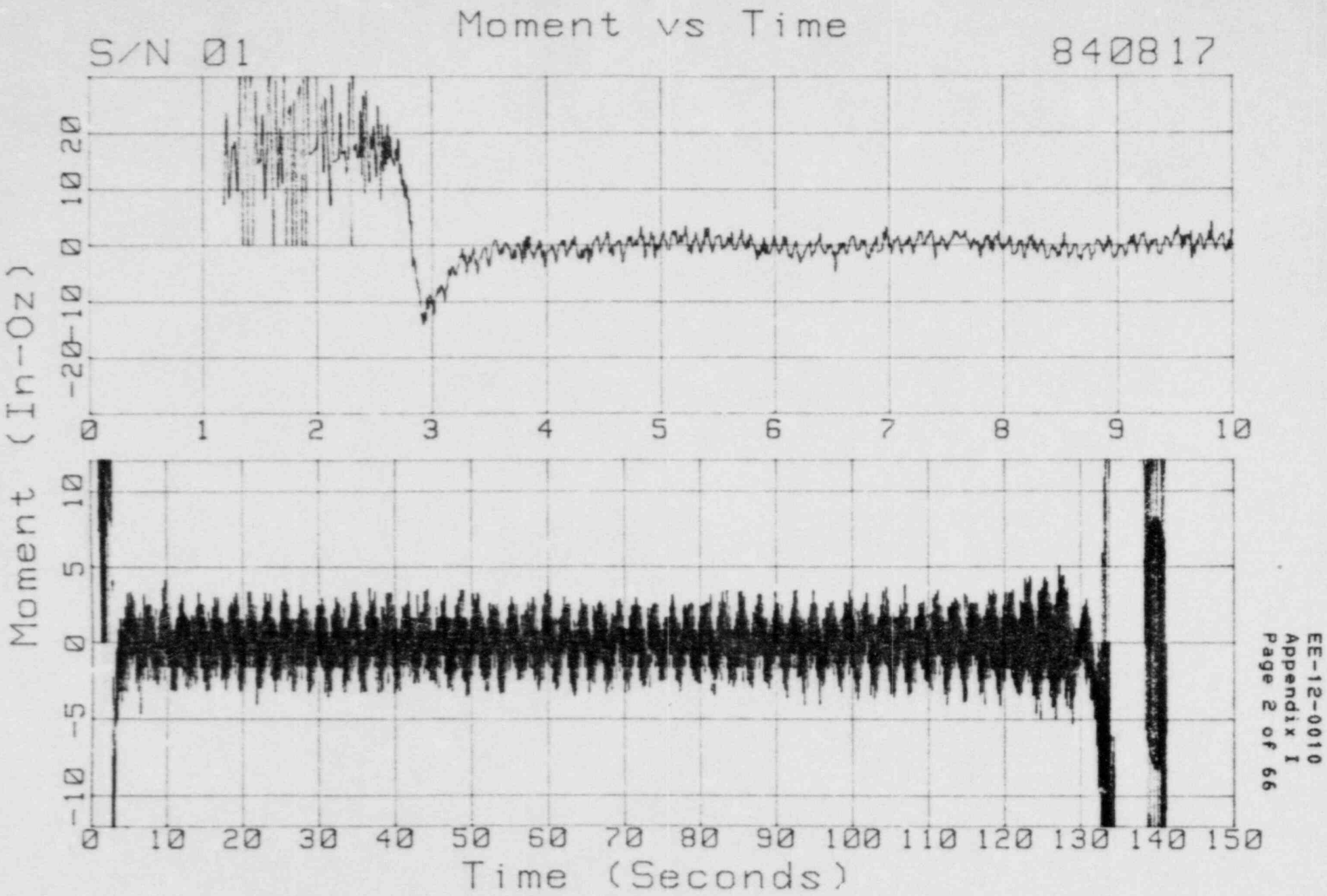
Moment vs Time
S/N 01
840817
Moment (In-Oz)
-20 -10 0 10 20
0 1 2 3 4 5 6 7 8 9 10
-10 -5 0 5 10
0 10 20 30 40 50 60 70 80 90 100 110 120 130 140 150
Time (Seconds)

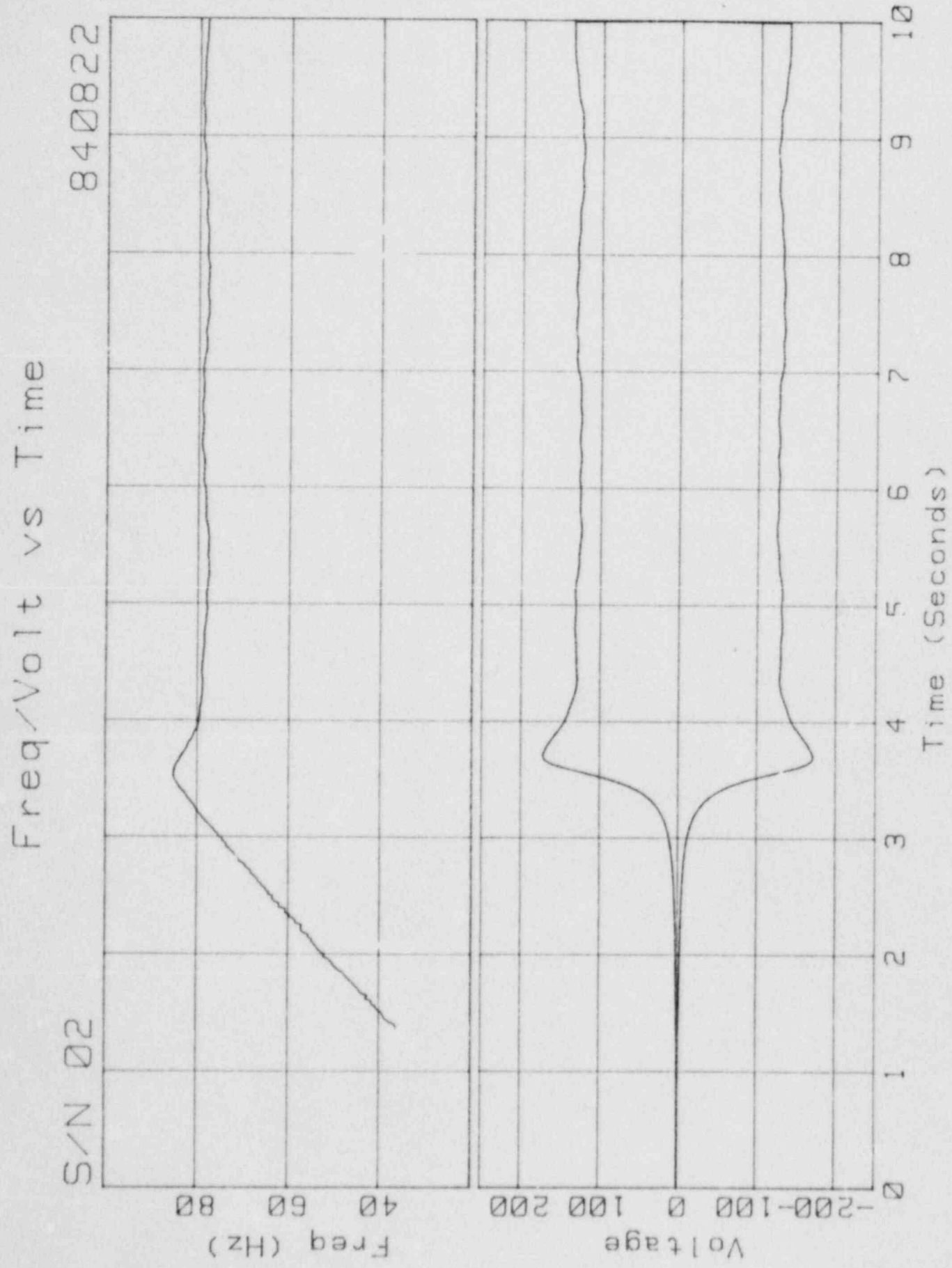
Freq/Volt vs Time
840822
S/N 02
Freq (Hz)
40
60
80
Voltage
-200 -100 0 100 200
Time (Seconds)
0 1 2 3 4 5 6 7 8 9 10

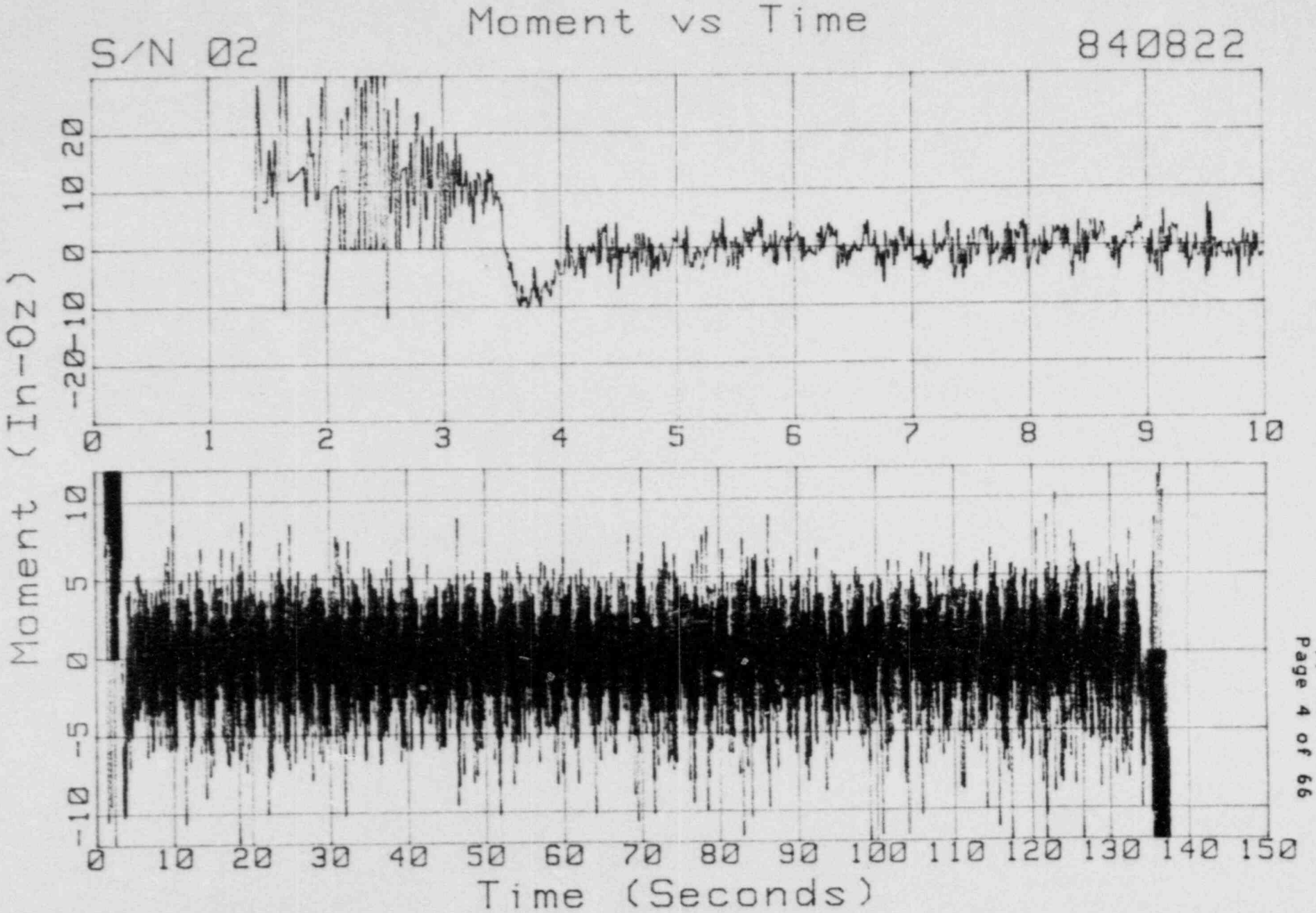
Moment vs Time
S/N 02
840822
Moment (In-Oz)
-20 -10 0 10 20
0 1 2 3 4 5 6 7 8 9 10
-10 -5 0 5 10
0 10 20 30 40 50 60 70 80 90 100 110 120 130 140 150
Time (Seconds)

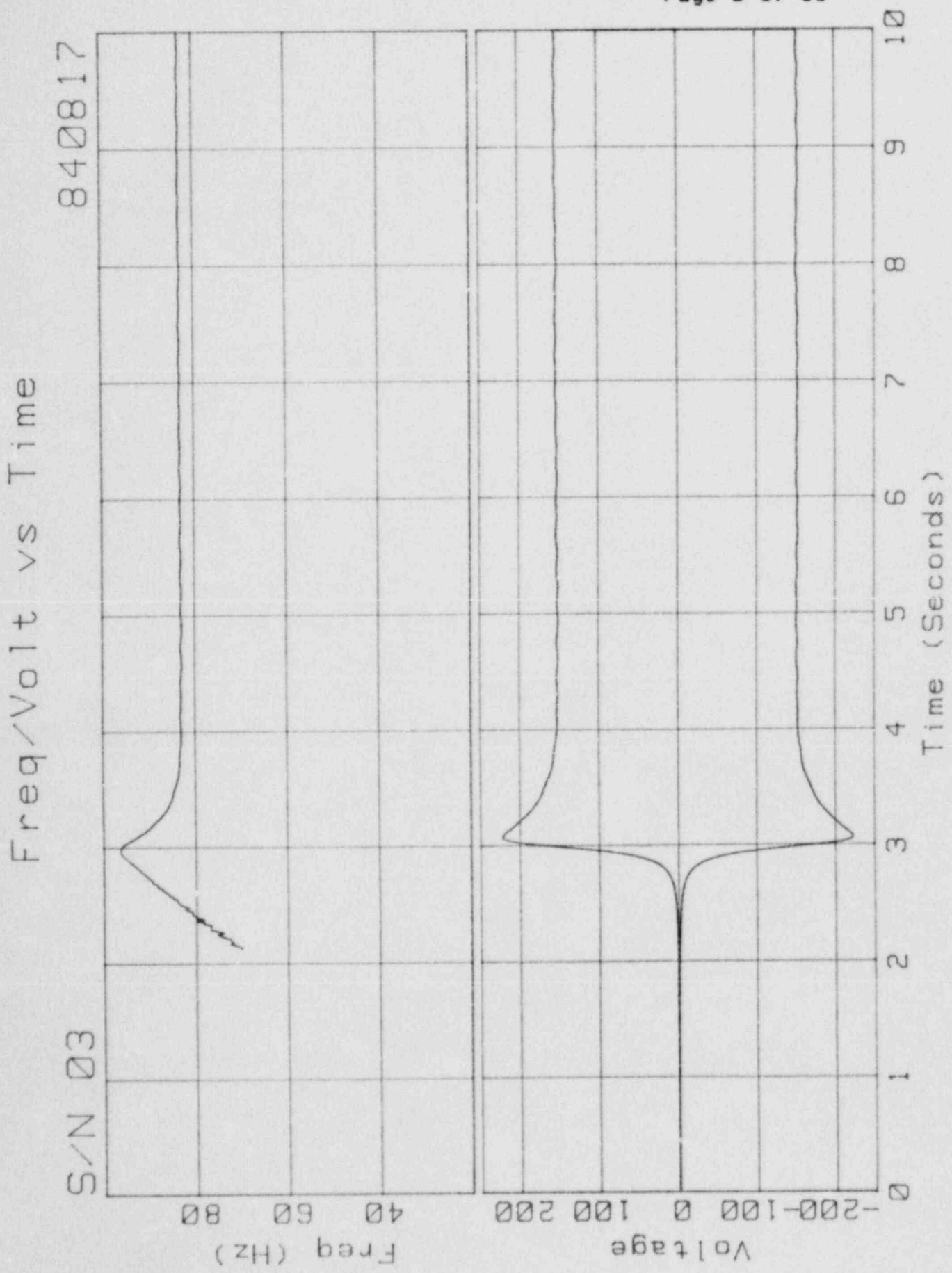
Freq/Volt vs Time
840817
S/N 03
Freq (Hz)
40
60
80
Voltage
-200
-100
0
100
200
0
1
2
3
4
5
6
7
8
9
10
Time (Seconds)

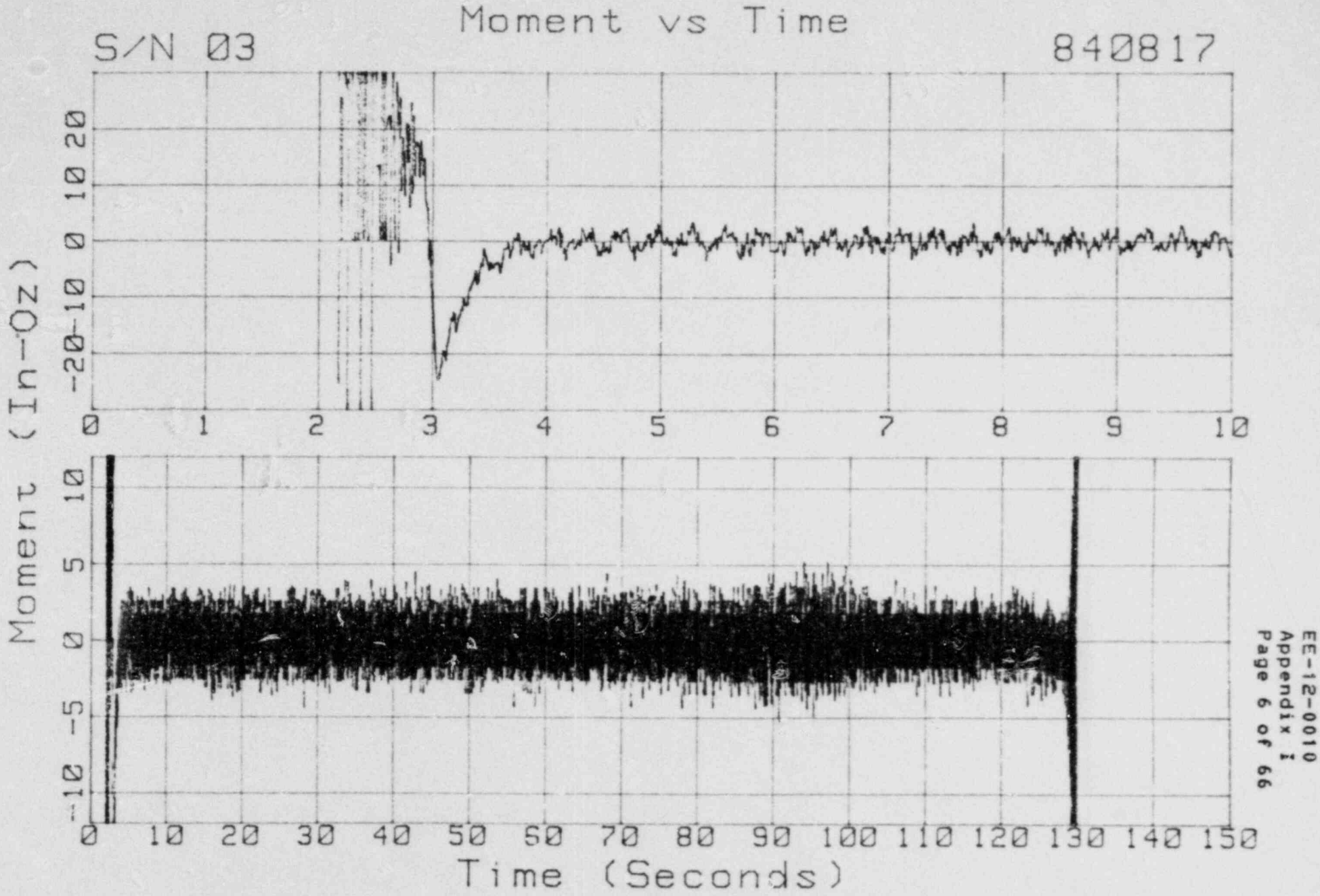
Moment vs Time
S/N 03
840817
Moment (In-Oz)
-20 -10 0 10 20
0 1 2 3 4 5 6 7 8 9 10
-10 -5 0 5 10
0 10 20 30 40 50 60 70 80 90 100 110 120 130 140 150
Time (Seconds)

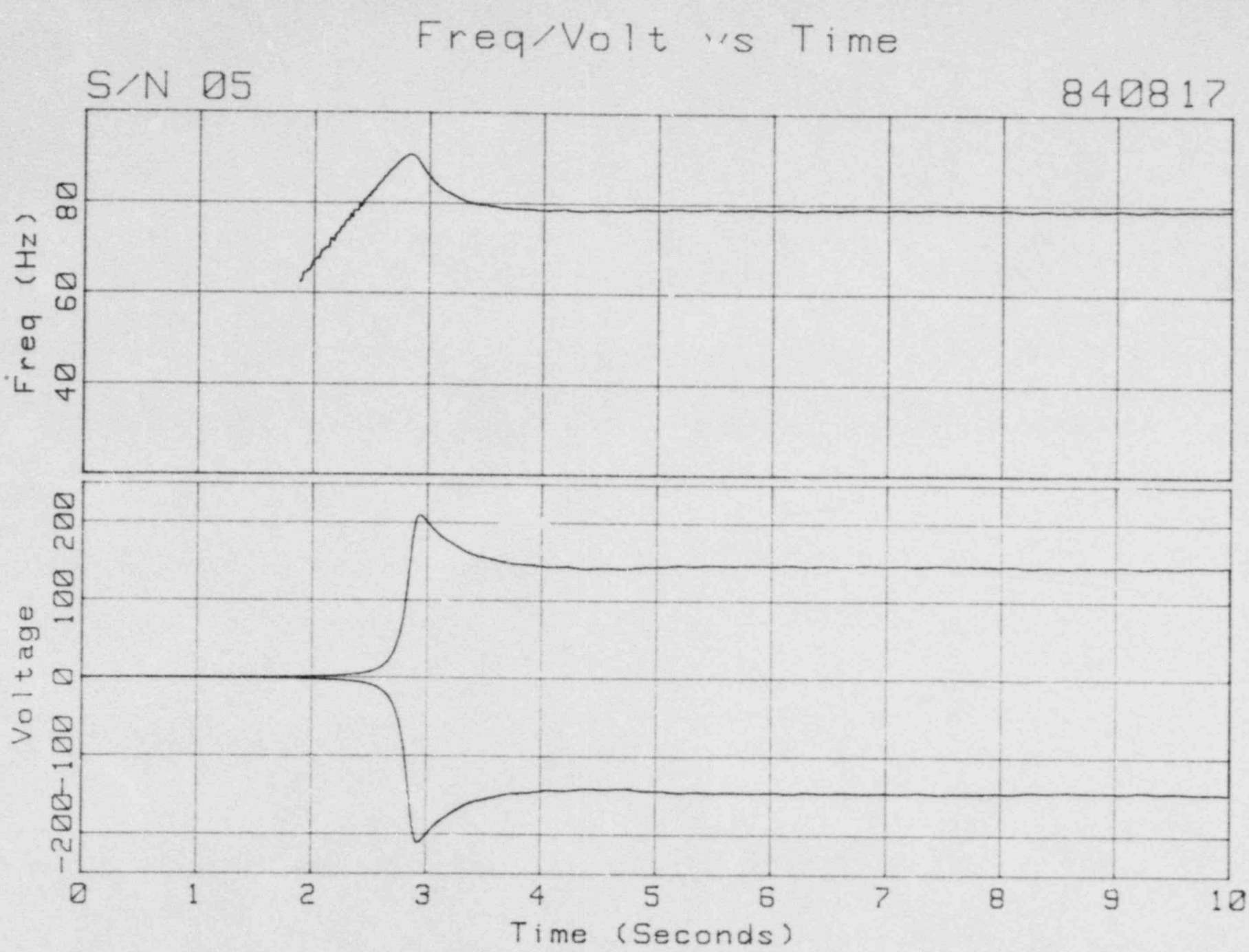
Freq/Volt vs Time
S/N 05
840817
Freq (Hz)
40
60
80
Voltage
-200
-100
0
100
200
0
1
2
3
4
5
6
7
8
9
10
Time (Seconds)

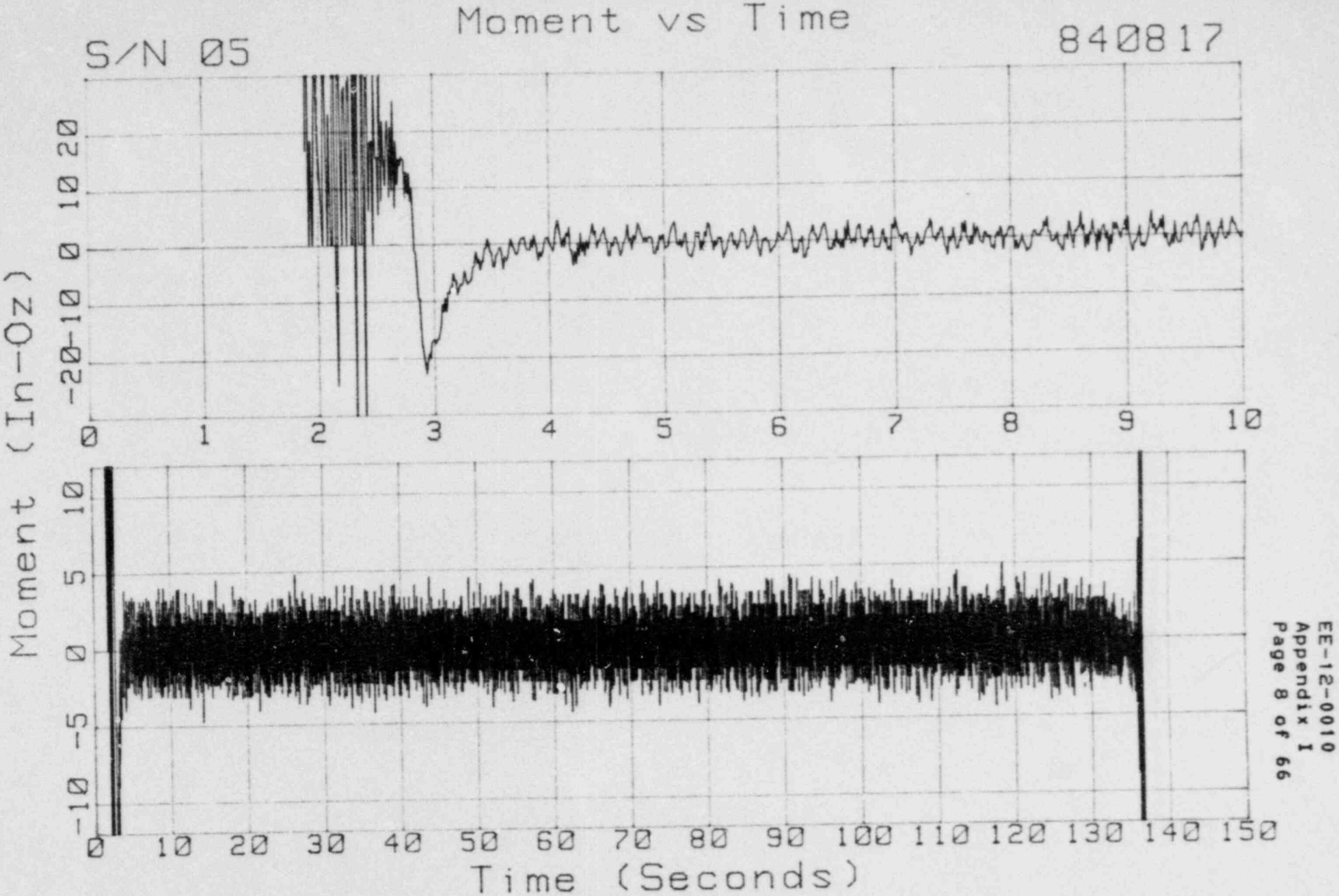
Moment vs Time
S/N 05
840817
Moment (In-Oz)
-20 -10 0 10 20
0 1 2 3 4 5 6 7 8 9 10
-10 -5 0 5 10
0 10 20 30 40 50 60 70 80 90 100 110 120 130 140 150
Time (Seconds)

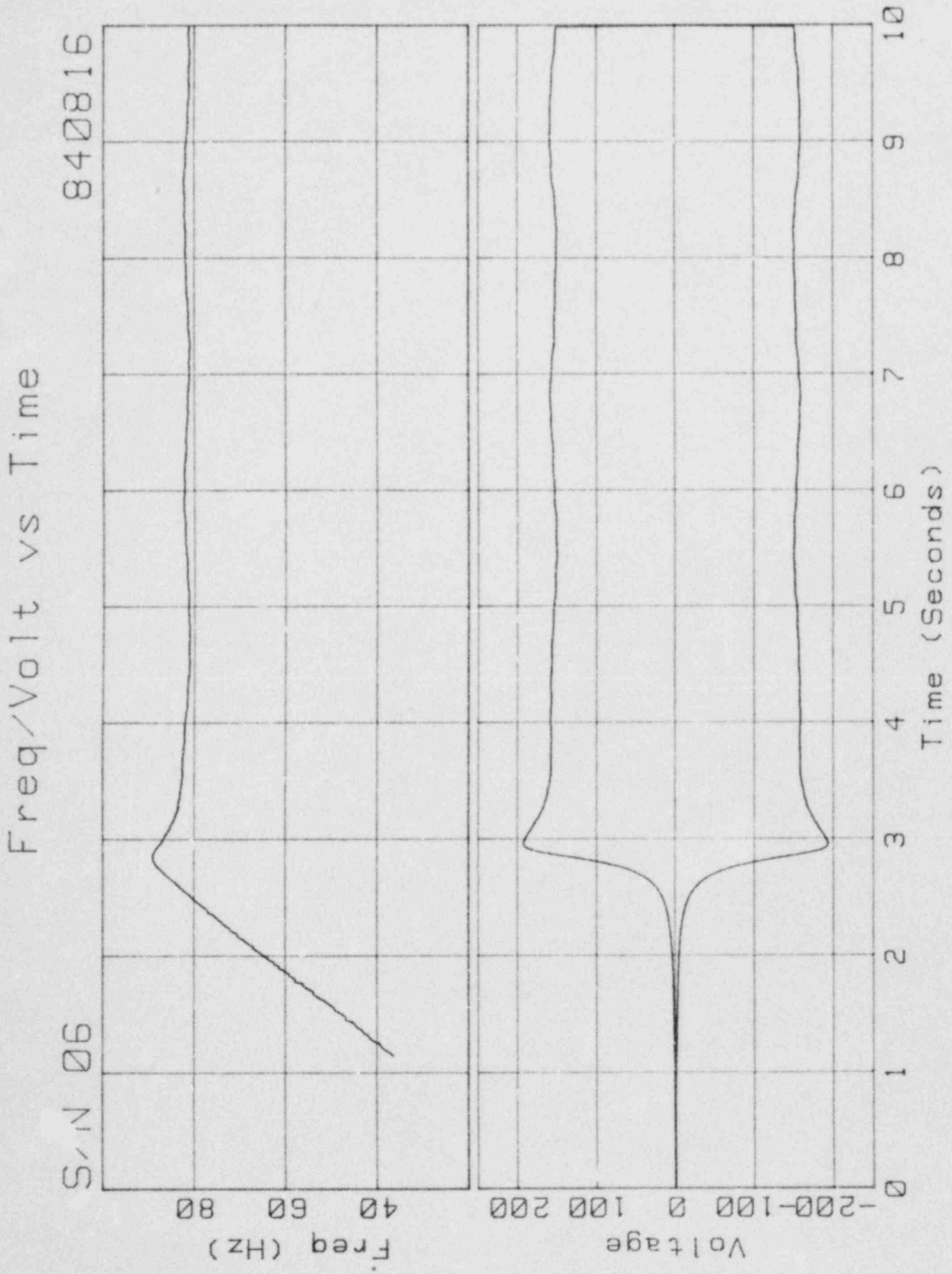
Freq/Volt vs Time
840816
S/N 06
Freq (Hz)
40
60
80
Voltage
-200
-100
0
100
200
0
1
2
3
4
5
6
7
8
9
10
Time (Seconds)

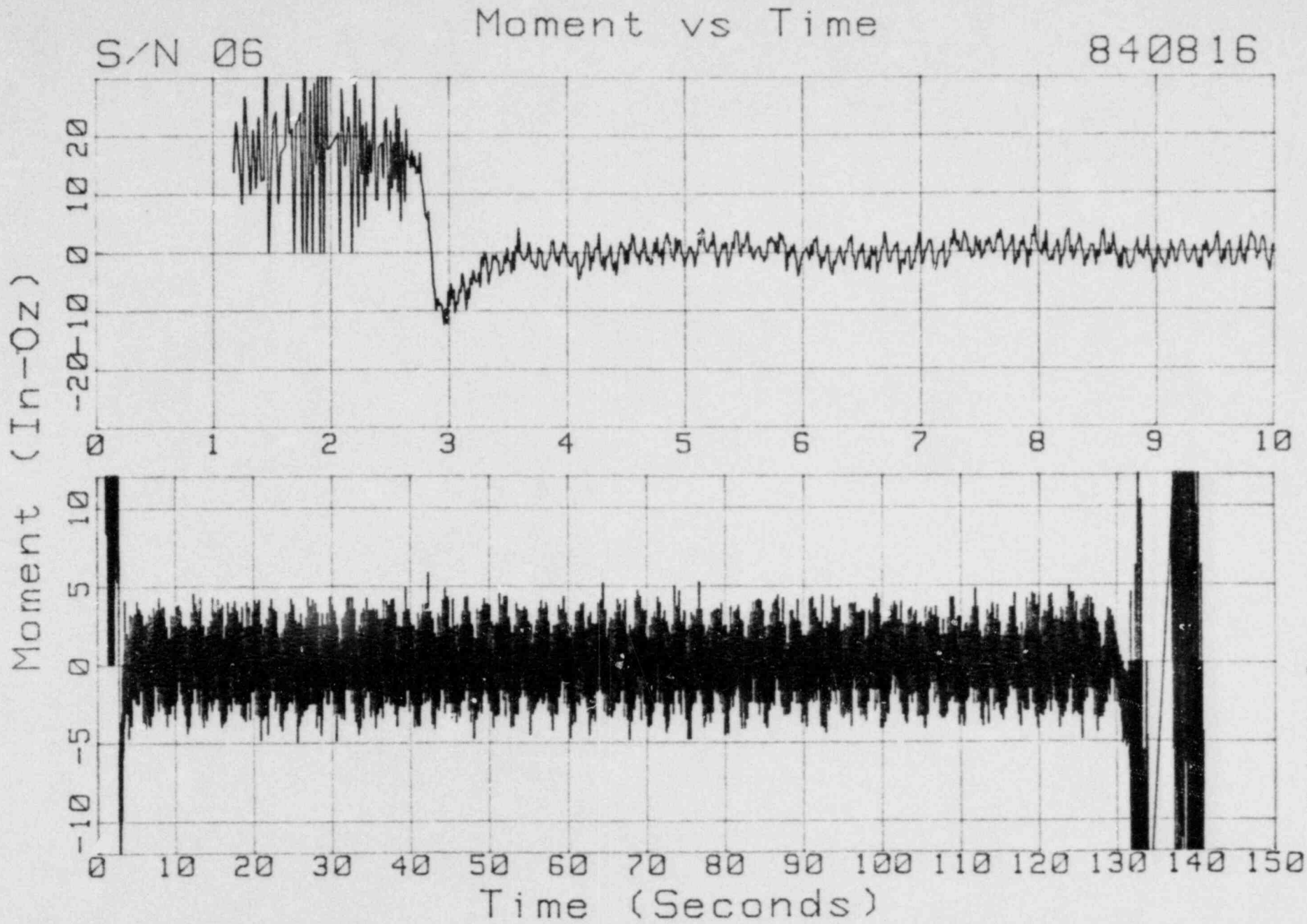
Moment vs Time
S/N 06
840816
Moment (In-Oz)
-20 -10 0 10 20
0 1 2 3 4 5 6 7 8 9 10
-10 -5 0 5 10
0 10 20 30 40 50 60 70 80 90 100 110 120 130 140 150
Time (Seconds)

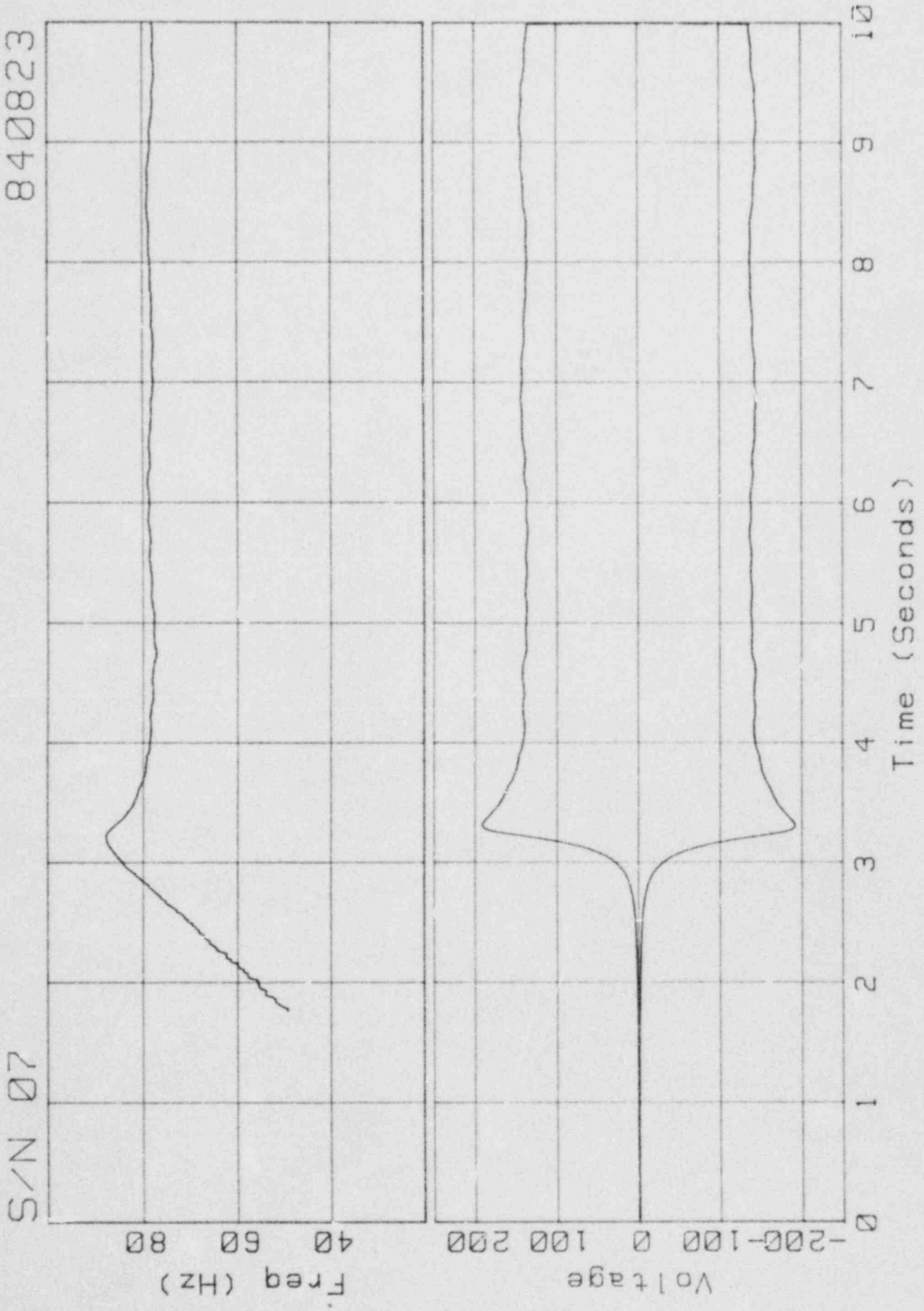
Freq/Volt vs Time
840823
S/N 07
Freq (Hz)
40
60
80
Voltage
-200
-100
0
100
200
0
1
2
3
4
5
6
7
8
9
10
Time (Seconds)

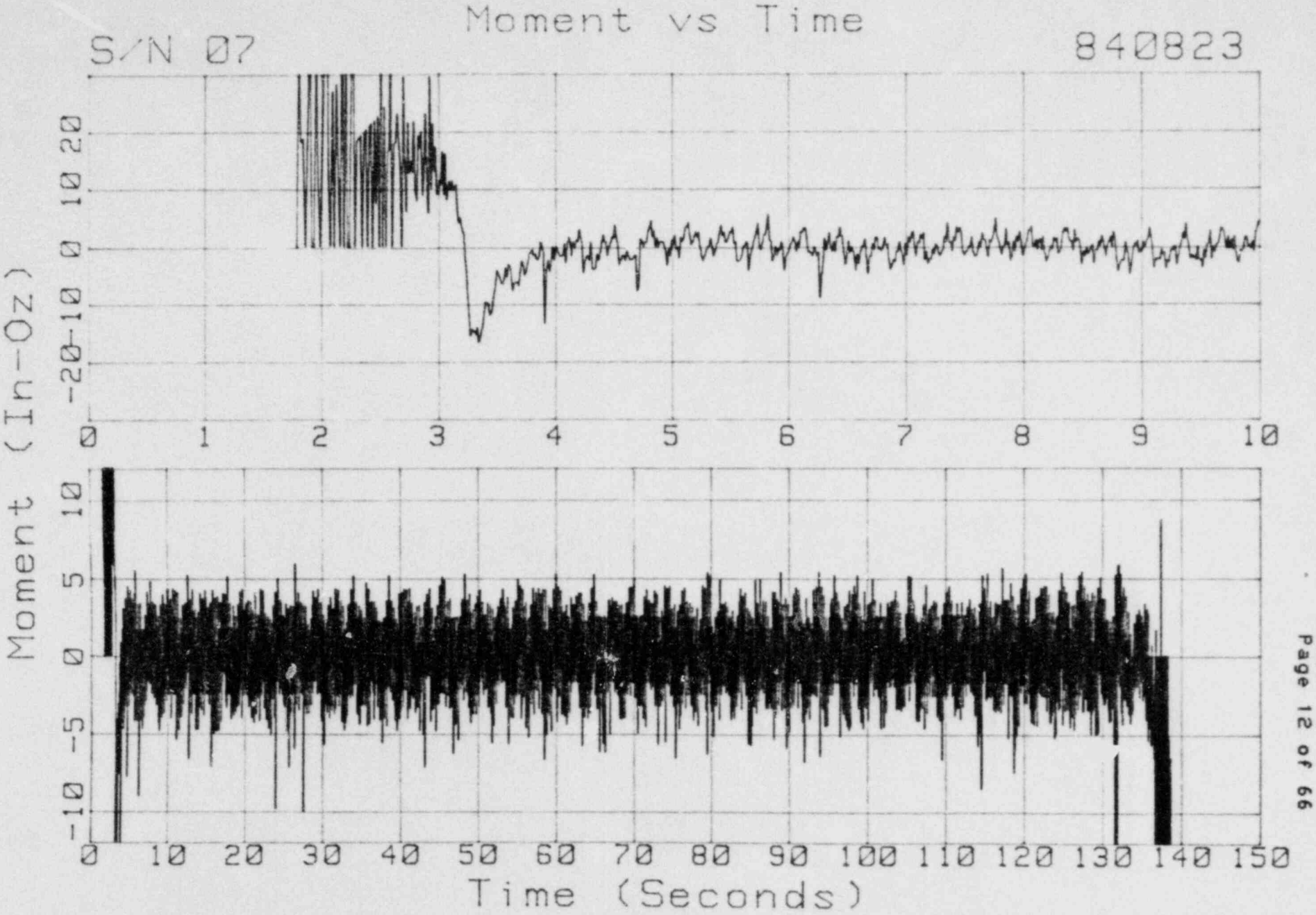
Moment vs Time
S/N 07
840823
Moment (In-Oz)
-20 -10 0 10 20
0 1 2 3 4 5 6 7 8 9 10
-10 -5 0 5 10
0 10 20 30 40 50 60 70 80 90 100 110 120 130 140 150
Time (Seconds)

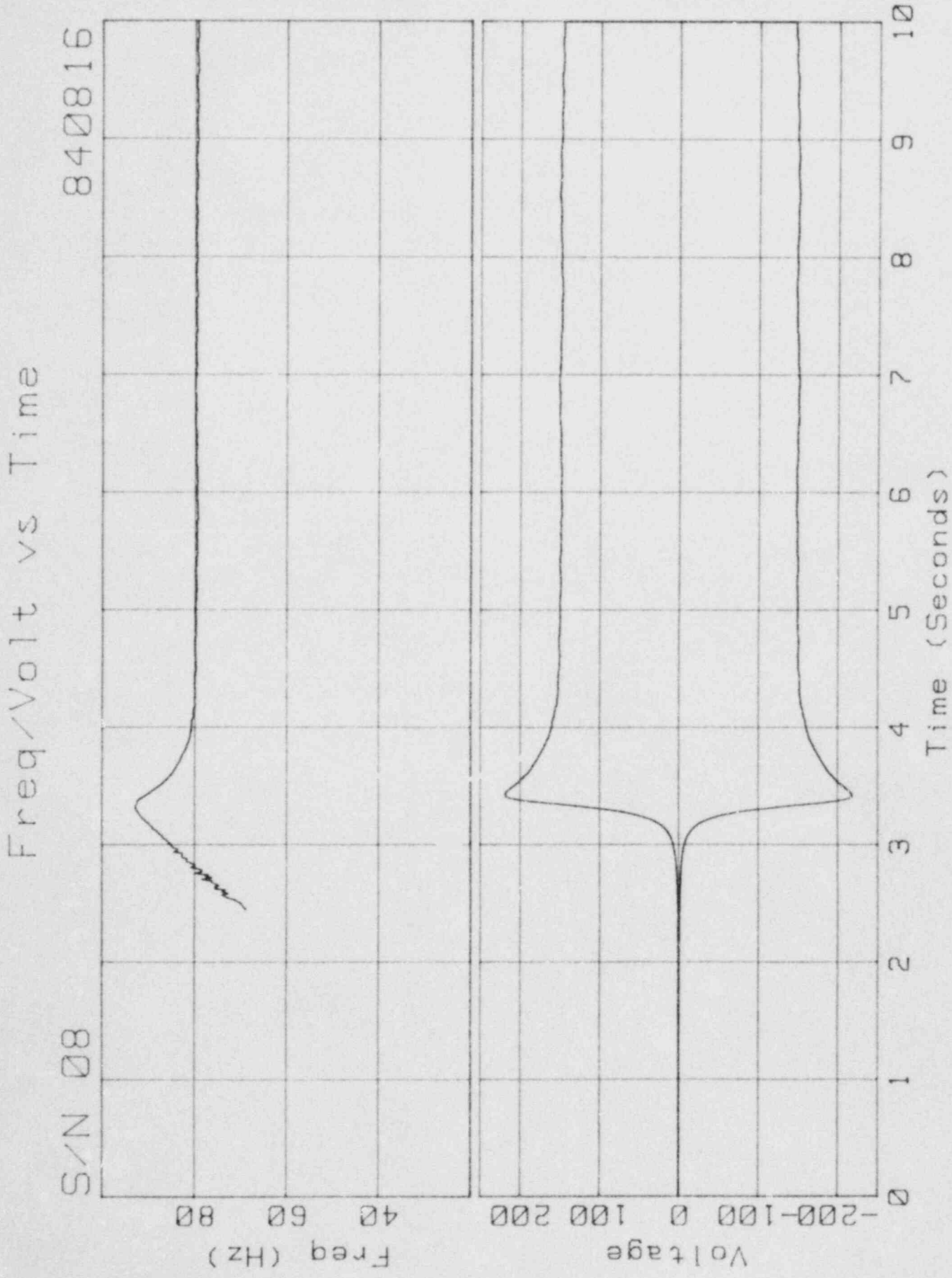
Freq/Volt vs Time
840816
S/N 08
Freq (Hz)
40
60
80
Voltage
-200
-100
0
100
200
0
1
2
3
4
5
6
7
8
9
10
Time (Seconds)

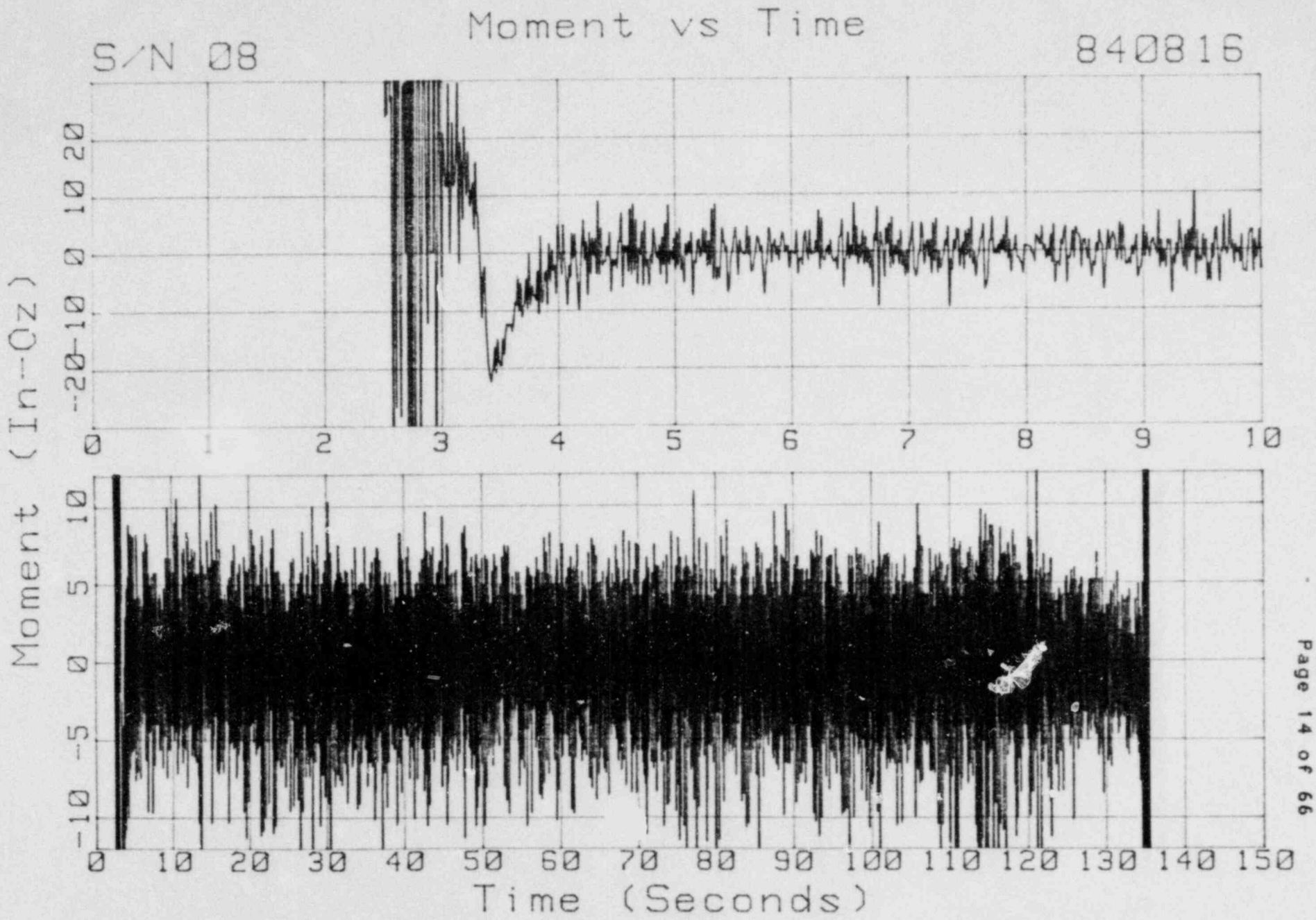
Moment vs Time
S/N 08
840816
Moment (In-Oz)
-20 -10 0 10 20
0 1 2 3 4 5 6 7 8 9 10
-10 -5 0 5 10
0 10 20 30 40 50 60 70 80 90 100 110 120 130 140 150
Time (Seconds)

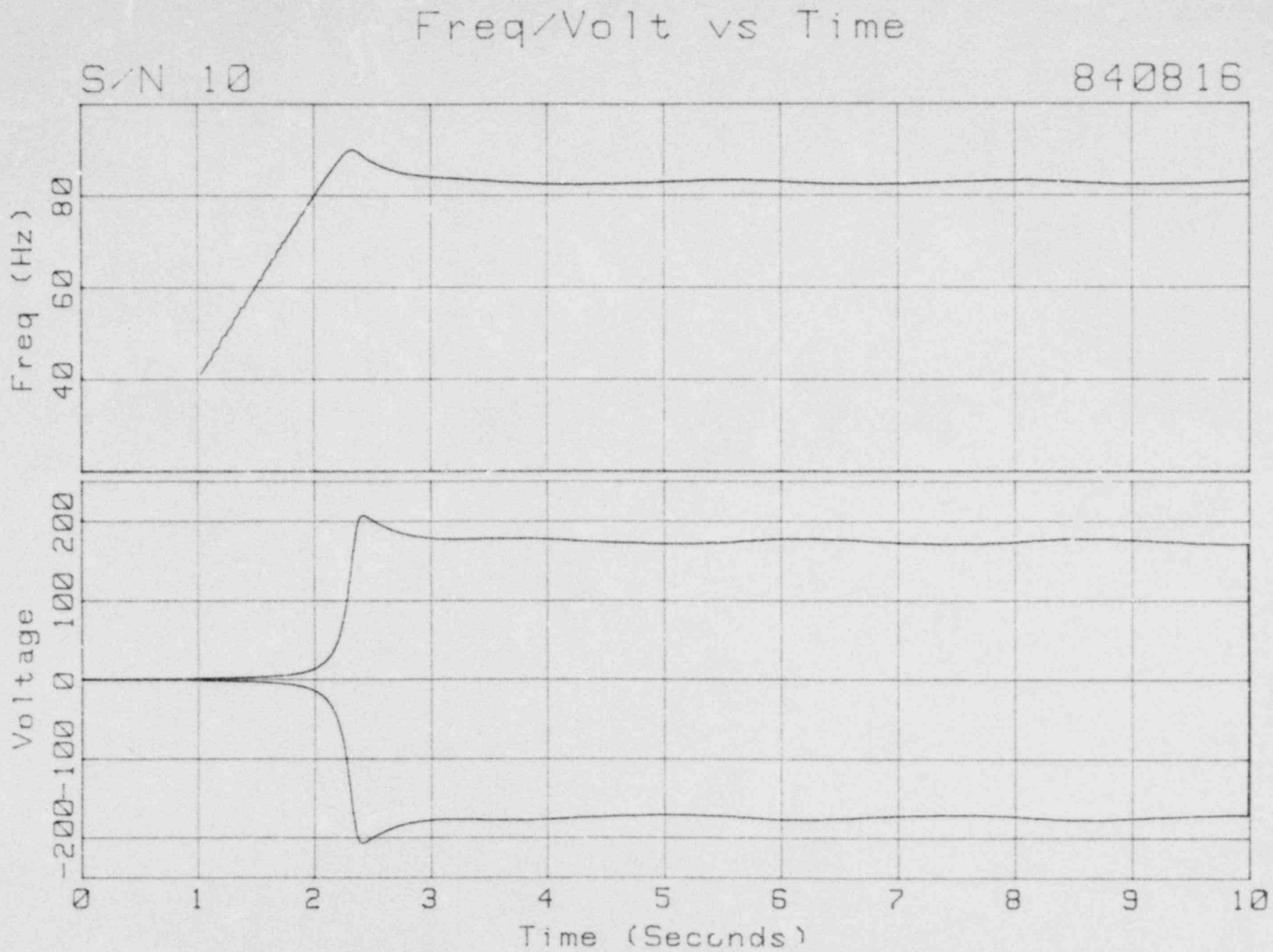
Freq/Volt vs Time
S/N 10
840816
Freq (Hz)
40
60
80
Voltage
-200
-100
0
100
200
0
1
2
3
4
5
6
7
8
9
10
Time (Seconds)

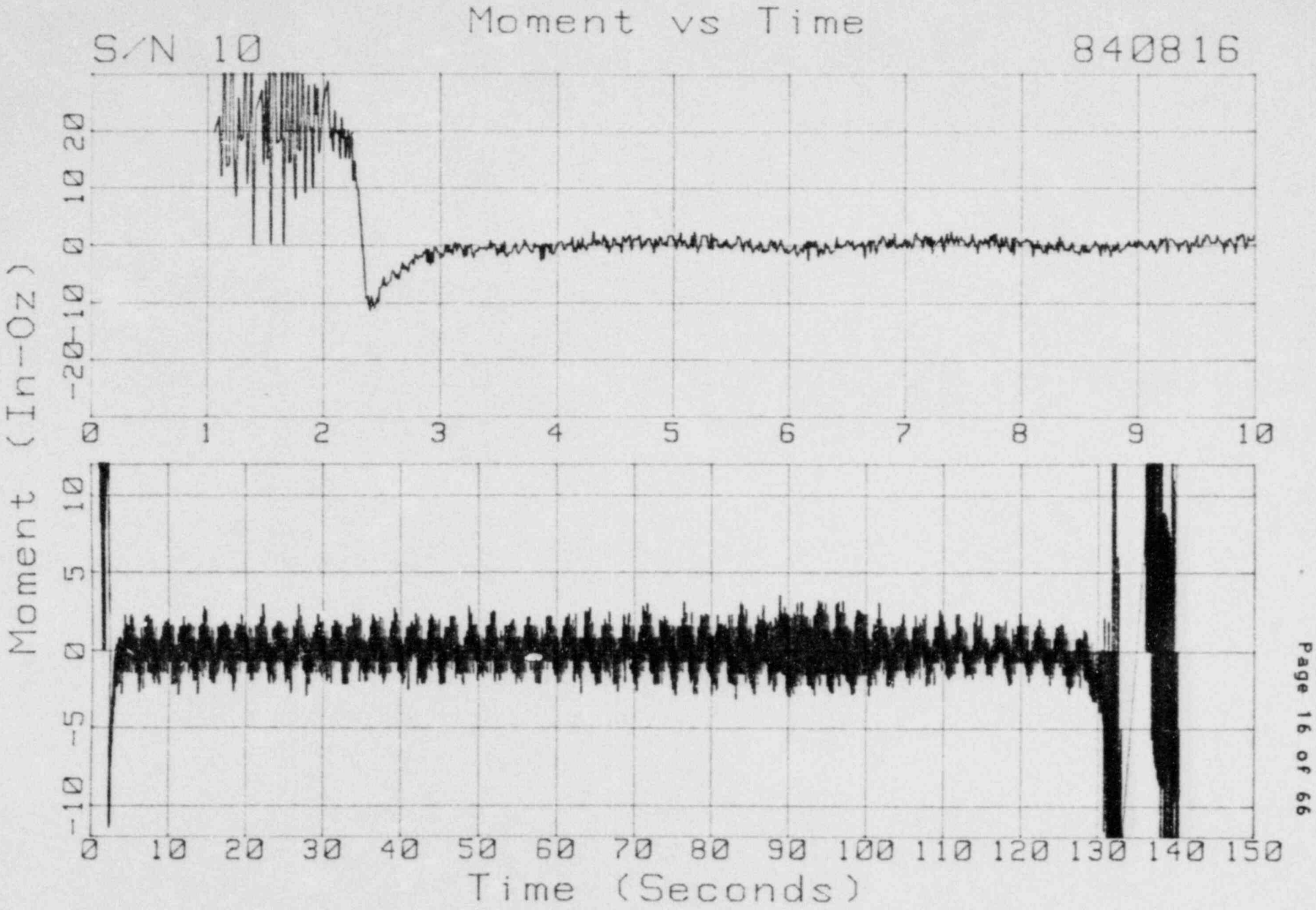
Moment vs Time
S/N 10
840816
Moment (In-Oz)
-20 -10 0 10 20
0 1 2 3 4 5 6 7 8 9 10
-10 -5 0 5 10
0 10 20 30 40 50 60 70 80 90 100 110 120 130 140 150
Time (Seconds)

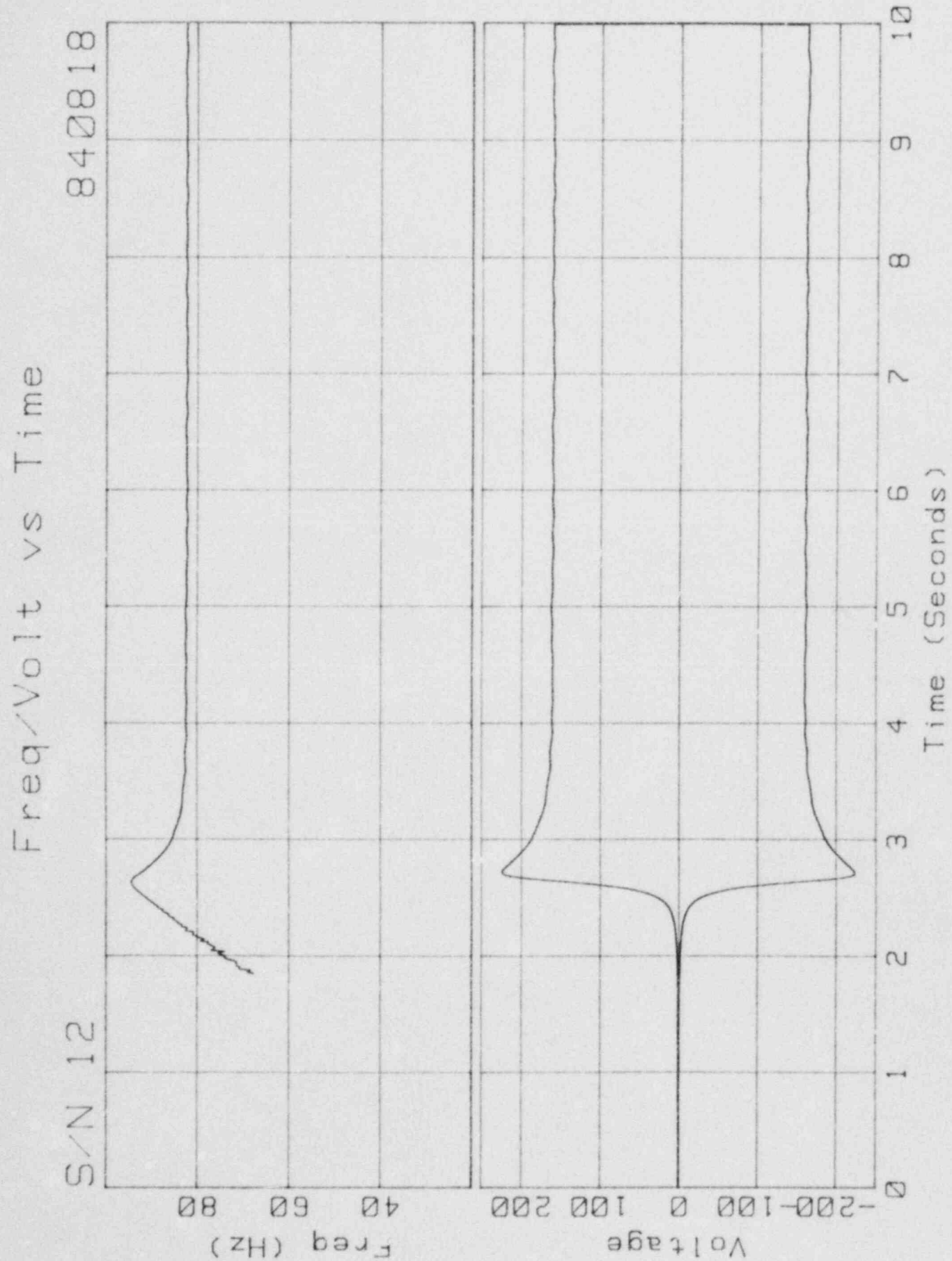
Freq/Volt vs Time
8408818
S/N 12
Freq (Hz)
40
60
80
Voltage
-200
-100
0
100
200
Time (Seconds)
0
1
2
3
4
5
6
7
8
9
10

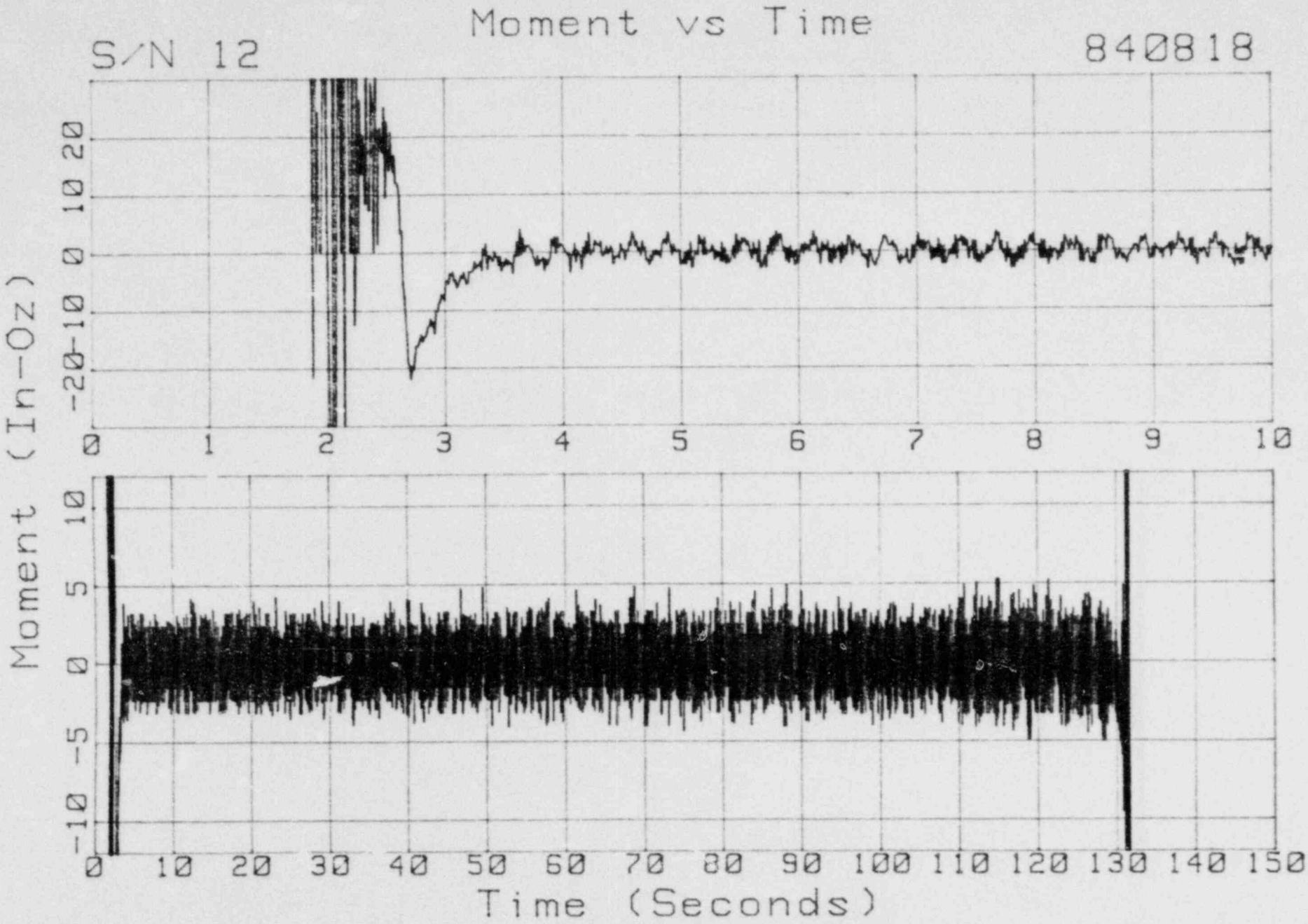
Moment vs Time
S/N 12
840818
Moment (In-Oz)
-20 -10 0 10 20
0 1 2 3 4 5 6 7 8 9 10
-10 -5 0 5 10
0 10 20 30 40 50 60 70 80 90 100 110 120 130 140 150
Time (Seconds)

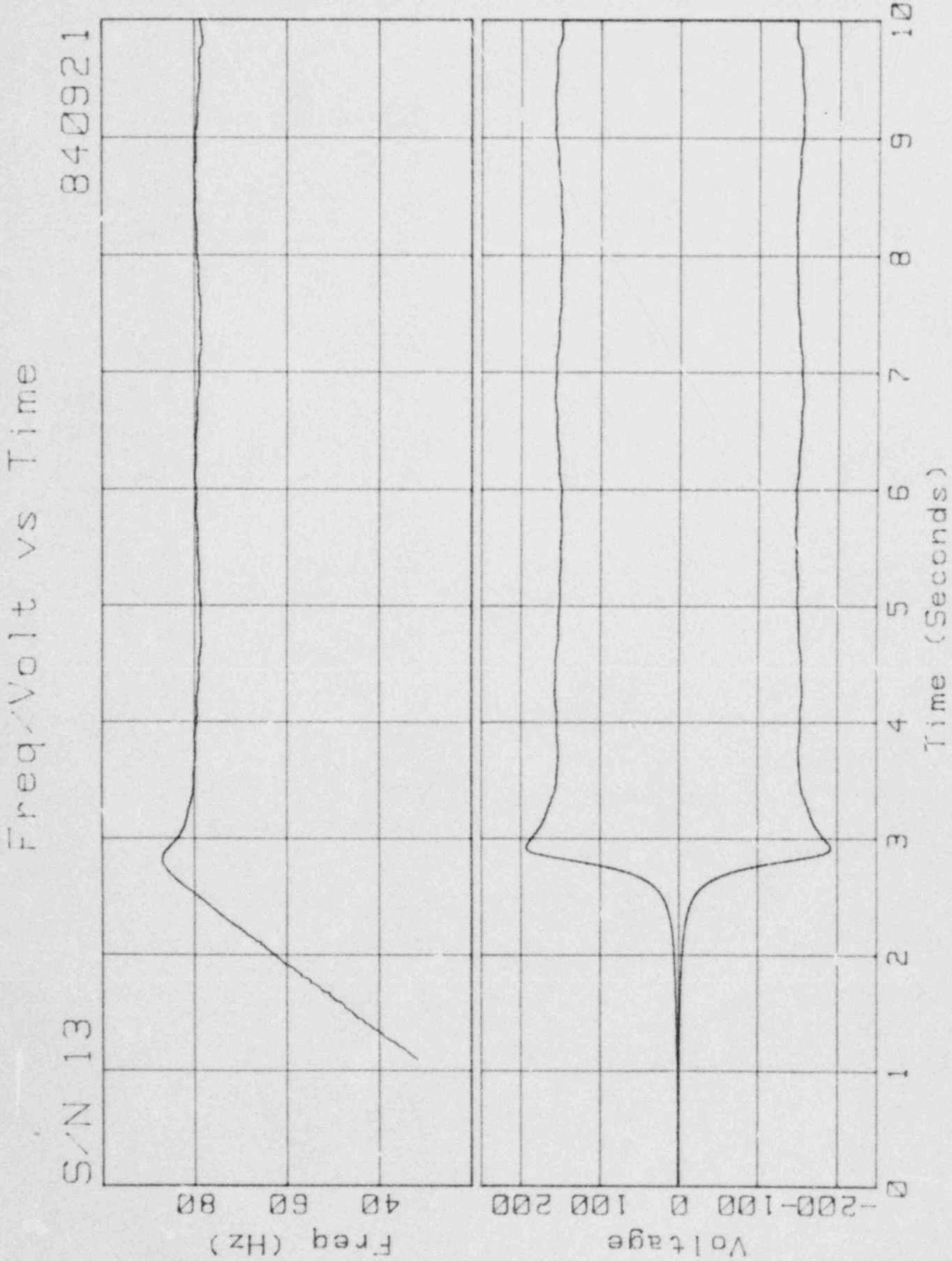
Freq/Volt vs Time
840921
S/N 13
Freq (Hz)
40
60
80
Voltage
-200
-100
0
100
200
0
1
2
3
4
5
6
7
8
9
10
Time (Seconds)

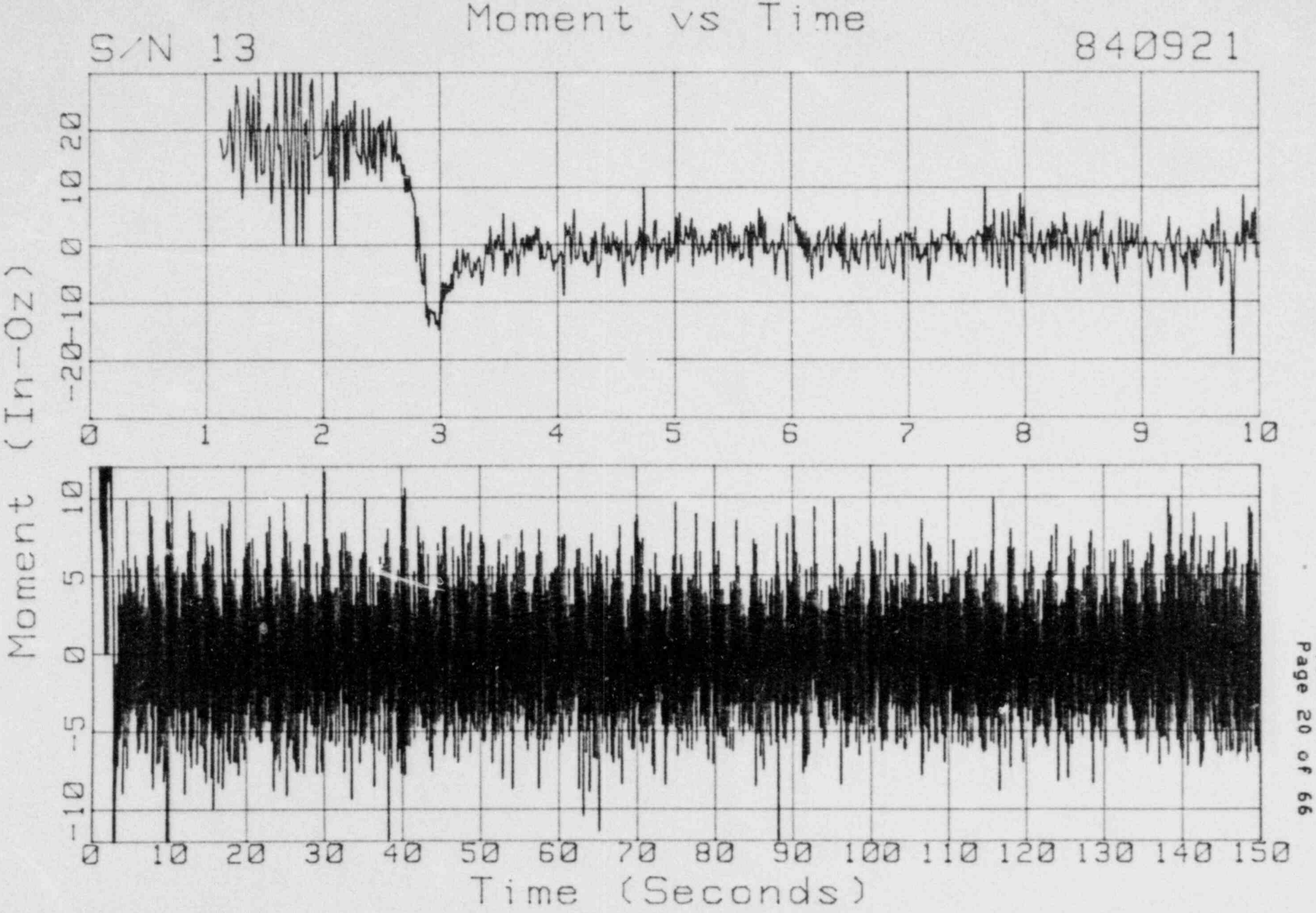
Moment vs Time
S/N 13
840921
Moment (In-Oz)
-20 -10 0 10 20
0 1 2 3 4 5 6 7 8 9 10
-10 -5 0 5 10
0 10 20 30 40 50 60 70 80 90 100 110 120 130 140 150
Time (Seconds)

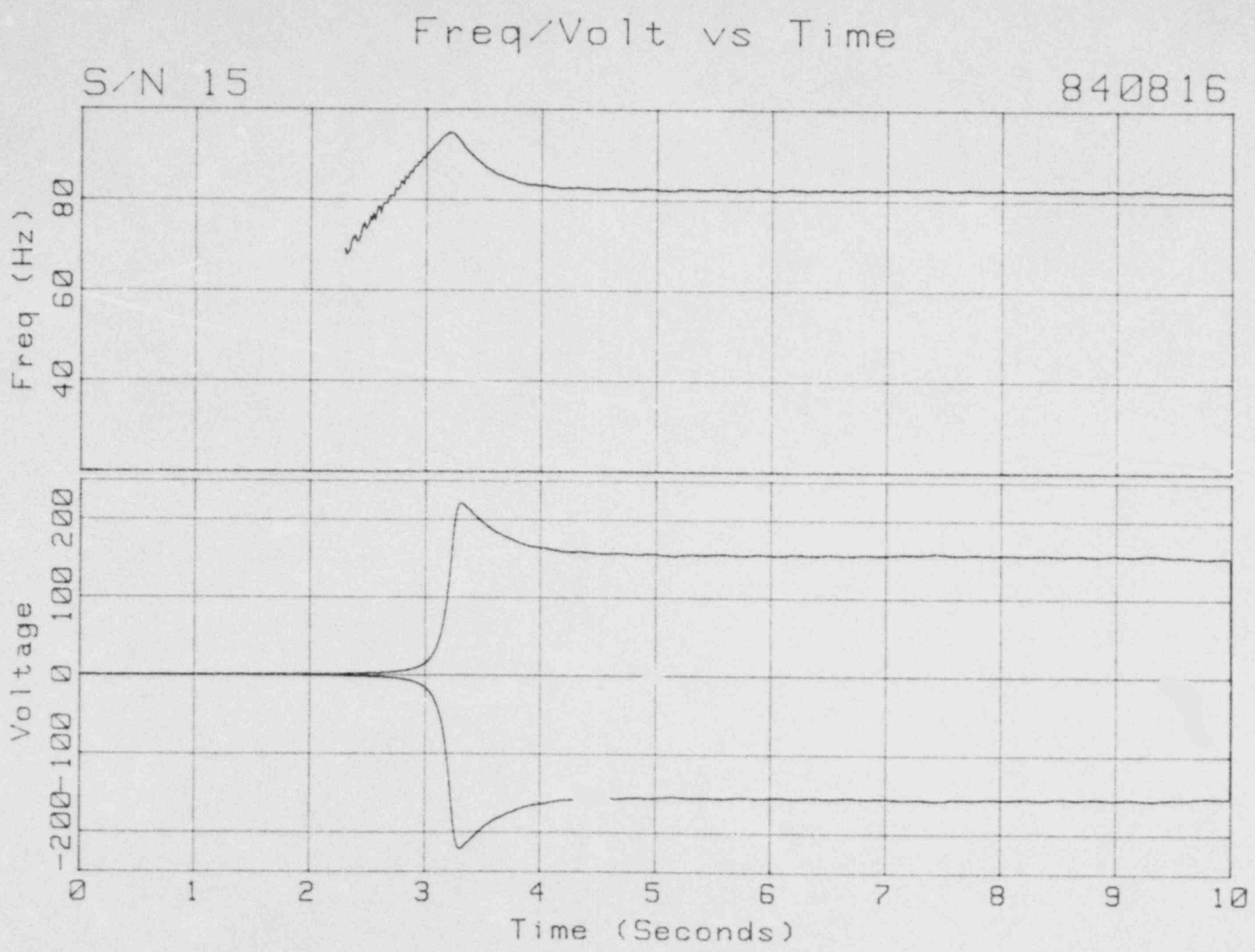
Freq/Volt vs Time
S/N 15
840816
Freq (Hz)
40 60 80
Voltage
-200 -100 0 100 200
0 1 2 3 4 5 6 7 8 9 10
Time (Seconds)

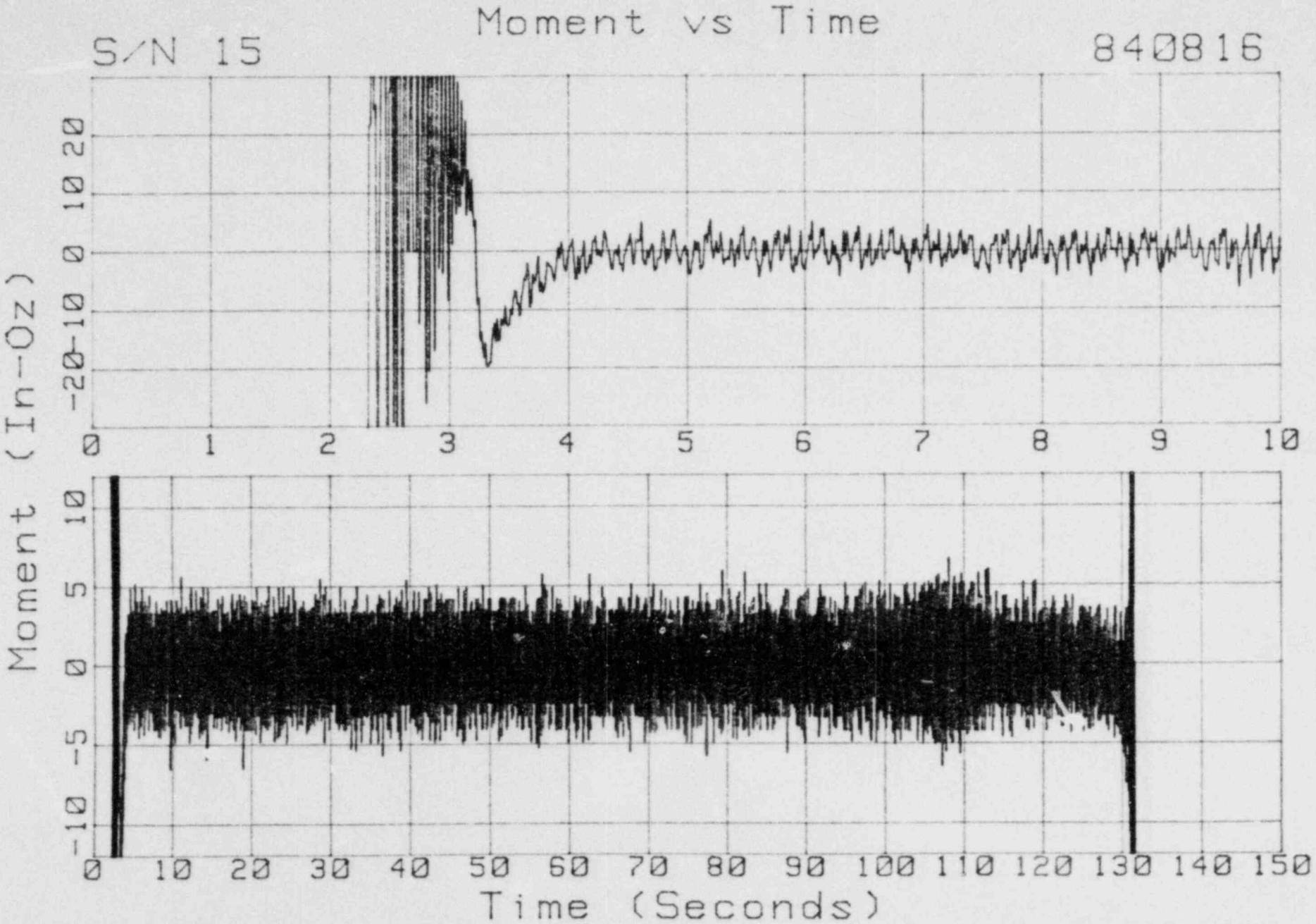
Moment vs Time
S/N 15
840816
Moment (In-Oz)
-20 -10 0 10 20
0 1 2 3 4 5 6 7 8 9 10
-10 -5 0 5 10
0 10 20 30 40 50 60 70 80 90 100 110 120 130 140 150
Time (Seconds)

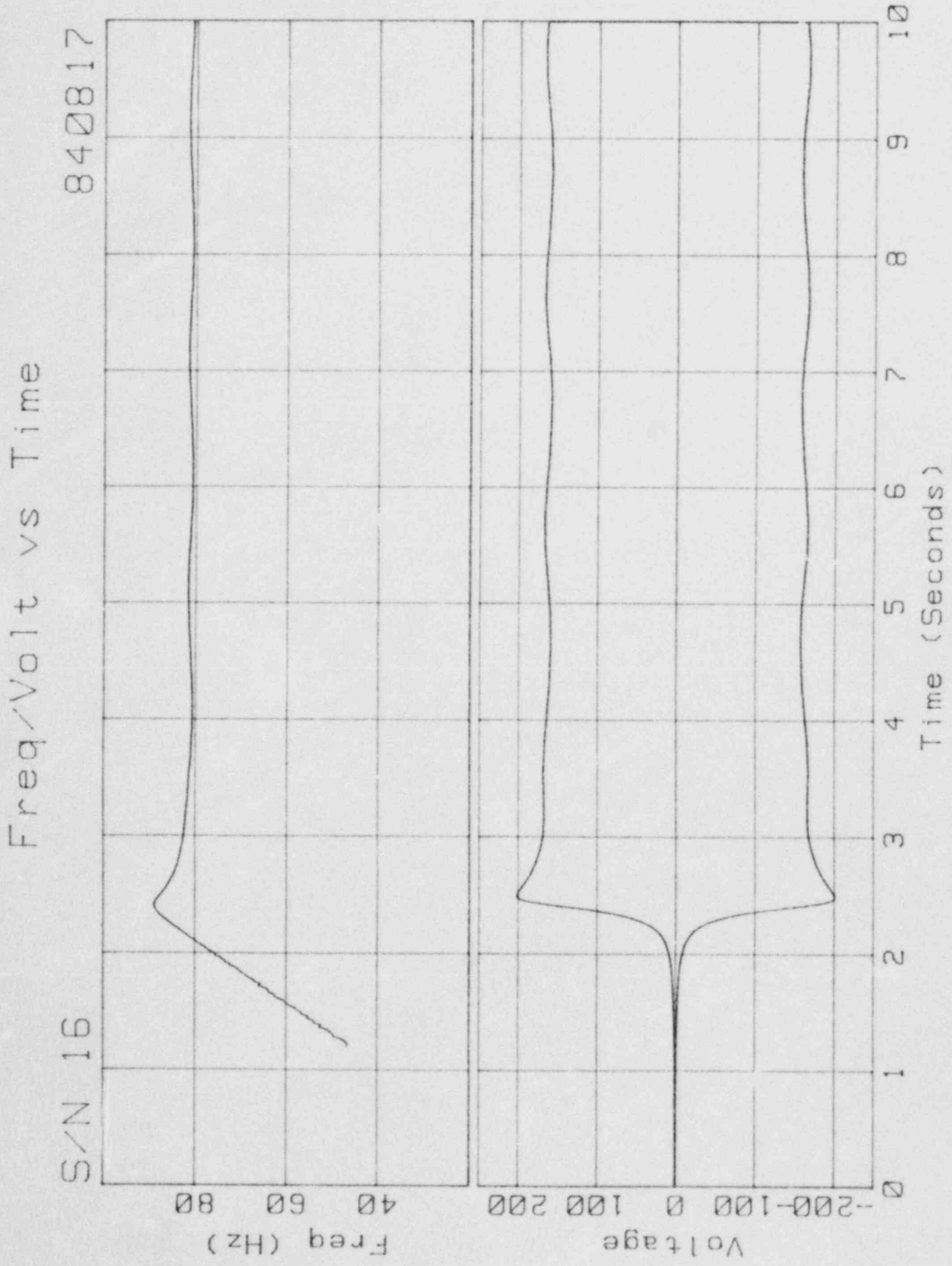
Freq/Volt vs Time
840817
S/N 16
Freq (Hz)
40
60
80
Voltage
-200
-100
0
100
200
0
1
2
3
4
5
6
7
8
9
10
Time (Seconds)

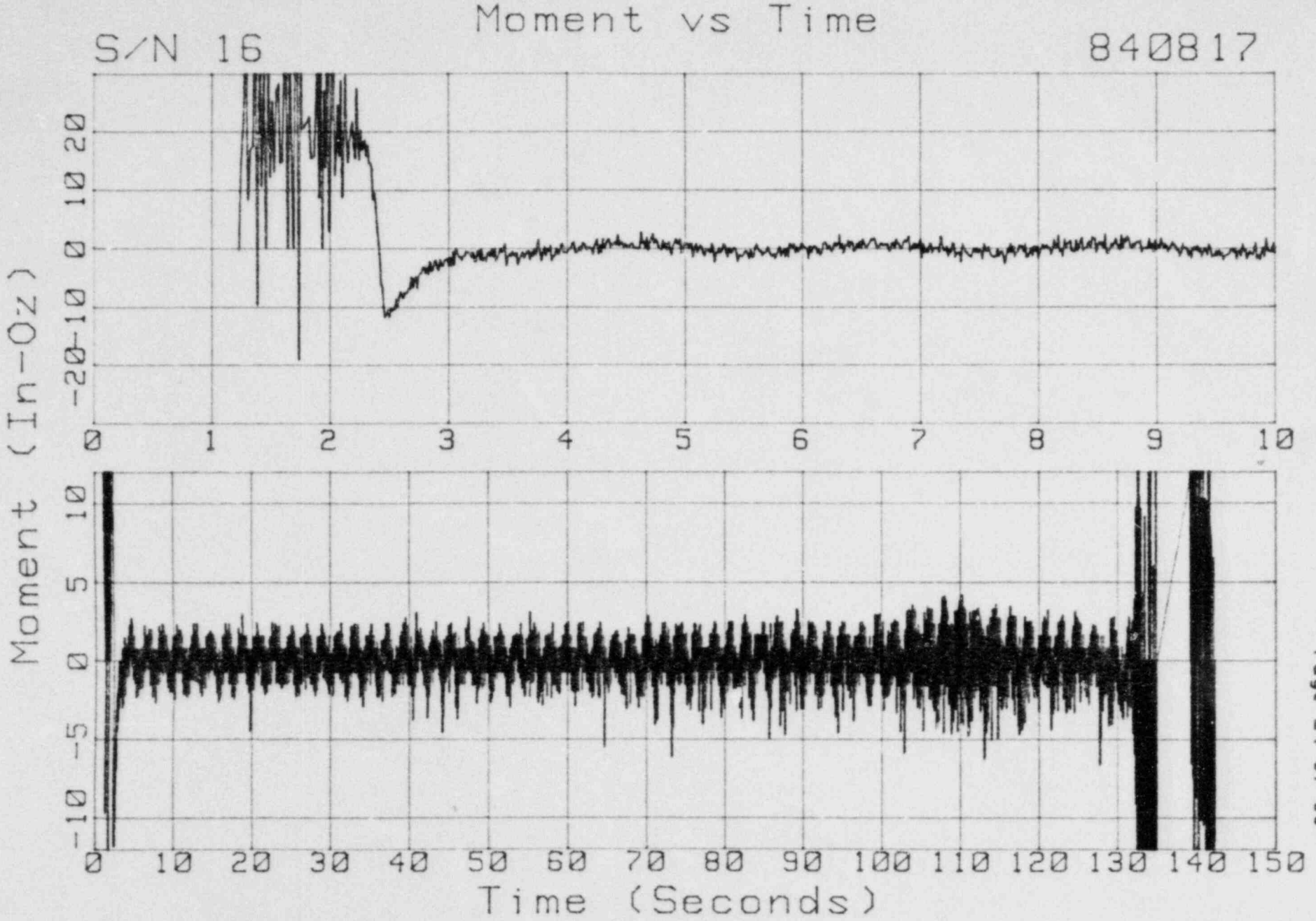
Moment vs Time
S/N 16
840817
Moment (In-Oz)
-20 -10 0 10 20
0 1 2 3 4 5 6 7 8 9 10
-10 -5 0 5 10
0 10 20 30 40 50 60 70 80 90 100 110 120 130 140 150
Time (Seconds)

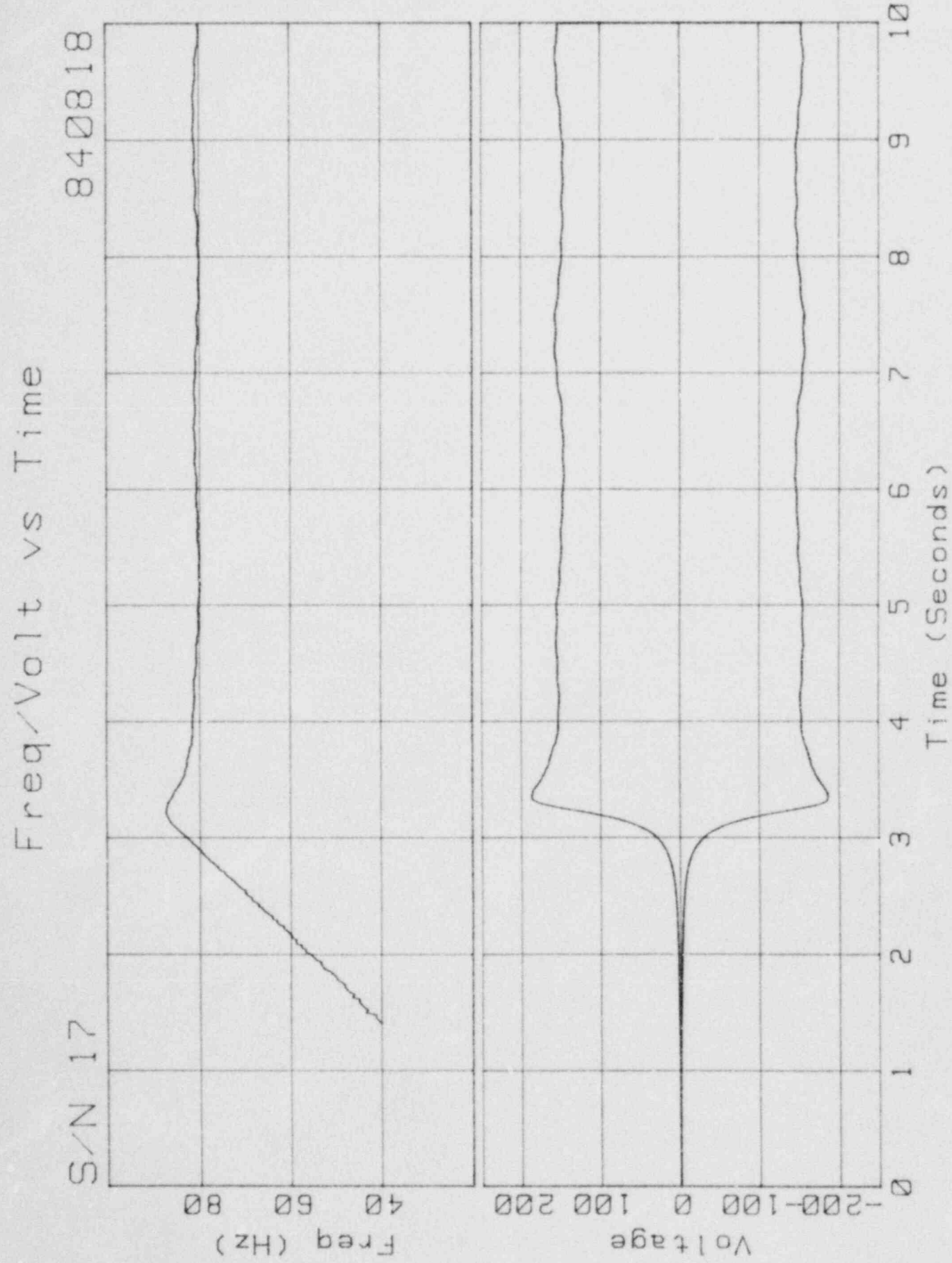
Freq/Volt vs Time
840818
S/N 17
Freq (Hz)
40
60
80
Voltage
-200
-100
0
100
200
0
1
2
3
4
5
6
7
8
9
10
Time (Seconds)

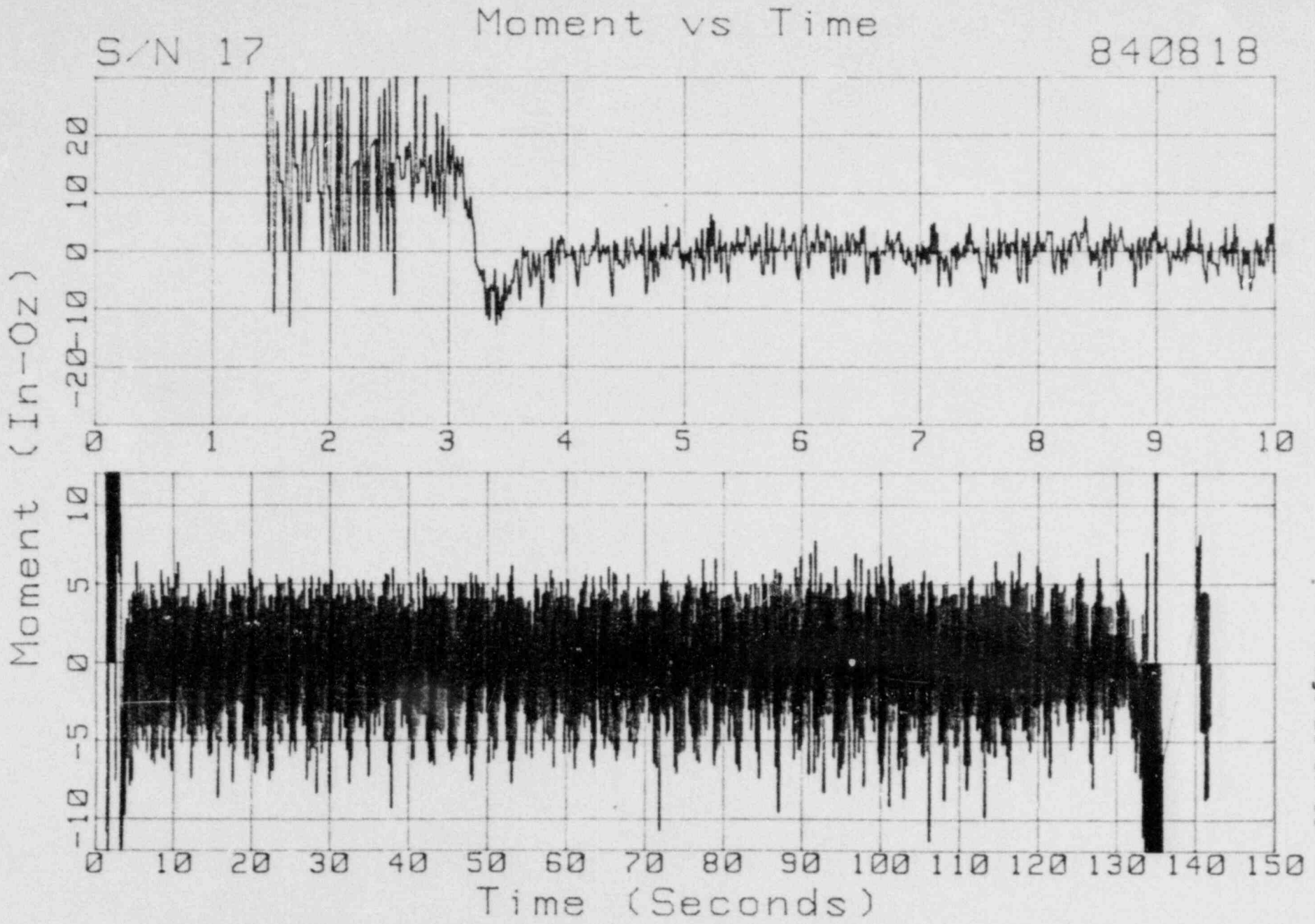
Moment vs Time
S/N 17
840818
Moment (In-Oz)
-20 -10 0 10 20
0 1 2 3 4 5 6 7 8 9 10
-10 -5 0 5 10
0 10 20 30 40 50 60 70 80 90 100 110 120 130 140 150
Time (Seconds)

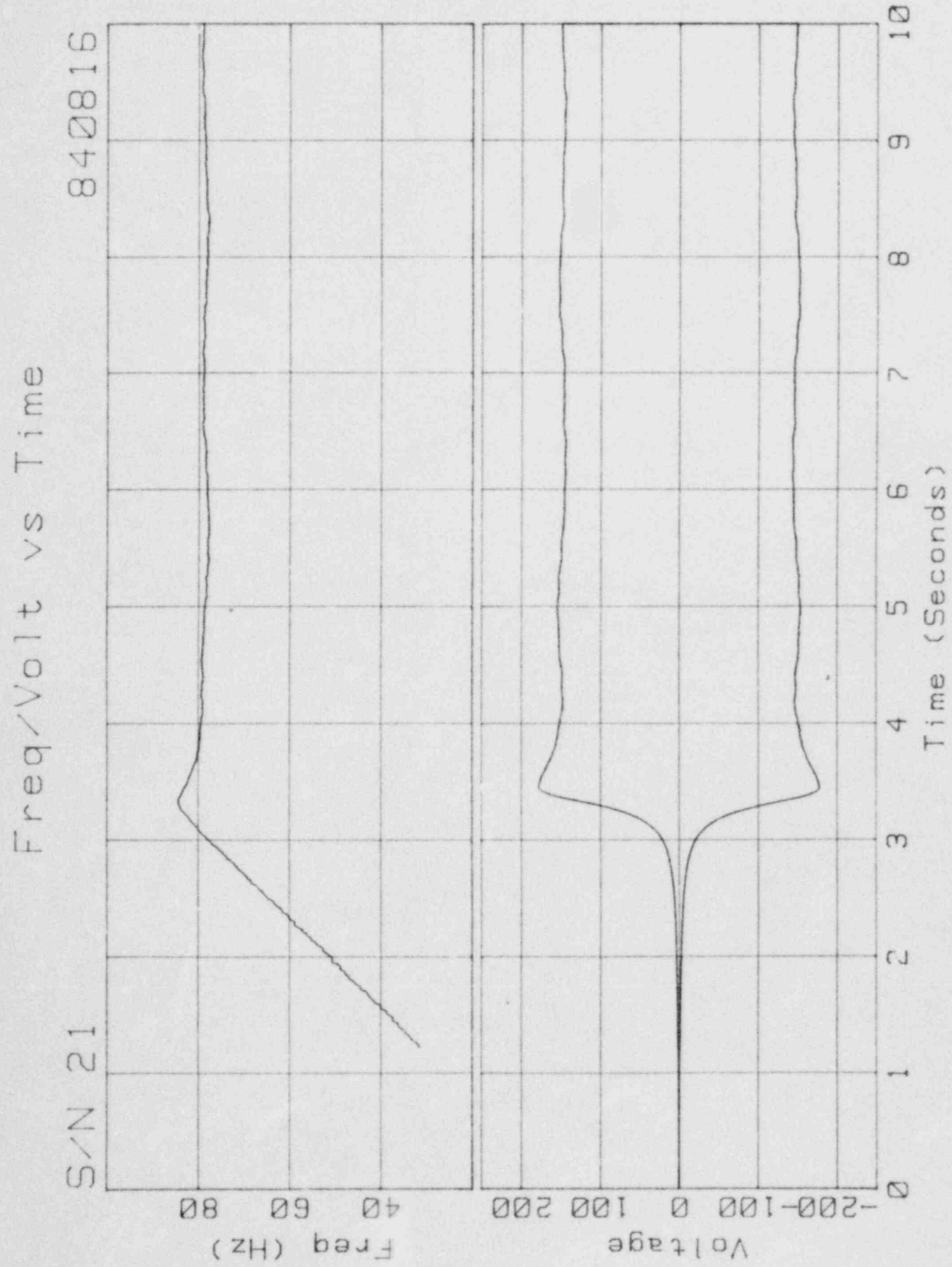
Freq/Volt vs Time
8408816
S/N 21
Freq (Hz)
40
60
80
Voltage
-200
-100
0
100
200
0
1
2
3
4
5
6
7
8
9
10
Time (Seconds)

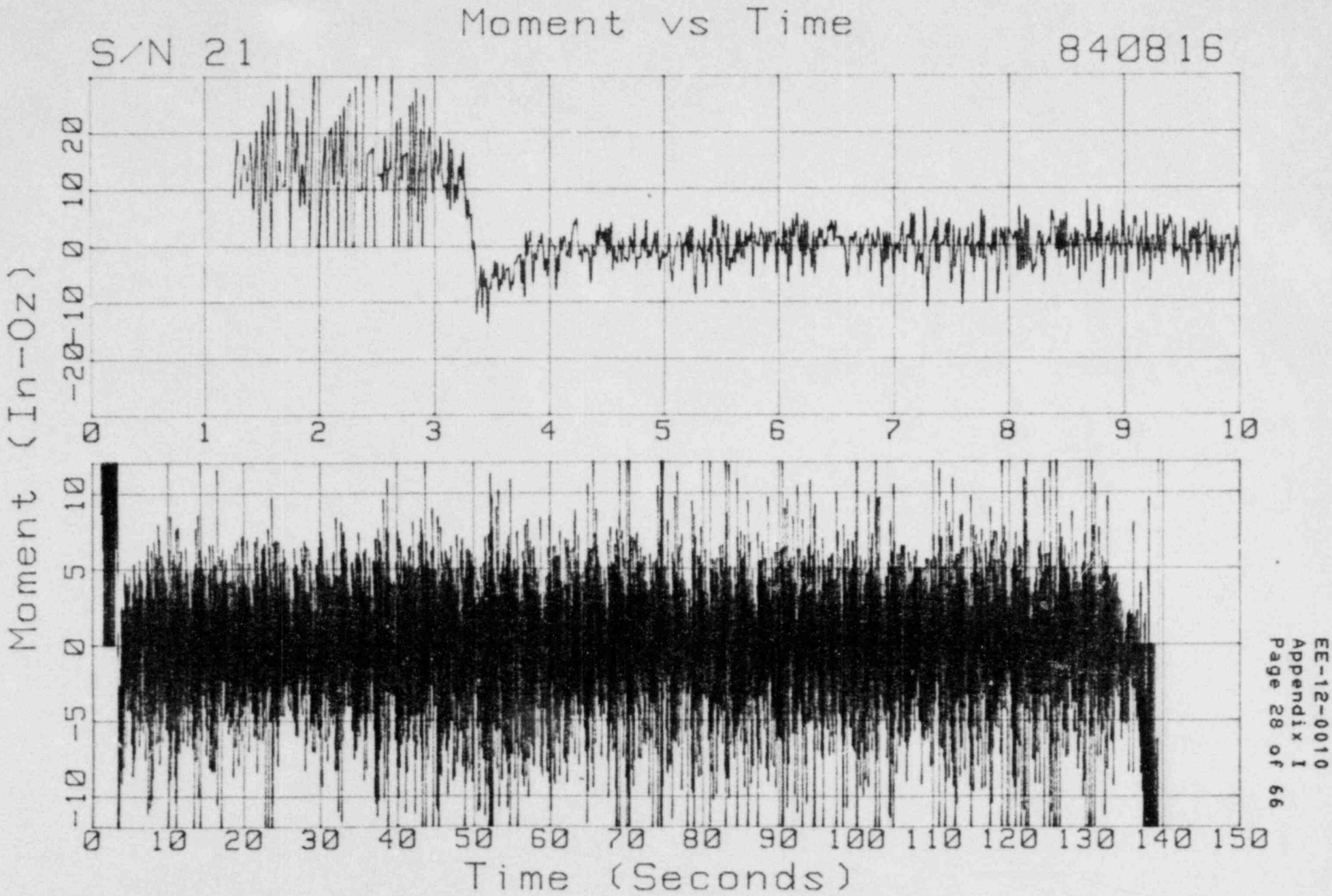
Moment vs Time
S/N 21
840816
Moment (In-Oz)
-20 -10 0 10 20
0 1 2 3 4 5 6 7 8 9 10
-10 -5 0 5 10
0 10 20 30 40 50 60 70 80 90 100 110 120 130 140 150
Time (Seconds)

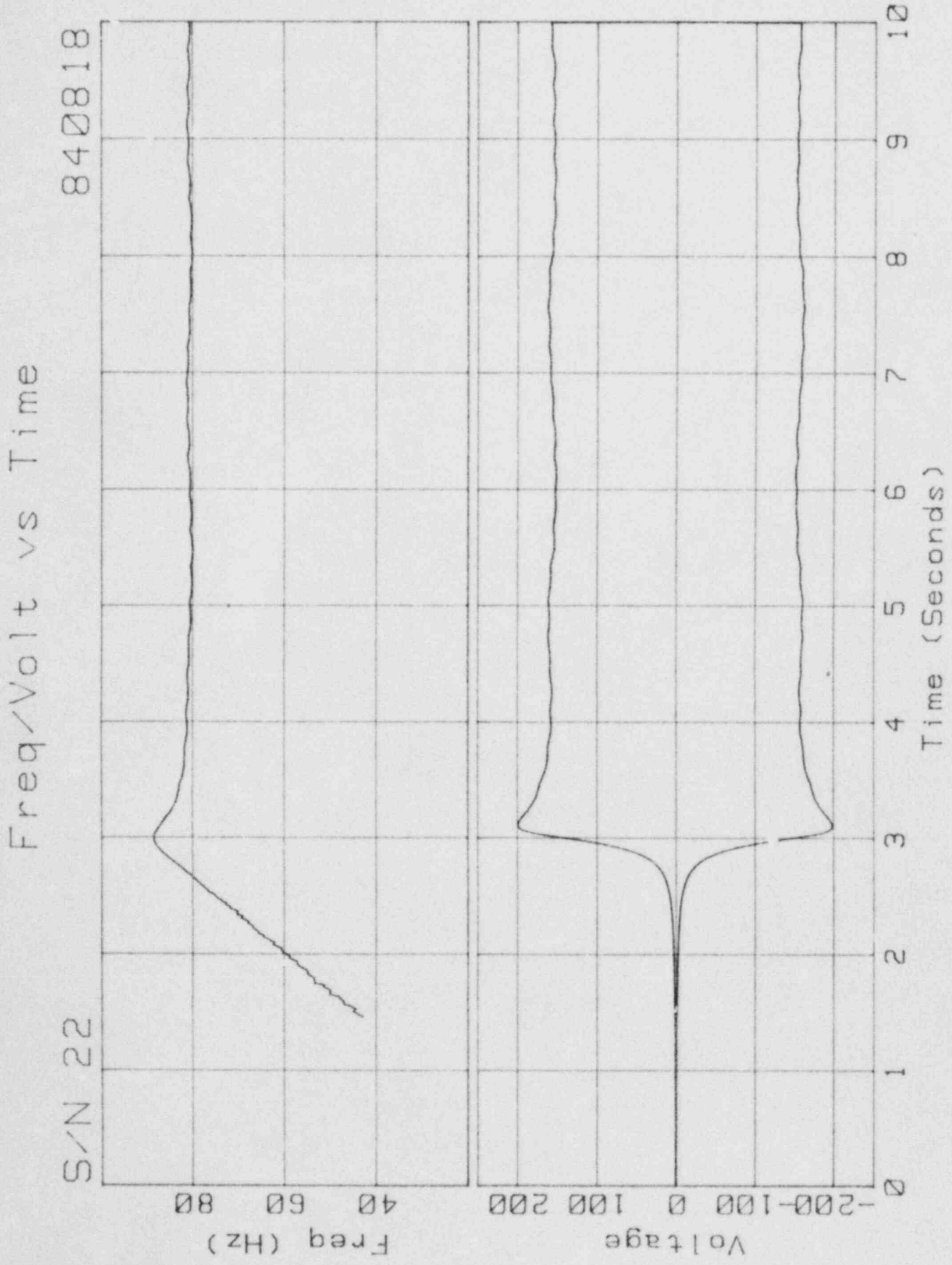
Freq/Volt vs Time
8408818
S/N 22
Freq (Hz)
40
60
80
Voltage
-200
-100
0
100
200
0
1
2
3
4
5
6
7
8
9
10
Time (Seconds)

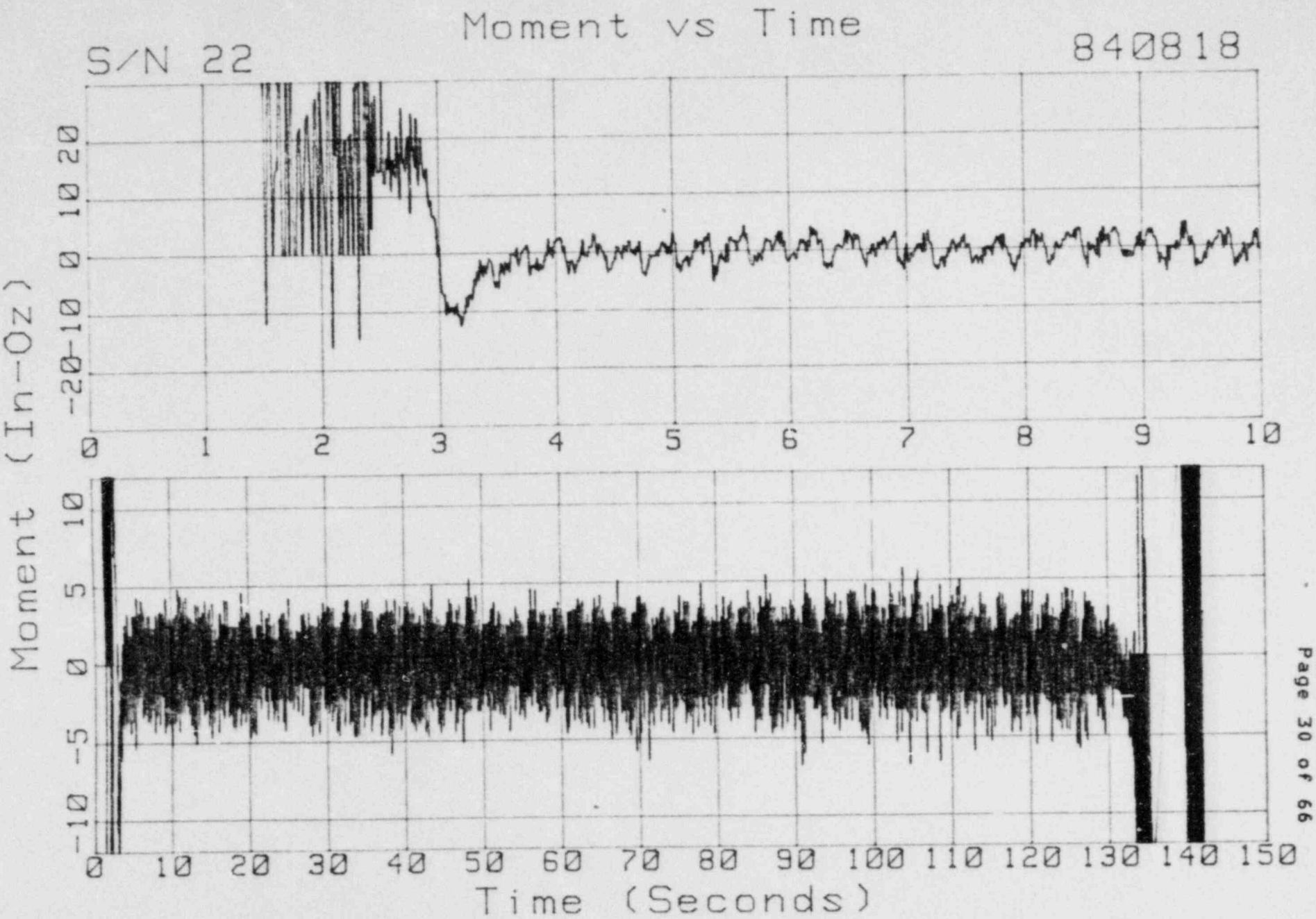
Moment vs Time
S/N 22
840818
Moment (In-Oz)
-20 -10 0 10 20
0 1 2 3 4 5 6 7 8 9 10
-10 -5 0 5 10
0 10 20 30 40 50 60 70 80 90 100 110 120 130 140 150
Time (Seconds)

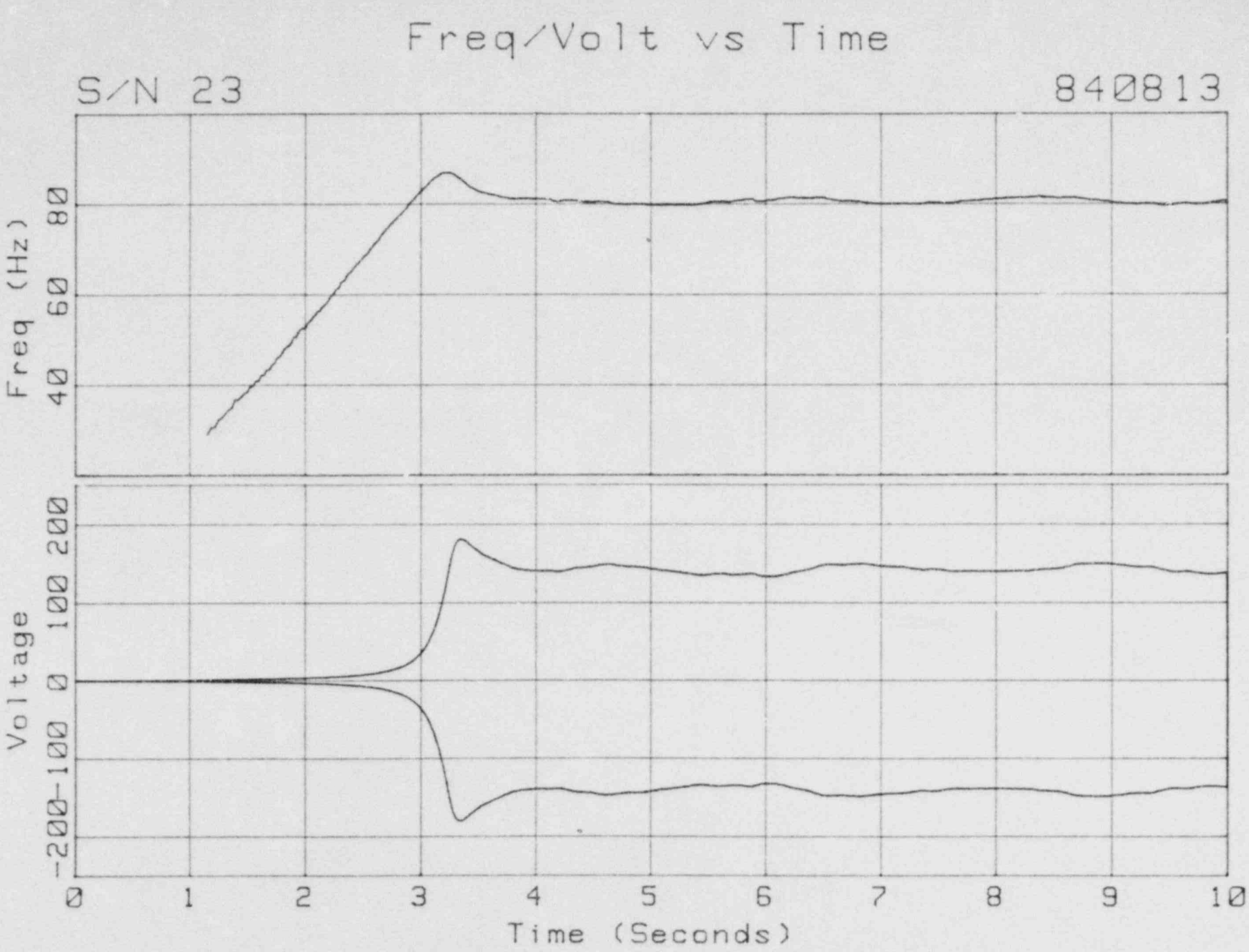
Freq/Volt vs Time
S/N 23
840813
Freq (Hz)
40
60
80
Voltage
-200
-100
0
100
200
0
1
2
3
4
5
6
7
8
9
10
Time (Seconds)

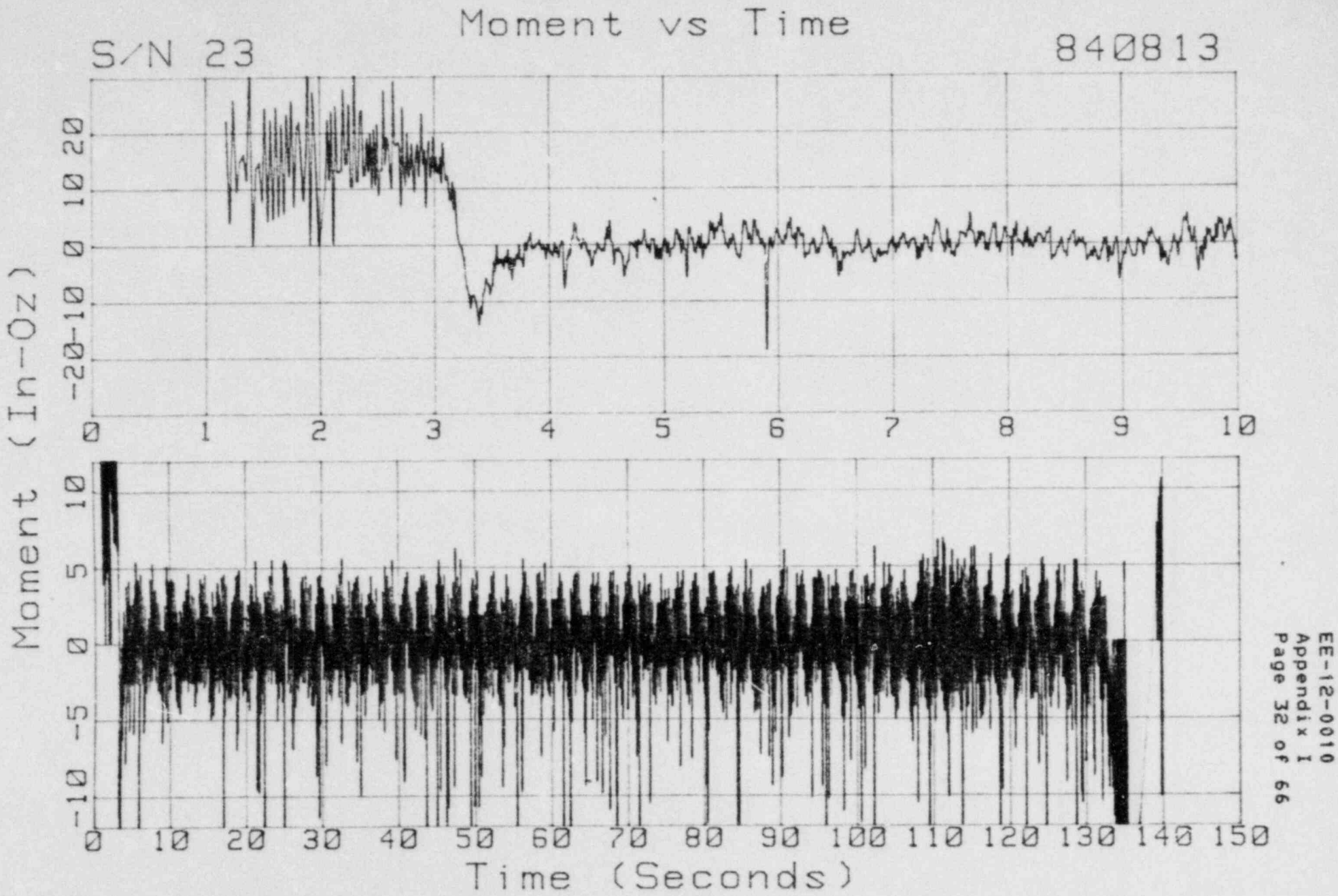
Moment vs Time
S/N 23
840813
Moment (In-Oz)
-20 -10 0 10 20
0 1 2 3 4 5 6 7 8 9 10
-10 -5 0 5 10
0 10 20 30 40 50 60 70 80 90 100 110 120 130 140 150
Time (Seconds)

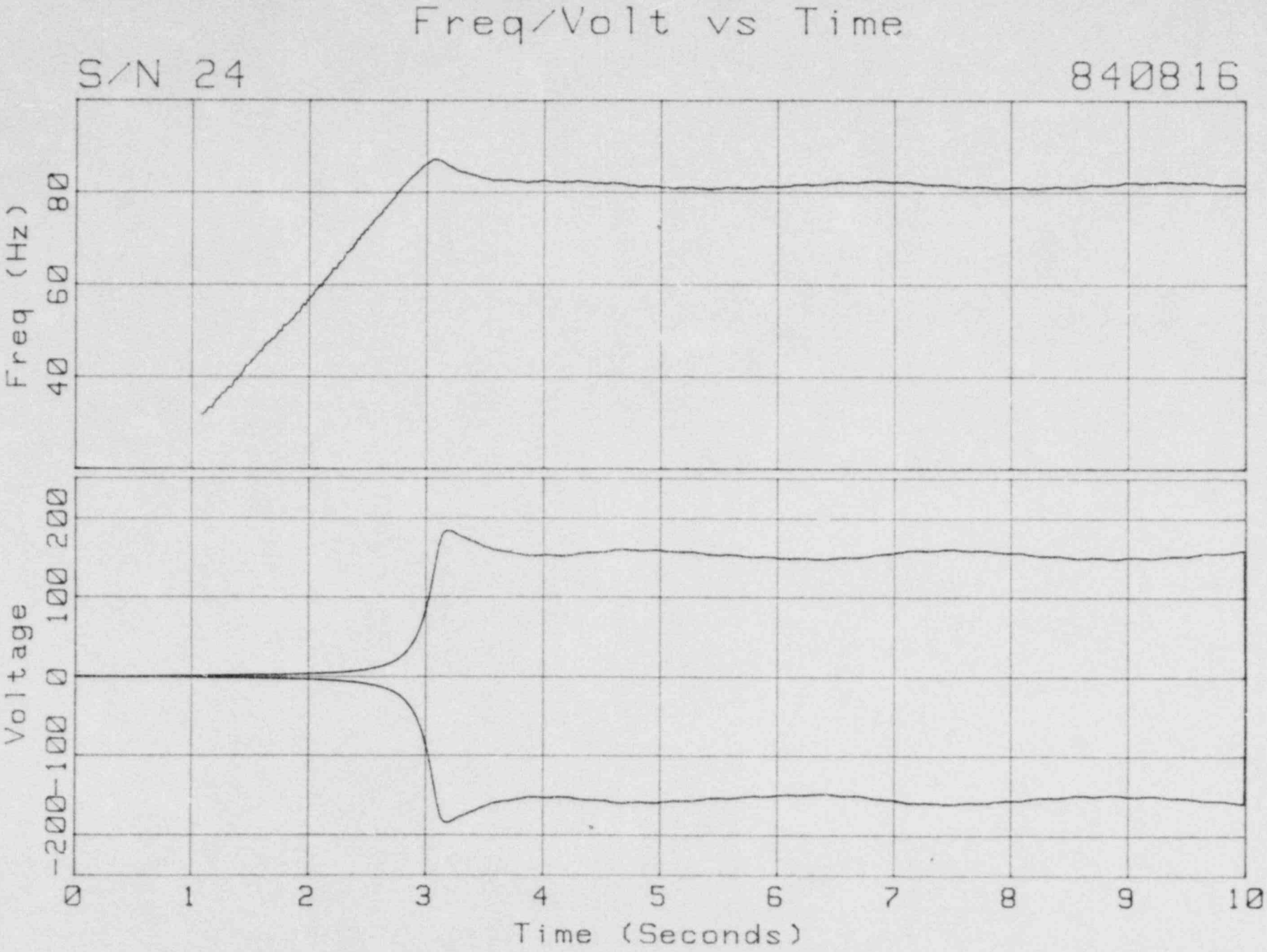
Freq/Volt vs Time
S/N 24
840816
Freq (Hz)
40
60
80
Voltage
-200
-100
0
100
200
0
1
2
3
4
5
6
7
8
9
10
Time (Seconds)

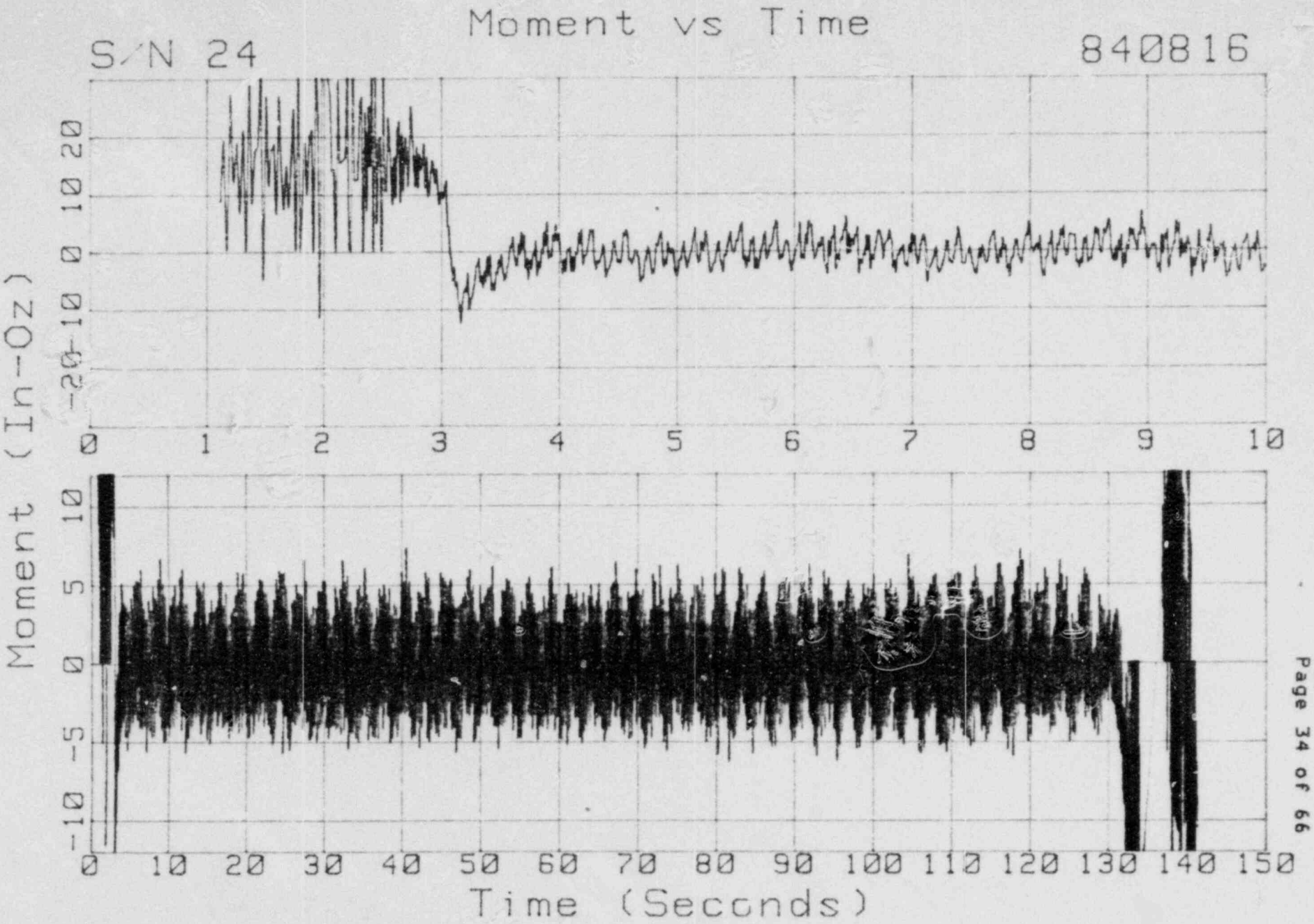
Moment vs Time
S/N 24
840816
Moment (In-Oz)
-20 -10 0 10 20
0 1 2 3 4 5 6 7 8 9 10
-10 -5 0 5 10
0 10 20 30 40 50 60 70 80 90 100 110 120 130 140 150
Time (Seconds)

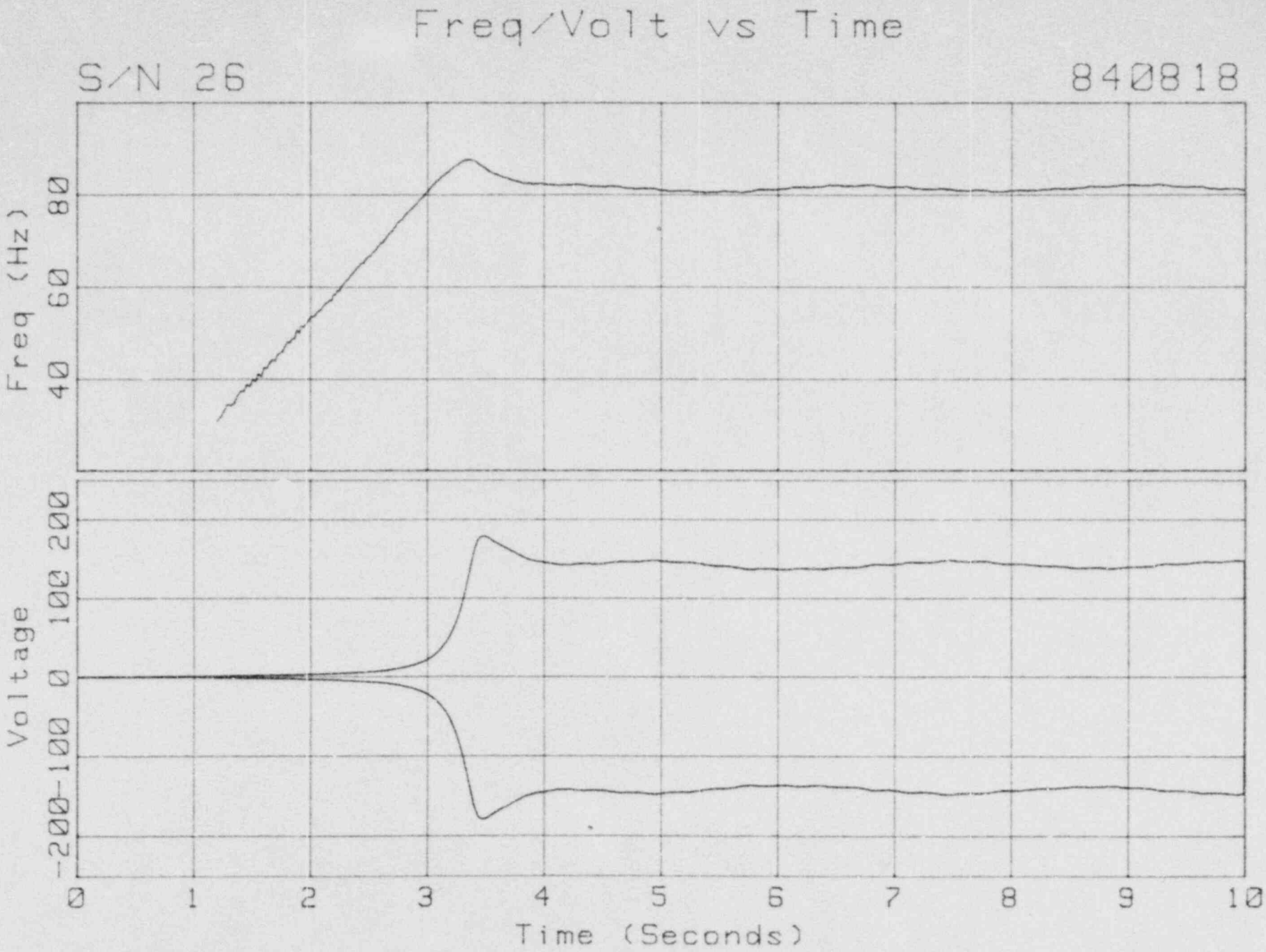
Freq/Volt vs Time
S/N 26
840818
Freq (Hz)
40
60
80
Voltage
-200
-100
0
100
200
0
1
2
3
4
5
6
7
8
9
10
Time (Seconds)

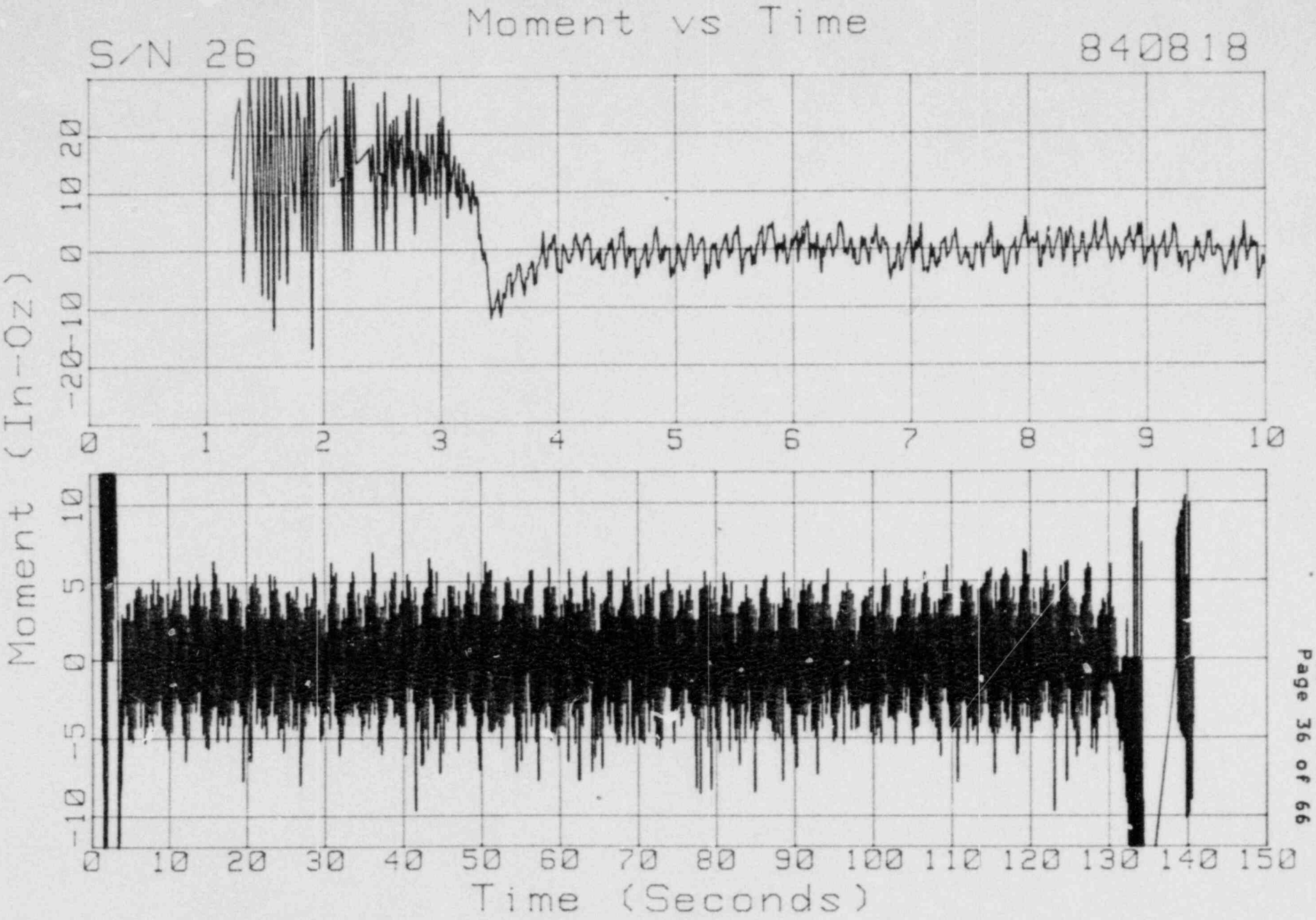
Moment vs Time
S/N 26
840818
Moment (In-Oz)
-20 -10 0 10 20
0 1 2 3 4 5 6 7 8 9 10
-10 -5 0 5 10
0 10 20 30 40 50 60 70 80 90 100 110 120 130 140 150
Time (Seconds)

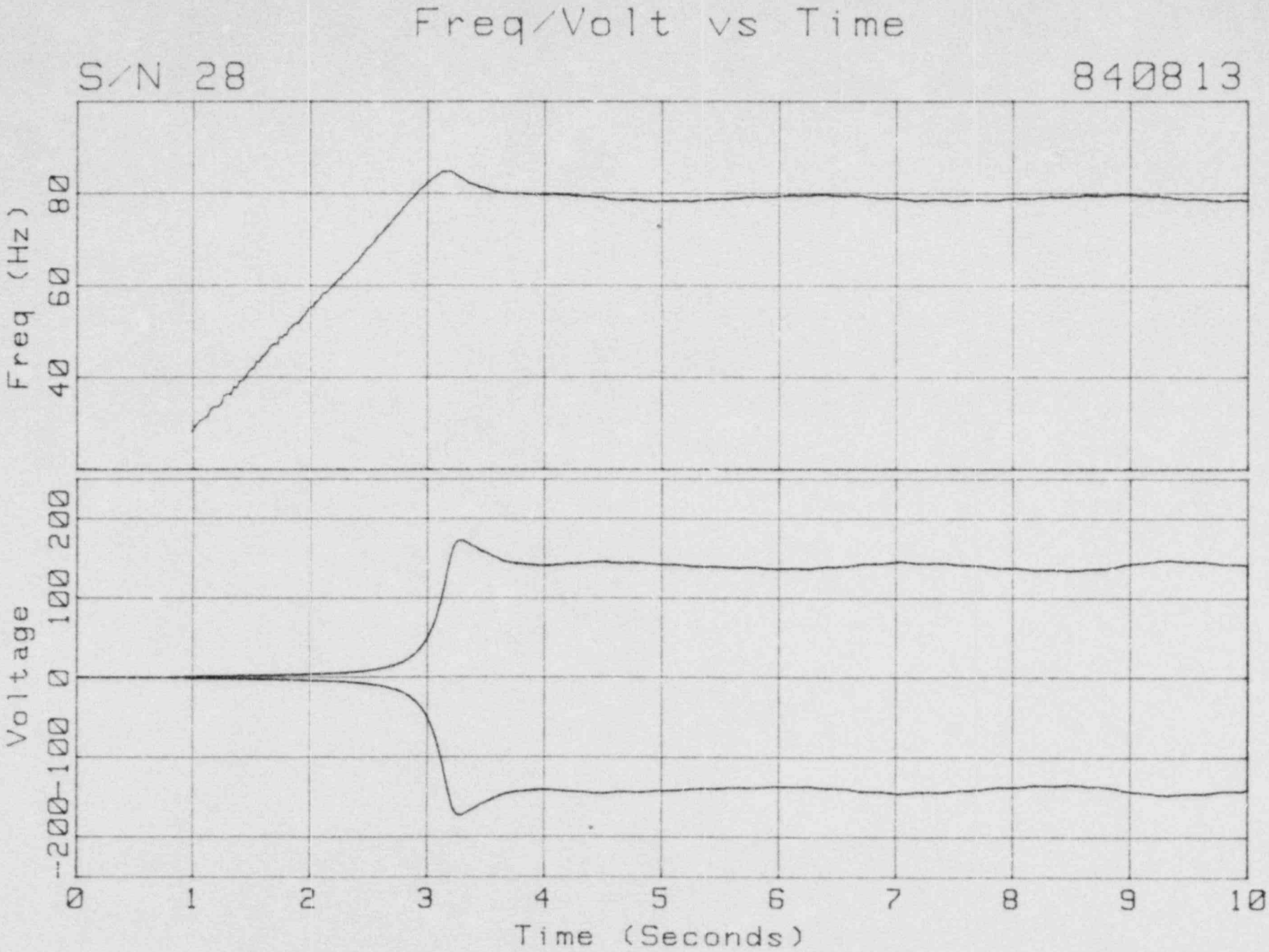
Freq/Volt vs Time
S/N 28
840813
Freq (Hz)
40
60
80
Voltage
-200
-100
0
100
200
0
1
2
3
4
5
6
7
8
9
10
Time (Seconds)

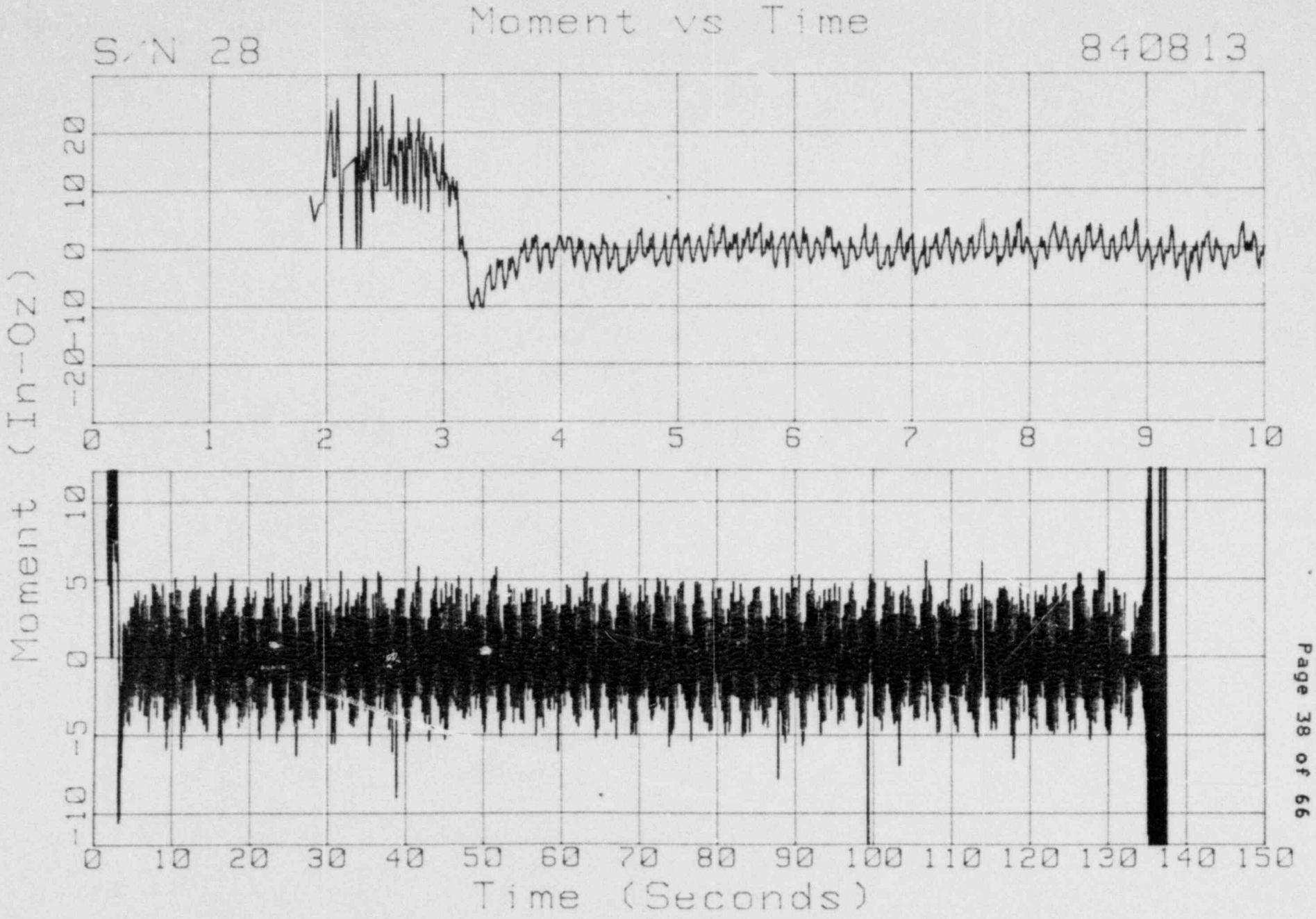
Moment vs Time
S/N 28
840813
Moment (In-Oz)
-20 -10 0 10 20
0 1 2 3 4 5 6 7 8 9 10
-10 -5 0 5 10
0 10 20 30 40 50 60 70 80 90 100 110 120 130 140 150
Time (Seconds)

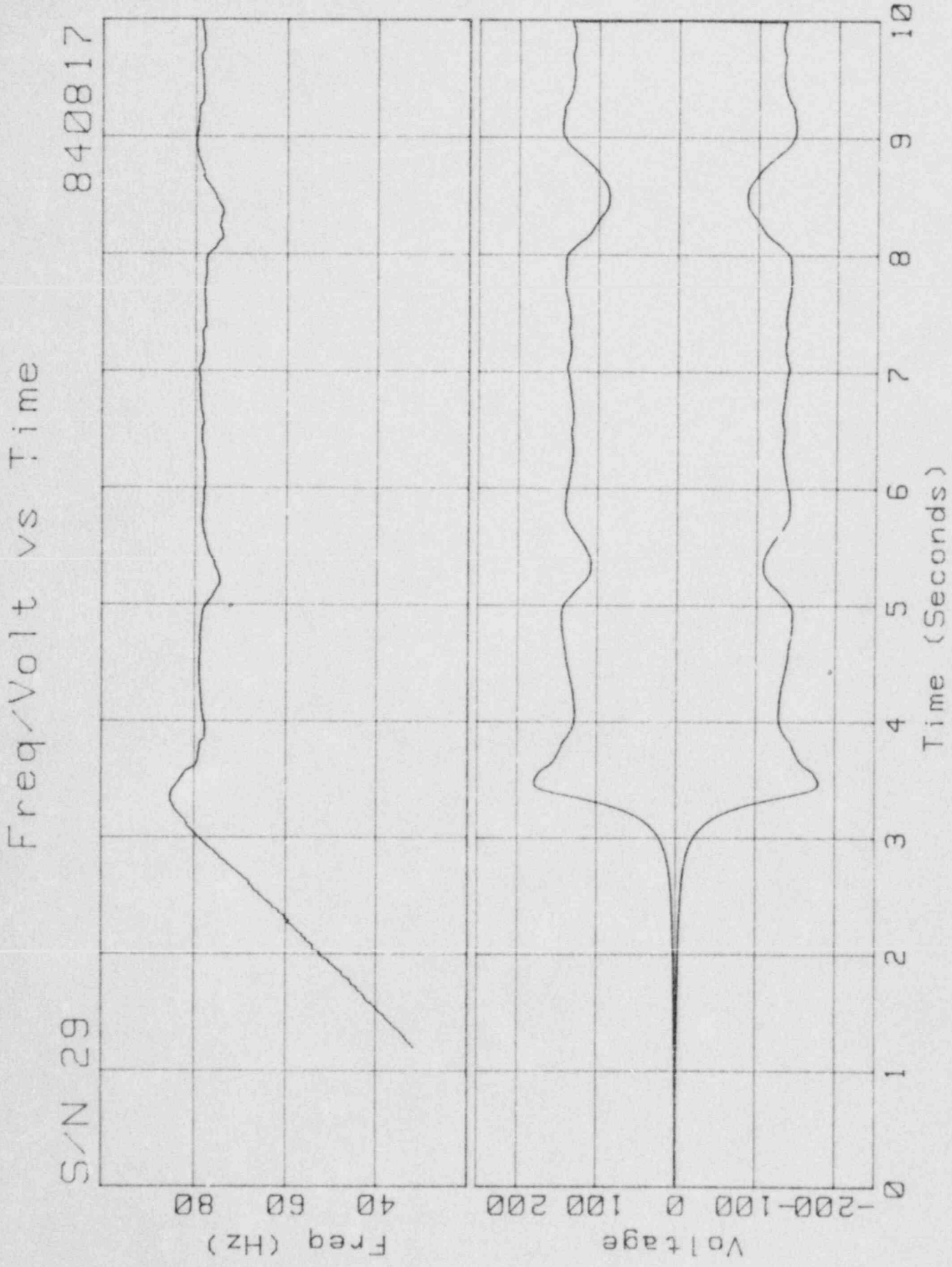
Freq/Volt vs Time
840817
S/N 29
Freq (Hz)
40
60
80
Voltage
-200
-100
0
100
200
0
1
2
3
4
5
6
7
8
9
10
Time (Seconds)

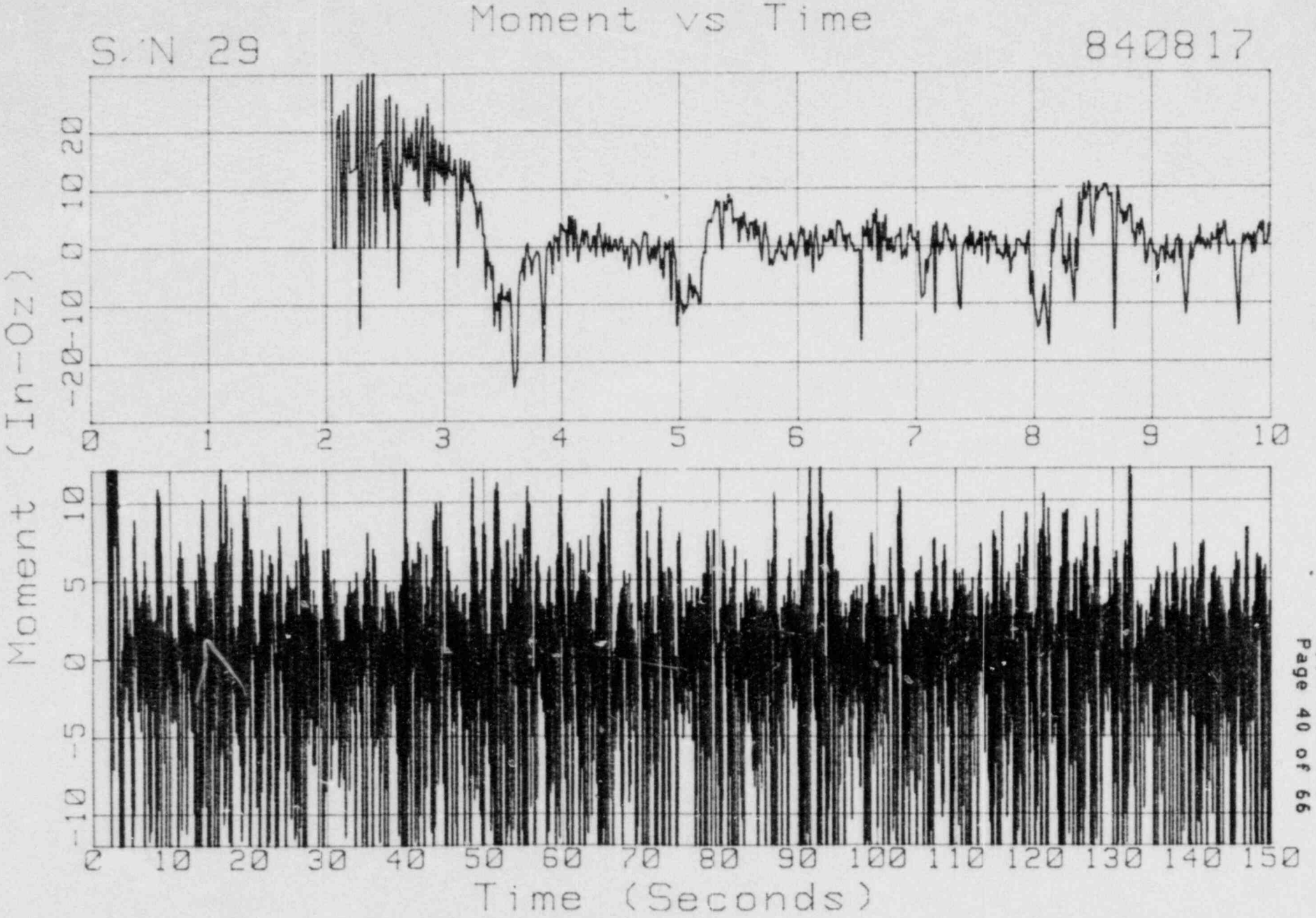
Moment vs Time
S/N 29
840817
Moment (In-Oz)
-20 -10 0 10 20
0 1 2 3 4 5 6 7 8 9 10
-10 -5 0 5 10
0 10 20 30 40 50 60 70 80 90 100 110 120 130 140 150
Time (Seconds)

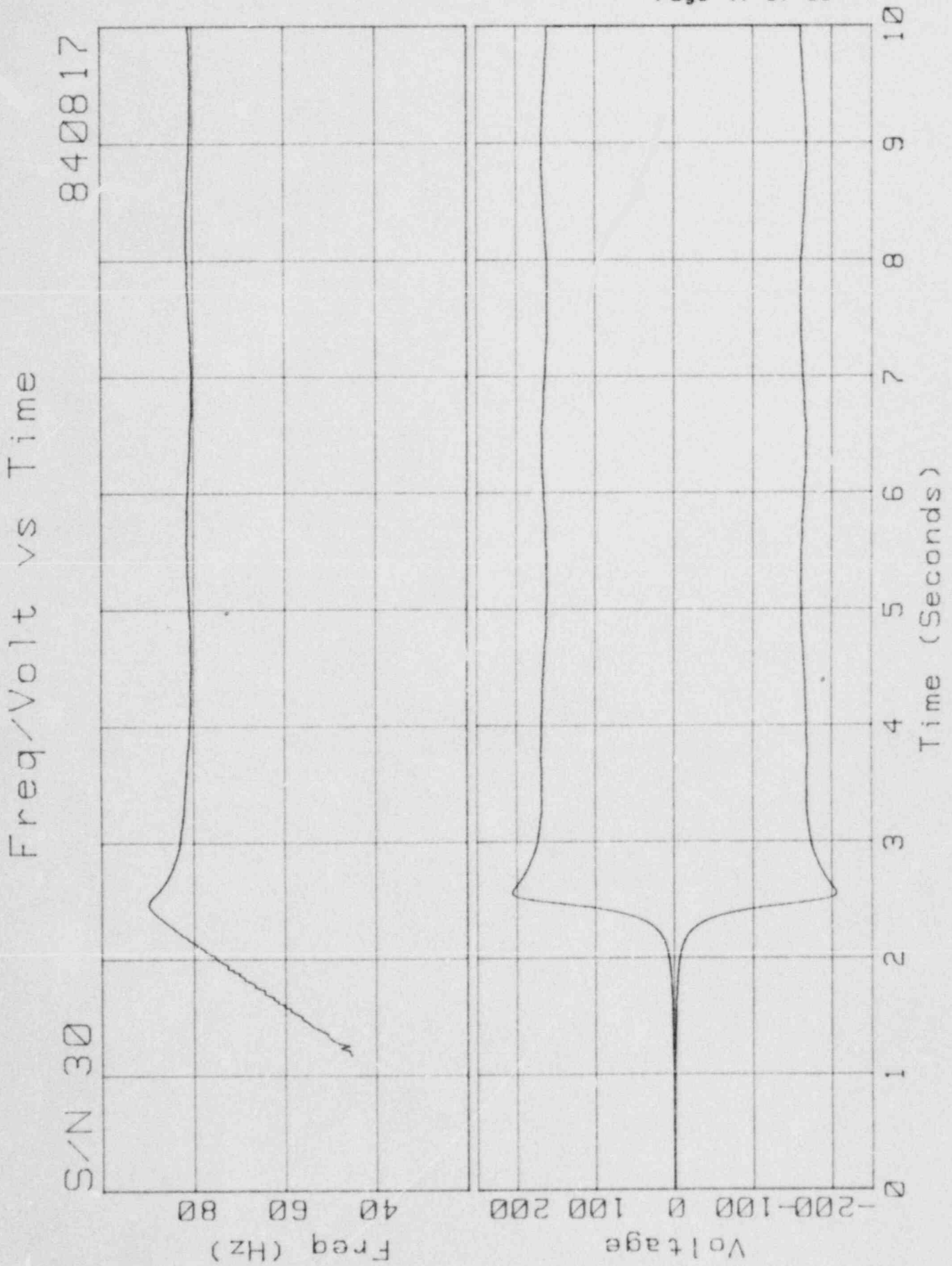
Freq/Volt vs Time
8408817
S/N 30
Freq (Hz)
40
60
80
Voltage
-200
-100
0
100
200
0
1
2
3
4
5
6
7
8
9
10
Time (Seconds)

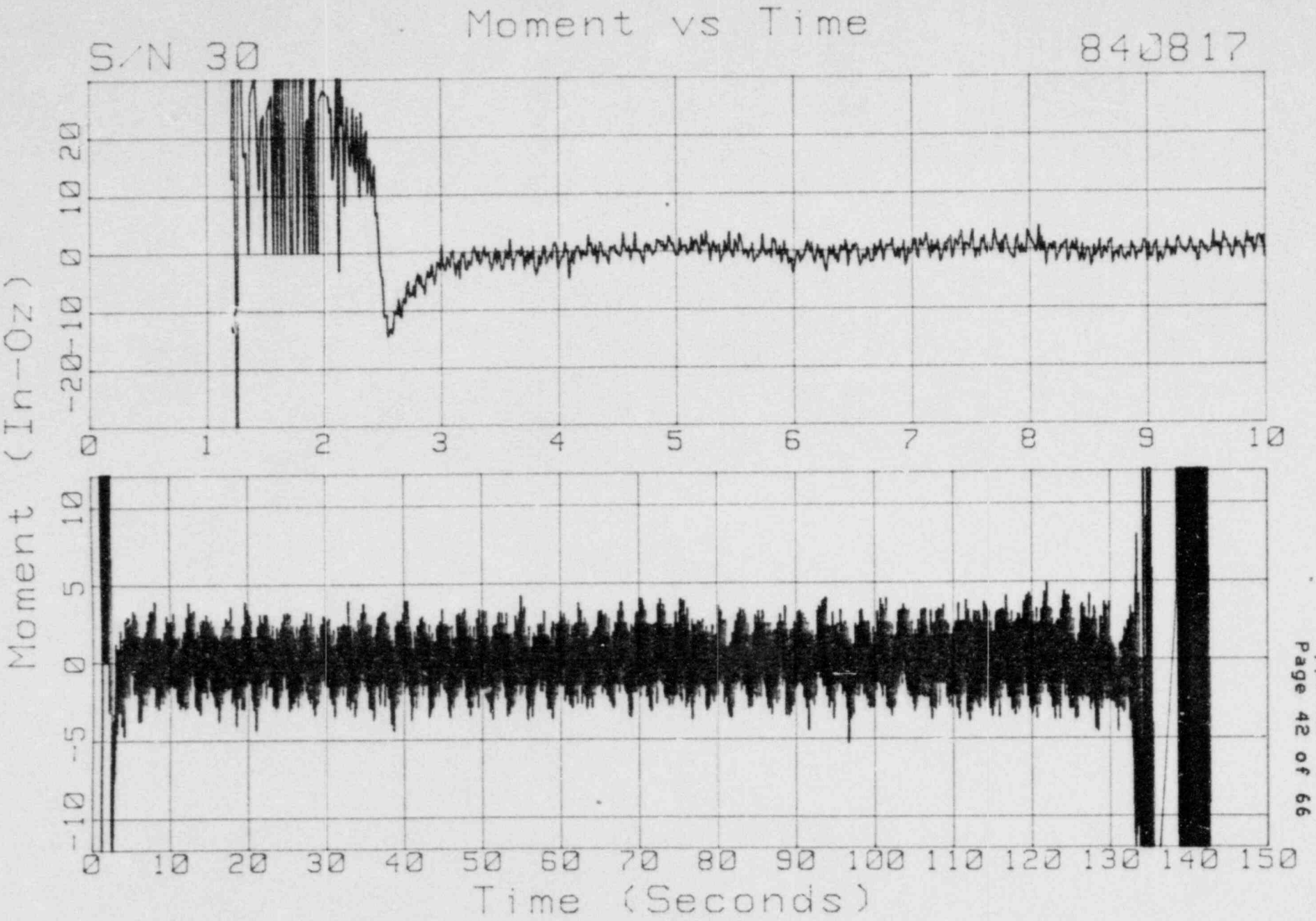
Moment vs Time
S/N 30
840817
Moment (In-Oz)
-20 -10 0 10 20
0 1 2 3 4 5 6 7 8 9 10
-10 -5 0 5 10
0 10 20 30 40 50 60 70 80 90 100 110 120 130 140 150
Time (Seconds)

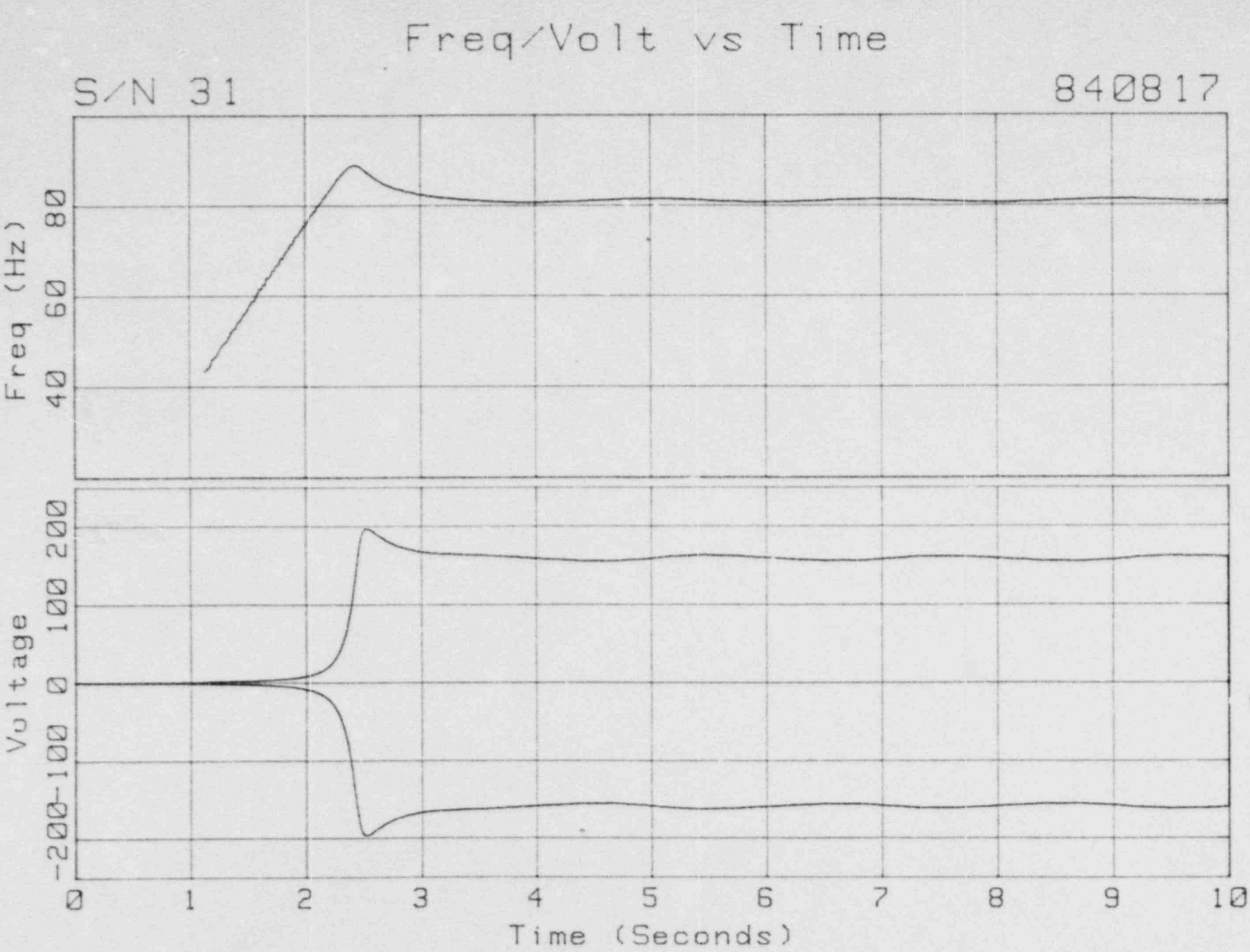
Freq/Volt vs Time
S/N 31
840817
Freq (Hz)
40
60
80
Voltage
-200
-100
0
100
200
0
1
2
3
4
5
6
7
8
9
10
Time (Seconds)

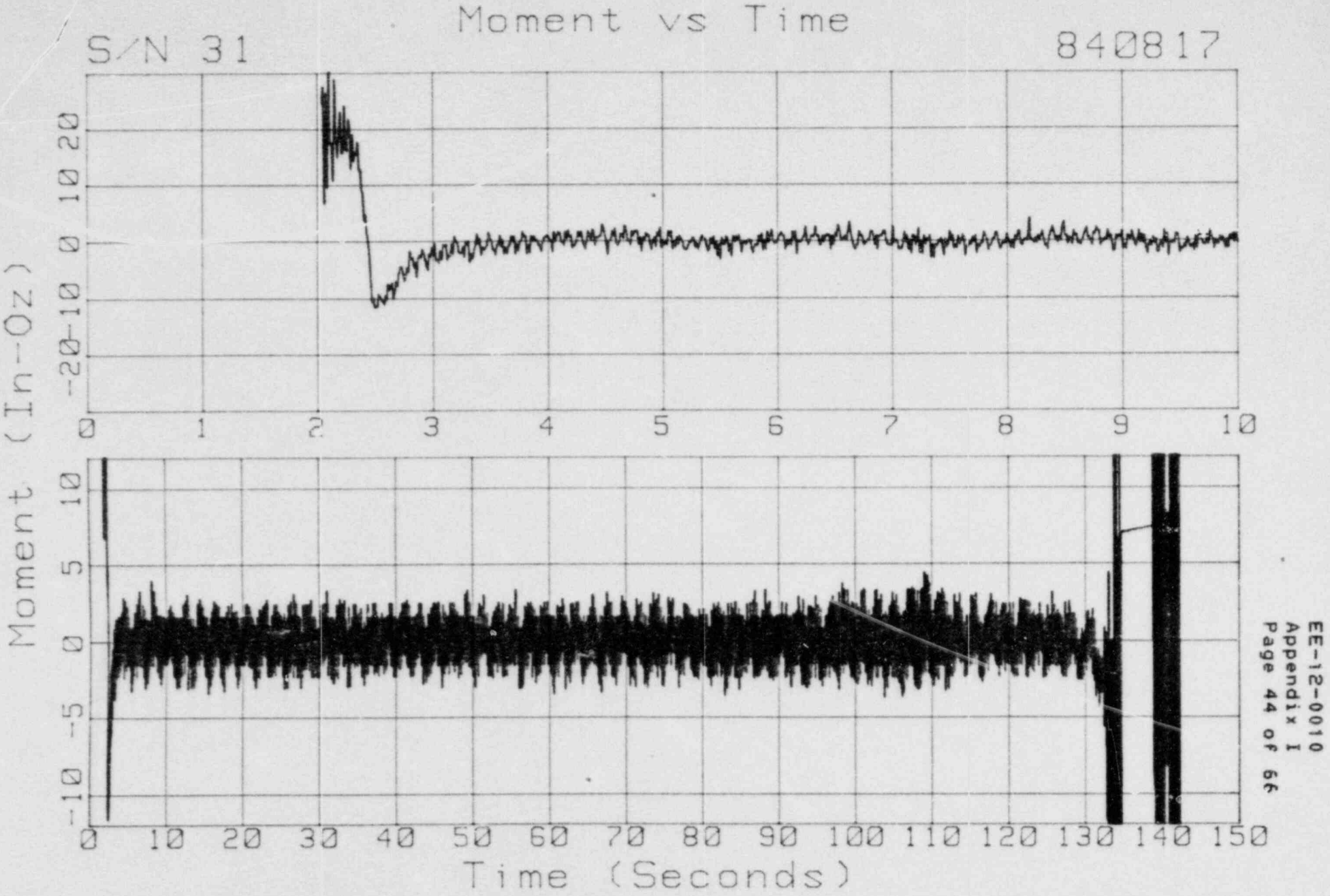
Moment vs Time
S/N 31
840817
Moment (In-Oz)
-20 -10 0 10 20
0 1 2 3 4 5 6 7 8 9 10
-10 -5 0 5 10
0 10 20 30 40 50 60 70 80 90 100 110 120 130 140 150
Time (Seconds)

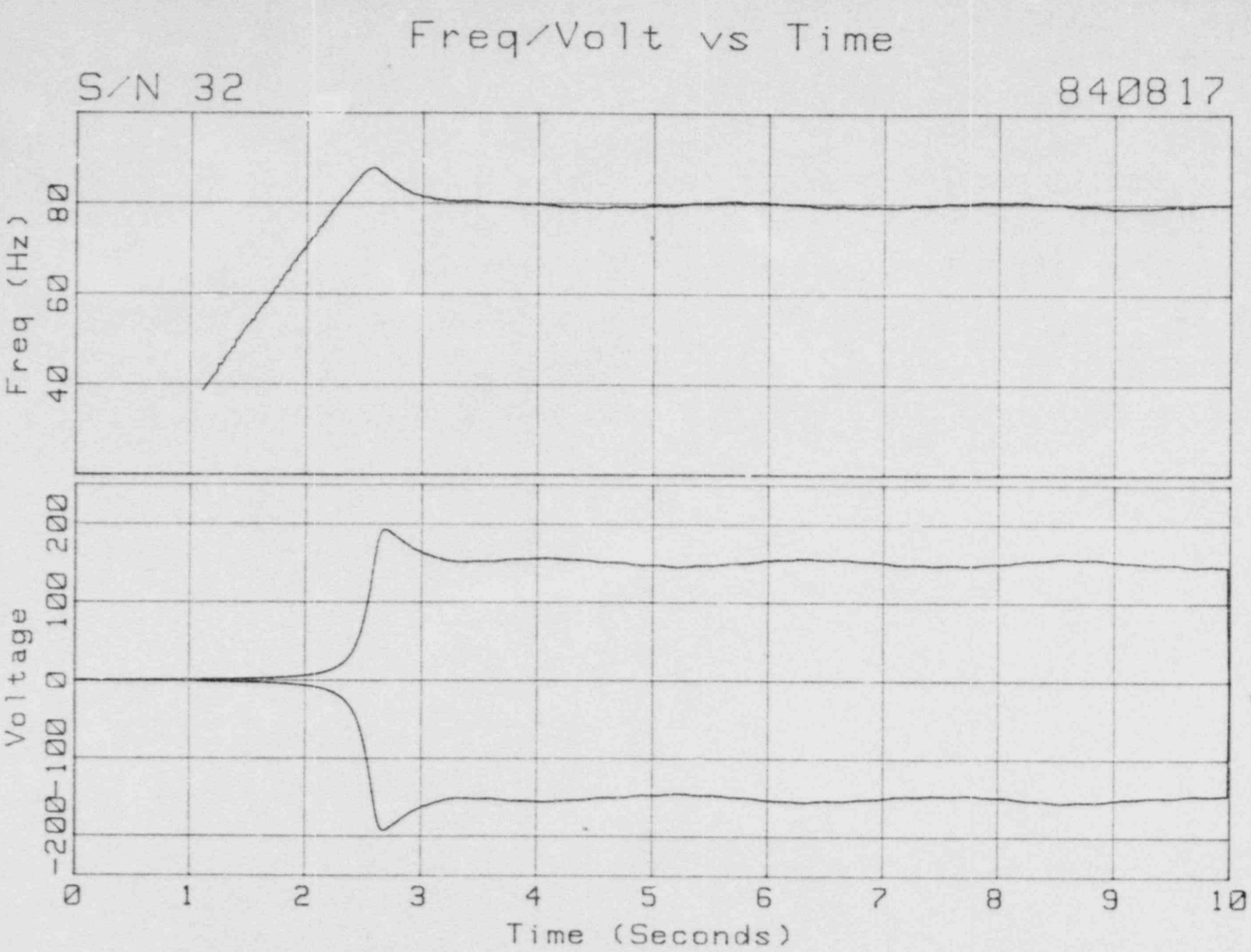
Freq/Volt vs Time
S/N 32
840817
Freq (Hz)
40 60 80
Voltage
-200 -100 0 100 200
0 1 2 3 4 5 6 7 8 9 10
Time (Seconds)

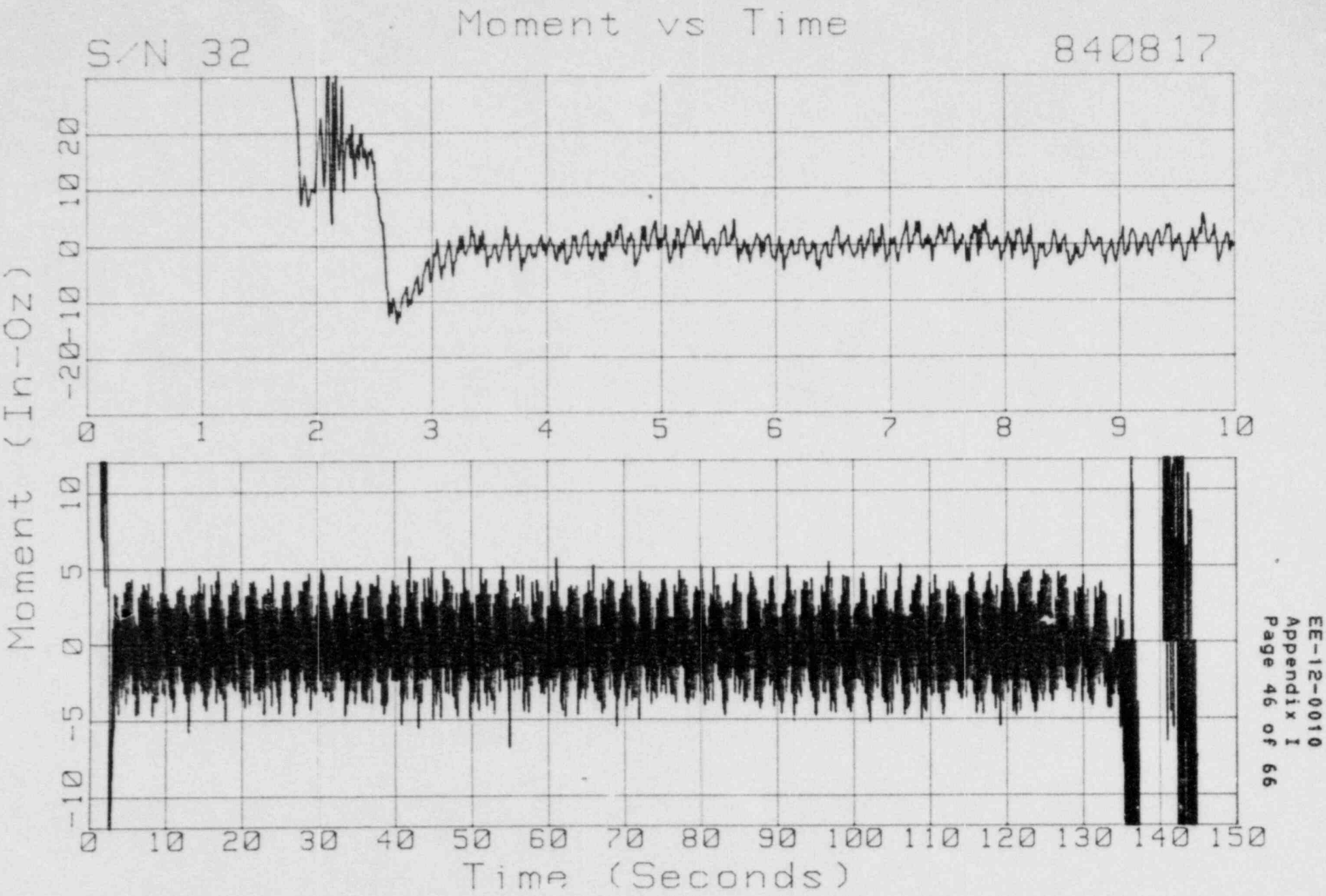
Moment vs Time
S/N 32
840817
Moment (In-Oz)
-20 -10 0 10 20
0 1 2 3 4 5 6 7 8 9 10
-10 -5 0 5 10
0 10 20 30 40 50 60 70 80 90 100 110 120 130 140 150
Time (Seconds)

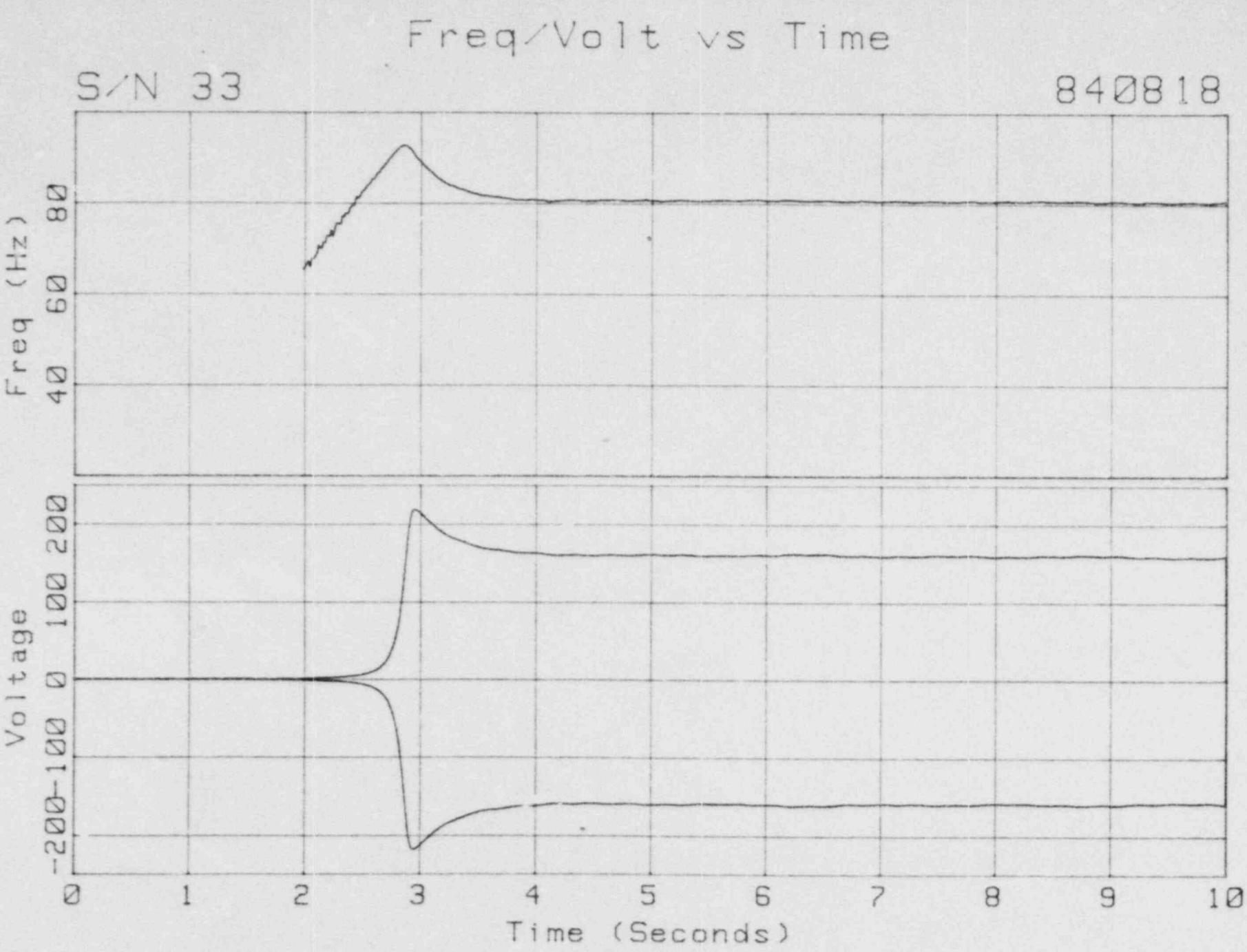
Freq/Volt vs Time
S/N 33
840818
Freq (Hz)
40
60
80
Voltage
-200
-100
0
100
200
0
1
2
3
4
5
6
7
8
9
10
Time (Seconds)

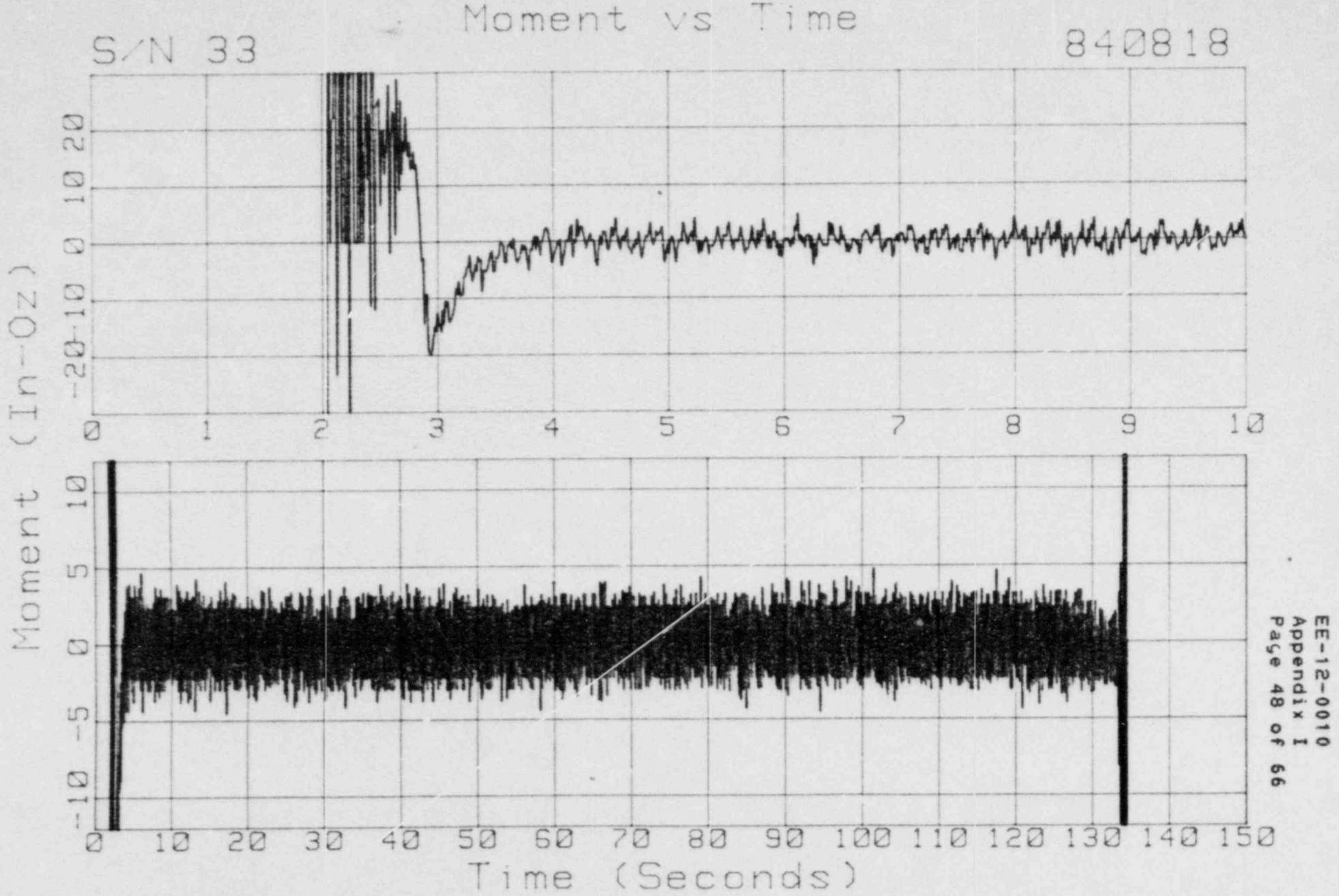
Moment vs Time
S/N 33
840818
Moment (In-Oz)
-20 -10 0 10 20
0 1 2 3 4 5 6 7 8 9 10
-10 -5 0 5 10
0 10 20 30 40 50 60 70 80 90 100 110 120 130 140 150
Time (Seconds)

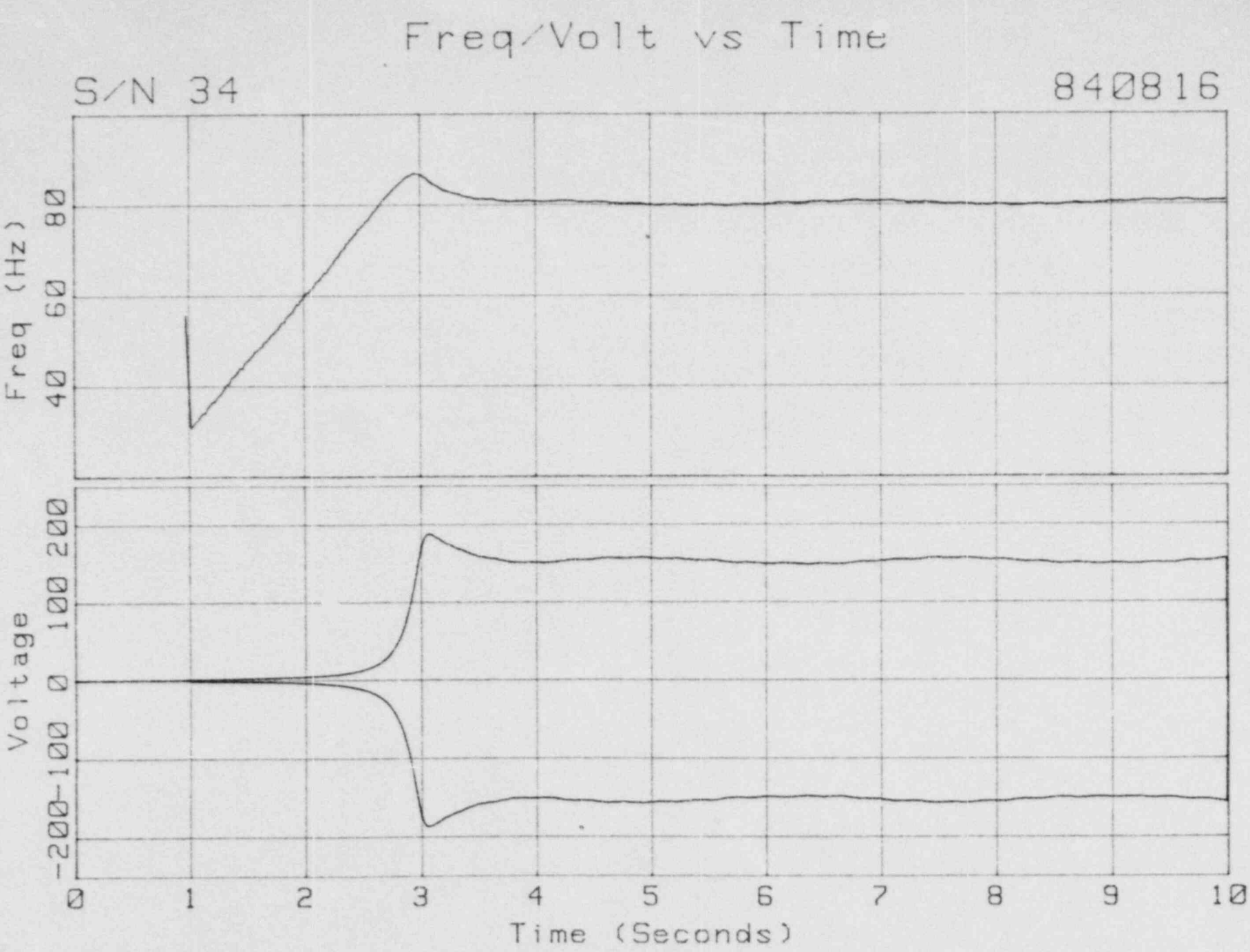
Freq/Volt vs Time
S/N 34
840816
Freq (Hz)
40
60
80
Voltage
-200
-100
0
100
200
0
1
2
3
4
5
6
7
8
9
10
Time (Seconds)

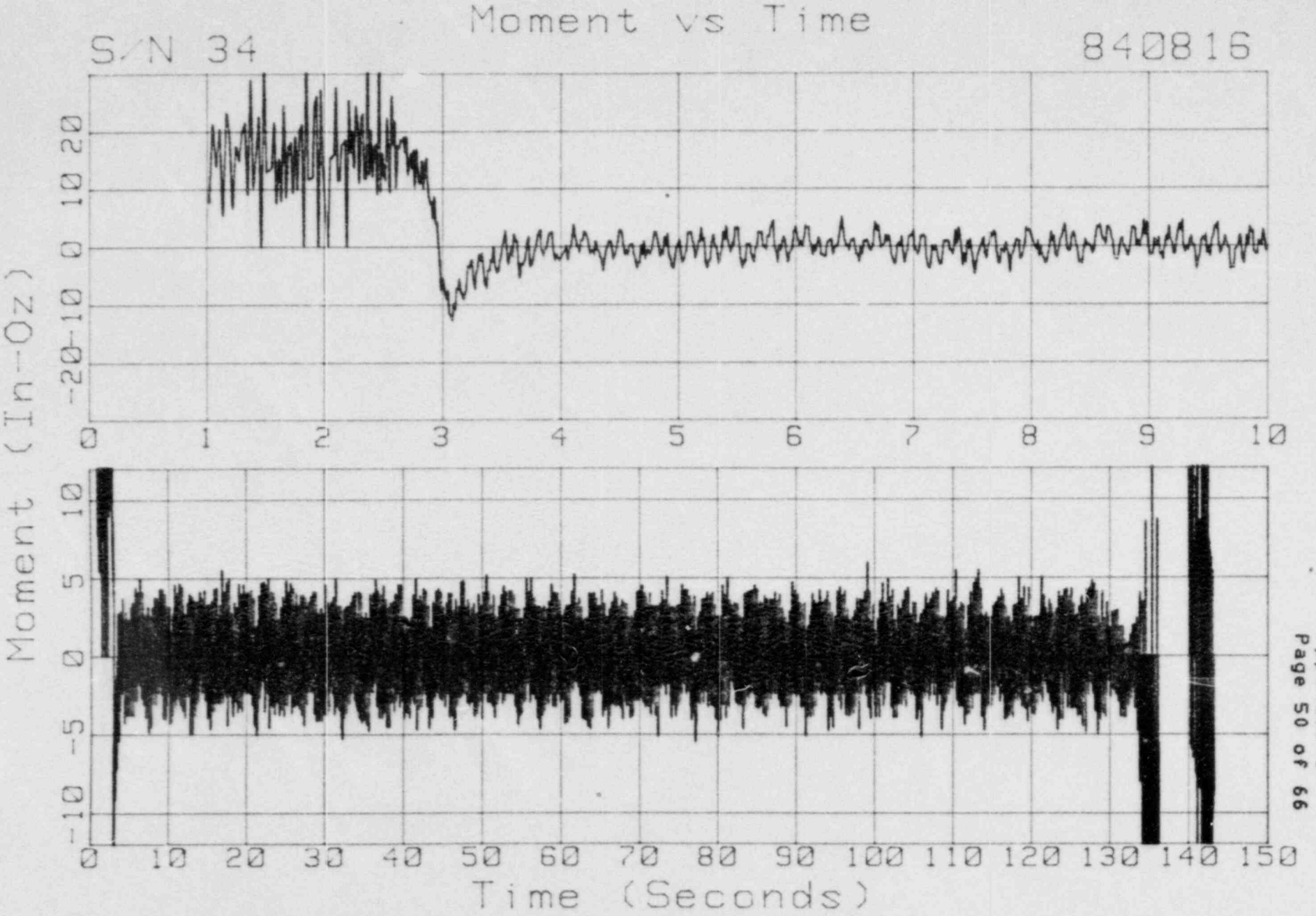
Moment vs Time
S/N 34
840816
Moment (In-Oz)
-20 -10 0 10 20
0 1 2 3 4 5 6 7 8 9 10
-10 -5 0 5 10
0 10 20 30 40 50 60 70 80 90 100 110 120 130 140 150
Time (Seconds)

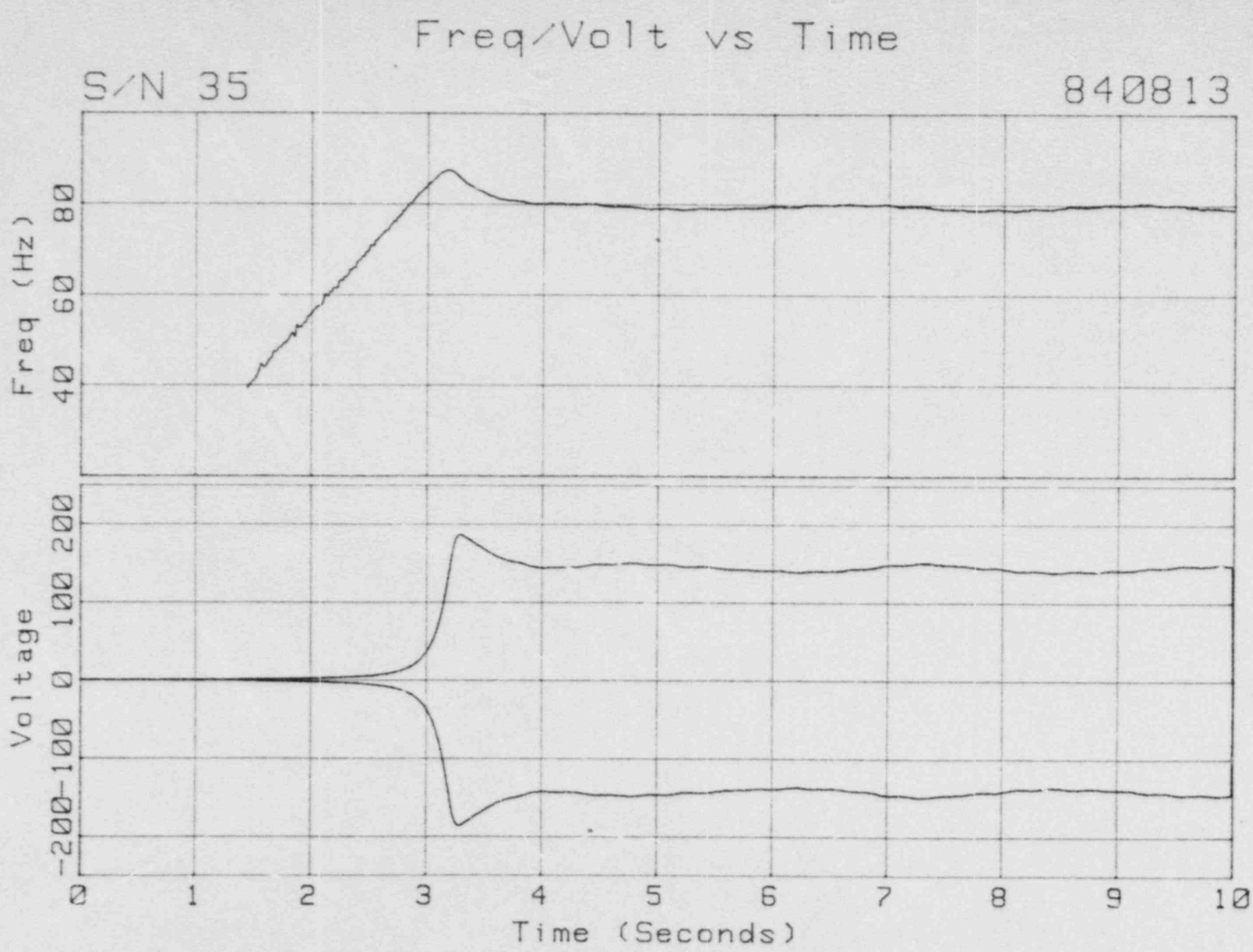
Freq/Volt vs Time
S/N 35
840813
Freq (Hz)
40
60
80
Voltage
-200
-100
0
100
200
0
1
2
3
4
5
6
7
8
9
10
Time (Seconds)

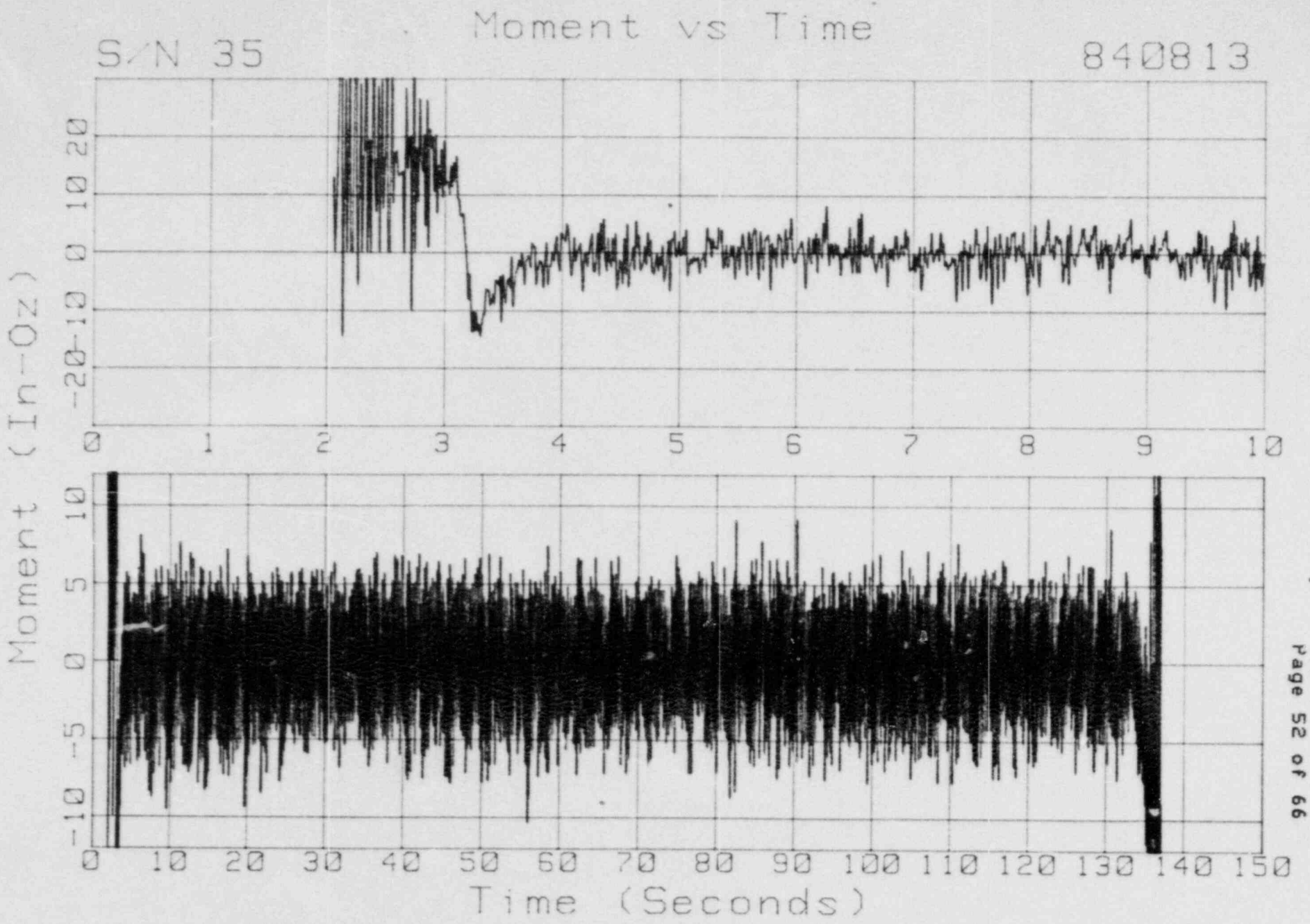
Moment vs Time
S/N 35
840813
Moment (In-Oz)
-20 -10 0 10 20
0 1 2 3 4 5 6 7 8 9 10
-10 -5 0 5 10
0 10 20 30 40 50 60 70 80 90 100 110 120 130 140 150
Time (Seconds)

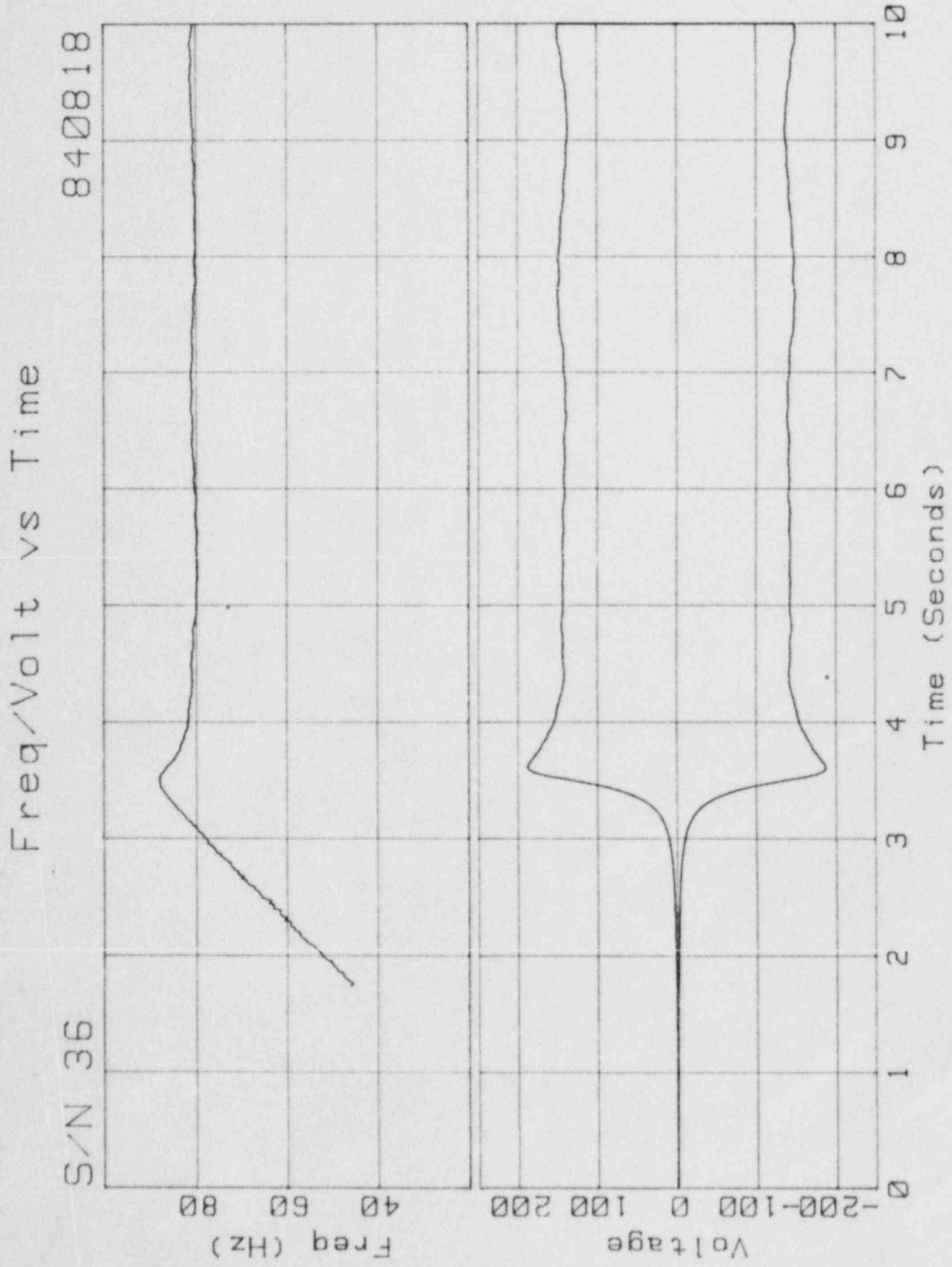
Freq/Volt vs Time
8408818
S/N 36
Freq (Hz)
40
60
80
Voltage
-200
-100
0
100
200
0
1
2
3
4
5
6
7
8
9
10
Time (Seconds)

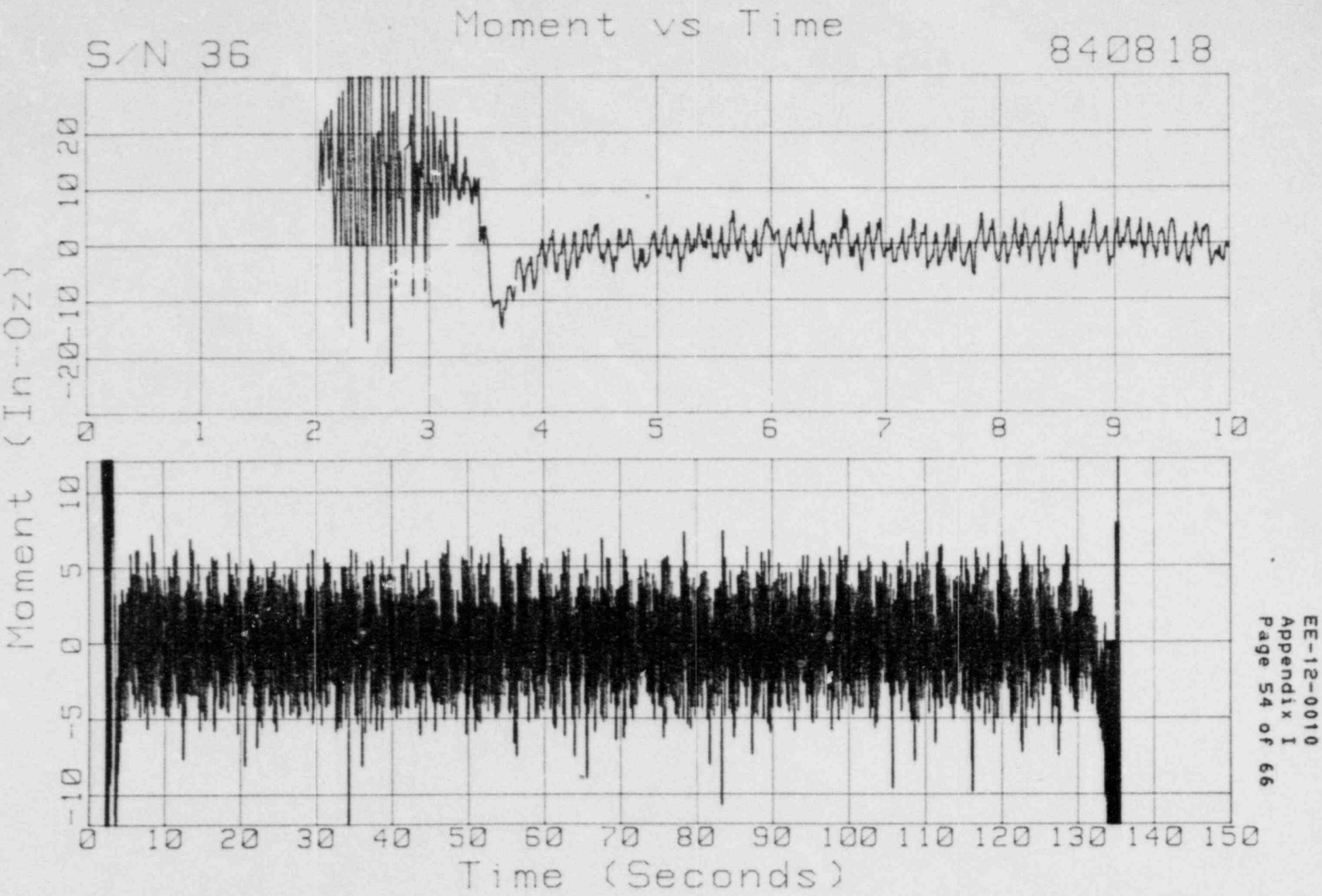
Moment vs Time
S/N 36
840818
Moment (In-Oz)
-20 -10 0 10 20
0 1 2 3 4 5 6 7 8 9 10
-10 -5 0 5 10
0 10 20 30 40 50 60 70 80 90 100 110 120 130 140 150
Time (Seconds)

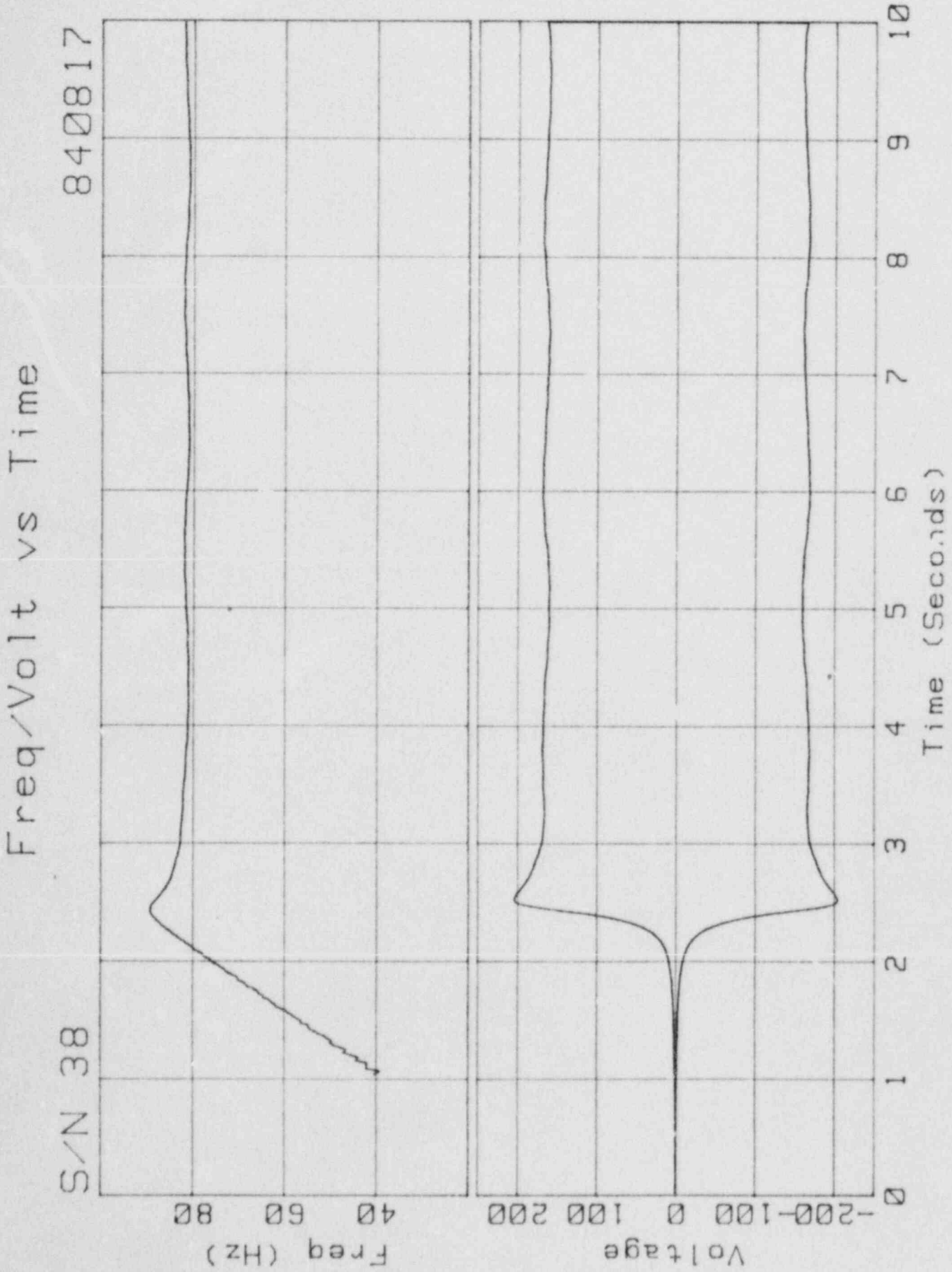
Freq/Volt vs Time
8408817
S/N 38
Freq (Hz)
40
60
80
Voltage
-200
-100
0
100
200
0
1
2
3
4
5
6
7
8
9
10
Time (Seconds)

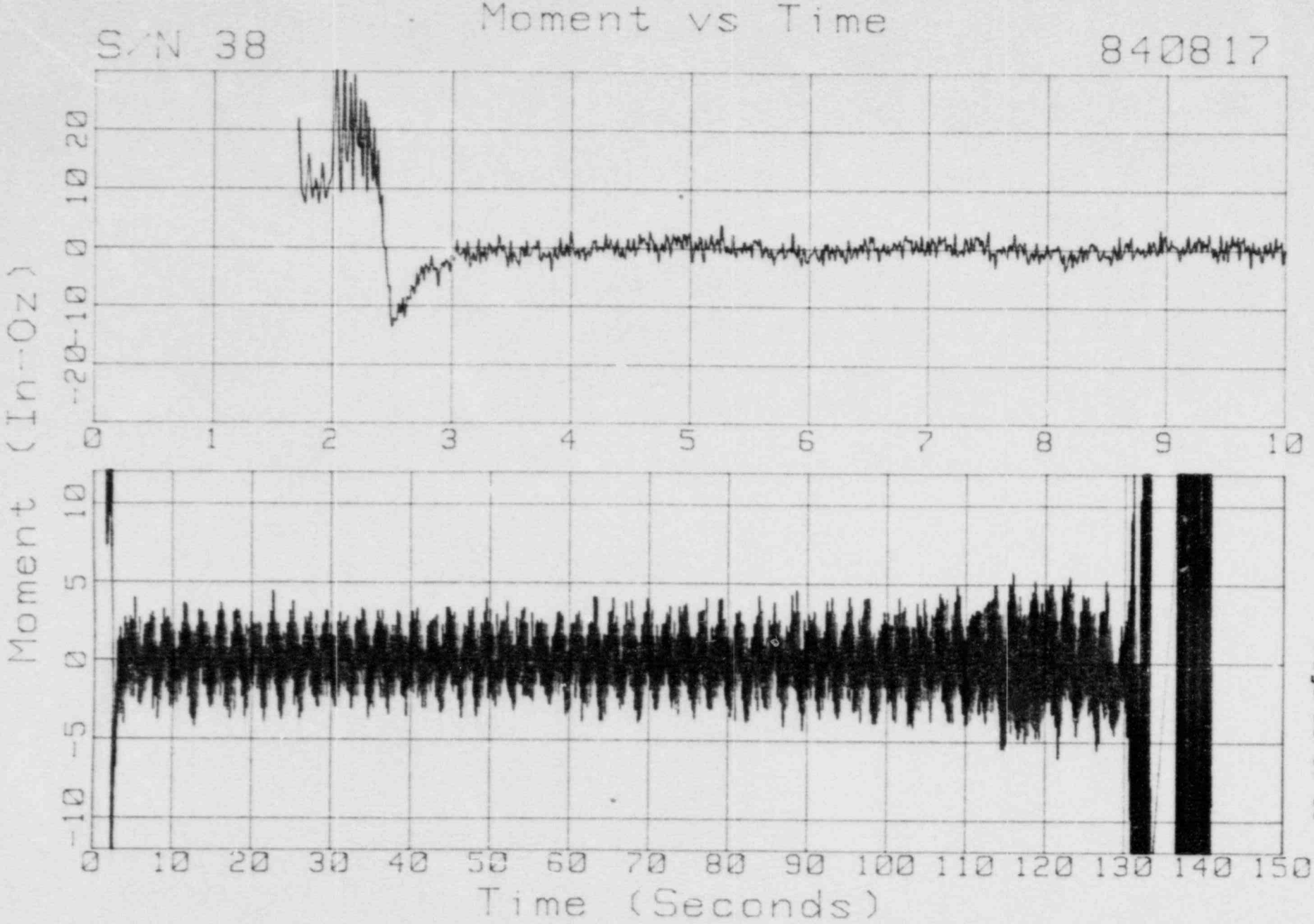
Moment vs Time
S/N 38
840817
Moment (In--Oz)
-20 -10 0 10 20
0 1 2 3 4 5 6 7 8 9 10
-10 -5 0 5 10
0 10 20 30 40 50 60 70 80 90 100 110 120 130 140 150
Time (Seconds)

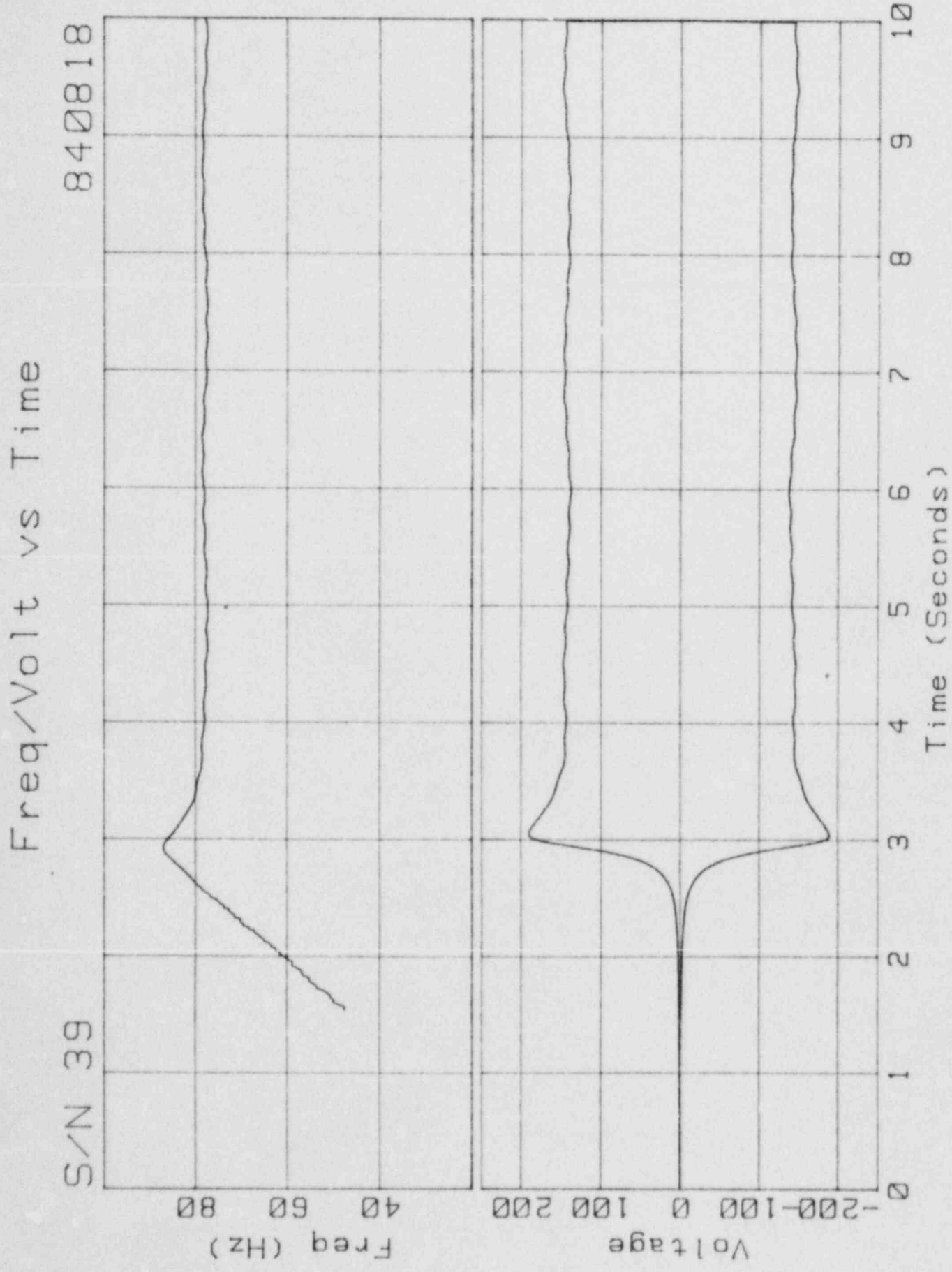
Freq/Volt vs Time
840818
S/N 39
Freq (Hz)
40
60
80
Voltage
-200
-100
0
100
200
Time (Seconds)
0
1
2
3
4
5
6
7
8
9
10

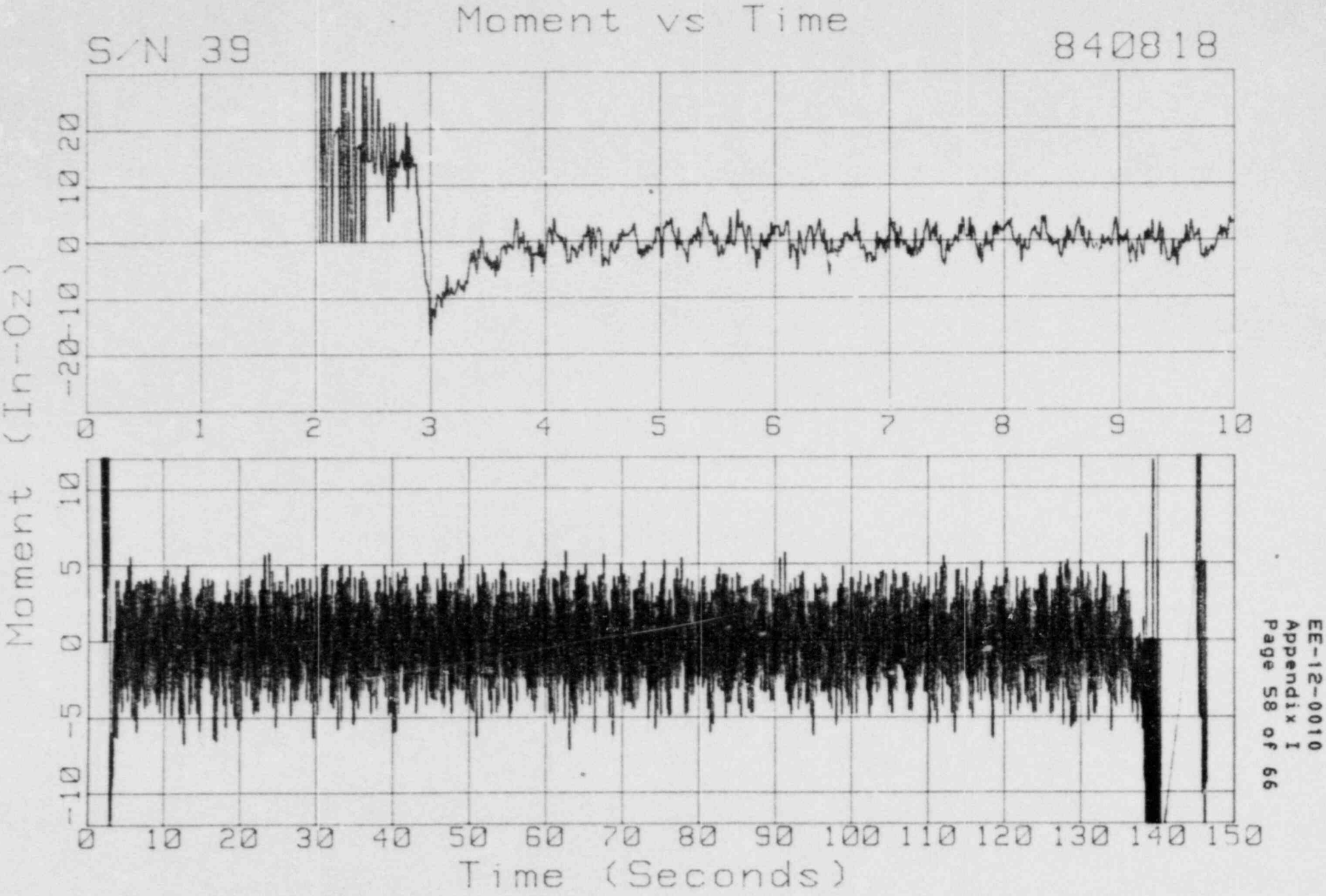
Moment vs Time
S/N 39
840818
Moment (In-Oz)
-20 -10 0 10 20
0 1 2 3 4 5 6 7 8 9 10
-10 -5 0 5 10
0 10 20 30 40 50 60 70 80 90 100 110 120 130 140 150
Time (Seconds)

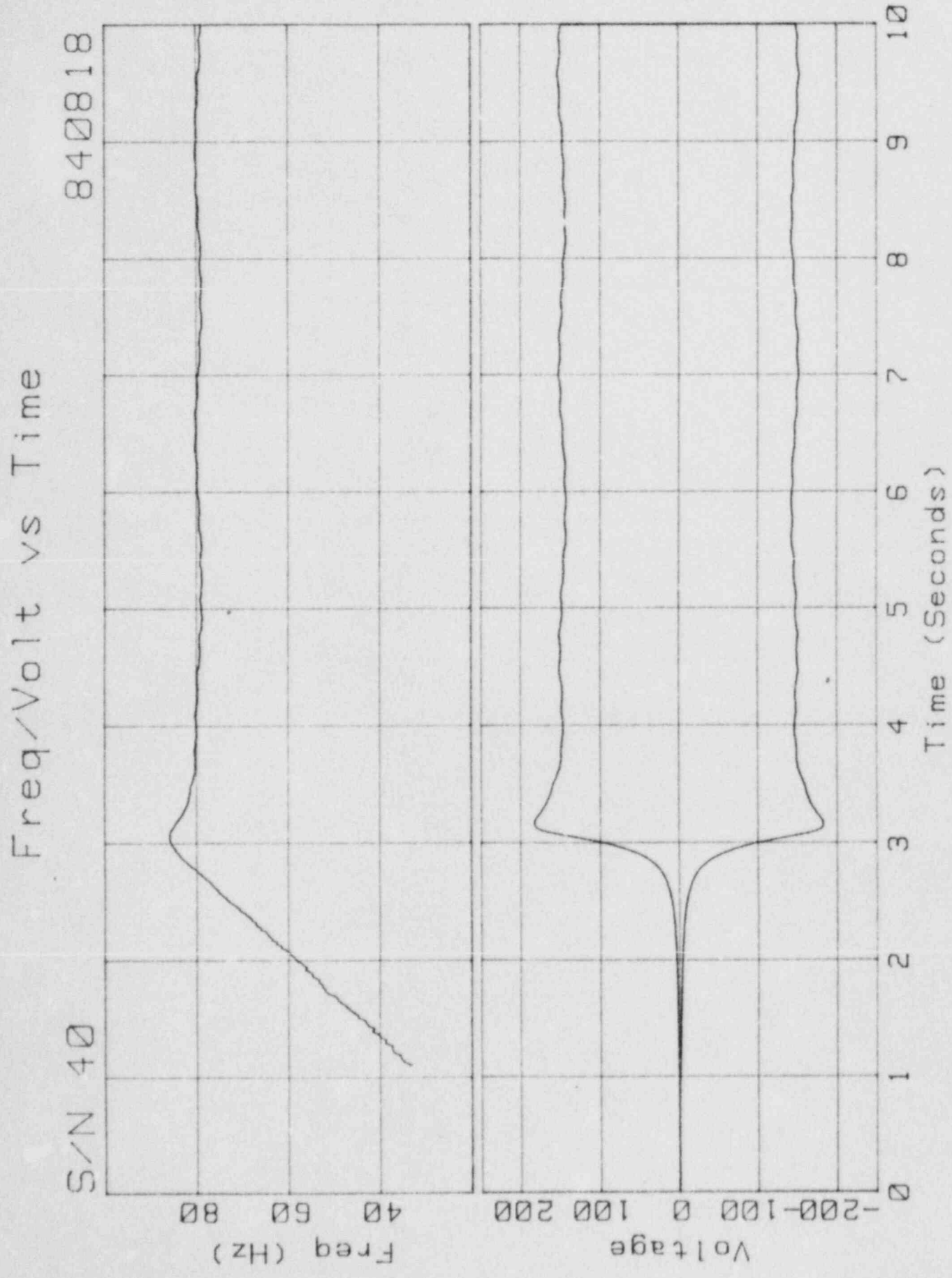
Freq/Volt vs Time
S/N 40
8408818
Freq (Hz)
40
60
80
Voltage
-200
-100
0
100
200
0
1
2
3
4
5
6
7
8
9
10
Time (Seconds)

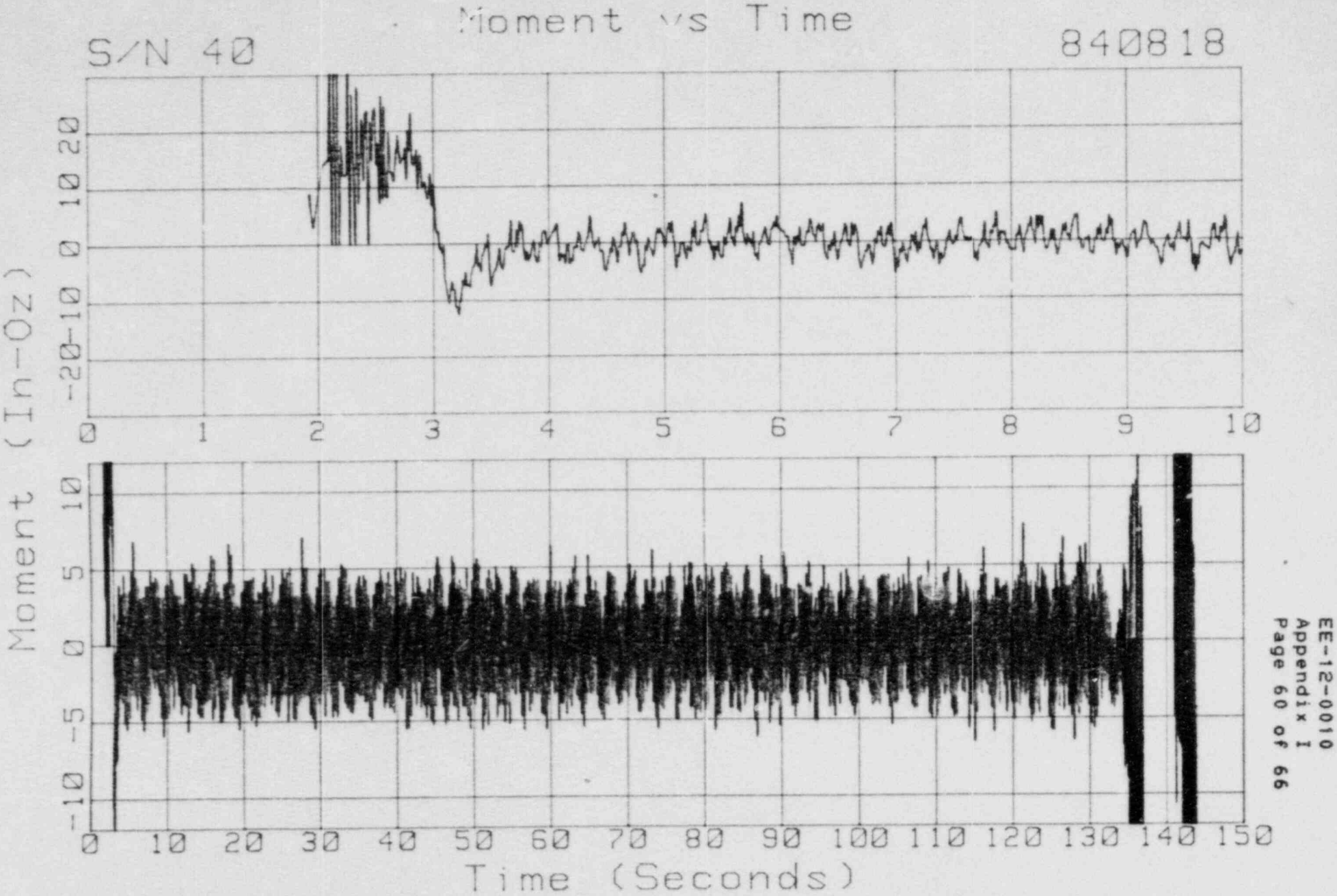
Moment vs Time
S/N 40
840818
Moment (In-Oz)
-20 -10 0 10 20
0 1 2 3 4 5 6 7 8 9 10
-10 -5 0 5 10
0 10 20 30 40 50 60 70 80 90 100 110 120 130 140 150
Time (Seconds)

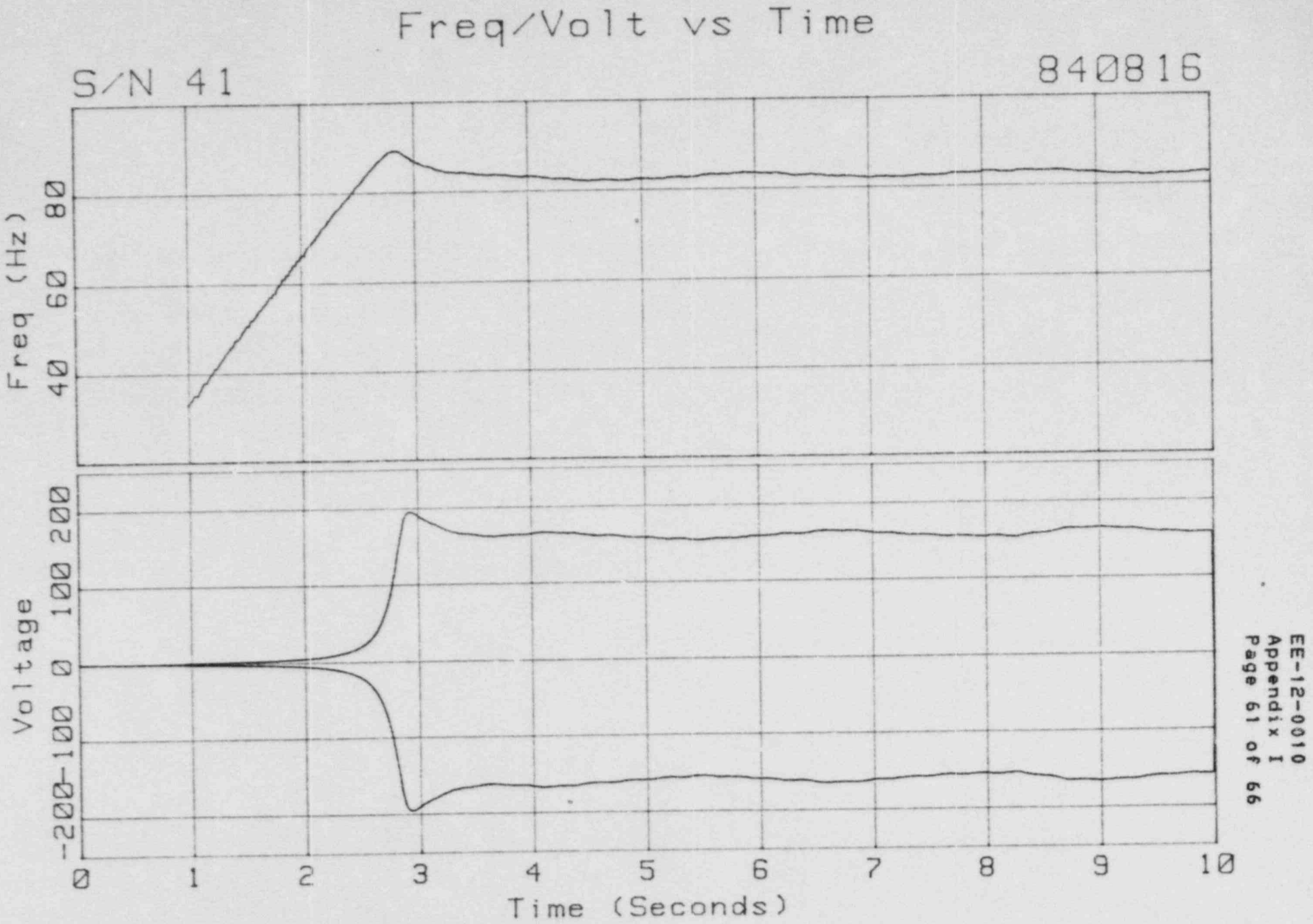
Freq/Volt vs Time
S/N 41
840816
Freq (Hz)
40
60
80
Voltage
-200
-100
0
100
200
0
1
2
3
4
5
6
7
8
9
10
Time (Seconds)

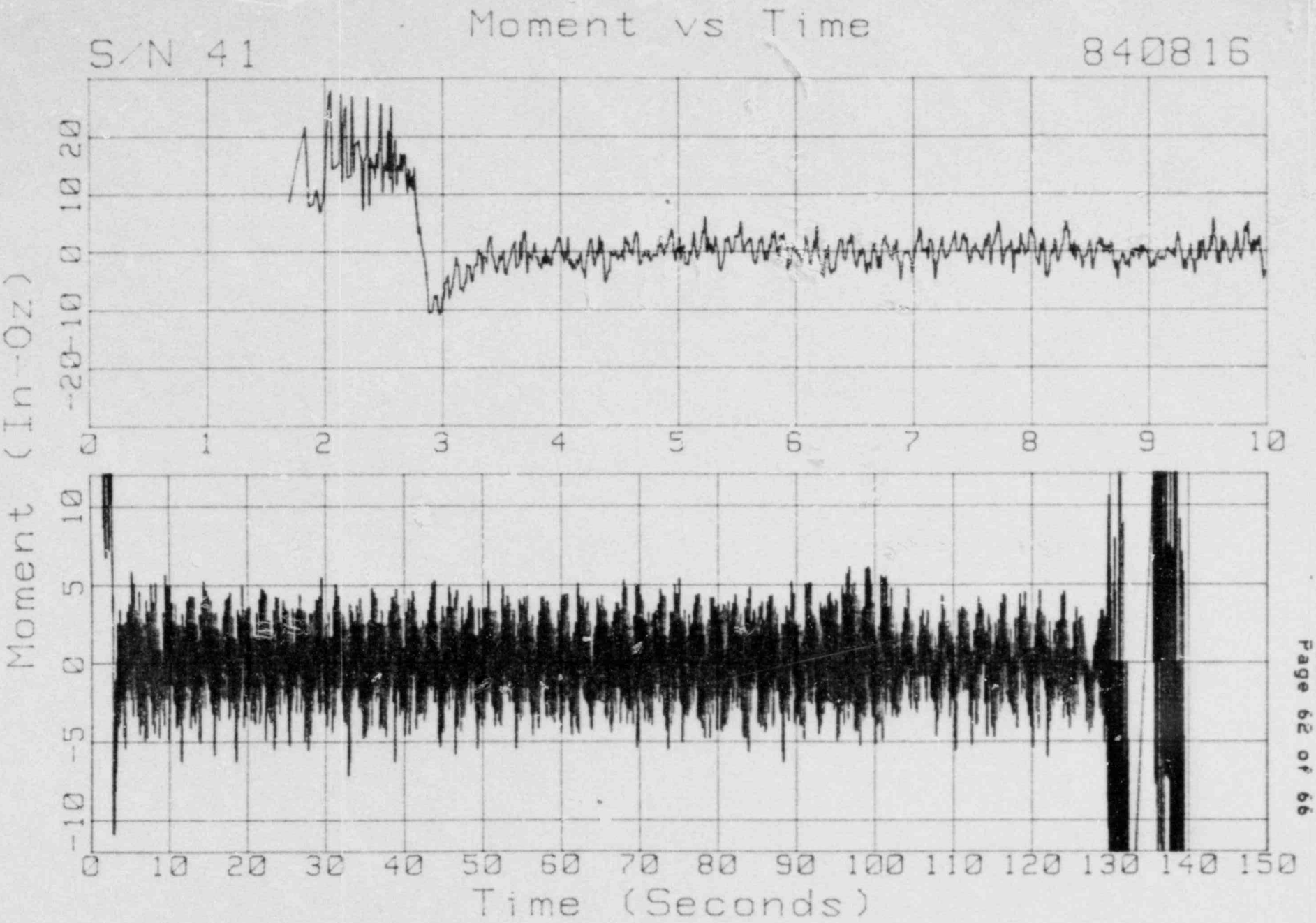
Moment vs Time
S/N 41
840816
Moment (In-Oz)
-20 -10 0 10 20
0 1 2 3 4 5 6 7 8 9 10
-10 -5 0 5 10
0 10 20 30 40 50 60 70 80 90 100 110 120 130 140 150
Time (Seconds)

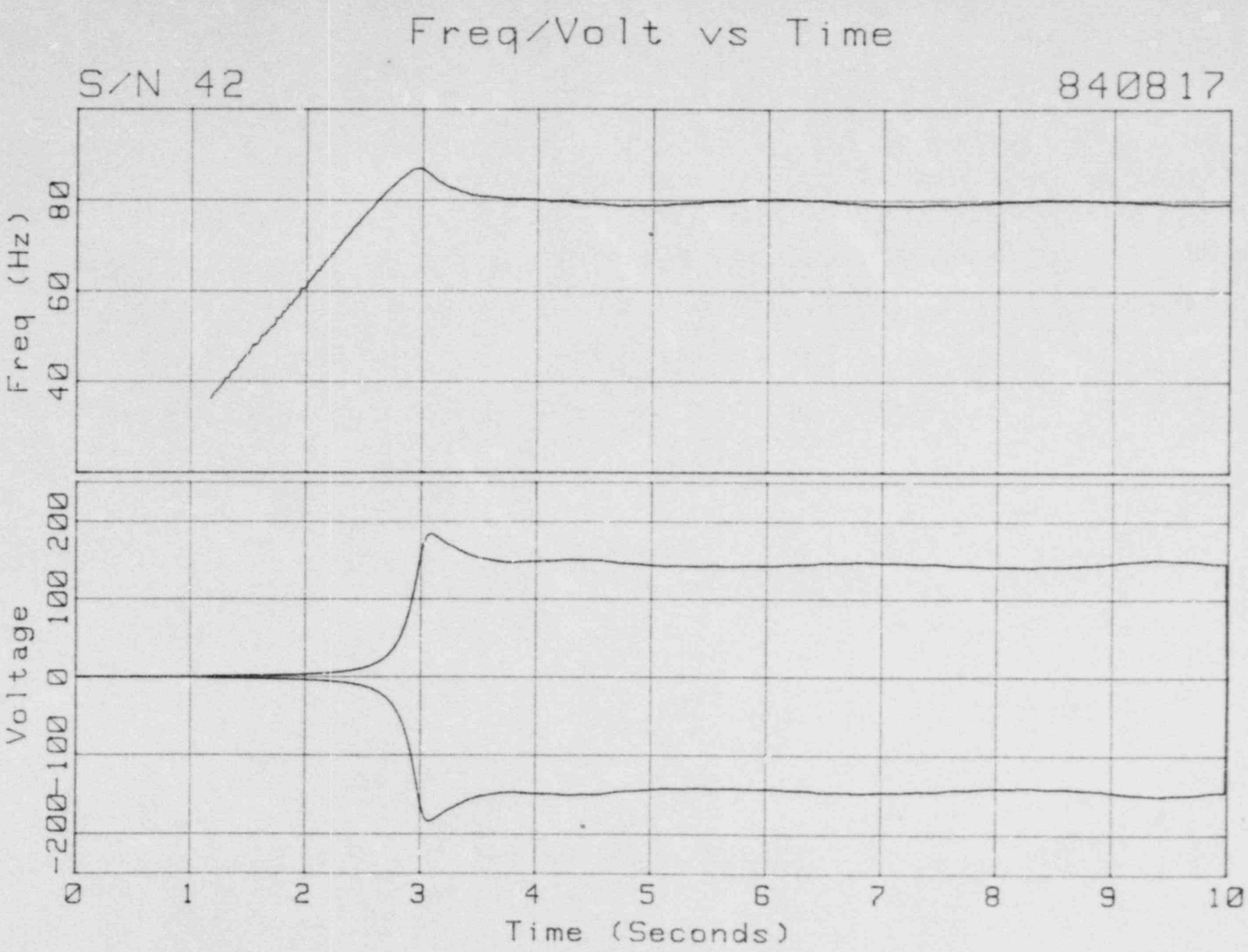
Freq/Volt vs Time
S/N 42
840817
Freq (Hz)
40
60
80
Voltage
-200
-100
0
100
200
0
1
2
3
4
5
6
7
8
9
10
Time (Seconds)

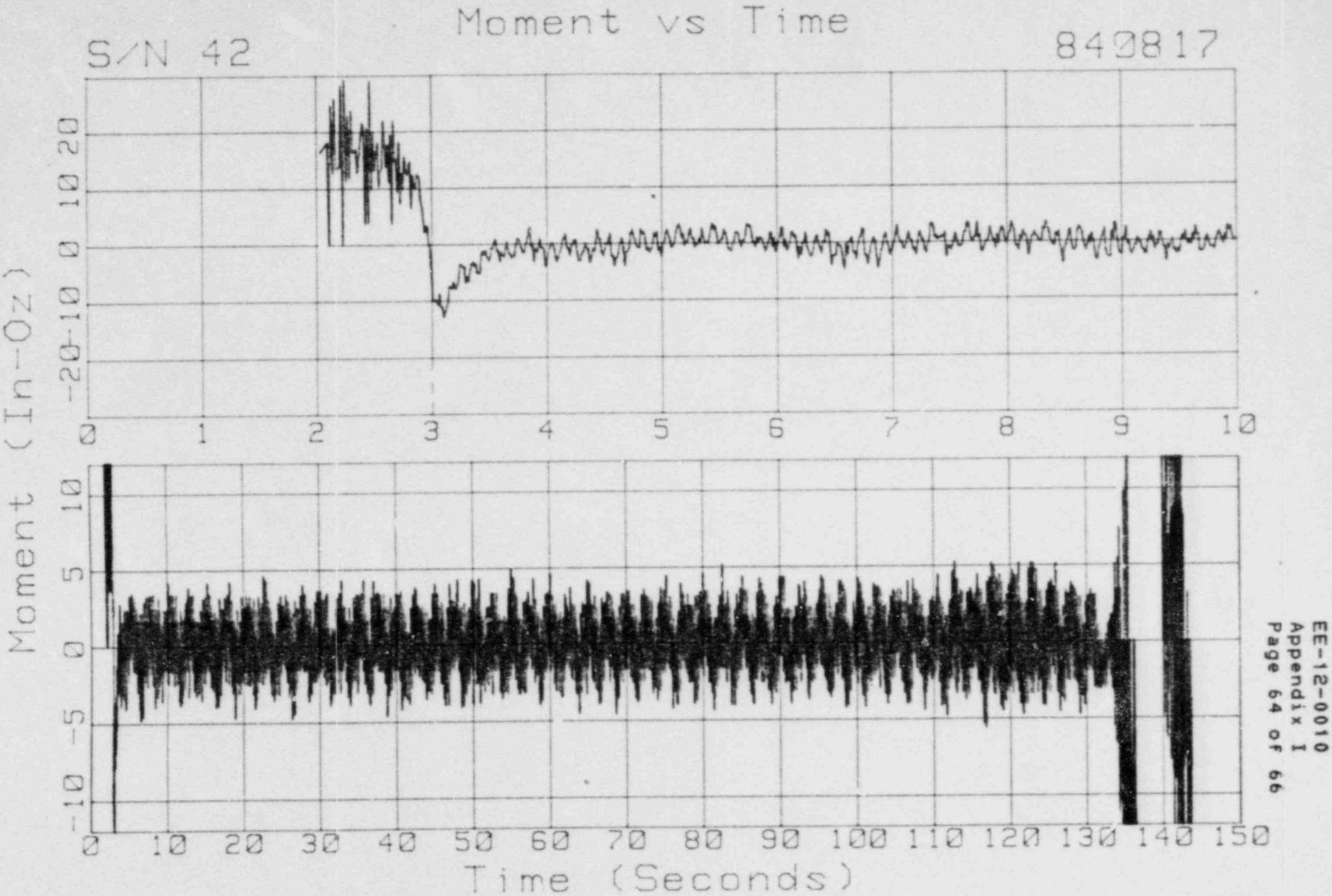
Moment vs Time
S/N 42
840817
Moment (In-Oz)
-20 -10 0 10 20
0 1 2 3 4 5 6 7 8 9 10
10 5 0 -5 -10
0 10 20 30 40 50 60 70 80 90 100 110 120 130 140 150
Time (Seconds)

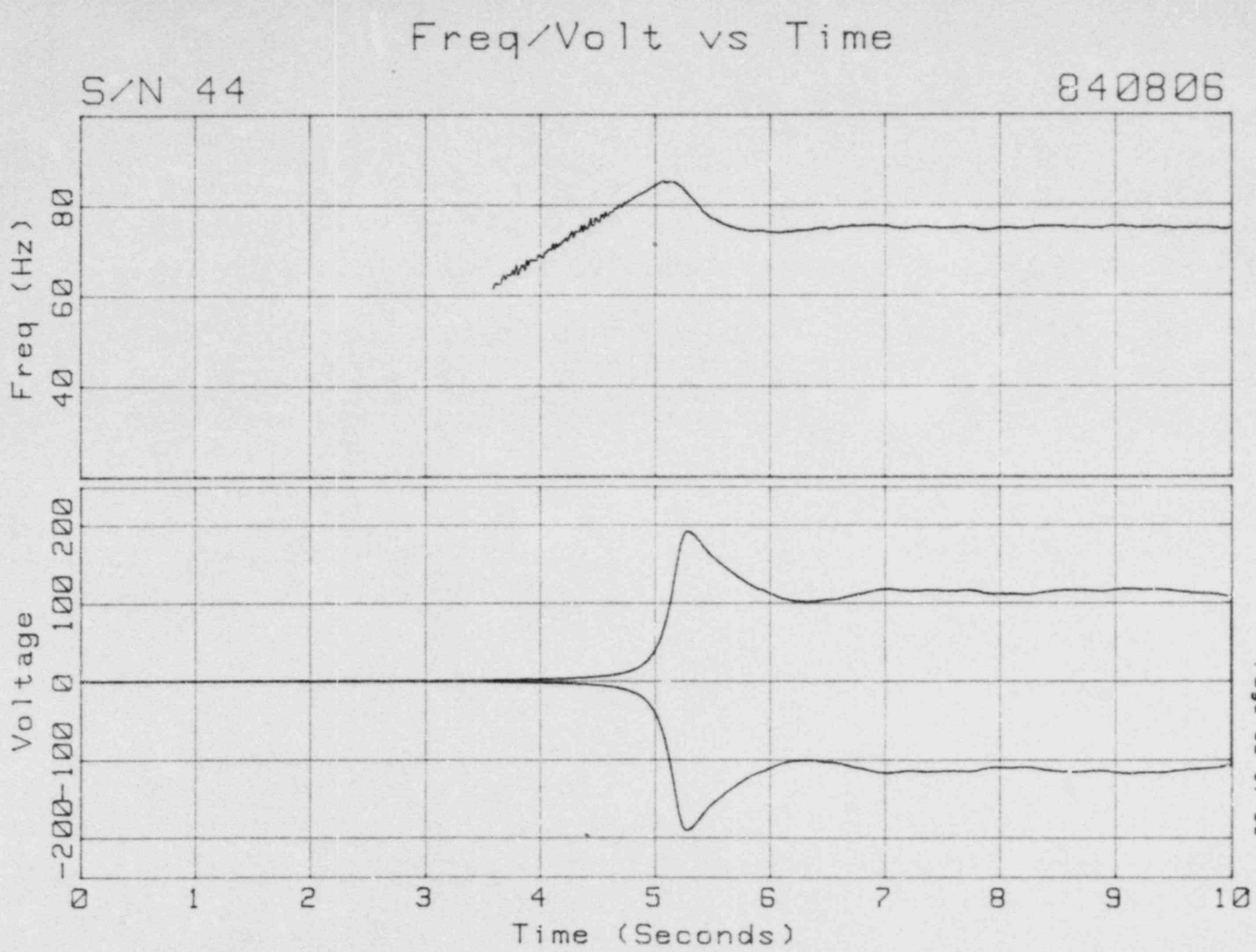
Freq/Volt vs Time
S/N 44
840806
Freq (Hz)
40 60 80
Voltage
-200 -100 0 100 200
0 1 2 3 4 5 6 7 8 9 10
Time (Seconds)

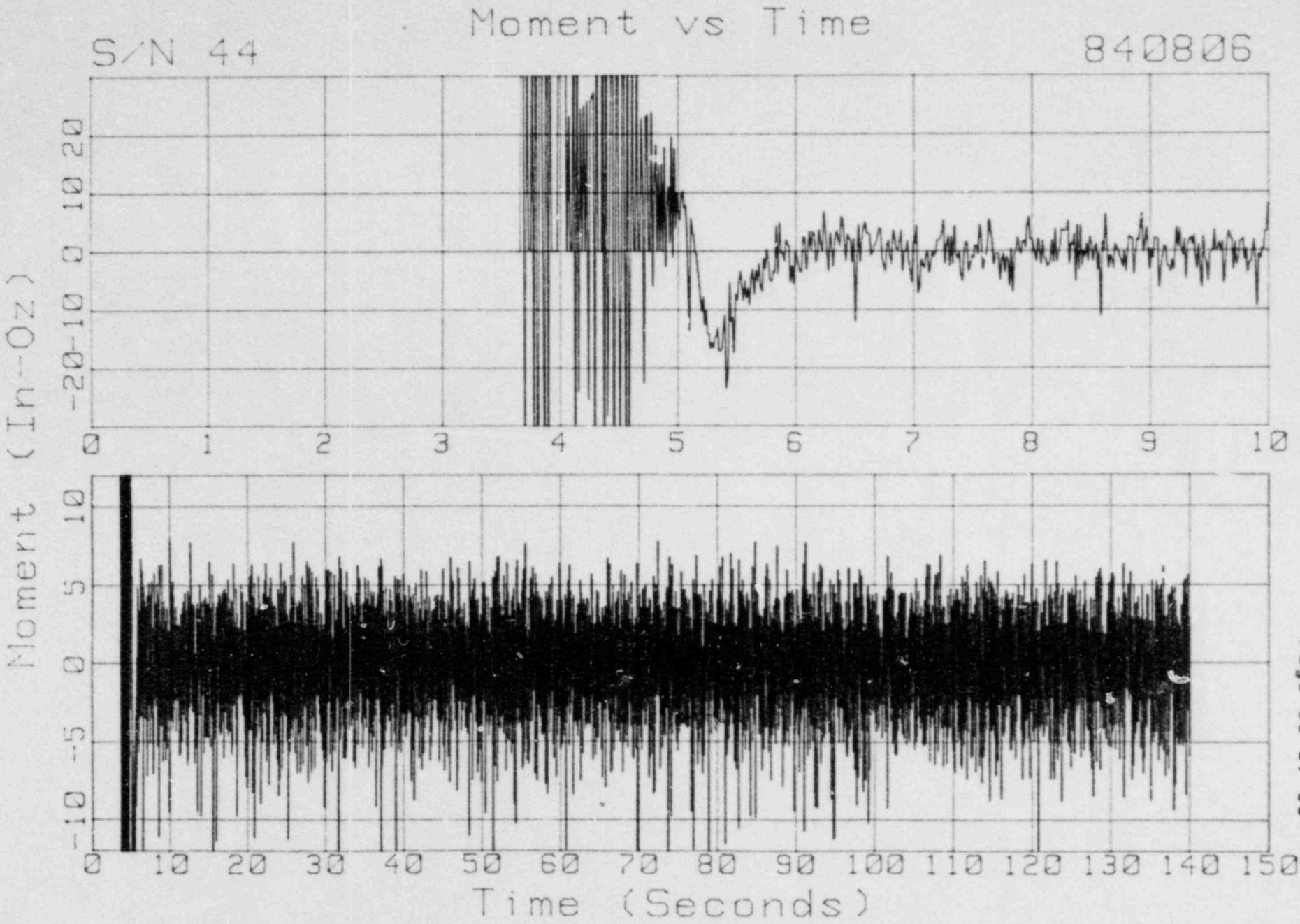
Moment vs Time
S/N 44
840806
Moment (In-Oz)
-20 -10 0 10 20
0 1 2 3 4 5 6 7 8 9 10
-10 -5 0 5 10
0 10 20 30 40 50 60 70 80 90 100 110 120 130 140 150
Time (Seconds)